New Routes To Fluorocarbon-Containing Phosphines

A thesis submitted to the University of Manchester for the degree of Doctor of

Philosophy in the Faculty of Engineering and Physical Sciences.

2010

Christopher James Herbert

School of Chemistry

Table of Contents

Final Word Count: 47968

Abstract

Routes to sterically demanding organofluorine-containing phosphines are described, and the stereoelectronic properties and chemistry of the resulting new ligands investigated.

The synthesis of $Cy_2P(CF=CF_2)$, **3**, has been accomplished. The nucleophilic substitution of $Ph_2P(CF=CF_2)$ with ^tBuLi produces the (*Z*)-isomer, $Ph_2P(Z-CF=CF(^tBu))$, **5-(*Z*)**, predominantly, which has been shown to be less electron-withdrawing than $Ph_2P(CF=CF_2)$, and similar in size to **3**.

The *bis*-trifluoropropynyl substituted phosphine $PhP(tfp)_2$, **7**, has been prepared, and its reaction with ^tBuLi investigated. This results in the formation of three previously unknown species, the *gem*-difluorocyclopropenyl-containing compound, $Ph^tBuP(dfcp)$, **8**, (*Z*)-$Ph_2P(CH=C(^tBu)CF_3)$, **9**, and $Ph^tBuP(tfp)$, **10**. The nucleophilic substitution occurs preferentially at the phosphorus centre, as shown by the reaction with one equivalent of ^tBuLi at -60°C, where compounds **9** and **10** are formed.

A new route to perfluoroalkyl-containing phosphines has been discovered. The addition of a perfluoroalkyl iodide to Ph_2PSiMe_3 results in the formation of six new phosphines, and has been shown to be extendable to partially fluorinated systems. The route can also be applied to $^iPr_2PSiMe_3$, and to the chiral phosphine $PhMePSiMe_3$. Three examples, Ph_2PR_f ($R_f = CF(CF_3)_2$, **15**, ($^sC_4F_9$), **18**, (*cyc*-C_6F_{11}), **19**), have been produced on a preparative scale.

The reaction of the *bis*-trimethylsilyl phenyl phosphine with $(CF_3)_2CFI$ has been investigated, though it does not result in the production of the *bis*-perfluoroalkyl-substituted phosphine, instead the previously unknown *P*-chiral compound, $PhP(H)CF(CF_3)_2$, **27** is formed.

Mechanistic studies have indicated that Ph_2P-PPh_2 is the intermediate, and that there is no evidence of a radical mechanism. There is no reaction between $Me_2(S)P-P(S)Me_2$ and $(CF_3)_2CFI$, though there is when $Me_2P-P(S)Me_2$ is used, suggesting that the lone pair of the intermediate diphosphine is necessary for the reaction to proceed. This has resulted in the formation of the new compound, $Me_2PCF(CF_3)_2$, **28**.

The chemistry of the perfluoroalkyl-containing phosphines has been investigated; they do not quaternise, but are oxidatively sensitive. The phosphorus(V) selenides of **15**, **18**, and **19** have been prepared, and based on their $^1J_{PSe}$ coupling constants, the perfluoroalkyl-groups impart a greater electron-withdrawing effect than perfluorovinyl, trifluoropropynyl, or alkoxy fragments. The oxidation of **15** and **18** with XeF_2 has also been accomplished, and shown to yield the corresponding $F_2PPh_2R_f$ compounds.

The molybdenum(0) pentacarbonyl complexes of **3**, **7**, and **15** have been synthesised and perfluoroalkyl-groups have again been shown to be more electron-withdrawing than perfluorovinyl and trifluoropropynyl groups by comparison of v(CO) values. The gold(I) chloride complexes of Ph_2PCF_3, **15**, and **18** and the platinum(II) dichloride complexes of **3** and **15** have been prepared, and the size of these ligands has been estimated from the crystal structures. Compound **18** has been shown to be the largest of these compounds, with a cone angle of 187°.

Declaration

I hereby declare that no portion of the work referred to in the thesis has been submitted in support of an application for another degree or qualification of this or any other university or other institute of learning.

Signed……….

Copyright

The author of this thesis (including any appendices and/or schedules to this thesis) owns any copyright in it (the "Copyright") and he has given The University of Manchester the right to use such Copyright for any administrative, promotional, educational and/or teaching purposes.

Copies of this thesis, either in full or in extracts, may be made **only** in accordance with the regulations of the John Rylands University Library of Manchester. Details of these regulations may be obtained from the Librarian. This page must form part of any such copies made.

The ownership of any patents, designs, trademarks and any and all other intellectual property rights except for the Copyright (the "Intellectual Property Rights") and any reproductions of copyright works, for example graphs and tables ("Reproductions"), which may be described in this thesis, may not be owned by the author and may be owned by third parties. Such Intellectual Property Rights and Reproductions cannot and must not be made available for use without the prior written permission of the owner(s) of the relevant Intellectual Property Rights and/or Reproductions.

Further information on the conditions under which disclosure, publication and exploitation of this thesis, the Copyright and any Intellectual Property Rights and/or Reproductions described in it may take place is available from the Head of School of Chemistry.

Acknowledgements

First and foremost, I would like to say that this would not have been possible without the continuing support of the Bank of Mum & Dad, especially its two long-suffering principal shareholders, to whom I owe a great debt (both literally and figuratively).

Many thanks are owed to my supervisor, Alan, for obtaining the funding for my position, and then taking me on as a student. His seemingly boundless patience, advice and suggestions have been gratefully received, and his witticisms and comic relief have made the laboratory and office a fantastic environment in which to work. Cheers Chief.

Speaking of the lab/office environment, many thanks must also go to those who have also inhabited it over the years (in no particular order), Nick "duplo" Barnes, Gavin "what's a backpack?" Potter, Andy "give me value" Ballantyne, Paul "out-first" Hurst, Mark Sadler, Rana Khan (whose limitless verbal diarrhoea will amuse me until the end of my days), Phil Miles, Phil Mallender, Shane Ratcliffle, Dave Meehan, Andy Jolleys, Scott Sulway, Sophia Solomon, Danny Woodruff, and the many other project students that have been and gone from Alan's group.

Outside of the four walls of the chemistry department, a great deal of gratitude is owed to Luke Thompson, Liam Marsh, Dave Mansell, Gavin Blackburn, and the aforementioned Mark Sadler, with whom I have lived and who have put up with me, and provided many moments of laughter that I will look back on fondly. A special thank you must also go to Laura, who took it upon herself to take in a homeless PhD student, look after me and give me love and support whilst I penned my *magnum opus*.

For all those who I've not mentioned, my apologies, and thank you anyway.

1 Introduction

The chemistry of phosphorus has been extensively studied since its discovery in 1669; this being largely due to the widespread utility of phosphorus compounds in a variety of processes and applications. Phosphorus-containing compounds are used widely in industry, they form the basis of the Wittig reaction,[1] and are perhaps the most important class of co-ligands in transition metal complexes with applications in a number of processes, such as hydroformylation,[2-4] Diels-Alder reactions,[5-7] and olefin polymerization.[8-10] Phosphorus compounds exhibit two common oxidation states, +III and +V, and frequently adopt coordination numbers of 3, 4, 5, and 6.

1.1 Phosphorus(III) Compounds

There are three major types of organophosphorus(III) compounds, those containing P–R bonds (R = alkyl/aryl), those with P–ER linkages (E = heteroatom such as O/N, R = alkyl/aryl), and those containing a combination of the two.

A smaller but related group of secondary (R_2PH) and primary (RPH_2) phosphines are also known, but their use is largely limited to precursors to tertiary phosphines, and they typically have an exceptionally foul odour. Halo-containing phosphines have also been extensively studied, again largely as starting materials for the formation of PR_3 compounds, often via their reaction with Grignard or organolithium reagents, but also as ligands in their own right (especially PF_3).

This ability to modify the properties of phosphorus(III) compounds has resulted in their use in a large number of diverse applications,[11-13] and their synthesis/coordination chemistry has been the subject of numerous reviews.[14-20] Typically, phosphorus(III) compounds are air sensitive (though

this stability depends on the nature of the organic substituents), and are often malodorous.

PR_3 compounds are σ-donors (due to the lone pair of electrons on the phosphorus centre) and π-acceptors. For the majority of phosphines, especially those that contain groups with a positive inductive effect (e.g. Me, ^{i}Pr, Cy etc) σ-donation is the dominant effect.

Phosphines that contain P–OR or P–NR$_2$ are generally better π-acceptors than alkyl/aryl containing analogues, and as a result $R_nP(ER_x)_{3-n}$ (n = 0-2, E = O, x = 1, E = N, x = 2) compounds have been extensively studied, as a way of tailoring (within reason) the steric and electronic properties of the phosphine ligand.

There are fewer π-acceptor ligands known than σ-donor ligands. The most widely studied of these π-acceptor ligands is C≡O, which is often used to stabilise low-valent metal complexes by accepting electron density from the metal centre into the π* anti-bonding molecular orbitals. The majority of other π-accepting ligands are analogous, e.g. cyanide and C≡NR. Many of these ligands are susceptible to nucleophilic addition,[21] as well as insertion[22,23] and coupling reactions.[23] It has been asserted that the only phosphorus ligand with similar π-acceptor properties to C≡O is PF_3.[24] These are small ligands, and it is thought that several processes would benefit from the availability of sterically demanding π-acceptor ligands.[11-13]

It is thought that phosphines containing perfluoro-organo groups will have π-acceptor properties approaching that of PF_3, but with the added advantage of steric modification, as the R/R$_f$ groups can be changed to modify the steric demand of the ligand.

1.2 Phosphorus Coordination Chemistry

The binding of phosphorus to metal centres is usually described as σ-donation and π-acception, as first proposed in the 1950s by Dewar,[25] Chatt and Duncansen.[26] The phosphorus lone pair is donated into a d-orbital of the metal that has the appropriate symmetry for efficient overlap, which gives rise to the σ-component of the bond. The orbitals involved in the π-bonding component are less clear cut. Initially it was proposed that the phosphorus low lying 3d orbitals were available for use in π-back bonding.[27,28] This view was widely accepted until several reports were published that proposed instead that anti-bonding P-R orbitals can act as the accepting orbitals without requiring the direct participation of the phosphorus 3d orbitals. These reports contained *ab initio* studies on PR$_3$ compounds,[29] and metal-PR$_3$ complexes[30] (along with analysis of experimental metal-PR$_3$ and P-R bonds in compounds where the molecular charge was varied)[31] and showed that while the 3d orbitals play some part in π-back bonding, it essentially occurs through the formation of hybridised orbitals with the anti-bonding P-R orbitals. Anti-bonding P-R orbitals are still able to participate in π-back bonding in the absence of the 3d orbitals,[32] though the effect is reinforced by the presence of the 3d orbitals.[32] The effect of the phosphorus d orbitals is less important for phosphines that contain electron-withdrawing groups, as it is now thought that the σ-donating ability does not vary significantly upon altering the substituents, but that π-acidity is much more sensitive.[33]

1.3 Electronic Properties of Phosphorus(III) Compounds

The net effect of the σ-donating and π-bonding ability of PR$_3$ compounds can be measured in several ways.[33] The most commonly used method is that of measuring the position(s) of the ν(CO) stretch in the infra-red spectrum of a transition metal carbonyl phosphine complex (e.g. [Ni(CO)$_3$PR$_3$],

[Mo(CO)$_5$PR$_3$], [Rh(CO)Cl(PR$_3$)$_2$]), shown by Strohmeier to be generally valid for a range of transition metal carbonyl complexes of phosphines, including manganese, vanadium, iron and nickel.[34] The position of this stretch varies according to the amount of electron density accepted by the π* anti-bonding orbital of the CO group *trans* to the PR$_3$ ligand, as the PR$_3$ group will compete with the CO moiety for electron density. Therefore, a metal complex containing a PR$_3$ ligand that is a strong π-acceptor will result in less electron density being donated to the CO π* anti-bonding orbital. This means that the C≡O bond will be stronger, resulting in a higher energy v(CO) stretch (since the vibrational frequency of the stretch is proportional to the square root of the force constant, which is in turn related to the strength of the bond). Historically, the major objection to this method of quantifying the electronic properties of the phosphine was that there is no way to separate the σ and п components. However, it is a useful measure of the electronic properties of PR$_3$ ligands, and recent research suggests that the σ-component does not vary significantly with different substituents.[33] Tolman compared a wide range of v(CO) stretching frequencies in [Ni(CO)$_3$L] complexes, and assigned the substituents attached to phosphorus a value (χ_i) based on an additive relationship (Equation 1.1) for estimating the electronic parameter of a given phosphine. These χ values are relative to a ^{t}Bu group, which has a χ value of 0, and for example a phenyl group has a value of 4.3, and CF$_3$ has a value of 19.6.

$$\text{Substituent contribution to } v \text{ for PXYZ: } v = 2056.1 + \sum_{i=1}^{3} \chi$$

Equation 1.1 Tolman's equation for estimating v(CO) stretching frequencies of [Ni(CO)$_3$L] complexes (L = phosphine).

The values obtained in this manner can be correlated empirically against those obtained for different metal centres. There is a strong positive

correlation when comparing the values for nickel and molybdenum (Figure 1.1) or rhodium (Figure 1.2) carbonyl complexes, though not quite so strong when comparing the nickel carbonyl stretching frequency with calculated values, such as the Semi-Empirical Electronic Parameter (SEP)[35] as can be seen in Figure 1.3.
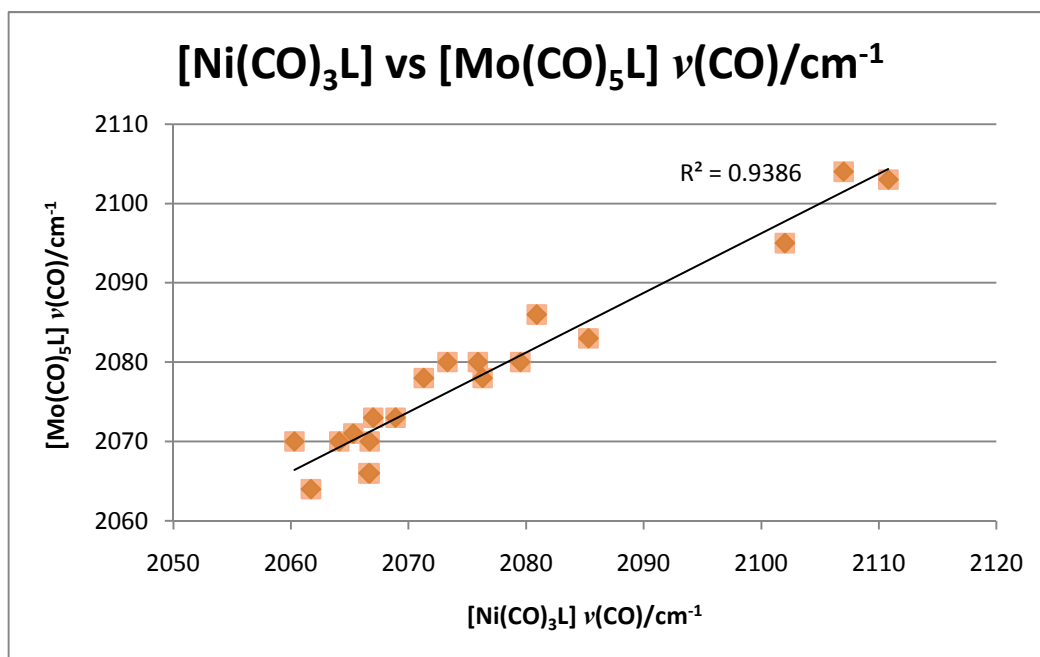
Figure 1.1 $v(CO)/cm^{-1}$ in [Mo(CO)$_5$L] vs [Ni(CO)$_3$L] (L = phosphine).
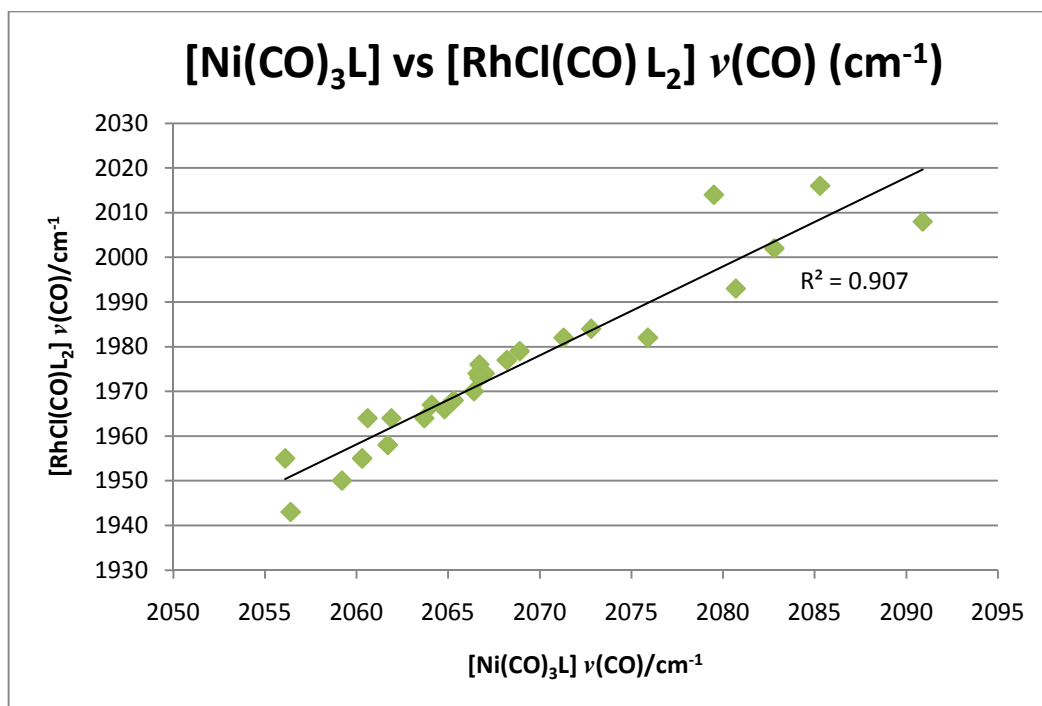
Figure 1.2 v(CO)/cm^{-1} in [RhCl(CO)L$_2$] vs [Ni(CO)$_3$L] (L = phosphine).

Due to the fact that the trend is unchanged when varying the metal centre, Banger *et al.*[36] have compared the v(CO) stretching frequencies of a series of [Mo(CO)$_5$L] complexes (Table 1.1).

PR$_3$, L	v(A$_1$)/cm^{-1}
Ph$_2$P(CF=CF$_2$)	2077
PhP(CF=CF$_2$)$_2$	2084
PMe$_3$	2070
Me$_2$PPh	2071
Ph$_2$PMe	2071
PPh$_3$	2072
P(OEt)$_3$	2078
P(OPh)$_3$	2084
PI$_3$	2087
PBr$_3$	2093
PCl$_3$	2095
PF$_3$	2104

Table 1.1 v(CO) stretching frequencies for [Mo(CO)$_5$L] complexes (only highest carbonyl stretching mode shown).[36]
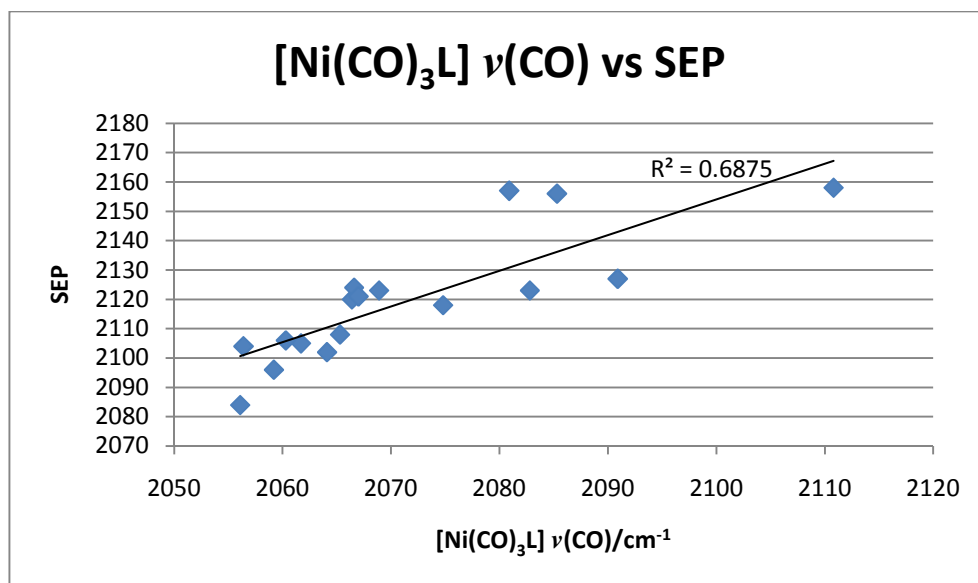
Figure 1.3: SEP v(CO)/cm^{-1} vs [Ni(CO)$_3$L]. SEP values taken from Ref. 35

A variety of NMR coupling constant information can also be used as a gauge of the electronic properties of a ligand, such as $^1J_{PtP}$ or $^1J_{PSe}$ values, and these can be compared with v(CO) stretching frequencies (Figure 1.4). It has been shown that the magnitude of $^1J_{PSe}$ coupling constants is dependent on the nature of the organic substituents bound to the phosphorus centre, with electron withdrawing substituents causing it to increase, and electron donating substituents causing it to decrease. Allen and Taylor state that electron withdrawing groups result in an increase in the s character of the lone pair, and electron donating fragments result in a reduction in the s character.[37] Hope *et al*.[38] have prepared a variety of phosphorus(V) selenides for this purpose, although care is needed, since the values of the coupling constant are solvent dependant.[38,39]
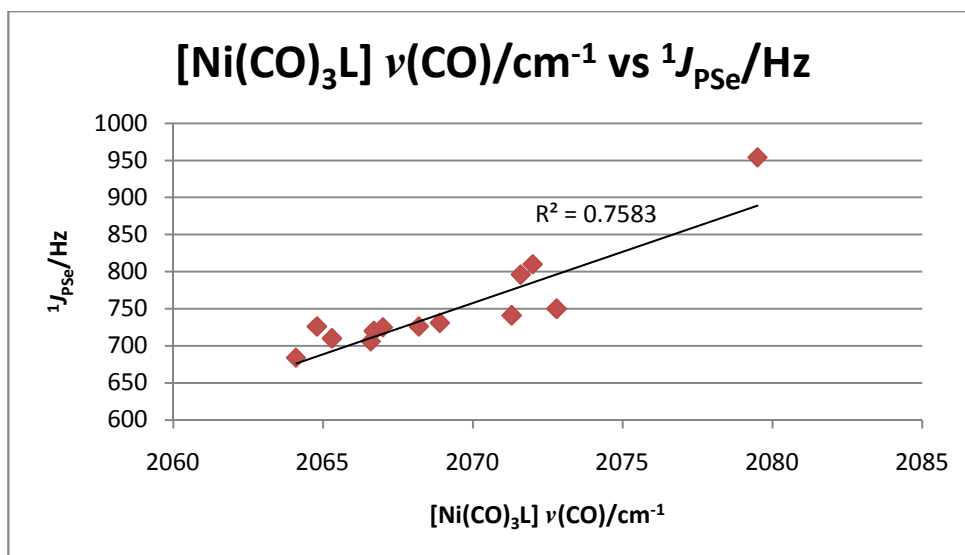
Figure 1.4: $^1J_{PSe}$/Hz for LSe vs v(CO)/cm^{-1} in [Ni(CO)$_3$L] (L = phosphine).

It can be seen from the above data that a number of alternative methods can be used to measure the electronic properties of phosphines (relative to [Ni(CO)$_3$L]), although the calculated SEP (Figure 1.4) shows the poorest agreement with the data from the nickel complexes.

1.4 Steric Properties of Phosphorus(III) Compounds

1.4.1 Tolman Cone Angle

The steric parameter of phosphines is also very important when considering their coordination chemistry. The most commonly used method of quantifying the size of a phosphine is the cone angle (θ) concept, developed by Tolman[40] in the late 1970s, and is based on data taken from [Ni(CO)$_3$L] systems. The Tolman Cone Angle is defined as:

"*The apex angle of a cylindrical cone, based about the Ni centre, which is 2.28 Å from the phosphorus centre, to the edge of the van der Waals' radius of the outermost atoms on the phosphine.*"[40] (Figure 1.5)
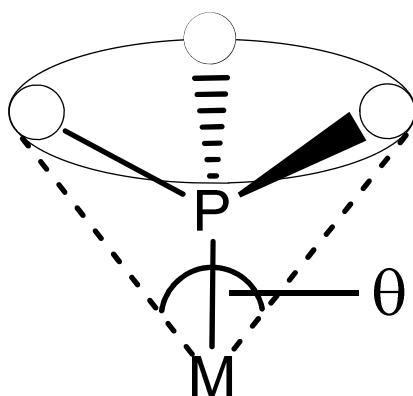
Figure 1.5: Diagram showing Tolman Cone Angle.

However, this has its limitations, since the apex is defined as being 2.28 Å from the phosphorus centre, this creates problems as metal-phosphorus bond lengths differ, which can result in the measurement of an approximate cone angle since the length of the cone is different. Furthermore, it is also possible for the ligand substituents to "intermesh" and this becomes considerably more important if the metal-phosphorus bond is significantly longer than 2.28 Å, or if the metal coordination number is low, as the ligand will (potentially) have more space to "relax" into, thus adopting a larger cone angle.

1.4.2 Solid Angle, Ω

An alternative to the Tolman Cone Angle is the solid angle, Ω. The concept of the solid angle was developed at a similar time to the Tolman Cone Angle, after Immirzi *et al*.[41] formed $[Pt(PCy_3)_3]$.1.5heptane by crystallising $[Pt(PCy_3)_2]$ from heptane at -15°C in the presence of an excess of PCy_3. The Tolman Cone Angle for PCy_3 is 170°, and so the formation of $[Pt(PCy_3)_3]$ would be unexpected and this compound should contain steric strain. However, the cyclohexyl groups "mesh" resulting in a measured cone angle of 157° in this particular complex. The solid angle of an object results from the area of the shadow of the object projected onto a surface, and is the

measure of the steric size of the object in question. This is represented by the integral, where **r** is the position vector of an element of a surface with respect to O (the origin) and r is the magnitude of **r**.[42,43]

$$\Omega = \int_S \frac{\boldsymbol{r}.dS}{r^3}$$

This is expressed in steradians, not a particularly common measure, so if the solid angle is assumed to be that of a cone, then the solid cone angle $\Omega°$ follows from the relationship.[41-43]

$$\Omega° = 2\, arccos\left(1 - \frac{\Omega}{2\Pi}\right)$$

The solid angle is a very reasonable alternative to the Tolman Cone Angle, however it is rather less intuitive and offers few significant advantages and has therefore never acquired a prominent role as a descriptor for the steric demand of ligands. There is a reasonably good correlation between the solid cone angle and the Tolman Cone Angle although unsurprisingly the solid cone angles are smaller.

1.4.3 Buried Volume, $\%V_{Bur}$

Another alternative for measuring the steric demand of ligands, developed to describe the size of N-heterocyclic carbenes, is the buried volume, $\%V_{Bur}$,[44-50] as the Tolman Cone Angle is not a particularly efficient descriptor for these ligands owing to their shape (see Figure 1.6).
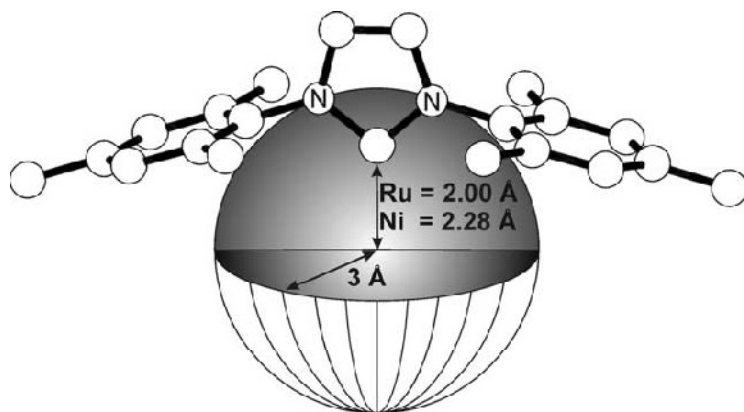
Figure 1.6: Representation of the dimensions used for the determination of %V_{Bur}.[48]

The concept of buried volume can be extended to include other, more classical ligands, such as phosphines and cyclopentadienyl derivatives. The buried volume refers to the amount of a sphere centred on the metal that is buried by overlap with atoms of the various ligands. Thus, the bulkier the ligand is, the greater the value of %V_{Bur}. However, this approach is largely computational in nature, and involves "fixing" the ligand to metal distance at an arbitrary length, and iteratively arriving at a "reasonable" radius for the sphere, as shown in Figure 1.6. This has been developed into a web-based %V_{Bur} calculator.[51]

1.4.4 Symmetric Deformation Coordinate, S$_4$'

Orpen *et al.*[52] have used the angles around the coordinated phosphorus atom to measure the steric effect of phosphines, via a symmetric deformation coordinate (S$_4$'). The S$_4$' is defined as Σ(M–P–R) – Σ(R–P–R) (see Figure 1.7).
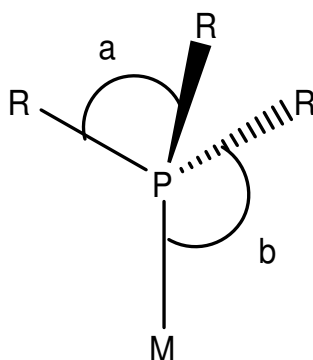
Figure 1.7: Representation of angles used in calculating S$_4$' parameter.

This parameter does not directly take into account the geometry of the external atoms of the ligand, and one can envisage ligands that would be considered small by their S$_4$', yet large by θ. There is also the possibility (as mentioned above) that the ligands may intermesh, giving rise to situations where the S$_4$' value is large despite the phosphine occupying relatively little space remote from the metal centre. However, in spite of these issues, the correlation between S$_4$' and θ is good.[52]

1.4.5 Stereo-Electronic Maps

It was noted by Roddick and Schnabel[53] that there was a lack of large, electron poor phosphorus(III) ligands. This was taken further by Cundari and co-workers[35] who used computational methods to calculate the S$_4$' and SEP values of a range of phosphines and generated the plot shown in Figure 1.8. This approach attempts to identify "gaps" where there were few ligands possessing those particular steric and electronic properties.
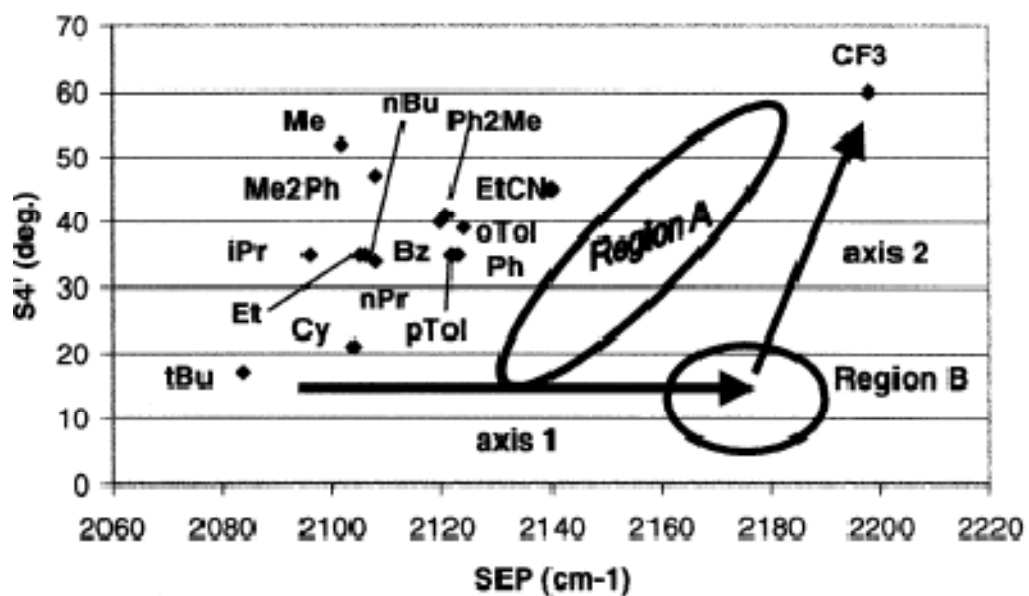
Figure 1.8: Calculated stereoelectronic map for phosphines derived from PM3 calculations on *trans*-[Rh(PR$_3$)$_2$(CO)Cl]. Taken from Ref. 35.

The graph shows that there is a lack of medium to large electron-poor phosphines, though they do not include any fluoroaryl-containing phosphines, which do indeed fall into this gap. Cundari *et al*. also note that with the exception of P(CF$_3$)$_3$, that all the other commonly studied phosphines are very similar, highlighting the sensitivity obtainable by varying the phosphine in a catalytic process.[35] The one exception cited in their work is P(CF$_3$)$_3$; however since this compound is spontaneously flammable[54] (Figure 1.9), and only weakly coordinates to metal centres[55] P(CF$_3$)$_3$ has been largely disregarded as a useful ligand.

Figure 1.9: Reaction of P(CF$_3$)$_3$ with atmospheric oxygen.[56]

It can be difficult to distinguish between the impact of steric and electronic parameters on the overall properties of a phosphine. This is because of the inter-play between them. The angular separation between the substituents bound to the phosphine will affect the s-character of the lone pair on the phosphorus centre, altering its σ-donating properties. Thus, modification of the steric bulk is expected to also have an effect on the electronic properties of the phosphine ligand.

1.5 Fluoroalkyl Phosphines

Phosphines that contain one or more perfluorinated moieties are thought to offer access to an unusual combination of steric and electronic properties, with the ability to "fine-tune" these properties as required. However, for a class of compounds that conveys very different properties there are surprisingly few examples compared to the number of non-fluorinated analogues. Phosphines containing fluoroaryl groups are commercially available and/or easily prepared from readily available starting materials, and have been the subject of a recent review by Saunders and co-workers[20] and as such they will not be discussed here.

1.5.1 Synthesis of Fluoroalkyl Phosphines

The first synthesis of a fluoroalkyl-containing phosphine was reported in the early 1950s by Bennett *et al.*[54] who utilized the reaction of trifluoromethyl iodide and white phosphorus at ~200°C in an autoclave, to obtain a mixture of products including $P(CF_3)_3$, $(CF_3)_2PI$, $(CF_3)PI_2$, and PI_3.[57] They discovered that by altering the reaction temperature and time they could tailor the ratio of products that they obtained, and in particular that at temperatures above 200°C over 80% $P(CF_3)_3$ was generated; but at temperatures below 200°C the reaction is slow and greater proportions of the iodo-phosphines were produced (Scheme 1.1). This method has also been shown to be applicable to $^nC_3F_7I$,[58] C_2F_5I,[59] and $^iC_3F_7I$,[60] but yielding only $(R_f)_2PI$ and $(R_f)PI_2$, with none of the tri-substituted compound.

$P(CF_3)_3$ is readily hydrolysed by weak aqueous alkaline solutions at room temperature,[61] and is spontaneously flammable in air (Figure 1.9).[57] $P(CF_3)_3$ also disproportionates when heated above 100°C in the presence of iodine,[57] giving a mixture of PI_3, CF_3PI_2, $(CF_3)_2PI$ and $P(CF_3)_3$. Of these materials, CF_3PI_2 and $(CF_3)_2PI$ are liquids that liberate iodine in the presence of light, and the latter is rapidly oxidised on exposure to air.[57]

$$CF_3I + P_4 \xrightarrow[\text{48 h}]{195 - 230^oC} P(CF_3)_3 + (CF_3)_2PI + (CF_3)PI_2 + PI_3$$
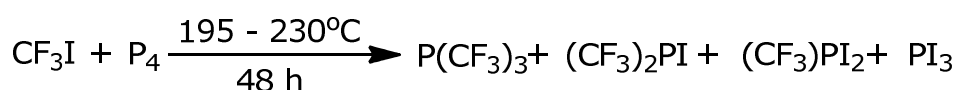
Scheme 1.1: Reaction of CF_3I with elemental phosphorus in an autoclave.

In 1957 Burg and Mahler reported that the reaction of $AgCO_2CF_3$, I_2, and red phosphorus in a steel bomb at 200°C for 120 hours also produces $P(CF_3)_2$, $(CF_3)_2PI$, $(CF_3)PI_2$ and PI_3 (Scheme 1.1).[62] However the potential side reactions between iodine and red phosphorus makes this procedure less

useful than the method of Bennett et al.[54] despite the dangers involved in handling white phosphorus.

$$AgCO_2CF_3 + P + I_2 \xrightarrow[120\ h]{200^o} P(CF_3)_3 + P(CF_3)_2I + P(CF_3)I_2 + PI_3$$
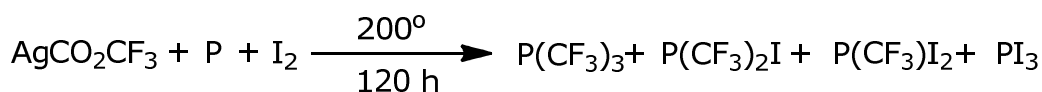
Scheme 1.2: Formation of trifluoromethyl phosphines using $AgCO_2CF_3$ as the source of CF_3 moiety.

The reaction of the iodo-containing phosphines $(CF_3)_2PI$ and CF_3PI_2 with AgCl at room temperature almost quantitatively produces the chloro-analogues[57] (Scheme 1.3), but takes 15 days.[63] $(CF_3)_2PCl$ and CF_3PCl_2 can also be formed via the reaction of the $(CF_3)_2PI$ and CF_3PI_2 with $HgCl_2$ (in 1 hour at room temperature),[64] or by the reaction with $SbCl_3$.[65] The fluoro-containing phosphines $(CF_3)_2PF$[66] and CF_3PF_2[67] can be formed in a similar fashion with SbF_3. The reactions involving SbX_3 (X = Cl, F) also produce $(CF_3)_2P\text{-}P(CF_3)_2$ as a minor by-product.[67]

$$(CF_3)_nPI_{3-n} \xrightarrow[RT]{AgCl\ or\ HgCl_2\ or\ SbCl_3} (CF_3)_nPCl_{3-n} + AgI\ or\ HgI_2\ or\ SbI_3$$
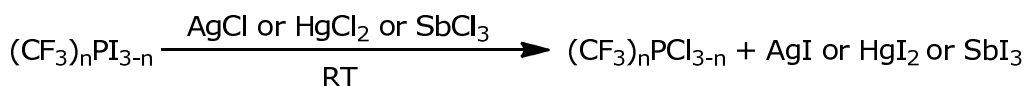
Scheme 1.3: Halogen exchange of iodo-fluoroalkylphosphines.

The latter compound is also formed when iodo-*bis*-trifluoromethylphosphine, $(CF_3)_2PI$ reacts with mercury at room temperature (with vigorous shaking over two days, Scheme 1.4).[57]

$$2(CF_3)_2PI + Hg \longrightarrow (CF_3)_2P\text{-}P(CF_3)_2 + HgI_2$$

Scheme 1.4: Reaction of *bis*-(trifluoromethyl)iodophosphine with mercury.

Haszeldine and West[68] showed that the reaction of PMe_3 with CF_3I at room temperature in the absence of a solvent forms Me_2PCF_3 (~50%), whilst

noting that the rate of reaction is accelerated by heat, and an equivalent amount of $[PMe_4]^+I^-$. Adding an excess of CF_3I however, did not result in the formation of any methyl*bis*-(trifluoromethyl)phosphine. Haszeldine and West also showed that CF_3I reacts with PH_3 to yield H_2PCF_3, though very low yielding (~13%). Further work[69] investigated the reaction of $P(CF_3)_3$ with MeI. It was found that the reaction only occurs at elevated temperatures (*ca.* 240°C or above), where $MeP(CF_3)_2$, and CF_3I are formed. They also found that $MeP(CF_3)_2$ will react with a further equivalent of MeI to yield Me_2PCF_3, albeit in low yield as the quaternary salt $[Me_3PCF_3]^+I^-$. Neither Me_2PCF_3 nor $MeP(CF_3)_2$ undergoes the reverse reaction with CF_3I (see Scheme 1.5).

$$PMe_3 \ + \ CF_3I \longrightarrow PMe_2(CF_3) \ + \ [PMe_4]^+I^-$$
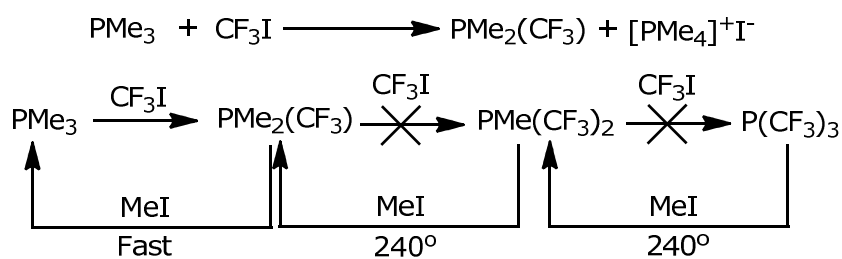
Scheme 1.5: Representation of the reactions of methyl(trifluoromethyl)phosphines and MeI/CF₃I.

Cullen[70] showed that it was also possible to form $^nBu_2PCF_3$ from P^nBu_3 and CF_3I at 100°C, but that the yields were very low, postulated as being due to the formation of a relatively stable phosphonium complex $[^nBu_3PCF_3]^+I^-$.

Mahler and Burg[71] reported the reaction of $(CF_3)PI_2$ with Hg at room temperature, resulting in the production of the cyclophosphines, $(CF_3P)_4$ (60%) and $(CF_3P)_5$ (40%) (Scheme 1.6). Reaction of these compounds with I_2 was shown to give complete reconversion to the starting material, whilst the reaction with chlorine yielded CF_3PCl_4, which could then be reduced to CF_3PCl_2 in the presence of Hg. They also showed that hydrolysis of the tetramer, $(CF_3P)_4$, yields CF_3PH_2 (21%), $(CF_3)PH(O)OH$ (24%) and the diphosphine $(CF_3PH)_2$. CF_3PH_2 was also obtained via the hydrolysis of the

27

pentamer, $(CF_3P)_5$, in diglyme along with the triphosphine $H_2(CF_3P)_3$. Surprisingly, similar treatment of $(C_2F_5)PI_2$ with Hg results in the formation of $(C_2F_5P)_3$ and $(C_2F_5P)_4$ in a 2:3 ratio,[59] perhaps due to the greater steric demand of the pentafluoroethyl group. Ang *et al.*[72] extended this work to include the $^nC_3F_7$ derivatives $(^nC_3F_7P)_n$ (n = 4, 5) and subsequently found that $(^nC_3F_7P)_5$ spontaneously converts into $(C_3F_7P)_4$ irreversibly over several days at room temperature.

$$(CF_3)PI_2 \xrightarrow{\text{Hg}} (CF_3P)_4 \ + \ (CF_3P)_5$$

$$(C_2F_5)PI_2 \xrightarrow{\text{Hg}} (C_2F_5P)_3 \ + \ (C_2F_5P)_4$$
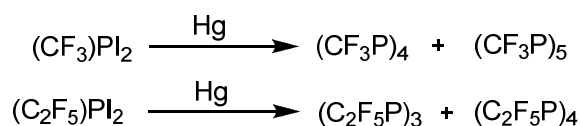
Scheme 1.6: Formation of cyclic perfluoroalkyl phosphines.

Bennett and co-workers reacted $(CF_3)_2PI$ with H_2 in the presence of Raney nickel to give $(CF_3)_2PH$ in a 65% yield.[61] They also reported the synthesis of the same compound via the reduction of $((CF_3)_2P)_2$ under similar conditions, but in a reduced yield. However, the reduction of *bis*-iodo(trifluoromethyl)phosphine, CF_3PI_2, with H_2 and Raney nickel does not proceed, perhaps due to complex formation with nickel.[61] The optimum procedure for the formation of $(CF_3)PH_2$ was found to be the hydrolysis in a highly concentrated aqueous solution of CF_3PI_2 followed by freeze-drying, yielding 24%.[61] Both the primary and secondary trifluoromethyl phosphines $(CF_3)_2PH$ and CF_3PH_2 are spontaneously flammable and susceptible to alkaline hydrolysis.[61]

Burg and Mahler[73] reported that the method of synthesizing $((CF_3)_2P)_2$ from $(CF_3)_2PI$ and Hg[57] is also a good way of producing $(CF_3)_2PH$ when the reaction is performed in the presence of a strong protic acid such as CF_3COOH, though the reported yield was only 35% (compared to 65% for the method of Bennett *et al.*).[61] An improved preparation for the synthesis of $(CF_3)_2PH$

and CF_3PH_2 was reported in the 1960s by Cavell and Dobbie,[74] which involves the reaction of $(CF_3)_2PI$ and CF_3PI_2 with Hg and HI (similar to that reported by Burg and Mahler described above) with yields of around 90% after fractionation (Scheme 1.7).

$$(CF_3)_nPI_{3-n} \xrightarrow[\substack{X = I, \text{ yields} \sim 90\% \\ X = CF_3COO^- \sim 35\% \\ n = 1,2}]{Hg, HX} (CF_3)_nPH_{3-n}$$
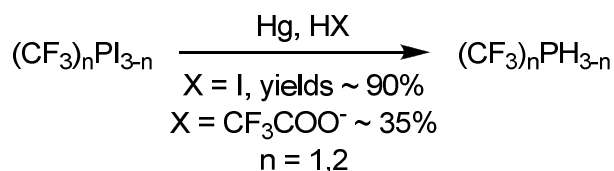
Scheme 1.7: Formation of trifluoromethyl phosphines.

Pyrolysis of C_2H_4, C_2F_4 and C_2H_2 with $(CF_3)_2P-P(CF_3)_2$ in the presence of a catalytic amount of iodine affords the bis(phosphino)alkanes $(CF_3)_2PCX_2CX_2P(CF_3)_2$ (X = H, F) and $(CF_3)_2PCH=CHP(CF_3)_2$ respectively.[75] Phillips *et al.*[76] reported an alternative procedure for producing the bis(phosphine)alkanes from the reaction of $((CF_3)_2P)_2$ and the corresponding diiodoalkane at 130°C (for between one and three days). Exploiting this method they formed $(CF_3)_2P(CH_2)_nP(CF_3)_2$ (n = 1-3) and $(CF_3)_2PCRR'P(CF_3)_2$ (R = R' = H, CH_3; R = H, R' = CH_3).

An alternative method for the production of $(CF_3)_2PCH_2CH_2P(CF_3)_2$ was reported by Field and Wilkinson,[77] via the reaction of *bis*(dichlorophosphino)ethane and CF_3Br in the presence of *tris*(diethylamino)phosphine at -60°C, though the reported yield was only 15% (Scheme 1.8). They also separately reported the synthesis of the unsymmetrical alkyl perfluoroalkyl *bis*-phosphine, $(CH_3)_2PCH_2CH_2P(CF_3)_2$, which utilized the same method for attaching the CF_3 groups, but requires rather more steps overall.[78] Kolomeitsev and co-workers[79] showed that replacing the chlorophosphine with $P(OPh)_3$ under the conditions used by

Field and Wilkinson results in the production of $P(CF_3)_3$ at -60°C in yields of up to 85%.

$$Cl_2PCH_2CH_2PCl_2 + CF_3Br + P(NEt_2)_3 \xrightarrow[\text{-60}^{\circ}\text{ - RT}]{\text{CH}_2\text{Cl}_2} (CF_3)_2PCH_2CH_2P(CF_3)_2 + X_2P(NEt_2)_3$$

$$X = Cl, Br$$
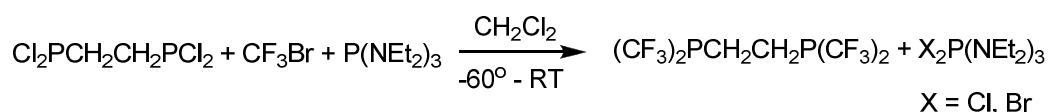
Scheme 1.8: Trifluoromethyl phosphines from CF$_3$Br and P(NEt$_2$)$_3$.

$(CF_3)_2PPh$ can be formed via the reaction of *tetrakis*-phenyltetraphosphine $(C_6H_5P)_4$ with CF_3I (Scheme 1.9), as part of a mixture that also contains $(CF_3)PhPI$, in an approximately 2:1 ratio,[80] the latter giving rise to $(CF_3)PhPH$ on hydrolysis.[80]

Bis-phenyl(trifluoromethyl)phosphine can be formed via the reaction of Ph_2P-PPh_2 and CF_3I at 185°C or by irradiation with ultraviolet light (Scheme 1.9).[81] Ph_2PCF_3 was found to be a colourless viscous liquid with a boiling point of 255-257°C, lower than that of Ph_2PH (b.p. 280°C),[82] as a result of weaker molecular interactions. Ph_2PCF_3 is only slightly hydrolysed by aqueous sodium hydroxide at 100°C,[81] unlike $PhP(CF_3)_2$, which is quantitatively hydrolysed in the same medium at 80°C.[80] In the early 1980s Maslennikov *et al.*[83] reported the synthesis of $Ph_2PC_2F_5$ via the method of Beg and Clark,[81] presumably from Ph_2P-PPh_2 and C_2F_5I.

$$(Ph_2P)_2 + CF_3I \xrightarrow{\text{UV or 185}^{\circ}\text{C}} Ph_2PCF_3 + Ph_2PI$$

$$(PhP)_4 + CF_3I \xrightarrow{\text{185}^{\circ}\text{C}} PhP(CF_3)_2 + Ph(CF_3)PI$$
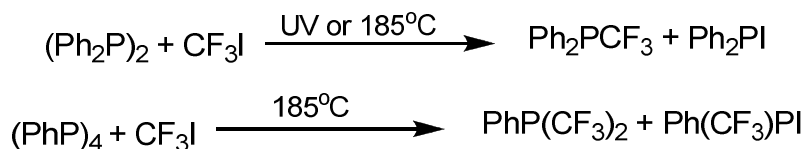
Scheme 1.9: Reaction of CF$_3$I with polyphosphines.

The synthesis of (dimethylamino)*bis*-(trifluoromethyl)phosphine, $Me_2NP(CF_3)_2$, was described by Nixon, from the reaction of $(CF_3)_2PF$ and Me_2NH by mixing the two compounds at -196°C and allowing them to warm

to room temperature.[84] The reaction of CF_3PF_2 with Me_2NH led to the formation of $(Me_2N)PF(CF_3)$,[64] which on further reaction with $HNMe_2$ yields $(Me_2N)_2PCF_3$.[64] This compound can be also be formed via the reaction of CF_3PCl_2 with an excess of dimethylamine.[64] Treatment of $(Me_2N)_2PCF_3$ with HCl results in the recovery of the starting CF_3PCl_2.[64] Adler and Kober[85] extended this method to include longer chain secondary amines (up to and including $-N(^nBu_2)$, and cyclic amines (pyrrolidine, piperidine). In 1968 Ang et al.[86] reported that the reaction of tris-(dimethylamino)phosphine with CF_3I or $(CF_3)_2CFI$ afforded $(Me_2N)_2PCF_3$ (71%) and $(Me_2N)PCF(CF_3)_2$ (68%), which have to be separated from the by-product of the reaction, $(Me_2N)_2P$-$P(NMe_2)_2$. Volbach and Ruppert[87] showed that it was possible to synthesise $(Et_2N)_2PCF_3$ directly from $CF_3Br/P(NEt_2)_3/PCl_3$, which on addition of HX (X = F, Cl, Br, I) yielded CF_3PX_2 quantitatively.

In the late 1960s Gosling et al.[88] showed that it is possible to form tertiary alkyl(perfluoroalkyl)phosphines via the reaction of $R_fPCl_2/(R_f)_2PCl$ with RLi (they state that using organolithium compounds is cleaner than utilising Grignard reagents), as summarised in Table 1.2. However, this route requires the formation of perfluoroalkyl chlorophosphines. They also found that the n-heptafluoropropyl alkyl phosphines hydrolysed more slowly than the corresponding trifluoromethyl derivative under similar conditions.[88] Subsequently, Maslennikov et al.[83] showed that $PhP(CF_3)_2$ could be prepared from PhMgBr and $(CF_3)_2PCl$, but only in approx 30% yield.

Phosphine	RLi	Product	Yield (%)
$(CF_3)_2PCl$	Me	$MeP(CF_3)_2$	24
$(CF_3)_2PCl$	^nBu	$^nBuP(CF_3)_2$	78
$(CF_3)_2PCl$	^iBu	$^iBuP(CF_3)_2$	Not given
$(CF_3)_2PCl$	Ph	$PhP(CF_3)_2$	54
$(^nC_3F_7)_2PCl$	^nBu	$^nBuP(^nC_3F_7)_2$	71
$(^nC_3F_7)_2PCl$	Ph	$PhP(^nC_3F_7)_2$	Not given
$CF_3PCl_2{}^a$	^nBu	$^nBuP(CF_3)_2$	40
Et_2PCl^b	$^nC_3F_7$	$Et_2P(^nC_3F_7)_2$	Not given
Ph_2PCl^b	$^nC_3F_7$	$Ph_2P(^nC_3F_7)_2$	Not given
$(CF_3)_2PCl^b$	$^nC_3F_7$	$(CF_3)_2P(^nC_3F_7)$	Not given
$CF_3PCl_2{}^b$	$^nC_3F_7$	$(CF_3)P(^nC_3F_7)_2$	15

(a)   This reaction also forms $^nBuPCl(CF_3) \sim 10\%$
(b)   This reaction involves the chlorophosphine, $^nC_3F_7I$, and a suspension of Li (2% Na)

Table 1.2: Compounds synthesised by Gosling *et al*.[88]

Some alternative, though non-specific, routes were published by Kang and Burg,[89] to $MeP(CF_3)_2$ and $^iBuP(CF_3)_2$ from $(CF_3)_2PCl$ and $ZnMe_2/Al(^iBu)_3$ respectively, as well as $(CF_3)_nP(Et)_{3-n}$ (n = 1, 2) from $PbEt_4$ and the requisite chloro-phosphine (Scheme 1.10).

$$2\ (CF_3)_2PCl + ZnMe_2 \longrightarrow 2\ (CF_3)_2PMe + ZnCl_2$$

$$3\ (CF_3)_2PCl + Al^iBu_3 \longrightarrow 3\ (CF_3)_2P^iBu_3$$

$$(CF_3)_nP_{3-n} + PbEt_4 \longrightarrow (CF_3)_nPEt_{3-n} + PbCl_4$$
$$n = 1, 2$$
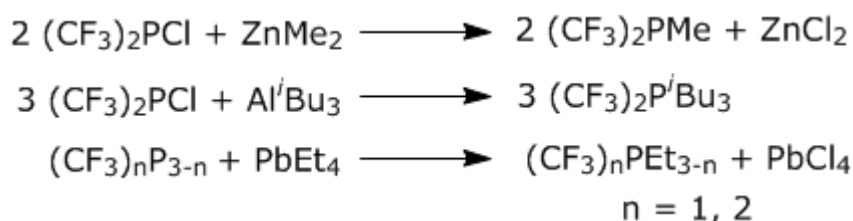
Scheme 1.10: Miscellaneous preparations of some fluoroalkyl phosphines.

Fields *et al*. showed that *bis*-(trifluoromethyl)phosphines react with olefins in the presence of UV radiation, yielding the corresponding tertiary phosphine $(CF_3)_2PR$ (R = Et, ^nPr, ^nBu, CHMeEt, CF_2CF_2H, $CFHCHF_2$, CH_2CHF_2 and $CH_2CH_2F)^{[90-92]}$ via a free-radical mechanism in which the most stable radical is formed when $(CF_3)_2P\cdot$ attacks the olefin.

The reaction of fluoroalkyl iodides with *tetrakis-*(trifluoromethyl)tetraphosphine was investigated by Lavrent'ev *et al.*[93] who reported that the formation of $CF_3P(^nC_3F_7)I$ and $CF_3P(^iC_3F_7)I$ is possible in this manner (with $^nC_3F_7I$ and $(CF_3)_2CFI$ respectively), but they could not reach any firm conclusions regarding the influence of the perfluoroalkyl iodide on the rate of reaction. Ganja *et al.*[94] showed that the reaction of $Hg(CF_3)_2$ and PI_3 at 160°C produces $P(CF_3)_3$ in approximately 60% yield, and that if excess PI_3 is used, then CF_3PI_2 can be isolated in 37% yield along with small ($\sim$ 8%) quantities of $(CF_3)_2PI$.

Semenii *et al.*[95] discovered that the electrochemical fluorination in anhydrous HF using Ni electrodes (Simon process) of *tris*-alkylphosphine oxides yielded the corresponding $(R_f)_3PF_2$ compounds (24-46% yields); this method also results in the production of OF_2, a toxic and explosive gas. This route was improved in the late 1990s by Ignat'ev and Sartori,[96] who used *tris*-alkylphosphines as the starting materials, which resulted in yields of 49-74%, and avoided the production of OF_2. However, neither of these reports include details of the subsequent reduction to the phosphorus(III) species.

Lagow and co-workers[97] reported an alternative route to *tris*-substituted perfluoroalkyl phosphines, via solution-phase direct elemental fluorination of trialkyl phosphines in Freon at -60°C, followed by reduction of the resulting phosphorus(V) species with *tris*-(trimethylsilyl)phosphine, yielding $P(C_nF_{2n+1})_3$ (n = 2-6) (Scheme 1.11). This method was also shown to be applicable to unsymmetrical phosphines, $(C_2F_5)_2P(^nC_4F_9)$ (from $Et_2P(^nBu)$) and the bridged diphosphine $(C_2F_5)_2PCF_2CF_2P(C_2F_5)_2$ (from $Et_2PCH_2CH_2PEt_2$).

$$P(C_nH_{2n+1})_3 \xrightarrow[\substack{2.\ P(SiMe_3)_3 \\ n = 2\text{-}6}]{1.\ F_2,\ Freon,\ -60°C} P(C_nF_{2n+1})_3$$
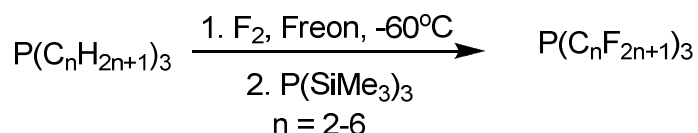
Scheme 1.11: Representation of direct fluorination of alkyl phosphines.

More recently, the Roddick group reported that the synthesis of $(C_2F_5)_2PCH_2CH_2P(C_2F_5)_2$ could be achieved by perfluoroalkylating $Cl_2PCH_2CH_2PCl_2$ with C_2F_5Li at -95°C, formed from C_2F_5X (X = Cl, I) and BuLi (Scheme 1.12).[98] Subsequently the same group reported the synthesis of $RP(C_2F_5)_2$ (R = Me, ^tBu, Ph, NEt$_2$),[99] $P(C_2F_5)_3$,[99] $Ph_2P(C_2F_5)$[100] and 1,3-$C_6H_4(CH_2P(C_2F_5)_2)_2$.[101] The majority of these ligands have been shown to coordinate to a variety of metal centres (see later).

$$C_2F_5X + {^n}BuLi \xrightarrow{-95°C} C_2F_5Li + {^n}BuH$$
$$X = Cl,\ I$$
$$\Big\downarrow 0.25\ Cl_2PCH_2CH_2PCl_2$$
$$0.25\ (C_2F_5)_2PCH_2CH_2P(C_2F_5)_2 + LiCl$$
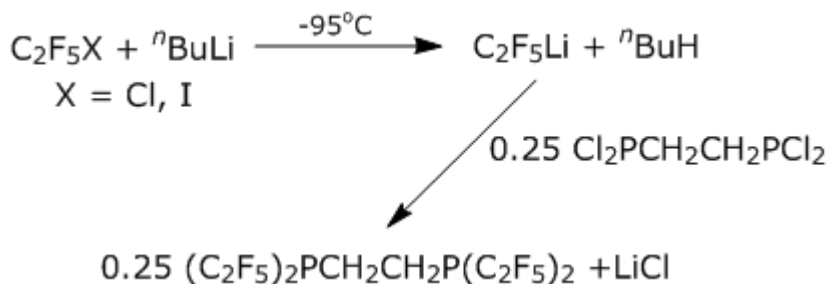
Scheme 1.12: Formation of C$_2$F$_5$Li, and reaction with Cl$_2$PCH$_2$CH$_2$PCl$_2$.

Fild *et al.* reported the synthesis of R_2PCF_2Br (R = Ph, ^tBu, Me) from R_2PSiMe_3 and CF_2Br_2 in chloroform at -20°C.[102] They also found that the reaction of $RP(SiMe_3)_2$ with CF_2Br_2 gives the diphosphetane $(CF_2PR)_2$. However, no experimental detail or yields are reported (see Scheme 1.13).

$$Ph_2PSiMe_3 + CF_2Br_2 \xrightarrow[-20°C]{CHCl_3} Ph_2PCF_2Br + Me_3SiBr$$
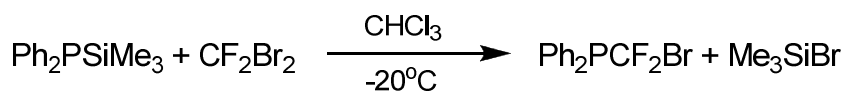
Scheme 1.13: Formation of Ph$_2$PCF$_2$Br from Ph$_2$PSiMe$_3$ and CF$_2$Br$_2$.

Pringle and co-workers[103] extended this by coupling Ph_2PCF_2Br with Ph_2PSiMe_3 in the presence of $[NiCl_2(dippf)]$ (dippf = *bis-diisopropylphosphinoferrocene*) to form $R_2PCF_2PR_2$ (R = Ph, ^iPr, CH_2CH_2CN).

The reaction of Ph_2P^- with R_fI compounds has been shown to produce Ph_2PR_f ($R_f = {}^nC_4F_9$, $^nC_6F_{13}$) compounds in fairly good yields in liquid NH_3, HMPA, DMPU, or tetraglyme by Vaillard *et al.*,[104] although they deliberately isolated the phosphine oxides. These reactions generally worked better when irradiated with ultra-violet light, suggesting a free-radical mechanism. Rossi and co-workers[105] also showed that the palladium catalysed cross-coupling reactions of perfluoroalkyl iodides and organoheteroatom stannanes could be used to generate perfluoroalkyl-substituted phosphines, Ph_2PR_f, ($R_f = {}^nC_4F_9$, $^nC_8F_{17}$) though once again they were isolated as their corresponding oxides.

Michalski and co-workers reported that it was possible to introduce CF_3 groups onto a phosphorus centre via the nucleophilic trifluoromethylation of the corresponding PF compound.[106] They generated the fluorophosphine from the reaction of a phosphonite with a fluoride source, and then subsequently added Ruppert's reagent and another fluoride source (e.g. CsF) to synthesise the desired trifluoromethyl phosphine (Scheme 1.14).

$$R_2PF + Me_3SiCF_3 \xrightarrow{F^-} R_2PCF_3 + Me_3SiF$$

$$R_2 = -SCH_2CH_2S-$$
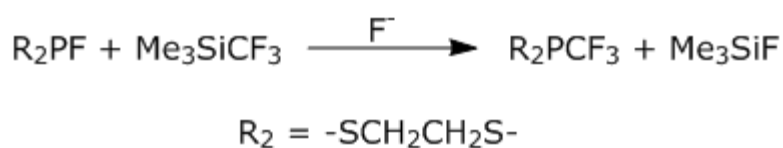
Scheme 1.14: Michalski's synthesis of trifluoromethyl-containing phosphines.

They also established that this procedure could be performed in a "one-pot fashion".[106] This method was subsequently expanded upon and the reaction of $P(OPh)_3$, $Ph_2P(OPh)$, $PhP(OPh)_2$ and $(PhO)_2PCH_2CH_2P(OPh)_2$ with

perfluoroalkyltrimethylsilanes in the presence of a source of fluoride results in the formation of $P(R_f)_3$ ($R_f = CF_3$, C_2F_5, $^nC_3F_7$ and $^nC_4F_9$), Ph_2PR_f, $PhP(R_f)_2$ and $(R_f)_2PCH_2CH_2P(R_f)_2$ ($R_f = CF_3$, C_2F_5) and Me_3SiOPh (Scheme 1.15).[107] As the length of the R_f chain increases, the rate of reaction and yield decreases (e.g. $CF_3 = 98\%$, $^nC_3F_7 = 35\%$). Roddick and co-workers have also utilised this method, to synthesise $1,3-((C_2F_5)PCH_2)_2C_6H_4$. This route, whilst appearing to be quite generic, is hindered by the lack of availability of Ruppert reagent analogues.[101] Me_3SiCF_3 is commercially available, whilst the C_2F_5 and $^nC_3F_7$ analogues are available as special request syntheses; the remainder require specialist methods of preparation, or are unknown compounds.

$$P(OPh)_3 + Me_3SiR_f \xrightarrow{\text{CsF}} P(R_f)_3 + Me_3SiOPh$$

$$R_f = CF_3, \; C_2F_5, \; ^nC_3F_7, \; ^nC_4F_9$$
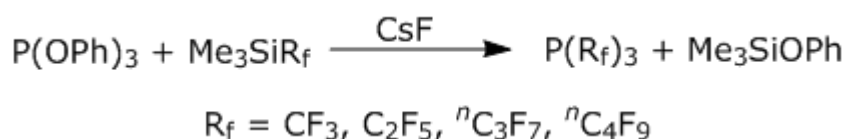
Scheme 1.15: Reaction of fluoroalkyl-silyl reagents and phosphites.

Recently, Togni and co-workers reported that trifluoromethylating primary and secondary phosphines could be achieved with hypervalent iodine(III)-CF_3 compounds (Scheme 1.16).[108] They have produced a number of CF_3PR_2 (R = Cy, Ph, o-Tol, p-Tol, β-Np, p-OMePh) and CF_3PHR (R = Cy, Ph) compounds. They also found that this reaction proceeds if the secondary phosphine is replaced with Ph_2PSiMe_3 with similar yields. The iodine(III)-CF_3 compound(s) are derived from Me_3SiCF_3 and iodobenzoic acid derivatives (see Scheme 1.16), thus this route currently is hampered in a similar manner to that reported by Murphy-Jolley et al.[107]
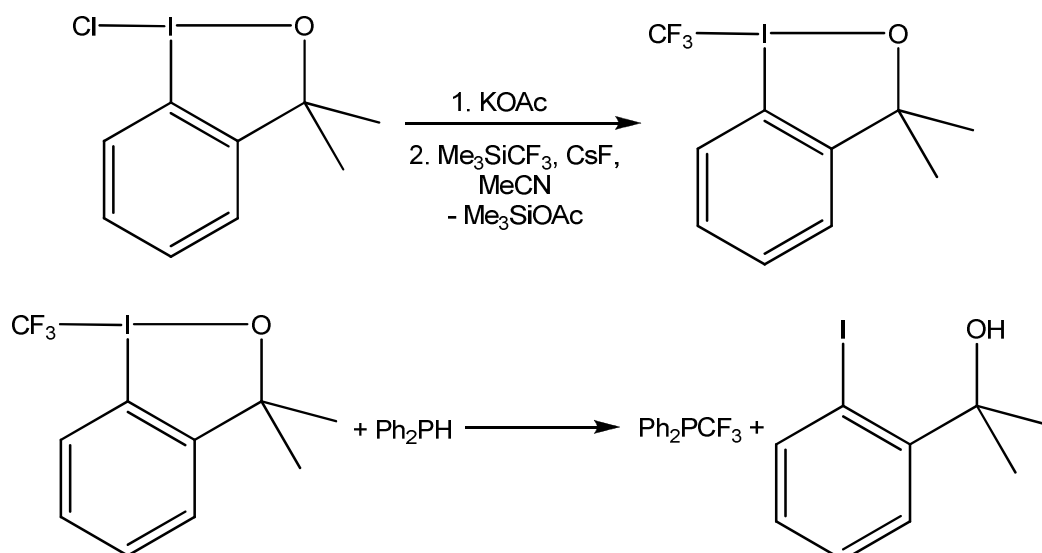
Scheme 1.16: Formation of trifluoromethyl-containing phosphines from secondary phosphines and hypervalent iodine(III) reagents.

In summary, a number of specialist routes exist that allow the synthesis of fluoroalkyl containing phosphines, principally those containing CF_3 groups. The methods with the most widely available starting materials require specialist equipment and/or hazardous chemicals. Those which are simplest to perform are hampered by a lack of available starting materials.

A summary of the known perfluoroalkyl-phosphines and the methods of preparation is given in Table 1.3.

Table 1.3: Fluoroalkyl Phosphines.

R_f	R_2PR_f	$RP(R_f)_2$	$P(R_f)_3$	Bridged Phosphines	Polyphosphines
CF_3	**R_2PCF_3** R = Me **m**,[68] H **n**,[74] Ph **c**[107] **e**[108] **j**,[81] F **p**,[67] Cl **p**,[57] I **a**,[54] ^nBu **b**[88] **q**,[84] Me_2N **q**,[84] Et_2N **q**,[84] $^nPr_2N$ **q**,[84] C_5H_5N **q**,[84] C_4H_4N **q**,[84] C_3F_7 **b**,[88] Et **t**,[89] Cy **e**,[108] o-Tol **e**,[108] p-Tol **e**,[108] Np **e**,[108] p-OMePh **e**[108] **$RR'P(CF_3)$** R = H, R' = Ph **e**,[108] Cy **e**,[108] R = I, R' = Ph **j**,[80] C_3F_7 **j**,[93] $^iC_3F_7$ **j**,[93] R = F, R' = Me_2N **q**[84]	**$RP(CF_3)_2$** R = H **n**,[74] Me **b**[88] **t**,[89] Ph **b**[88] **c**[107] **j**,[80] Cl **p**,[57] I **a**,[54] F **p**,[66] C_3F_7 **b**∗[88] Et **t**,[89] ^nBu **b**,[88] ^iBu **b**[88] **t**,[89] Me_2N **q**,[84] CHMeEt **k**,[90] CF_2CF_2H **k**,[90] $CFHCHF_2$ **k**,[90] CH_2CHF_2 **k**,[90] CH_2CH_2F **k**[90]	**$P(CF_3)_3$** **a**[54] **c**[107] **d**[79]	**$(CF_3)_2P(CH_2)_nP(CF_3)_2$,** n = 1 **t**,[76] 2 **c**[107] **d**,[77] 3 **t**[76] **$(CF_3)_2PCF_2CF_2P(CF_3)_2$, s**[75] **$(CF_3)_2PCH=CHP(CF_3)_2$, s**[75] **$(CF_3)_2PCRR'P(CF_3)_2$,** (R = R'= H, CH_3, R = H, R' = CH_3), **t**[76] **$(CH_3)_2PCH_2CH_2P(CF_3)_2$ d**[77] **$1,3$-$C_6H_4(CH_2P(CF_3)_2)_2$, g**[101]	**$(CF_3P)_4$, u**[71] **$(CF_3P)_5$, u**[71] **$(CF_3)_2PP(CF_3)_2$, u**[57] **$H_2(CF_3P)_3$, u**[71]
C_2F_5	**$R_2PC_2F_5$** R = I **a**,[60] Ph **g**[100] **j**[83]	**$RP(C_2F_5)_2$** R = $^nC_4F_9$ **g**,[99] Me **g**,[99] ^tBu **g**,[99] Ph **g**,[99] NEt_2 **g**[99]	**$P(C_2F_5)_3$** **c**[107] **f**[97] **g**[99]	**$(C_2F_5)_2PCF_2CF_2P(C_2F_5)_2$, f**[97] **$(C_2F_5)_2PCH_2CH_2P(C_2F_5)_2$, g**[98] **$1,3$-$C_6H_4(CH_2P(C_2F_5)_2)_2$, g**[101]	**$(C_2F_5P)_3$, u**[86] **$(C_2F_5P)_4$, u**[86]
$^nC_3F_7$	**$R_2P(^nC_3F_7)$** R = I **a**[58] Et **b**[88] Ph **b**[88], CF_3 **b**∗[88] **$RR'P(^nC_3F_7)$** R = I, R' = CF_3 **j**[93]	**$RP(^nC_3F_7)_2$** R = ^nBu **b**[88] Ph **b**[88] CF_3 **b**∗[88] Cl **p**[58] I **a**[58]	**$P(^nC_3F_7)_3$** **c**[107], **f**[97]		**$(^nC_3F_7P)_4$, u**[72] **$(^nC_3F_7P)_5$, u**[72]
$^iC_3F_7$	**$R_2P(^iC_3F_7)$** R = I **a**,[60] Me_2N **r**[86] **$RR'P(^iC_3F_7)$** R = I, R' = CF_3 **j**[93]	**$RP(^iC_3F_7)_2$** R = I **a**[60]			
$^nC_4F_9$	**$R_2P(^nC_4F_9)$** R = C_2F_5 **f**[97] Ph **h**[104]		**$P(^nC_4F_9)_3$** **c**[107] **f**[97]		
$^nC_5F_{11}$			**$P(^nC_5F_{11})_3$** **f**[97]		
$^nC_6F_{13}$	**$Ph_2P(^nC_6F_{13})$** **h**[104]		**$P(^nC_6F_{13})_3$** **c**[107] **f**[97]		

a synthesized in autoclave from phosphorus (any allotrope) and R_fI at ~200°C; **b** synthesized from chlorophosphine and RLi (∗ denotes from mixture of R_fI, Li, and chlorophosphine); **c** synthesized from phosphite and Rupperts' reagent (or analogue); **d** Synthesized from $CF_3Br/P(NEt_2)_3$/chlorophosphine; **e** synthesized from primary/secondary phosphine and iodine(III) reagent; **f** synthesized via direct fluorination; **g** synthesized from C_2F_5Li and chlorophosphine; **h** synthesized via PPh_2^-, and UV light; **j** from polyphosphine and R_fI; **k** reaction of $(CF_3)_2P\cdot$ with olefins under UV radiation; **m** CF_3 substituted phosphine and MeI; **n** reaction of phosphine with Hg and HI; **p** reaction of iodophosphine and SbX_3 (X = Cl, F)/$HgCl_2/AgCl$; **q** reaction of halophosphine with R_2NH; **r** Reaction of R_fI with $P(NEt_2)_3$; **s** Pyrolysis of secondary phosphine with olefin; **t** From $(R_f)_2PP(R_f)_2$ and di-iodoalkanes; **u** Other – see text

1.6 Perfluoroalkenyl Phosphines

The first report of a perfluoroalkenyl compound to appear in the literature was in the mid 1950s, $CF_2=CFI$.[109] Treatment of $CF_2=CFI$ with magnesium at 0°C gave poor yields of the corresponding Grignard reagent (~20%). This yield was later improved by Knunyants[110-112] who utilised lower temperatures and obtained ~70% yield. $CF_2=CFBr$ was also shown to be a suitable precursor for generating the Grignard reagent,[113] and $CF_2=CFMgX$ (X = Br, I) generated in this manner were used to prepare some early perfluorovinyl-containing compounds, *e.g.* $Si(CF=CF_2)_4$,[111] (Scheme 1.17) and $Hg(CF=CF_2)_2$.[109]

$$CF_2=CFX + Mg \xrightarrow{0^oC} CF_2=CFMgX \xrightarrow{1/4\ SiCl_4} Si(CF=CF_2)_4 + 4\ MgClX$$
$$X = Br,\ I$$
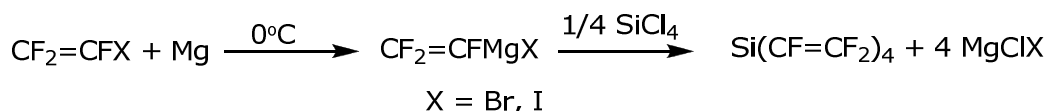
Scheme 1.17: Early perfluorovinyl organometallic compound synthesis.

The synthesis of perfluorovinyl lithium was first reported in 1962 by Seyferth via the transmetallation of triphenyl(perfluorovinyl)stannane with phenyl lithium at low temperature with a maximum yield of ~65% (Scheme 1.18).[110]

$$Ph_3Sn(CF=CF_2) + PhLi \longrightarrow CF_2=CFLi + SnPh_4$$
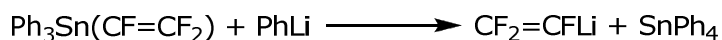
Scheme 1.18: Transmetallation of triphenyl(perfluorovinyl)stannane.

Subsequently, it was shown by Tarrant that perfluorovinyl lithium could be prepared from the reaction of $CF_2=CFX$ (X = Br, H) and alkyl lithium reagents at low temperature (Scheme 1.19).[111]

$$CF_2=CFX + RLi \xrightarrow[\substack{X = Br, H \\ R = Me, Bu}]{-78^0C} CF_2=CFLi + RX$$
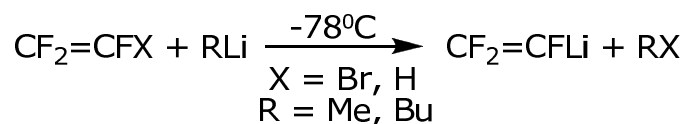
Scheme 1.19: Generation of $CF_2=CFLi$ from $CF_2=CFX$ and alkyl lithium reagents.

Perfluorovinyl lithium is much less stable than vinyl lithium, and it has been the subject of several studies.[110,111] Tarrant found that perfluorovinyl lithium was stable for several hours in diethyl ether at -78°C, and that it was more stable in pentanes than in diethyl ether. The concentration of perfluorovinyl lithium was also found to affect the rate of decomposition,[111] meaning that the decomposition must occur via an intermolecular pathway.

1.6.1 Synthesis of Perfluorovinyl Phosphines

The first report of a perfluorovinyl-containing phosphine was published in 1959 by Sterlin *et al.*,[112] who showed that $CF_2=CFMgI$ reacted with $(Et_2N)_nPCl_{3-n}$ (n = 0, 1, 2) in the appropriate stoichiometry to yield the corresponding perfluorovinyl phosphine (Scheme 1.20).

$$CF_2=CFMgI + PR_{3-n}Cl_n \longrightarrow P(NEt_2)_{3-n}(CF=CF_2)_n + MgICl$$
$$n = 1-3$$
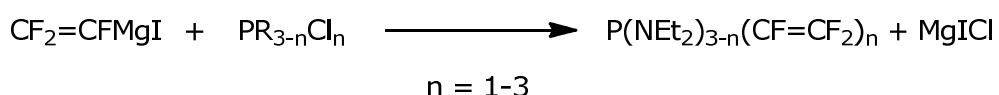
Scheme 1.20: Sterlin's synthesis of the first perfluorovinyl phosphines.

Treatment of $(CF=CF_2)_nP(NEt_2)_{3-n}$ (n = 1, 2) with dry HCl affords the corresponding chloro-perfluorovinyl phosphines,[112] (Scheme 1.21) and subsequent halogen exchange with SbF_3 gives the analogous fluorophosphines.[112]

$$(CF_2=CF)P(NEt_2)_2 \xrightarrow{HCl} (CF_2=CF)PCl_2$$
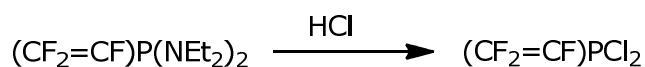
Scheme 1.21: Synthesis of chloroperfluorovinyl phosphines.

In 1969 Cowley and Taylor attempted the synthesis of some of the above compounds, using perfluorovinyl lithium instead of the Grignard reagent but reported that the reaction does not proceed.[113] However, a decade later, Horn *et al*. reported that this synthetic method does work, and they described the preparation of $Ph_nP(CF=CF_2)_{3-n}$ (n = 0-2), although the isolated yields were poor (in some cases, less than 2%).[114] This is probably due to the thermal instability of perfluorovinyl lithium, which decomposes at temperatures of ~ -50°C and above, yielding LiF and a viscous brown oil, which was shown to contain a greater than expected proportion of hydrogen and carbon-carbon double bonds.[111]

By the end of the 1980s, just a handful of perfluorovinyl phosphines had been reported, including $R_nP(CF=CF_2)_{3-n}$ (n = 0-2, R = Ph, NEt_2, NMe_2, Cl, F). This may be accounted for by the fact that the precursors ($CF_2=CFX$, X = Cl, Br, I) were difficult to acquire from commercial sources due to their potentially deleterious effect on the ozone layer.

Interest in perfluorovinyl containing compounds was revitalised in the 1990s following the discovery by Burdon *et al*.[115] that perfluorovinyl lithium could be generated from the recently commercialised CFC-replacement HFC-134a (CH_2FCF_3) and two equivalents of ^nBuLi in diethyl ether at -78°C (Scheme 1.22).
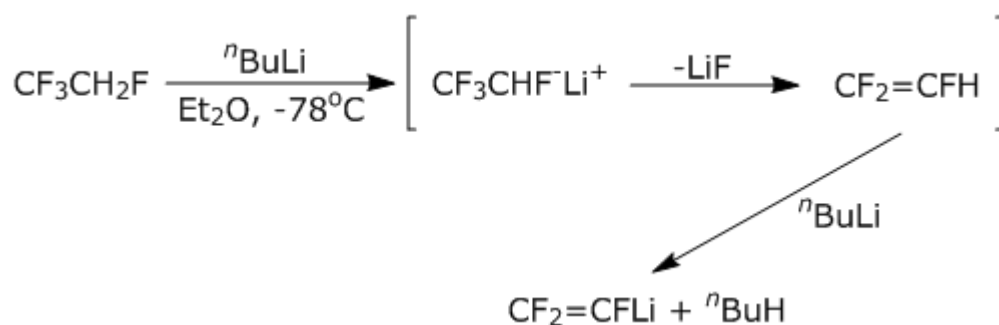
Scheme 1.22: Generation of $CF_2=CFLi$ from HFC-134a.

Perfluorovinyl lithium generated in this manner can then be reacted *in situ* with a wide variety of electrophiles, and its use in organic synthesis was the subject of a review by Coe in 1999.[116] This one-pot procedure was utilised by Banger *et al*.[117,118] to synthesise perfluorovinyl-containing organometallic compounds, and its application in this area was reviewed by Banger and Brisdon in 1999.[119] Banger *et al*.[36] also reported the synthesis of perfluorovinyl phosphines via this route, vastly improving on the yields obtained by Sterlin,[120] Cowley,[113] and Horn.[114] They reported the production of $R_nP(CF=CF_2)_{3-n}$ (n = 0-2, R = Ph), and $Cl_nP(CF=CF_2)_{3-n}$ (n = 1, 2), as well as the structure of $PhP(CF=CF_2)_2$ (determined via low-temperature X-ray crystallography). The same route has been extended to synthesise $R_2P(CF=CF_2)$ (R = Et, ^iPr, Cy).[121] Typically, perfluorovinyl phosphines are non-malodorous, air and moisture stable liquids that are soluble in most organic solvents.

1.6.2 Derivatisation of Perfluorovinyl Phosphines

Perfluorovinyl phosphines can exhibit more than one type of reactivity. There is a lone pair on the phosphorus atom, allowing them to react with electrophiles, and they should therefore be susceptible to quaternisation. However the perfluorovinyl moiety exhibits a negative inductive effect, which diminishes the availability of the lone pair, which in turn decreases or even prevents reactions such as quaternisation from taking place. Barnes *et al*.[121] have investigated the reactivity of some perfluorovinyl phosphines with the group 16 elements (O, S, Se). They found that *mono*-perfluorovinyl substituted phosphines reacted smoothly with aqueous H_2O_2 at 0°C (Scheme 1.23), whereas the reaction with elemental sulfur/selenium required several hours refluxing in toluene to go to completion. However, they were unable to completely convert $PhP(CF=CF_2)_2$ into the corresponding oxide, even after prolonged heating with H_2O_2.[121]

$$R_2P(CF=CF_2) + H_2O_2 \xrightarrow{\text{H}_2\text{O, 0}^{\circ}\text{C}} R_2P(O)CF=CF_2 + H_2O$$

$$R = Et, {}^{i}Pr, Cy, Ph$$
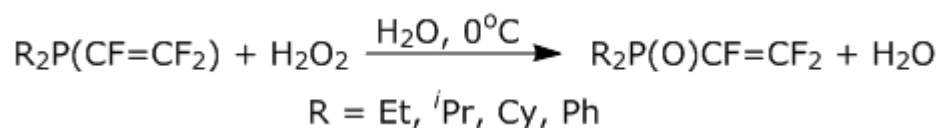
Scheme 1.23: Oxidation of perfluorovinyl phosphines.

However the oxide of the *bis*-substituted phosphine can be obtained in a two stage reaction. The perfluorovinyl phosphines react with XeF_2 to give the phosphorus(V) species $F_2PR_2(CF=CF_2)$ or $F_2PR(CF=CF_2)_2$. These compounds are extremely moisture sensitive, affording $O=PR_2(CF=CF_2)$ and $O=PR(CF=CF_2)_2$ respectively (Scheme 1.24) on exposure to moisture.[121]

$$R_2P(CF=CF_2) + XeF_2 \xrightarrow[-Xe]{} F_2PR_2(CF=CF_2) \xrightarrow{\text{H}_2\text{O}} R_2P(O)CF=CF_2 + 2HF$$

$$R = Et, {}^{i}Pr, Cy, Ph$$
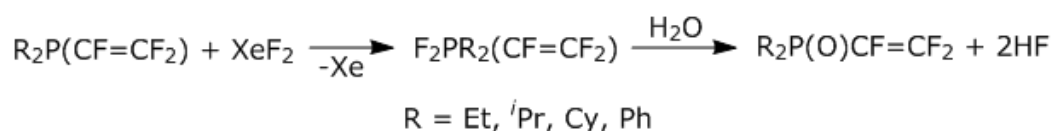
Scheme 1.24: Oxidation of perfluorovinyl phosphines by XeF_2.

The perfluorovinyl moiety can also react as an electrophile, but its reactivity will be diminished relative to perprotio vinyl groups, due to the presence of three electronegative fluorine atoms. This reactivity has been explored by Cowley,[113] and Barnes.[121] Both found that the addition of X_2 (X = Cl, Br, I)[113,121] or SO_2Cl_2[121] gave mixtures of products, due to the competition between addition across the double bond and oxidation of the phosphorus centre.

The presence of two fluorine atoms on the β-carbon means that the C_β-F bonds will have a greater ionic character than the C_α-F bond – therefore they should be more susceptible to nucleophilic attack. This hypothesis is also supported by steric arguments, and due to the size of PR_2 relative to F, suggests than any substitution should occur *trans* to the PR_2 group preferentially. Horn and Kolkmann[122] have reported the reaction of $P(CF=CF_2)_3$ with organolithium reagents, resulting in the formation of

43

P(CF=CFR)$_3$ though in all cases the yields were poor. Horn proposed that an excess of CF$_2$=CFLi resulted in a second addition of a –CF=CF$_2$ unit to generate –CF=CFCF=CF$_2$ systems. Barnes *et al.*[121] have reported the reaction of some perfluorovinyl phosphines with ^{n}BuLi and LiAlH$_4$/LiAlH(O^{t}Bu)$_3$, resulting in R$_2$P(CF=CF^{n}Bu) and R$_2$P(CF=CFH) respectively.

It is also possible that perfluorovinyl phosphines may be susceptible to nucleophilic attack at the phosphorus centre (known for aryl phosphines)[123] despite their apparent stability.

1.7 Perfluoroalkynyl Phosphines

The simplest fluoroalkynyl compound that can be prepared is *mono*-fluoroacetylene. This compound was first prepared in 1959 by Middleton and Sharkey,[124] by the pyrolysis of fluoromaleic anhydride at 650°C and 5-7 mmHg. This method produced essentially quantitative yields of *mono*-fluoroactylene, which is a colourless gas that freezes to a white solid at −196°C, and melts to a mobile liquid that boils just below −80°C. They also report that liquid samples can detonate with reasonable force, and describe the compound as being "treacherously explosive".[124] The obvious difficulties and risk associated in preparing and handling such a compound perhaps explains why there are no reports of *mono*-fluoroethynyl phosphines in the literature.

In contrast to the instability of *mono*-fluoroacetylene, trifluoromethylacetylene is much safer to handle. This was first prepared in the 1950s by Haszeldine[54,125] who irradiated CF$_3$I and acetylene with UV light or by heating the compounds together at 220°C, followed by dehydroiodination of the resulting 1-iodo-3,3,3-trifluoropropene with KOH. Haszeldine also reports the preparation of the Cu, Ag, and Hg

trifluoropropynyl (tfp) compounds.[54,125] Henne and Nager[126] also proposed several routes to trifluoropropyne at the same time, but did not recommend any of them. An alternative method for producing trifluoropropyne was reported by Finnegan and Norris,[127] who treated 1,1,2-trichloro-3,3,3-trifluoropropyne with Zn in DMF or *N,N*-diacetylamide to give the zinc acteylide complex which were then hydrolysed, allowing 3,3,3-trifluoropropyne to be collected in a cold trap in ~75% yield.

The tfp Grignard reagent was synthesised by Henne and Nager[128] shortly after Haszeldine's initial report. They prepared it via transmetallation of EtMgBr (Scheme 1.25).
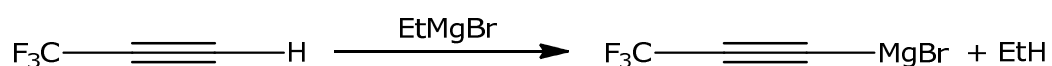
Scheme 1.25: Trifluoropropynyl Grignard/lithium generation.

The first report of Li(tfp) was by Tarrant in 1968,[129] who reacted 3,3,3-trifluoropropyne with ^{n}BuLi at -78°C, then subsequently added an electrophile (Et$_3$SiCl), whereupon Et$_3$Si(tfp) was generated (Scheme 1.26).
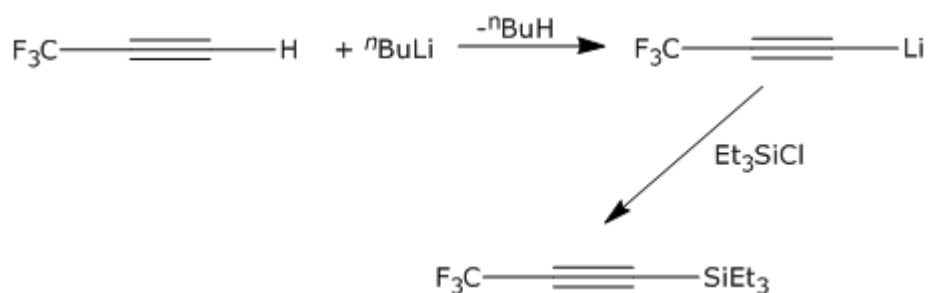
Scheme 1.26: Typical formation of main-group tfp compounds.

The major difficulty in handling 3,3,3-trifluoropropyne is that it is a very volatile gas with a boiling point of -48°C.[126,130] It is also relatively expensive.

As such there has been a search for an alternative method of introducing tfp moieties into compounds, or for generating Li(tfp). In 1996 Katritzky *et al*. reported that the generation of Li(tfp) was possible from 2-bromo-3,3,3-trifluoropropene and two equivalents of LDA in THF at -78°C (Scheme 1.27).[131]
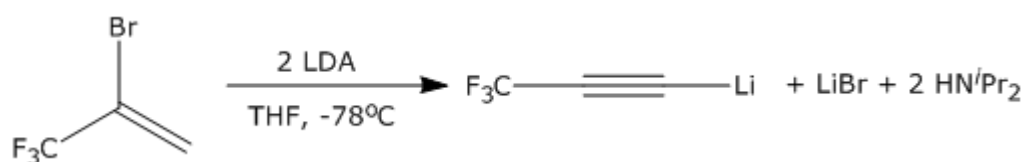
Scheme 1.27: 2-Bromo-1,1,1-trifluoroprop-3-ene as a precursor for the generation of Li(tfp).

More recently Brisdon and Crossley[132] reported that Li(tfp) could be generated via the slow addition of three equivalents of ^{n}BuLi to 1,1,1,3,3-pentafluoropropane (HFC-245fa) at -15°C (see Scheme 1.28).
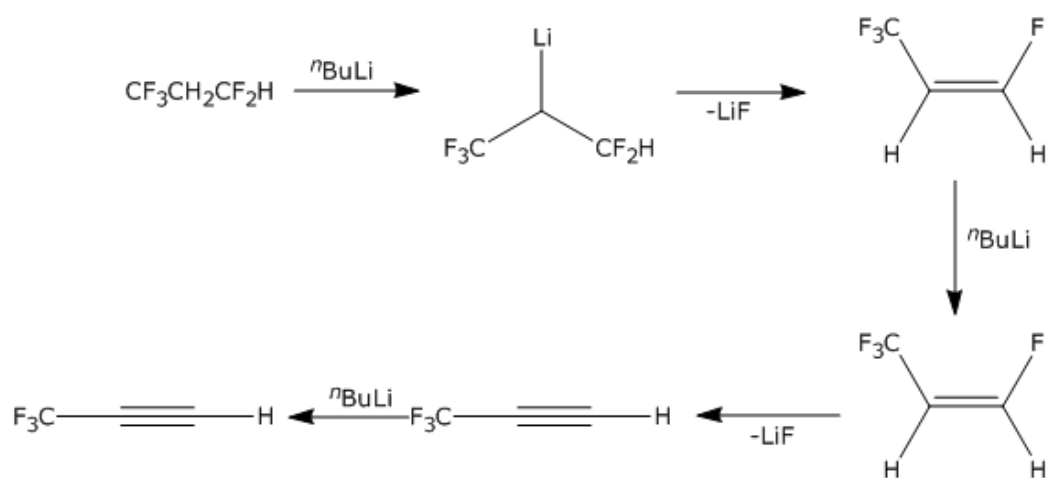
Scheme 1.28: Proposed mechanism of formation of Li(tfp) from HFC-245fa.

FC-245fa has a lower boiling point than 2-bromo-3,3,3-trifluoroprop-1-ene (15°C vs 33°C) but its greater commercial ability (it is available as a blowing agent) and easier removal of side products (butane vs diisopropylamine) makes it synthetically more useful.

A further method for the generation of Li(tfp) was published in 2007 by Shimuzu *et al.*[133] Treatment of the commercially available 1,1,1-trifluoro-3,3-dichloroacetone with tosyl chloride and triethylamine in DCM afforded the enol tosylate, which was isolated and then treated with two equivalents of ^{n}BuLi in THF at -78°C to afford Li(tfp) (Scheme 1.29). The major drawback of this route is that it is a two step reaction, though the lower volatility of the reagents is advantageous.
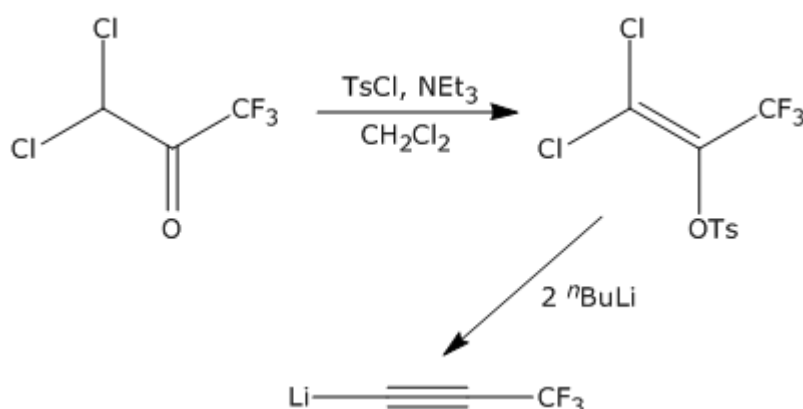
Scheme 1.29: Preparation of Li(tfp) from 1,1-dichloro-3,3,3-trifluoroacetone.

Despite the existence of a number of synthetic routes to Li(tfp), the only tfp-containing phosphorus(III) compounds that have been reported in the literature are $Ph_2P(tfp)$,[134] $PhP(tfp)_2$[135] and $P(tfp)_3$.[135,136] Banger *et al.*[137] have also shown that $^iPr_2P(tfp)$ can be formed from Li(tfp) and $^iPr_2PCl$. However, a greater range of P(V) species of the type $(RO)_2P(O)(C{\equiv}C\text{-}R_f)$ (R = Me, Et, ^iPr, Ph; R_f = CF_3, C_2F_5, $^nC_3F_7$, CF_2Cl and CF_2H) have been prepared and their applications and conversions, for example to fluoroalkylated vinylphosphonates, have been studied.[138-140]

1.7.1 Derivatisation of Perfluoroalkynyl Phosphines

The reactivity of the tfp group has been investigated by the Brisdon group.[137,141,142] Some group 14 tfp compounds ($R_3E(tfp)$, R = Et, Bu, Ph, E = C – Pb) have been reacted with RLi reagents (R = ^nBu, ^tBu, Ph).[142] When R =

^{n}Bu or Ph addition across the triple bond occurs, resulting in alkenic species with the *E* isomer formed predominantly. The *E* isomer is also formed as the major product during the reaction with R = ^{t}Bu at low (-60°C) temperature. However, when the tfp compound is added to a refluxing solution of ^{t}BuLi in THF, a remarkable cyclisation occurs, resulting in the formation of *gem*-difluorocyclopropenyl (dfcp) compounds (Scheme 1.30).
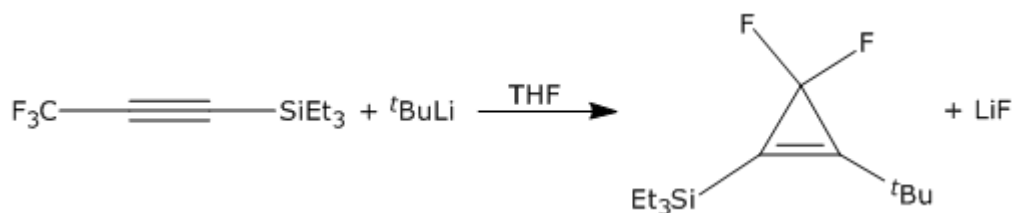
Scheme 1.30: Formation of *gem*-dfcp compounds.

The reactivity of ^{i}Pr$_2$P(tfp) under these conditions has also been explored,[137,141] with similar results. At higher temperatures the cyclisation is favoured, resulting in the dfcp compound as the major product.

The oxidation of ^{i}Pr$_2$P(tfp) with XeF$_2$ yields the expected P(V) species, F$_2$P^{i}Pr$_2$(tfp), cleanly.[141] The reaction of ^{i}Pr$_2$P(tfp) with H$_2$O$_2$ results in the formation of the corresponding phosphine oxide according to NMR spectroscopic studies, however, the same reaction with ^{i}PrP(tfp)$_2$ does not proceed cleanly resulting in a mixture of products.[141] Reaction of PhP(tfp)$_2$ with H$_2$O$_2$ results not only in the oxidation of the phosphorus centre but also nucleophilic substitution of a tfp group, resulting in PhP(O)(OH)(tfp), as shown by single crystal X-ray diffraction studies.[141]

1.8 Coordination Chemistry of Fluorinated Phosphines

1.8.1 Complexes of Fluoroalkyl Phosphines

The coordination chemistry of perfluoroalkyl phosphines has received far less attention than their non-fluorinated analogues; this is due to the paucity of synthetic routes to these ligands. The first transition metal complex of a perfluoroalkyl phosphine was reported independently in 1958 by Emeleus and Smith[55] and Burg and Mahler.[143] Emeleus and Smith showed that the reaction of an excess of $P(CF_3)_3$ with $[Ni(CO)_4]$ at room temperature gave a mixture of $[Ni(CO)_3P(CF_3)_3]$ and $[Ni(CO)_2\{P(CF_3)_3\}_2]$ (Scheme 1.31).[55] Both of these compounds are clear liquids which turn red on exposure to light, and are spontaneously flammable in air.

$$[Ni(CO)_4] + P(CF_3)_3 \longrightarrow [Ni(CO)_3P(CF_3)_3] + [Ni(CO)_2\{P(CF_3)_3\}_2]$$

Scheme 1.31: Reaction of an excess of $P(CF_3)_3$ with $[Ni(CO)_4]$.

The IR stretching frequencies of the carbonyl groups have been recorded for $[Ni(CO)_3P(CF_3)_3]$, $[Ni(CO)_2\{P(CF_3)_3\}_2]$, $[Ni(CO)_3PF_3]$, and $[Ni(CO)_2\{PF_3\}_2]$, so as to compare the electronic properties of the phosphines, and these are summarised in Table 1.4.

Complex	ν(CO)/cm^{-1}
$[Ni(CO)_3P(CF_3)_3]$	2107, 2116[89]
$[Ni(CO)_2\{P(CF_3)_3\}_2]$	2088
$[Ni(CO)_3PF_3]$	2110
$[Ni(CO)_2(PF_3)_2]$	2094

Table 1.4: Comparison of ν(CO) in $[Ni(CO)_{4-n}(L)_n]$ (L = PF$_3$, P(CF$_3$)$_3$).[144]

These data suggest that PF_3 and $P(CF_3)_3$ are electronically similar. However, PF_3 can form the tetra-substituted nickel complex $[Ni(PF_3)_4]$, whereas $P(CF_3)_3$ can only form the *bis*-substituted complex. This is probably due to the

greater steric demand of $P(CF_3)_3$ relative to PF_3, rather than their electronic properties.[145]

Burg and Mahler formed $[(CO)_3NiP(CF_3)_2P(CF_3)_2Ni(CO)_3]$ via the reaction of $[Ni(CO)_4]$ and $P_2(CF_3)_4$. They also reported that upon reacting the cyclic phosphine $(CF_3P)_4$ with $[Ni(CO)_4]$, an oily mixture of products with an average composition of $[Ni_{3.77}(CO)_{4.45}P(CF_3)_4]$ was produced, suggesting a mixture of compounds of the type $[(CF_3P)_4Ni(CO)_3]_n$ (n = 1-3).[143] Kang and Burg later showed that it was possible to synthesise $[Ni(CO)_3PR(CF_3)_2]$ (R = Me, Et, ^iBu) and $[Ni(CO)_3PEt_2(CF_3)]$ in a similar manner.[89] They also compared carbonyl stretching frequencies of these complexes to ascertain the trend in the π-acceptor strength for the phosphines (Table 1.5).

PR_3	$v(CO)/cm^{-1}$
$MeP(CF_3)_2$	2105
$EtP(CF_3)_2$	2103
$Me_2P(CF_3)$	2081
PMe_3	2064

Table 1.5: $v(CO)$ of some $[Ni(CO)_3L]$ complexes (L = PR_3).

The complexes $[Co(NO)(CO)_{2-n}\{P(CF_3)_3\}_n]$ (n = 1, 2) were also synthesised by Burg et $al.$, although they state that it is more difficult to prepare these than the corresponding nickel carbonyl complexes.[146] Burg and Street synthesised the complex $[Ni(CO)_2\{\kappa^2-(CF_3)_2PCH_2CH_2P(CF_3)_2\}]$ by reacting $[Ni(CO)_4]$ with the chelating ligand $(CF_3)_2PCH_2CH_2P(CF_3)_2$ in refluxing benzene.[147] The heteroatom bridged diphosphines $(CF_3)_2PEP(CF_3)_2$ (E = O,[148] S,[148,149] N-R where R = H[150] or Me[148]) have been shown to form nickel carbonyl complexes, resulting in the formation of dimetallic systems.

Trifluoromethyl-containing phosphine-substituted carbonyl complexes of other metals have also been synthesised, including rhodium, manganese, iron, chromium, molybdenum and cobalt. Khokhryakov et al. formed compounds of the type $[Rh(CO)Cl\{PPh_{3-n}(CF_3)_n\}_2]$ (n = 1, 2), and

$[RhCl_3\{PPh_{3-n}(CF_3)_n\}_3]$ (n = 1, 2).[151] However the only other reports of rhodium complexes of fluoroalkyl-containing phosphines in the literature are theoretical studies, and as such will not be considered further here.

Dobbie[152] has shown that trifluoromethyl phosphines, $(CF_3)_2PX$ react with pentacarbonyl manganese hydride, $[HMn(CO)_5]$, to yield complexes of the type $[HMn(CO)_4\{P(CF_3)_2X\}]$ (where X = F, CH_3, CF_3). Dobbie reports that these complexes are a mixture of *cis-* and *trans-* isomers according to NMR spectroscopy. However, when X = Cl, Br or I, $[XMn(CO)_5]$ is the recovered product, along with $HP(CF_3)_2$.[152]

The *tris*-(trifluoromethyl)phosphine iron carbonyl complexes $[Fe(CO)_{5-n}\{P(CF_3)_3\}_n]$ (n = 1-3), can also be formed by allowing $[Fe(CO)_5]$ and $P(CF_3)_3$ to react under "carefully controlled conditions in direct sunlight".[153] Brookhart *et al.*[154] showed that $(C_2F_5)_2PCH_2CH_2P(C_2F_5)_2$ (dfepe) reacts with [(benzylideneacetone)Fe(CO)_3] resulting in the synthesis of [(dfepe)Fe(CO)_3], the ruthenium analogue of which has been reported by Roddick *et al.*[155] Subsequently CO can then be photo-substituted for THF, C_2H_4, $P(OCH_3)_3$, and butadiene, yielding low valent iron complexes of dfepe.

Roddick and co-workers have shown that dfepe can also form carbonyl complexes with molybdenum,[98] chromium,[98] tungsten[98] and cobalt.[156] The thermal substitution reaction of dfepe and $[M(CO)_6]$ (M = Mo, Cr, W) afforded the tetracarbonyl complexes [(dfepe)M(CO)_4], and they report that dfepe rivals fluorophosphines in π-acceptor strength based on comparisons of IR data.[98] The same group have also reported the synthesis of several $[M(CO)_5L]$ species (L = $PhP(C_2F_5)_2$, M = Mo, Cr, L = $(Et_2N)P(C_2F_5)_2$, $MeP(C_2F_5)_2$, M = Mo), however, they did not observe any coordination of the *tris*-substituted ligand $P(C_2F_5)_3$, or the bulkier derivative $^tBuP(C_2F_5)_2$.[99] The cobalt complex, $[(dfepe)(CO)_2Co(H)]$ was prepared via the reaction of dfepe

with the $[(CO)_4Co]^-$ anion followed by acidification with $HBF_4.(Me_2O)$. The compound is an oil which decomposes after several hours. The $v(CO)$ bands of this complex are observed at higher energy than the analogous PPh_3 containing complex,[156] as expected based on the electronic properties of the two ligands.

Beg and Clark[157] synthesised $[PtCl_2\{PMe_2(CF_3)\}_2]$ and $[PtCl_2\{PMe(CF_3)_2\}_2]$ via the direct reaction of $PtCl_2$ and the phosphine in a sealed tube at room temperature (Scheme 1.32). The former was assigned as the *cis*-isomer, on the basis of the compound having a large dipole moment, whereas the latter has a dipole moment of zero, and therefore is the *trans* isomer. A similar reaction with $P(CF_3)_3$ in methanol was problematic, the solution acquired a yellow colour and some crystals appeared to form, but all attempts to isolate the material failed. Khokhyrakov *et al.*[158] passed gaseous $P(CF_3)_3$ through a methanolic solution of $Na_2[PtCl_4]$, resulting in a brown coloured compound, reported as "$[Pt\{P(CF_3)_3\}(P(CF_3)_2O)Cl_2]$"; subsequent work-up with pyridine was reported to afford $[Pt(P(CF_3)O)_2Py_2]$, which they state shows that $P(CF_3)_3$ does coordinate to platinum but the resulting complex is very readily hydrolysed by trace amounts of water.

$$[PtCl_2] + 2\ Me_nP(CF_3)_{3-n} \longrightarrow [PtCl_2\{Me_nP(CF_3)_{3-n}\}_2]$$

$$n = 1,\ trans\ \text{isomer}$$
$$n = 2,\ cis\ \text{isomer}$$
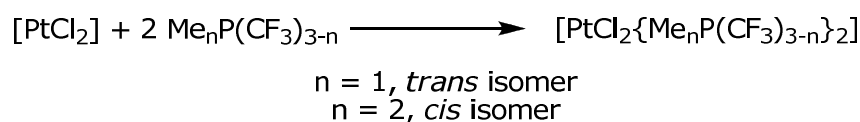
Scheme 1.32: Reaction of PtCl$_2$ with methyltrifluoromethylphosphines.

Beg and Clark[81] also reported the synthesis of $[PtCl_2\{PPh_2(CF_3)\}_2]$ and $[PtCl_2\{PPh(CF_3)_2\}_2]$, via the addition of an acetone solution of the phosphine to an aqueous solution of $K_2[PtCl_4]$. Both of these complexes formed the *trans*-isomer (again assigned based on their zero dipole moment), however, Rest[159] reports that the route used by Beg and Clark yielded exclusively the

cis-isomer of [PtCl$_2${PPh$_2$(CF$_3$)}$_2$], and that the *trans* isomer could be formed by changing the solvent of the reaction from acetone to methanol. Rest also reported the synthesis of *cis/trans*-[PtX$_2${PPh$_2$(CF$_3$)}$_2$] (X = Br, Cl) and *trans*-[PdX$_2${PPh$_2$(CF$_3$)}$_2$] (X = Cl, Br, I), along with the halide-bridged compounds [(CF$_3$Ph$_2$P)MX(μ^2-X)]$_2$ (M = Pd, X = Cl, Br, I, M = Pt X = I).[159] Grigorov and Khokhryakov[160] showed that *trans*-[PtCl$_2${PPh$_{3-n}$(CF$_3$)$_n$}$_2$] (n = 1, 2) isomerise to the *cis*-isomers upon heating, as evidenced by the presence of two Pt-Cl stretches in the infra-red spectrum (*cf.* one for the *trans*-isomer); this isomerisation was independently confirmed by Beg and Qaiser.[161]

Roddick and co-workers[100] have synthesised *trans*-[PtCl$_2${PPh$_2$(C$_2$F$_5$)}$_2$] and *trans*-[PtCl$_2${PPh(C$_2$F$_5$)$_2$}$_2$], from two equivalents of the corresponding phosphine and [PtCl$_2$(NCPh)$_2$] or [PtCl$_2$(cod)] respectively, although, when preparing the *bis*-C$_2$F$_5$ containing complex approximately 10% of the chloride bridged dimer, [{(C$_2$F$_5$)$_2$PhP}PtCl(μ^2-Cl)]$_2$ was also formed. They have also structurally characterised *trans*-[PtCl$_2${PPh$_2$(C$_2$F$_5$)}$_2$] and *trans*-[PtCl$_2${PPh(C$_2$F$_5$)$_2$}$_2$] via X-ray diffraction studies, which allows for estimates of the steric demand of the phosphines to be made. PhP(C$_2$F$_5$)$_2$ and Ph$_2$PC$_2$F$_5$ have estimated Tolman Cone Angles of 178° and 160° respectively (based on published data;[100] estimated using STERIC).[162] It can be seen from these data that the substitution of a phenyl ring for a C$_2$F$_5$ moiety increases the bulk of the phosphine considerably. The same group have also prepared complexes of the type [PtMeX{PMe(C$_2$F$_5$)$_2$}$_2$] (X = Me, O$_2$CCF$_3$, OTf, OSO$_2$F),[163,164] and have investigated their reactivity with CO and H$_2$, finding that [PtMe(CO){PMe(C$_2$F$_5$)$_2$}]$^+$X$^-$ results in reductive carbonylation under moderate pressures of CO to yield MeC(O)X anhydride products.[164]

Beg and Clark synthesised the complexes [NiX$_2${PMe$_2$(CF$_3$)}$_2$] (X = Cl, Br, I, NO$_3$, SCN), all of which are stable.[165] They report that the ligands MeP(CF$_3$)$_2$

and $P(CF_3)_3$ show no sign of reaction with Ni(II) salts. The reason for this may be down to steric factors, as nickel has a smaller van der Waals' radius than platinum (163 pm *vs.* 175 pm), since the electronic properties of $MeP(C_2F_5)_2$ and $MeP(CF_3)_2$ are expected to be very similar.

Manojlovic-Muir *et al*. were able to synthesise the dichloropalladium(II) complex *cis*-[PdCl$_2${κ^2-Ph$_2$PCH$_2$CH$_2$P(CF$_3$)$_2$}] of the unsymmetrical chelating phosphine (CF$_3$)$_2$PCH$_2$CH$_2$PPh$_2$, by the addition of the phosphine to [PdCl$_2$(NCPh)$_2$] in refluxing benzene.[166] They subsequently obtained the analogous dichloroplatinum(II) complex in the same manner.[167] Both of these complexes have been characterised via single crystal X-ray diffraction studies. Roddick and co-workers have also shown that the symmetrical *bis*-phosphine, dfepe, coordinates to a variety of metal centres including rhodium and iridium (affording [(dfepe)M(μ-Cl)]$_2$ where R = Rh, Ir)[168] and nickel, molybdenum and chromium as described above.

Pincer ligands of the type 1,3-(R$_{f2}$PCH$_2$)$_2$C$_6$H$_4$ (R$_f$ = CF$_3$, C$_2$F$_5$) have also been shown to coordinate to platinum forming [ClPt{κ^3-(1,3-R$_{f2}$PCH$_2$)$_2$C$_6$H$_4$}].[101] There has been considerable growth in the chemistry and application of these pincer "PCP" complexes; they have been used in alkene dehydrogenation chemistry of iridium for example, though to date no studies of fluorinated pincer ligand catalysis or applications have been published.

1.8.2 Complexes of Perfluorovinyl Phosphines

The synthesis and reactivity of perfluorovinyl phosphines has been widely explored in recent years, as has their coordination chemistry. They have been shown to coordinate to a variety of metals (Scheme 1.33), including molybdenum,[36,169] rhodium,[170,171] palladium,[170] platinum[36,170,172] and gold.[36]

$$[Rh_2Cl_2(CO)_4] + 4\ R_2PCF=CF_2 \longrightarrow 2\ [Rh(CO)Cl(PR_2CF=CF_2)_2]$$

$$K_2[MCl_4] + 2\ R_2PCF=CF_2 \longrightarrow [MCl_2(PR_2CF=CF_2)_2]$$

$$[AuCl\{S(CH_2CH_2OH)_2\}] + R_2PCF=CF_2 \longrightarrow [AuCl(PR_2CF=CF_2)] + S(CH_2CH_2OH)_2$$

Scheme 1.33: Coordination chemistry of perfluorovinyl phosphines.

The gold(I) complex of $Ph_2P(CF=CF_2)$ displays an interesting structure in the solid state, adopting a dimeric structure, $[\{AuCl[PPh_2(CF=CF_2)]\}_2]$. This complex contains a short gold-gold contact of 3.1945(5) Å, with the P – Au – Cl units almost perpendicular to one another (Cl1–Au1–Au2–P2 torsion angle is 98.6(1)°) in a "crossed swords" motif.[36]

The *trans*-palladium(II) and platinum(II) dihalide square-planar complexes contain intramolecular short contacts between the metal centre and the *cis*-fluorine atoms on the perfluorovinyl groups that are less than the sum of the van der Waals' radii, resulting in a pseudo-octahedral geometry.[170,173] A similar feature has also been observed in $[Rh(CO)Cl\ (PPh_2CF=CF_2)_2]$.[170]

There appears to be a fine balance as to whether the geometry of the platinum halide complexes is *cis* or *trans*. The *cis* complex is thermodynamically favoured, unless the ligands are sterically demanding, in which case the *trans* isomer will be formed preferentially. The complexes $[PtX_2\{PEt_2(CF=CF_2)\}_2]$ (X = Cl, Br, I) have been studied. In the case of the chloride, an oily product results, which based on the appearance of the $^{31}P[^1H]$ NMR spectrum and the magnitude of the $^1J_{PtP}$ coupling constant (3667 Hz) was assigned as the *cis* isomer. However, when X = iodide, a low melting solid forms which gives rise to a virtual triplet in the $^{31}P[^1H]$ NMR spectrum, confirming that the *trans* isomer has formed exclusively. Finally, when $Et_2PCF=CF_2$ is added to an ethanolic solution of $K_2[PtBr_4]$, the $^{31}P[^1H]$ NMR spectrum of the product contains resonances corresponding to both isomers.

Similarly, this *cis/trans* balance is also displayed in [PtCl$_2$(P^{i}Pr$_2$CF=CF$_2$)$_2$], perhaps the most interesting perfluorovinyl phosphine complex, which exists exclusively as the *trans* isomer in solution but crystallises as a mixture of both *cis* and *trans* isomers of the complex in the same unit cell (Figure 1.10). The *trans* isomers are located at the corners, and top and bottom faces of the cell, with the *cis*-isomers sited in-between, such that the unit cell containing 4 *cis* and 2 *trans* molecules.
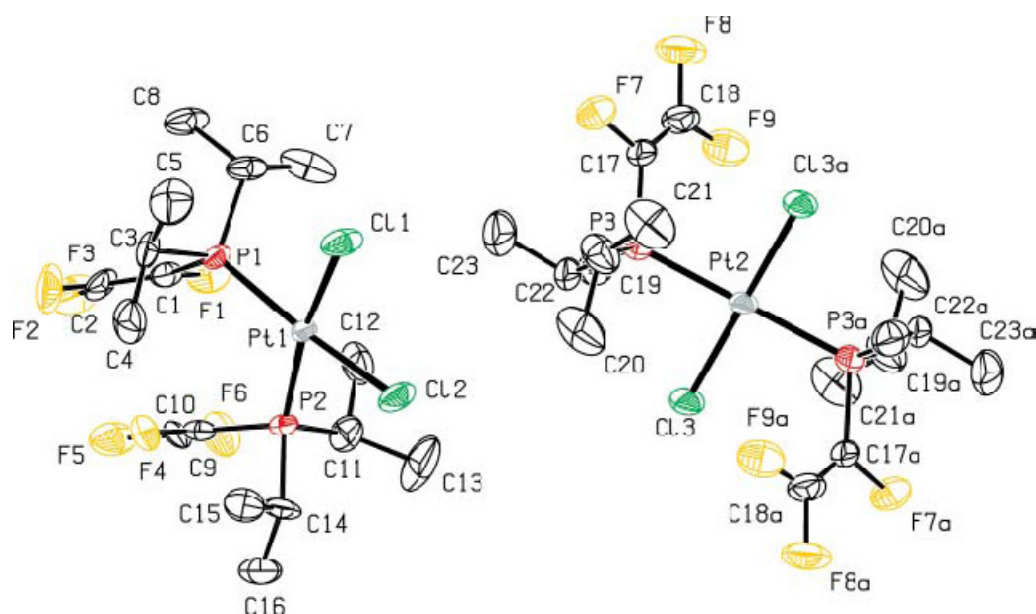
Figure 1.10 ORTEP[174] representation of the *cis* and *trans* isomers of [PtCl$_2${P^{i}Pr$_2$(CF=CF$_2$)}$_2$]. Thermal ellipsoids set to 50% and hydrogen atoms removed for clarity. Taken from Ref. 174

The Pt-P bond lengths are shorter in the *cis* molecule than in the *trans* (2.44(4) Å *vs* 2.290(3) Å), whilst the reverse is noted for the Pt-Cl bond, as expected based on the relative *trans* influences of phosphine and chloride ligands (where P > Cl).

The arrangement of the *cis/trans*-isomers in the solid state structure of [PtCl$_2${P^{i}Pr$_2$(CF=CF$_2$)}$_2$] results in the congregation of the fluorine substituents, forming isolated pockets of fluorous domains (Figure 1.11).
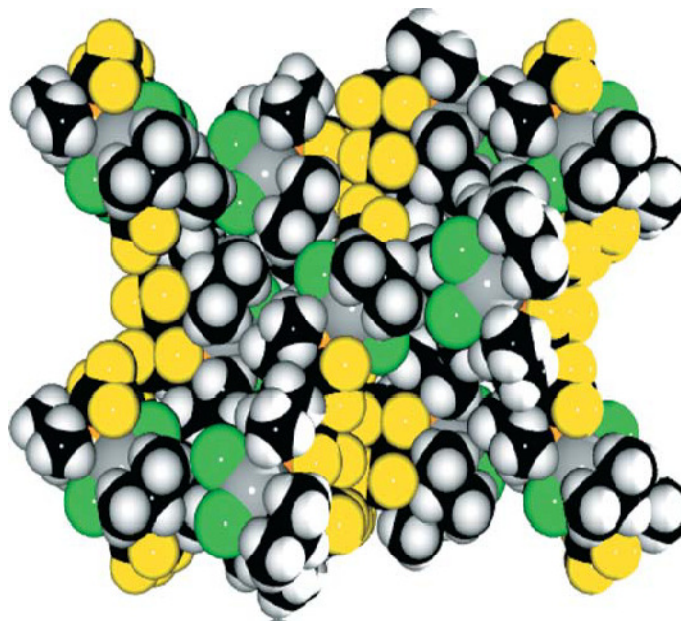
Figure 1.11: Space-filling diagram of *cis-/trans*-[PtCl$_2$\{(P^{i}Pr$_2$(CF=CF$_2$)\}$_2$], illustrating the fluorous domains. Taken from Ref. 170

The only other example of this co-crystallisation of isomers was observed in the complex [PtCl$_2$\{P(C$_6$H$_4$C$_6$F$_{13}$-4)$_3$\}$_2$], which was found to a adopt a similar packing arrangement to give a *cis* : *trans* ratio of 2:1.[175] It is thought that in this complex the long fluorous chains are responsible for the packing. However, it is unlikely that the CF=CF$_2$ unit is capable of giving rise to fluorophilic/fluorophobic interactions, though they are shown to aggregate (Figure 1.11).

Comparisons of the v(CO) stretching frequencies of the molybdenum and rhodium complexes has been achieved.[170] As mentioned previously, these data can be empirically related to the data obtained from [Ni(CO)$_3$L] complexes, and it has been shown that the perfluorovinyl group imparts a similar electron-withdrawing effect to an alkoxy group, and a slightly greater effect than a perfluoroaryl moiety. The compound [Mo(CO)$_5$\{PPh$_2$(CF=CF$_2$)\}] has also been shown to crystallise at very low temperature.[176]

The rhodium complexes [Cp*RhCl$_2$\{PR$_{3-x}$(CF=CF$_2$)\}$_x$] (x = 1, R = Ph, ^{i}Pr, Et, x= 2, R = Ph)[171] have also been prepared, via treatment of [Cp*RhCl(μ-Cl)]$_2$ with the corresponding phosphine. When reacted with ^{t}BuCN in the presence of NaBF$_4$, the salts [Cp*RhCl(NC^{t}Bu)\{PR$_{3-x}$(CF=CF$_2$)$_x$\}]BF$_4$ were formed (Scheme 1.34).

[\{Cp*RhCl(μ-Cl)\}$_2$] + R$_{3-x}$P(CF=CF$_2$)$_x$ $\xrightarrow{\text{DCM}}$ [Cp*RhCl$_2$\{PR$_{3-x}$(CF=CF$_2$)$_x$\}]

^{t}BuCN / NaBF$_4$

[Cp*RhCl(NC^{t}Bu)\{PR$_{3-x}$(CF=CF$_2$)$_x$\}]BF$_4$ + NaCl

x = 1, R = Ph, ^{i}Pr, Et
x= 2, R = Ph
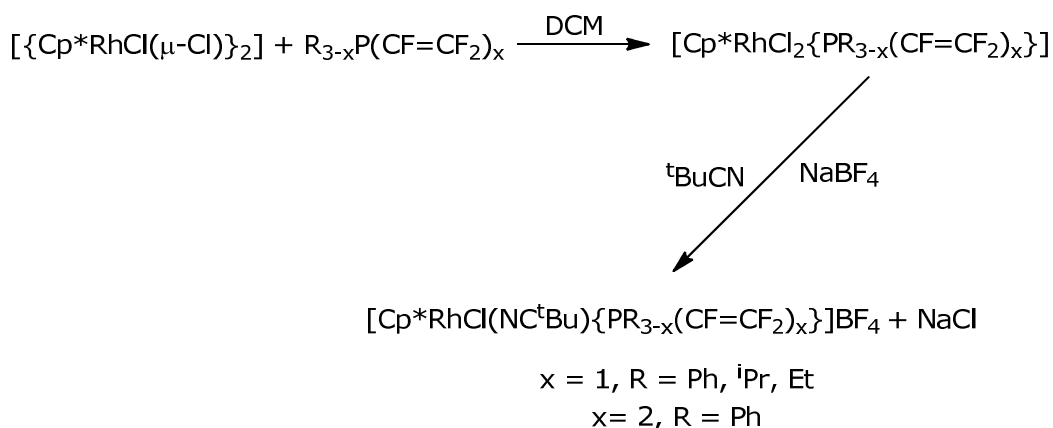
Scheme 1.34: Formation of pentamethylcyclopentyl rhodium complexes of perfluorovinyl phosphines.

Similarly, the salt [Cp*RhCl\{κ-P,κ-S-PPh(CF=CF$_2$)\}(C$_6$H$_4$SMe-2)]BF$_4$ was produced as a mixture of enantiomers which differ in the relative positions of the perfluorovinyl and pentamethylcyclopentadienyl groups, of which the *cis* isomer is formed preferentially. The reaction of these salts with proton sponge has been investigated and it was found that [Cp*RhCl\{κ-P,κ-S-PPh(CF=CF$_2$)\}(C$_6$H$_4$SMe-2)]BF$_4$ undergoes dehydrofluorinative coupling, although not cleanly and that some products due to HF addition across the vinyl bond are also formed (Scheme 1.35).[171]

$[\{Cp^*RhCl(\mu\text{-}Cl)\}_2] \xrightarrow[\text{NaBF}_4]{\text{PRR'(CF=CF}_2)} cis/trans\text{-}[Cp^*RhCl\{\kappa\text{-}P,\kappa\text{-}S\text{-}PRR'(CF=CF_2)\}]BF_4$

Proton sponge
CDCl$_3$

R = Ph, R' = PhP(C$_6$H$_4$SMe-2)(CF=CF$_2$)
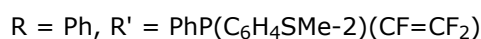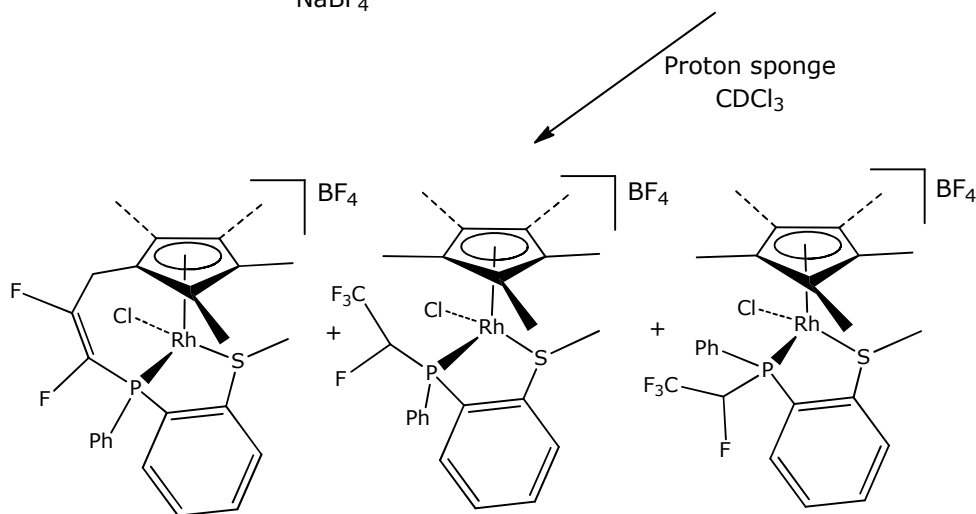
Scheme 1.35: Dehydrofluorinative coupling of [Cp*RhCl{κ-P,κ-S-PPh(CF=CF$_2$)}(C$_6$H$_4$SMe-2)]BF$_4$.

1.8.3 Fluoroalkynyl Phosphine Complexes

There are few fluoroalkynyl phosphine complexes in the literature; those that are known are limited to complexes of Ph$_2$P(tfp). This phosphine has been coordinated to palladium and platinum. The square planar *cis*-[PtCl$_2$\{PPh$_2$(tfp)\}$_2$] complex is formed from the reaction between the phosphine and [PtCl$_2$(cod)], whereas the square planar *cis*-[PdCl$_2$\{PPh$_2$(tfp)\}$_2$] is made from [PdCl$_2$(NCPh)$_2$] and the phosphine.

Other complexes of this phosphine have been synthesised, to investigate the potential of the alkyne bond to participate in coordination, for example, the complex [Co$_4$(CO)$_{10}$\{PPh$_2$(tfp)\}$_2$] was prepared by the addition of two equivalents of the phosphine to [Co$_2$(CO)$_8$] and has been structurally characterised via single crystal x-ray diffraction studies. The molecular structure shows that the alkyne moiety is coordinated to two cobalt atoms (of Co(CO)$_5$ fragments), whilst the phosphorus atom of the same ligand is coordinated to an adjacent Co(CO)$_5$ unit. This leads to the formation of a

59

"puckered" 6-membered $Co_2C_2P_2$ ring, probably via the intermolecular displacement of two CO groups by the uncoordinated phosphorus atoms of $\{Ph_2P(tfp)\}Co_2(CO)_6$.

The zerovalent complexes $[M\{Ph_2P(tfp)\}_2]_2$ and $[Ph_3PM\{Ph_2P(tfp)\}_2]_2$ (M = Pd, Pt] have also been synthesised, and coordination of the acetylene bond was found to occur in these complexes as well. The complexes $[M\{Ph_2P(tfp)\}_2]_2$ are prepared via the reduction of the cis-$[MCl_2\{PPh_2(tfp)\}_2]$ derivatives with $NaBH_4$, and the presence of metal-acetylene interactions confirmed via IR/raman spectroscopy. The complexes $[Ph_3PM\{Ph_2P(tfp)\}_2]_2$ were prepared from $[M(PPh_3)_4]$ (M = Pd, Pt) and one equivalent of $Ph_2P(tfp)$ in dry benzene, and again the presence of a coordinated triple bond was indicated by IR/raman spectroscopic studies. The palladium derivative was also analysed by single crystal X-ray diffraction studies, finding that the C≡C bond length was (on average) 1.285(28) Å, longer than "free" C≡C distances of 1.20 Å,[177] giving further evidence of metal – acetylene interaction.

1.9 Summary

Several research groups have identified a gap in the stereoelectronic profile of phosphorus(III) ligands, with only a few large, electron-poor phosphines currently known. A number of reports have suggested that perfluoroalkyl-containing phosphines will fill this void; however, as described above, there are no generic, simple methods available for the synthesis (and subsequent investigation) of these ligands. This lack of available methodology has hindered the development of their chemistry, as evidenced by the extremely low number of coordination complexes of this class of compound compared with their perprotio analogues. Those examples that are known are essentially limited to CF_3, C_2F_5, and C_2F_3 and $CCCF_3$ substituted examples.

2. Unsaturated Fluoro-organo Phosphines

In recent years the protocol for introducing perfluorovinyl groups into phosphorus systems has been well established.[36,121,137,170,172,173] However, as most of this work has focussed on phosphines bearing relatively small perprotio groups; it was decided to investigate the synthesis of bulkier analogues, which as described above are of interest.

2.1 Perfluorovinyl Phosphines

2.1.1 MesP(CF=CF$_2$)$_2$ (1)

A diethyl ether solution of MesPCl$_2$ was synthesised (Scheme 2.1) via the slow addition of mesitylmagnesium bromide to PCl$_3$ at -78°C; this was subsequently added cautiously (at -95°C) to an excess of CF$_2$=CFLi (synthesised from HFC-134a and 2 equivalents of ^{n}BuLi) resulting in a dark brown oil.

$$MesMgBr + PCl_3 \xrightarrow[-78°C]{THF} MesPCl_2 + MgBrCl$$

$$\downarrow \begin{array}{c} Et_2O \\ -90°C \end{array} 2\ LiCF=CF_2$$

$$MesP(CF=CF_2)_2 + 2\ LiCl$$
$$\mathbf{1}$$
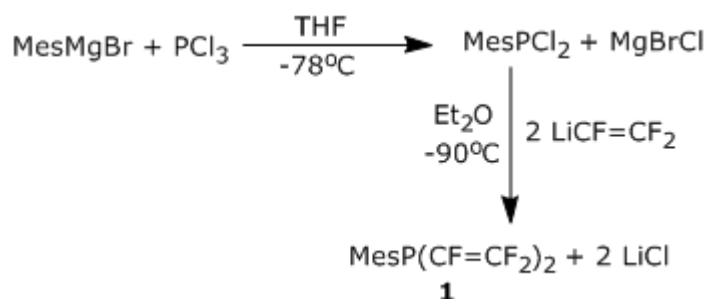
Scheme 2.1: Synthesis of MesP(CF=CF$_2$)$_2$.

The ^{31}P{^{1}H} NMR spectrum of the resulting oil shows a complex triplet based pattern at δ -63.3 ppm ($J_{PF} \sim$ 54 Hz), consistent with the presence of two perfluorovinyl groups attached to the phosphorus centre, *cf.* PhP(CF=CF$_2$)$_2$ lit. δ -51.0 ppm.[36]

The ^{19}F NMR spectrum contains the expected three signals for the three chemically unique fluorine environments of a perfluorovinyl group, at δ -

84.5, -107.0 and -170.7 ppm (see Figure 2.1, Figure 2.3, and Figure 2.2 respectively); these are all doublets of doublets of doublets.
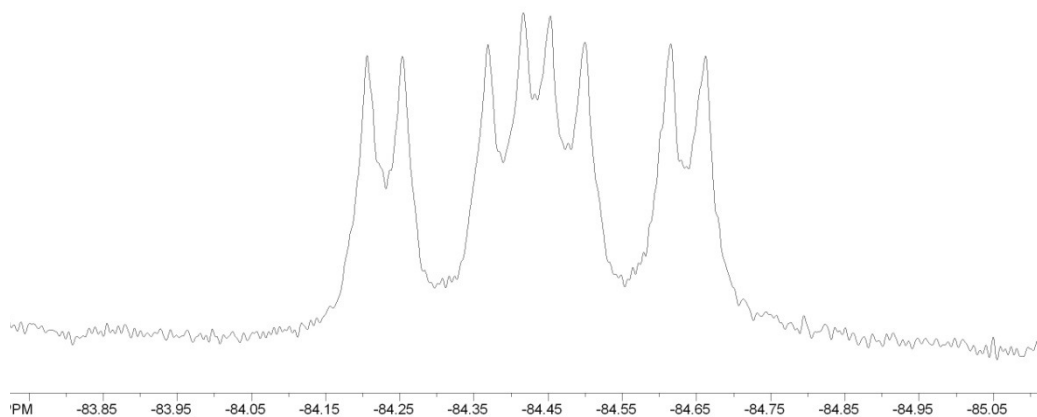
Figure 2.1: Expansion of the signal observed at δ –84.5 ppm in the ^{19}F NMR spectrum of 1.

The signal at -84.5 ppm (Figure 2.1) is assigned as the fluorine atom *trans* to the phosphorus centre, as it does not have a large (>100 Hz) F–F coupling constant characteristic of *trans* fluorine-fluorine interactions.[178] The signal at δ -170.7 ppm (Figure 2.2) is assigned to the fluorine atom *geminal* to the phosphorus atom, based on its chemical shift, and that it shares a coupling constant of 30 Hz with the signal at δ -84.5 ppm, indicative of *cis* fluorine-fluorine interaction.[178]

PM	-169.7	-169.9	-170.1	-170.3	-170.5	-170.7	-170.9	-171.1	-171.3	-171.5	-171.7
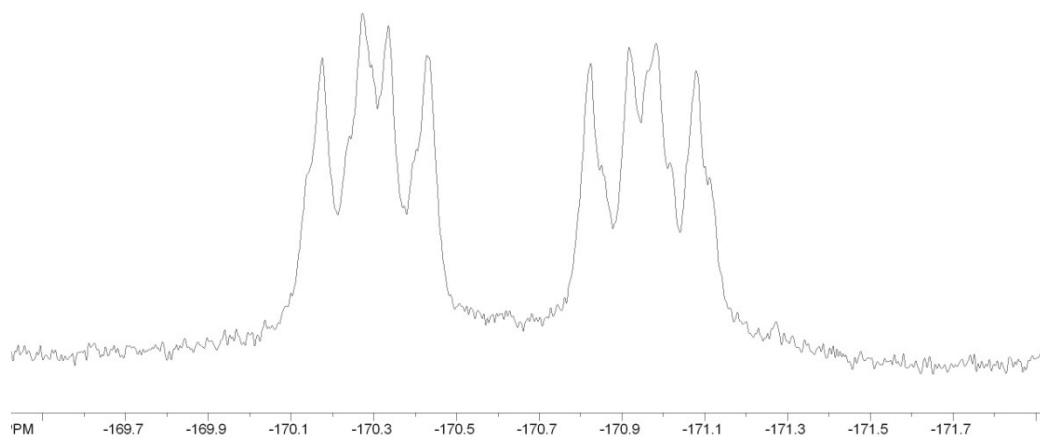
Figure 2.2: Expansion of the signal observed at δ -170.7 ppm in the ^{19}F NMR spectrum of 1.

Therefore the signal at δ -107.0 ppm (Figure 2.3 is assigned to the fluorine atom *cis* to the phosphorus nuclei; it shares a large coupling constant (121 Hz, mutual *trans* $^{3}J_{FF}$ coupling) with the signal at -170.7 ppm.
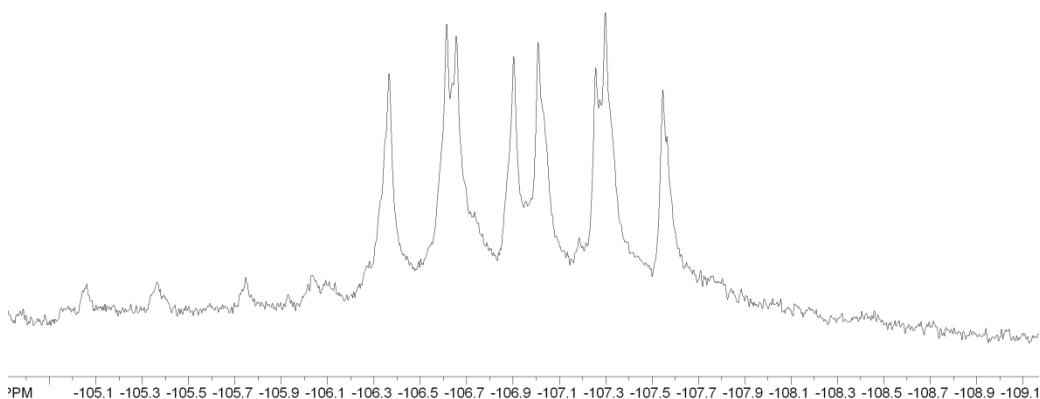
Figure 2.3: Expansion of the signal observed at δ -107.0 ppm in the ^{19}F NMR spectrum of 1.

This signal also has a doublet coupling of 54.6 Hz, shared with the signal observed at δ -63.3 ppm in the ^{31}P{^{1}H} NMR spectrum. The magnitude of the coupling constant is also consistent with that observed between the phosphorus centre and the *cis*-fluorine atom in related systems (e.g. $Ph_2P(CF=CF_2)$ and $PhP(CF=CF_2)_2$, where $^{3}J_{PFcis}$ = 61 and 57 Hz respectively).

The ^{1}H NMR spectrum confirms the presence of the aromatic protons, with a singlet observed at δ 6.97 ppm, the *ortho*-methyl protons are observed at δ 2.44 ppm, and the *para*-methyl protons seen at δ 2.29 ppm, integrating in the expected ratio of 2:6:3.

Whilst the data above unequivocally allows the compound to be assigned as $MesP(CF=CF_2)_2$, the yield of the reaction is poor, and despite repeated attempts insufficient quantities of material for further analysis/study were obtained.

2.1.2 Attempted Synthesis of $Mes_2P(CF=CF_2)$ (2)

The synthesis of compound **2** was attempted in a similar manner to that described for **1**, again resulting in a dark brown oil.

However, the $^{31}P\{^1H\}$ NMR spectrum of the oil only contained a signal corresponding to the starting chlorophosphine, Mes_2PCl (lit. δ 76.0 ppm),[179] and it seems as though this reaction does not proceed under these conditions. As Mes_2PCl is a rather bulky electrophile, this may mean that the activation energy of this reaction is large, and as such at the low temperatures required to prevent the decomposition of $CF_2=CFLi$, there is not enough energy for the reaction to proceed, resulting in the recovery of Mes_2PCl.

2.1.3 $Cy_2P(CF=CF_2)$ (3)

The synthesis of this compound has been previously reported,[121] and was repeated so as to investigate its stereoelectronic properties (Sections 2.5.1 and 2.5.2).

$$Cy_2PCl + LiCF{=}CF_2 \xrightarrow{\text{Et}_2\text{O, -90°C}} Cy_2PCF{=}CF_2 + LiCl$$
3
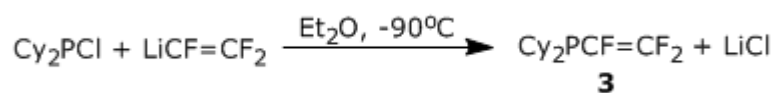
Scheme 2.2: Synthesis of compound 3.

Following the reported procedure[121] a mobile dark brown oil was obtained in very high yield. The $^{31}P\{^1H\}$ NMR spectrum of the oil displays a single resonance at δ -16.3 ppm (lit: -16.2 ppm)[121] which is an overlapping doublet of doublet of doublets (Figure 2.4).

x 0.500

-14.8   -15.2   -15.6   -16.0   -16.4   -16.8   -17.2   -17.6   -18.0   -18.4

PM   260.0   220.0   180.0   140.0   100.0   60.0   20.0   -20.0   -60.0   -100.0   -140.0   -180.0   -220.0   -260.0
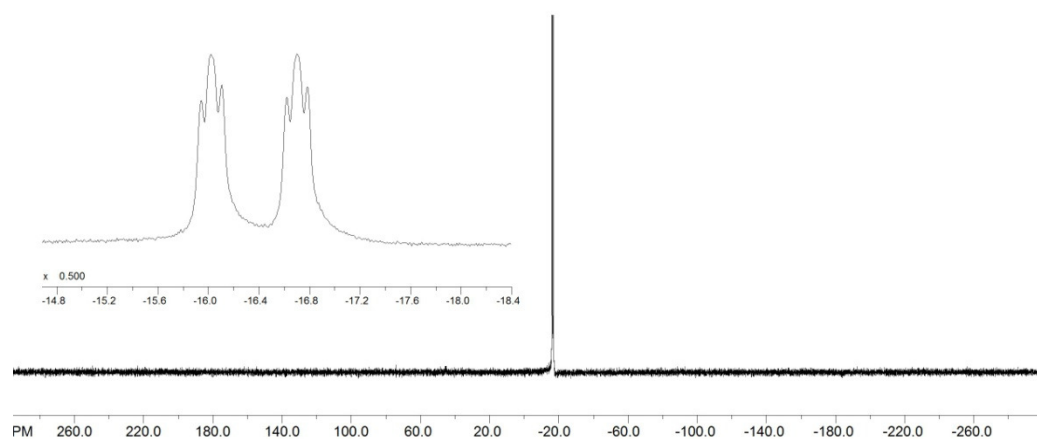
Figure 2.4: $^{31}P\{^1H\}$ NMR spectrum of 3.

The ^{19}F NMR spectrum displays the three characteristic resonances of a fluorovinyl group, at δ -86.5, -110.7, and -177.5 ppm (lit: δ -86.4, -110.5, -177.3 ppm).[121] These data confirm the identity of the compound, and its chemistry/stereoelectronic properties are detailed in Section 2.5.

2.2 Difluorovinyl Phosphines

Introducing bulk at the phosphorus centre appears to have a potential limit *i.e. bis*-mesitylchlorophosphine is sterically too demanding for the low-temperature reaction with Li(pfv) to proceed. In order to remedy this, an alternative strategy to synthesising bulky phosphines is required. As

65

fluorovinyl groups have been shown to be susceptible to nucleophilic substitution (Section 1.6.2), adding bulk to perfluorovinyl phosphines in this manner provides an alternative route to synthesising sterically demanding ligands possessing electron-withdrawing substituents.

2.2.1 (*E/Z*)-^{i}Pr$_2$P(CF=CF^{t}Bu) (4(*E*)/(*Z*))

The addition of ^{t}BuLi to ^{i}Pr$_2$P(CF=CF$_2$) at -78°C was undertaken (Scheme 2.3), resulting in the formation of a dark brown oil.

$$^i\text{Pr}_2\text{PCF=CF}_2 + {}^t\text{BuLi} \xrightarrow[\text{Et}_2\text{O}]{-78°\text{C}} E/Z\text{-}^i\text{Pr}_2\text{PCF=CF}^t\text{Bu} + \text{LiF}$$
$$\mathbf{4\text{-}E/Z}$$
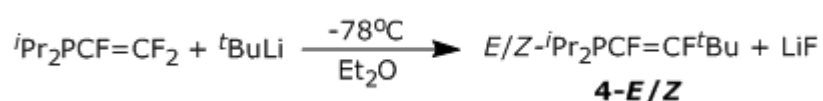
Scheme 2.3: Derivatisation of perfluorovinyl group.

The ^{31}P{^{1}H} NMR spectrum of the resulting oil shows two signals, both doublets of doublets, centred at δ -2.3 and -4.9 ppm (in the ratio 1:5), with no signal observed for the starting phosphine ^{i}Pr$_2$P(CF=CF$_2$) (δ −7.6 ppm).

The signal at δ -4.9 ppm is more intense, and exhibits coupling constants of 96 and 6.3 Hz, whilst the signal at δ -2.3 ppm has a coupling constant of 11 Hz, with another doublet coupling that is too small to determine accurately.

The ^{19}F NMR spectrum of the oil shows two pairs of signals, also in the ratio 1:5. The more intense pair of signals are observed at δ -136.9 and -156.2 ppm; these are a doublet of doublets and a doublet respectively. The resonance at δ -136.9 ppm has coupling constants of 144 Hz (indicative of a *trans* fluorine-fluorine interaction; these are typically 120–140 Hz)[178] and 96 Hz, consistent with that observed in the signal at δ -4.9 ppm in the ^{31}P{^{1}H} NMR spectrum. This coupling ($^3J_{PF}$) is also similar in magnitude to that observed for P–F$_{cis}$ couplings in perfluorovinyl phosphines, such as **3** and ^{i}Pr$_2$P(CF=CF$_2$) (54 and 53 Hz)[121] and difluorovinyl phosphines such as

Ph$_2$PCF=CF^{n}Bu (89 Hz).[121] The magnitudes of these coupling constants suggest that the major coupling mechanism in the *Z*-compounds (and in the P-F$_{cis}$ coupling constants in compounds **3**, ^{i}Pr$_2$P(CF=CF$_2$), and Ph$_2$P(CF=CF^{n}Bu) above) is "through-space" coupling. The "through-bond" contribution to coupling constants involving fluorine nuclei are known to be small when the number of bonds between the interacting nuclei is greater than three.[180] Some systems that require phosphorus-fluorine couplings through four bonds have a much greater magnitude than would be expected, *e.g.* in Ph$_2$P(5,6,7,8-tetrafluoronaphthalene) the phosphorus–fluorine coupling constant is 198 Hz.[181] This has been interpreted in terms of through-space coupling. The remaining doublet, observed at δ -156.2 ppm has a $^3J_{FF}$ coupling constant of 144 Hz, and some additional fine structure, suggesting that it may be a poorly resolved doublet of doublets, with a small coupling constant of *ca*. 5 Hz, possibly corresponding to $^3J_{PF}$.

The lower intensity pair of signals observed at δ -112.2 and -139.3 ppm are both doublets, though the signal at δ -139.3 ppm is poorly resolved. The doublet at δ -112.2 ppm has a $^2J_{PF}$ coupling constant of 11 Hz. The signal observed at δ -139.3 ppm is broad, but appears as a doublet with a coupling constant of *ca*. 3 Hz.

The ^{1}H NMR spectrum contains two resonances, both singlets, at δ 0.96 and 0.89 ppm. The peak at δ 0.89 ppm is more intense, though accurate integration is not possible owing to overlap of the signals. The chemical shifts are consistent with that of methyl groups adjacent to quaternary carbons, suggesting two similar species have been formed, each containing a tertiary butyl moiety.

On the basis of multinuclear NMR data, it appears that both the *E* and *Z* isomers have been formed, with the *Z*-isomer formed predominantly as

evidenced by the presence of the large $^3J_{FF}$ coupling constant (in the approximate ratio 1:5, from integration of the NMR data, Scheme 2.4). Unfortunately, due to the similar solubilities of these compounds, separation was not achieved.
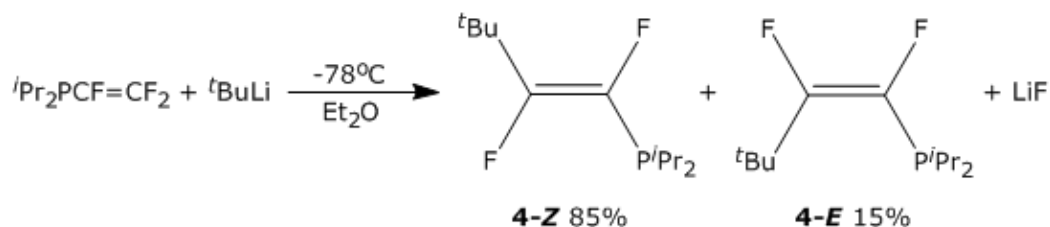
Scheme 2.4: Outcome of nucleophilic substitution of $^iPr_2PCF=CF_2$ with ^tBuLi.

2.2.2 (*E/Z*)-Ph$_2$P(CF=CF^{t}Bu) (5(*E*)/(*Z*))

In a similar fashion Ph$_2$P(CF=CF$_2$) was treated with ^tBuLi at -78°C, which after work-up afforded a viscous dark brown oil.

The $^{31}P\{^1H\}$ NMR spectrum of the resulting oil contains two resonances, at δ -23.6 (>94 % based on integration) and -19.6 ppm (see Figure 2.5).

Figure 2.5: Expansion of $^{31}P\{^1H\}$ NMR spectrum of *E/Z*-Ph$_2$PCF=CF^{t}Bu.

Similarly, the ^{19}F NMR spectrum of this oil contains two pairs of resonances, in relative intensities which agree with the integration data from the ^{31}P{^{1}H} NMR spectrum.

The major signals are observed at δ -134.1 (doublet of doublets, $^3J_{FF}$ = 143.4 Hz, $^3J_{PF}$ = 112 Hz) and -156.3 ppm (doublet of doublets, $^3J_{FF}$ = 143.4 Hz, $^2J_{PF}$ = 5.6 Hz). Both these signals have a $^3J_{FF}$ coupling of 144 Hz, suggesting that they arise from fluorine nuclei that are *trans* to one another across a double bond. The remaining coupling constants (112, 5.6 Hz) are shared with the signal at δ -23.6 ppm in the ^{31}P{^{1}H} NMR spectrum. The signal at δ -134.1 ppm is assigned as the fluorine nucleus *cis* to the phosphorus centre, on the basis of the large (112 Hz) shared coupling constant, and therefore the signal at δ -156.3 ppm is assigned as the *geminal* fluorine nucleus which exhibits smaller phosphorus fluorine coupling, as has been noted before by Barnes *et al.*[121] for (Z)-Ph$_2$P(CF=CF^{n}Bu).

The minor signals are observed at δ -108.3 and -139.5 ppm, similar to those found in (Z)-^{i}Pr$_2$P(CF=CF^{t}Bu), and are a doublet and a singlet respectively. The signal at δ -108.5 ppm has a doublet coupling of 16 Hz, shared by the signal at δ -18.3 ppm in the ^{31}P{^{1}H} NMR spectrum.

The ^{1}H NMR spectrum is as expected – there are complex aromatic signals at δ 7.24–7.30 and 7.33–7.43 ppm, and a triplet centred at δ 1.19 ppm, with a coupling constant of ~2 Hz.

Taken together, the multinuclear NMR data shows that the major product of this reaction is (Z)-Ph$_2$P(CF=CF^{t}Bu), and that contrary to earlier reports[121] a small amount of (E)-Ph$_2$P(CF=CF^{t}Bu) is also formed.

2.3 Chemistry of Difluorovinyl Phosphines

As outlined previously, quantifying the electronic parameter of a phosphine is possible by a variety of methods, of which the most straightforward is based on $^1J_{PSe}$ coupling constants derived from the phosphorus(V) selenide (Scheme 2.5).

2.3.1 Se=PPh$_2$(Z-CF=CF^{t}Bu) (6)

The synthesis of this compound was attempted according to the method of Barnes *et al.*,[121] by refluxing **5-(Z)** in toluene in the presence of elemental selenium (Scheme 2.5), which after work-up and purification via column chromatography resulted in a light brown solid.

$$(Z)\text{-Ph}_2\text{P(CF=CF}^t\text{Bu)} + \text{Se} \xrightarrow[\text{Toluene}]{\triangle} (Z)\text{-Ph}_2\text{P(Se)(CF=CF}^t\text{Bu)}$$
$$\textbf{5-(Z)} \qquad\qquad\qquad\qquad\qquad\qquad \textbf{6}$$
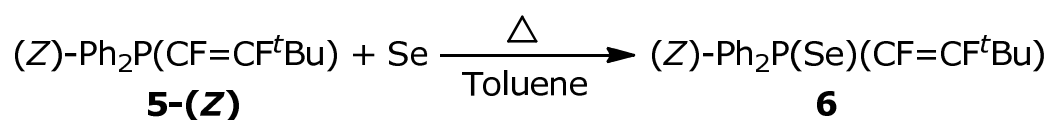
Scheme 2.5: Reaction of 5-(Z) with elemental selenium.

The ^{31}P{^{1}H} NMR spectrum of this solid (Figure 2.6) in CDCl$_3$ contains a doublet of doublets, (J = 70.9, 4.4 Hz) at δ 24.4 ppm, with ^{77}Se (I = ½, 7.6%) satellites ($^1J_{PSe}$ = 764 Hz).
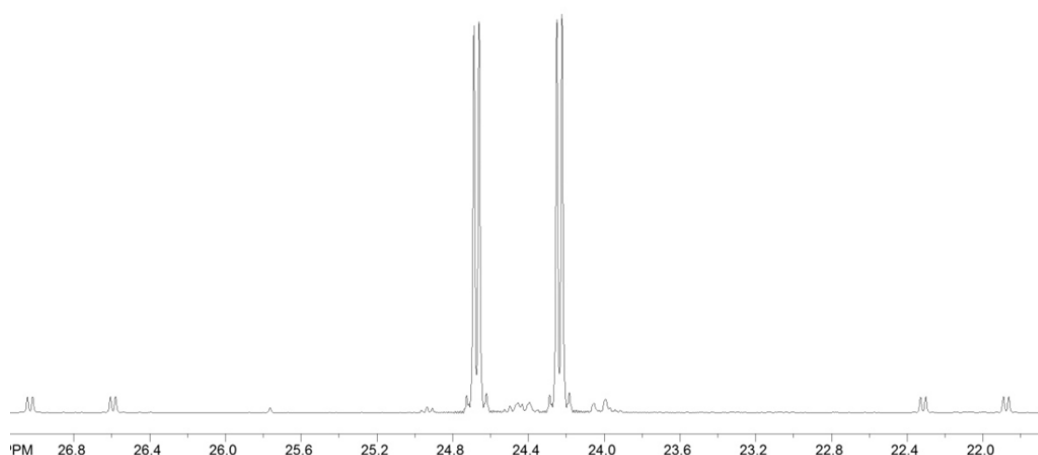
Figure 2.6: Expansion of signal observed at δ 24.4 ppm in the ^{31}P{^{1}H} NMR spectrum of the product from the reaction between 5-(Z) and selenium.

The $^1J_{PSe}$ coupling constant obtained from the ^{31}P{^{1}H} NMR spectrum is consistent with the data obtained from the ^{77}Se{^{1}H} NMR spectrum (Figure 2.7) of this material, which exhibits an overlapping doublet of doublet of doublets ($^1J_{PSe}$ = 764 Hz, $^3J_{SeF}$ = 5.0, $^5J_{SeF}$ = 5.0 Hz) at δ -294.8 ppm.
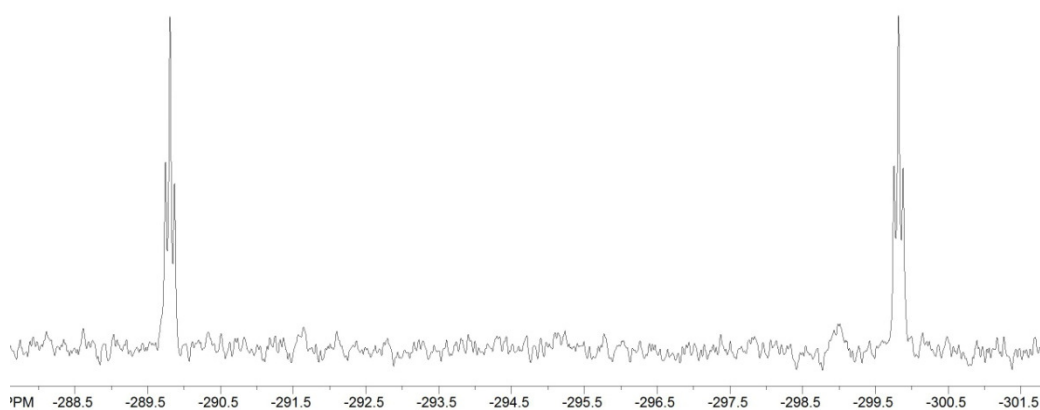
Figure 2.7: Expansion of signal observed at δ -294.8 ppm in the ^{77}Se{^{1}H} NMR spectrum of the product from the reaction between 5-(Z) and selenium.

The ^{19}F spectrum of the brown solid (Figure 2.7) displays two complex resonances at δ -126.1 and -156.8 ppm; they are interpreted as a doublet of

dectets ($^3J_{FF}$ = 141.4 Hz, $^5J_{FH}$ = 2.0 Hz) and a doublet of doublet of dectets ($^3J_{FF}$ = 141.4 Hz, $^3J_{PF}$ = 70.8 Hz, and $^4J_{FH}$ = 2.0 Hz, Figure 2.8) respectively.

| | -156.35 | -156.45 | -156.55 | -156.65 | -156.75 | -156.85 | -156.95 | -157.05 | -157.15 | -157.25 |
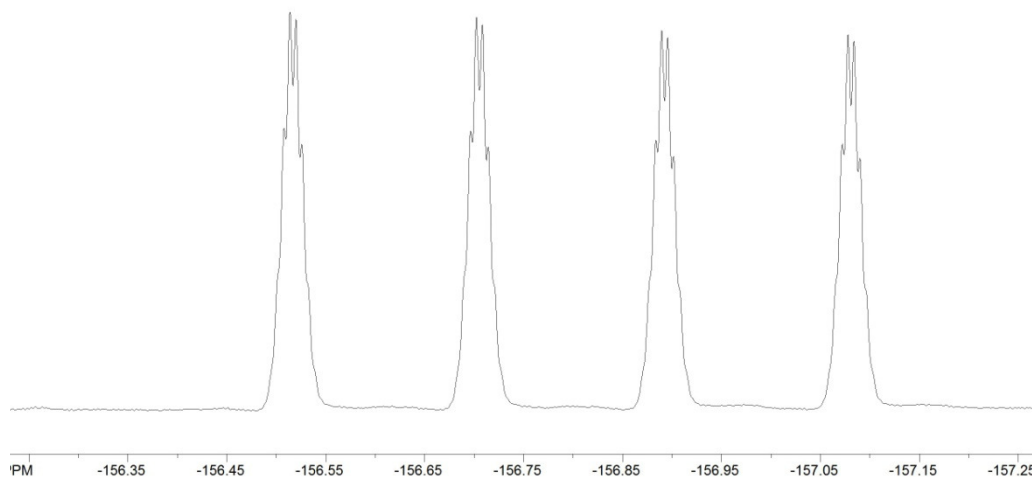
Figure 2.8: Expansion of the doublet of doublet of dectets observed at δ – 156.8 ppm in the ^{19}F NMR spectrum of 6.

The presence of the large (141.3 Hz) mutual coupling between the fluorine signals confirms that the fluorine nuclei are *trans* to one another across the double bond The signal at δ -156.8 ppm also shares a coupling constant with the signal observed at δ 24.4 ppm in the ^{31}P{^{1}H} NMR spectrum, and is assigned as the fluorine nucleus *geminal* to the phosphorus centre on the basis of this (and its chemical shift), therefore the other signal at δ -126.1 ppm is assigned to the fluorine nucleus bonded to the β-carbon. The magnitude of the coupling between the nuclei differs from that of **5-(Z)**, the precursor phosphorus(III) compound. In **5-(Z)** the largest P-F coupling constant is to the *cis*-fluorine nuclei (possibly owing to a "through-space" coupling mechanism), whilst it has decreased to zero upon oxidation to the phosphorus(V) species. This is consistent with the change observed for the oxidation of perfluorovinyl phosphines, $PR_2CF=CF_2$ (R = Ph, Et, ^{i}Pr) to $E=PR_2CF=CF_2$ (E = O, S, Se).[121]

The magnitude of the phosphorus–selenium coupling constant is interesting, which at 764 Hz is lower than observed in $Se=PPh_2(CF=CF_2)$ (785 Hz),[121] which is consistent with having replaced an electron withdrawing fluorine atom for an electron-donating *tert*-butyl group. However it is larger than observed in $Se=PPh_3$ ($^1J_{PSe}$ = 732 Hz),[37] showing that the electron withdrawing effect of the difluorovinyl group is still present.

2.4 Trifluoropropynyl Phosphines

As discussed in Section 1.7, there are very few tfp phosphines known, and only the coordination chemistry of $Ph_2P(tfp)$ has been examined in any detail.

The following tfp-containing compounds were synthesised via the HFC-245fa/^{n}BuLi route as pioneered by Brisdon *et al.*,[132] and described in Section 1.7.

2.4.1 PhP(tfp)$_2$ (7)

This compound has been previously synthesised by the Brisdon group, though not reported.[141] The slow addition of a diethyl ether solution of $PhPCl_2$ to a cold, stirred solution of Li(tfp) results in the formation of compound **7** in high yield as a pale yellow liquid after distillation (Scheme 2.6). It can be stored for a reasonable lengths of time if kept cold, but discolours slowly at room temperature, though there is no discernible change in any of the NMR spectra.[182]

$$PhPCl_2 + 2\ Li(tfp) \xrightarrow[-15^\circ C]{Et_2O} PhP(tfp)_2 + 2\ LiCl$$
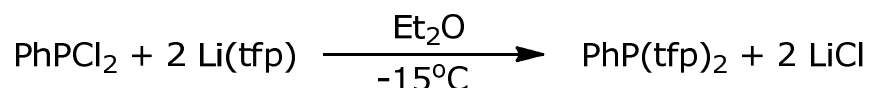
Scheme 2.6: Formation of 7

The $^{31}P\{^1H\}$ NMR spectrum of **7** in CDCl$_3$ shows a single resonance at δ -67.2 ppm as a septet with $^4J_{PF}$ = 6.4 Hz (Figure 2.9). The ^{19}F NMR spectrum shows a doublet ($^4J_{PF}$ = 6.4 Hz) at δ -51.9 ppm.
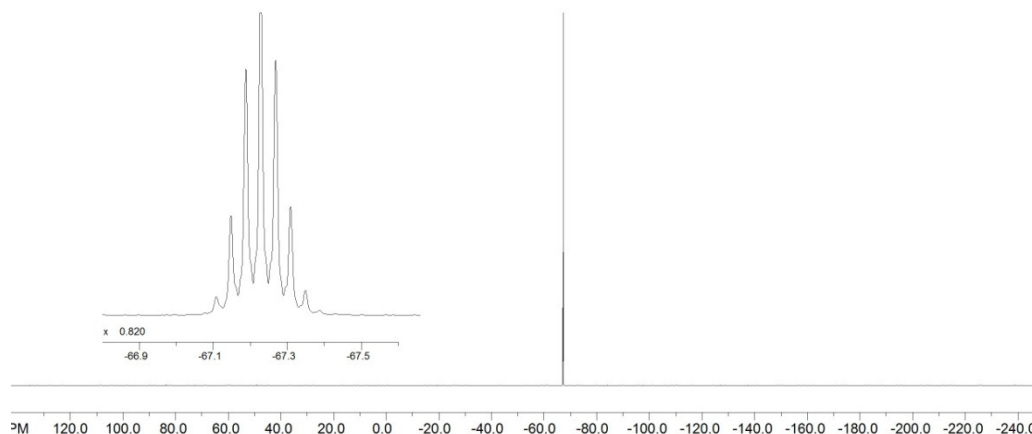
Figure 2.9: $^{31}P\{^1H\}$ NMR spectrum of PhP(tfp)$_2$. *Inset:* **Expansion of the signal observed at δ -67.2 ppm.**

For details on the stereoelectronic properties of this compound, see Section 2.5.2.

2.4.2   PhP(tfp)$_2$ + ^{t}BuLi

The addition of a sterically demanding nucleophile to tfp compounds results in the formation of a dfcp compound, as described in Section 1.7.1. In this manner ^{i}Pr$_2$P(dfcp) has been produced from ^{i}Pr$_2$P(tfp).[137,141] However, introducing two of these groups into a compound has not yet been explored.

The addition of 2 equivalents of ^{t}BuLi to a heated THF solution of **7** results in the formation of a dark oil. The $^{31}P\{^1H\}$ NMR spectrum of this oil shows three major signals, at δ -1.6, -6.0 and -14.4 ppm; they are a doublet of doublets, a quartet and a quartet respectively (Figure 2.10).
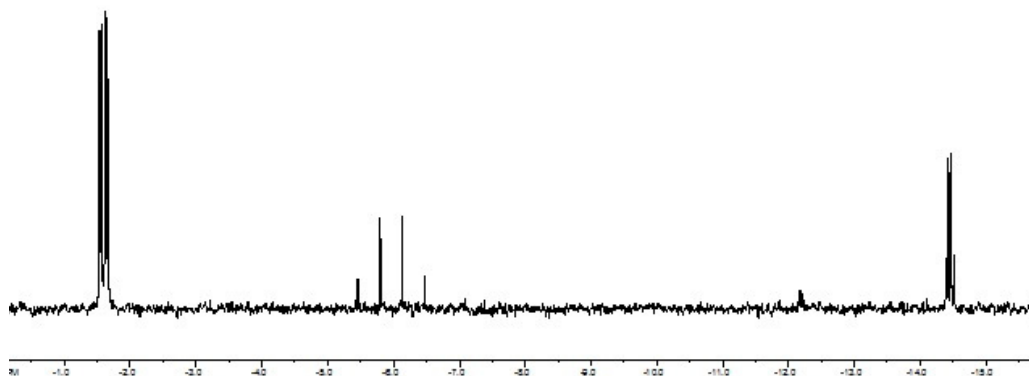
Figure 2.10: $^{31}P\{^1H\}$ NMR spectrum showing the major signals observed after the reaction between PhP(tfp)$_2$ and ^{t}BuLi.

The ^{19}F NMR spectrum of the brown oil also contains three major signals; a doublet centred at δ -50.2 ppm, another doublet centred at δ -54.2 ppm, and a pair of doublet of doublets centred at δ -99.1 and -101.9 ppm, which display slight second order effects.

The doublet of doublets observed at δ -1.6 ppm in the $^{31}P\{^1H\}$ NMR spectrum suggests the presence of only one cyclised tfp group; if both tfp groups had been converted into dfcp units then the signal observed in the $^{31}P\{^1H\}$ NMR spectrum would be expected to be a triplet of triplets (or a doublet of doublet of doublet of doublets). The signal has coupling constants of 14.6 and 4.9 Hz, which are shared with those observed in the pair of second order doublet of doublets centred at δ -99.1 and -101.9 ppm (these two signals are in the ratio 1:1) in the ^{19}F NMR spectrum (14.5 and 4.9 Hz respectively). The ^{19}F NMR signals also share a mutual coupling constant of 122 Hz, and their chemical shifts are in the region of the spectrum dfcp groups have been observed in other compounds, *cf*. Ph$_3$Si(dfcp) δ -103.1 ppm,[142,183] and ^{i}Pr$_2$P(dfcp) δ -103.3 ppm.[137] The ^{19}F NMR signals of Ph$_3$Si(dfcp) and ^{i}Pr$_2$P(dfcp) are a singlet and a doublet respectively, suggesting that the fluorine nuclei are magnetically equivalent. However, for the signals described above, the appearance of two mutually coupled

75

doublets of doublets (with slight second order effects) suggests that the product formed contains non-equivalent fluorine nuclei, for example due to the presence of a stereocentre, therefore making the fluorine nuclei of the dfcp group diastereotopic. This means that both tfp groups cannot have been cyclised. Cyclisation of one tfp group would give rise to the P-chiral compound Ph(tfp)P(dfcp), that would contain two different fluorinated groups however there is no evidence in either the $^{31}P\{^1H\}$ or ^{19}F NMR spectra to support this. The chemical shifts of phosphorus(III) compounds can be predicted with reasonable accuracy (to within a few ppm) by an additive relationship based on which R groups are bound to the phosphorus centre. This is known as Grim's Law (Figure 2.11).[184,185]

$$\delta = -62 + \sum_{i=0}^{n} \sigma P$$

Figure 2.11: Grim's Law for estimating the chemical shift of phosphines (σP is the value in ppm for each substituent).

Based on Grim's Law,[184] the predicted chemical shifts of PhP(dfcp)$_2$ and Ph(tfp)P(dfcp) are -50 and -51 ppm respectively; however, there are no signals observed around δ -50 ppm in the $^{31}P\{^1H\}$ NMR spectrum of the brown oil. Indeed, the multi-nuclear NMR data suggests that only one of the groups attached to the phosphorus centre contains fluorine.

It appears as though one of the tfp groups has been replaced, perhaps via substitution by a *tert*-butyl group. Grim's Law predicts that Ph^{t}BuP(dfcp) will have a chemical shift of δ -1 ppm, which is in good agreement with the observed value (δ -1.6 ppm). This compound will also be P-chiral, which would account for the signals observed in the ^{19}F NMR spectrum. Based on these data, the signal observed at δ -1.6 ppm in the $^{31}P\{^1H\}$ NMR spectrum is Ph^{t}BuP(dfcp), **8**.

The quartet observed at δ -6.0 ppm in the $^{31}P\{^1H\}$ NMR spectrum of the brown oil has a J_{PF} coupling constant of 54.4 Hz, which is shared with the doublet observed at δ -54.2 ppm in the ^{19}F NMR spectrum.

The multiplicity of the $^{31}P\{^1H\}$ NMR signal and the chemical shift observed in the ^{19}F NMR spectrum suggest that the coupling is between the phosphorus centre and a single CF_3 group – this corresponds to a species where no cyclisation has taken place, and also that (as in **8** above), only one fluorine-containing is group attached to the phosphorus centre. However, the magnitude of the coupling is markedly larger than that expected for a tfp-containing phosphine, for example in the starting phosphine **7**, the phosphorus–fluorine coupling is 6.0 Hz. This value of 54.4 Hz is similar to coupling constants observed within the Brisdon group in systems where a CF_3 group is *cis* to a phosphorus centre across a double bond. For comparison, in (*E*)-$PPh_2(CF=CFCF_3)$ and (*E*)-$PPh(CF=CFCF_3)_2$ the $^4J_{PF}$ coupling constants are 58.3 and 58.9 Hz respectively,[186] whereas in the *trans* compounds (*Z*)-$PPh_2(CF=CFCF_3)$ and (*Z*)-$P^iPr_2(CF=CFCF_3)$ the coupling constants are 1.8 Hz and 1.7 Hz respectively.[187] Grim's Law predicts a phosphorus chemical shift of δ -2 ppm for (*E*)-$PPh_2(CF=CFCF_3)$, so based on this and the above data, the signal observed at δ -6.0 ppm is assigned as (*Z*)-$PPh_2(CH=C(^tBu)CF_3)$, **9.**

The remaining signal in the $^{31}P\{^1H\}$ NMR spectrum, the quartet observed at δ −14.4 ppm, shares a coupling constant of 6.5 Hz with the doublet occurring at δ -50.2 ppm in the ^{19}F NMR spectrum. This is consistent with those observed in tfp-containing phosphines (e.g. **7**, $^4J_{PF}$ = 6.0 Hz, and $Ph_2P(tfp)$, $^4J_{PF}$ = 6.0 Hz) as is the ^{19}F chemical shift (*cf.* **7**, δ -51.9 ppm, see above). Taken together this suggests the presence of an uncyclised tfp group, but as in the other species identified in this mixture, only one such fluorinated fragment is present. The substitution of one tfp group of $PhP(tfp)_2$ would lead

to the formation of Ph^{t}BuP(tfp), which Grim's Law predicts would have a ^{31}P chemical shift of δ -12 ppm. Based on the above data the signal observed at δ -14.4 ppm in the ^{31}P{^{1}H} NMR spectrum is assigned as Ph^{t}BuP(tfp), **10**.

^{31}P{^{1}H}/ppm (multiplicity)	^{19}F/ppm (multiplicity)	J/Hz	Compound
-1.6 (dd)	-99.1 (dd) -101.9 (dd)	122, 14.6 122, 4.9	Ph^{t}BuP(dfcp), **8**
-6.0 (q)	-54.2 (d)	54.4	(Z)-PPh$_2$P(CH=C(^{t}Bu)CF$_3$), **9**
-14.4 (q)	-50.2 (d)	6.5	Ph^{t}BuP(tfp), **10**

Table 2.1: Summary of the compounds produced in the reaction shown in Scheme 2.7.

It appears that the *tert*-butyl group has attacked the phosphorus centre resulting in the replacement of one of the fluorinated groups. This attack at the phosphorus centre has not been observed by previous members of the group who have synthesised and derivatised tfp-containing phosphines. So as to ascertain whether the attack occurs preferentially at the β-carbon or at the phosphorus centre, the reaction was repeated with 1.1 equivalents of *tert*-butyl lithium at -80°C. This resulted in the isolation of a brown oil after work-up. The ^{31}P{^{1}H} NMR spectrum of this brown oil shows two signals at δ -5.9 ppm and -14.4 ppm; both are observed as binomial quartets. For these signals the chemical shifts agree with those ascribed to compounds **9**, (Z)-^{t}BuPhP(CH=C(^{t}Bu)CF$_3$) and **10**, ^{t}BuPhP(tfp) respectively. Integration suggests that **10** accounts for almost 90% of the mixture, which suggests that the nucleophilic attack of the *tert*-butyl group at the phosphorus centre occurs preferentially.
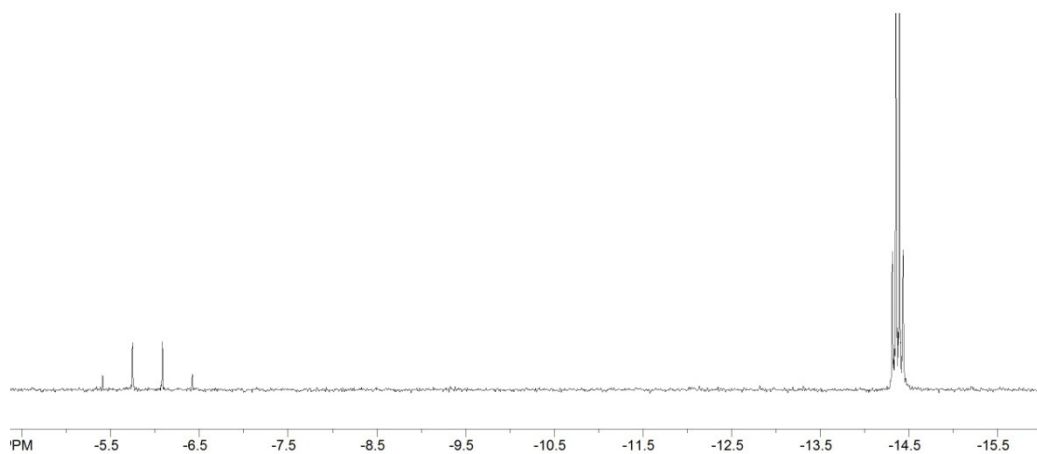
Figure 2.12: $^{31}P\{^1H\}$ NMR spectrum following the reaction between 1.1 equiv. ^{t}BuLi and 11.

Both the ^{19}F and ^1H NMR spectra confirm this distribution of products and the absence of any other by-products.

$$PhP(tfp)_2 + 1.1\ ^t\text{BuLi} \longrightarrow Z\text{-}^t\text{BuPhP}(CH=C(^t\text{Bu})CF_3) + {}^t\text{BuPhP}(tfp)$$

<div align="center">

9, 10%   **10**, 90%

</div>
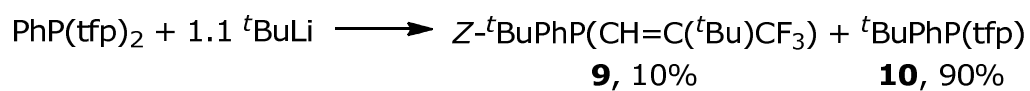
Scheme 2.7: Reaction of 11 with ^{t}BuLi.

2.5 Coordination Chemistry of Unsaturated Fluoro-organo Phosphines

2.5.1 Group 10 Complexes of $Cy_2P(CF=CF_2)$

The square-planar palladium and platinum complexes of **3**, $[MCl_2\{PCy_2(CF=CF_2)\}_2]$ (M = Pd, **11**, Pt, **12**) have been previously synthesised[188] but no structural data was reported for either compound. Both complexes were synthesised from two equivalents of **3** and $K_2[MCl_4]$ (M = Pd, Pt) (Scheme 2.8).

$$Cy_2P(CF=CF_2) + K_2[MCl_4] \xrightarrow[\text{M = Pd, Pt}]{\text{EtOH/H}_2\text{O}} [MCl_2\{PCy_2(CF=CF_2)\}_2] + 2\ KCl$$
$$\mathbf{3} \qquad\qquad\qquad\qquad\qquad Pd = \mathbf{11},\ Pt\ = \mathbf{12}$$
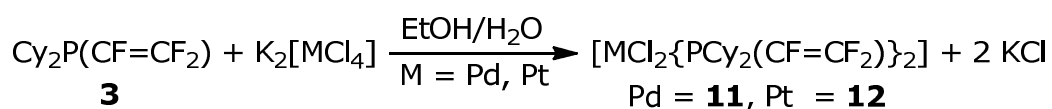
Scheme 2.8: Formation of Group 10 complexes of 3.

The $^{31}P\{^1H\}$ NMR spectrum of **11** contains a resonance at δ 24.1 ppm, a "virtual triplet", with $\frac{1}{2}|^2J_{PF} + {}^4J_{PF}|$ = 15.0 Hz. The ^{19}F NMR spectrum is consistent with the presence of a perfluorovinyl group, though shifted slightly compared to **3**.

The $^{31}P\{^1H\}$ NMR spectrum of the product from the reaction with M = Pt contains a resonance at δ 19.8 ppm (Figure 2.13). The signal is observed as a "virtual triplet" with ^{195}Pt satellites (I = ½, 33%, $^1J_{PtP}$ = 2654 Hz), with $\frac{1}{2}|^2J_{PF} + {}^4J_{PF}|$ = 16 Hz. The magnitude of the coupling constant and the appearance of the signal suggest that the *trans*-isomer of $[PtCl_2\{PCy_2(CF=CF_2)\}_2]$ has been formed. The ^{19}F NMR spectrum contains three signals, as expected for a perfluorovinyl group, slightly shifted relative to **3**, as observed in **11**.
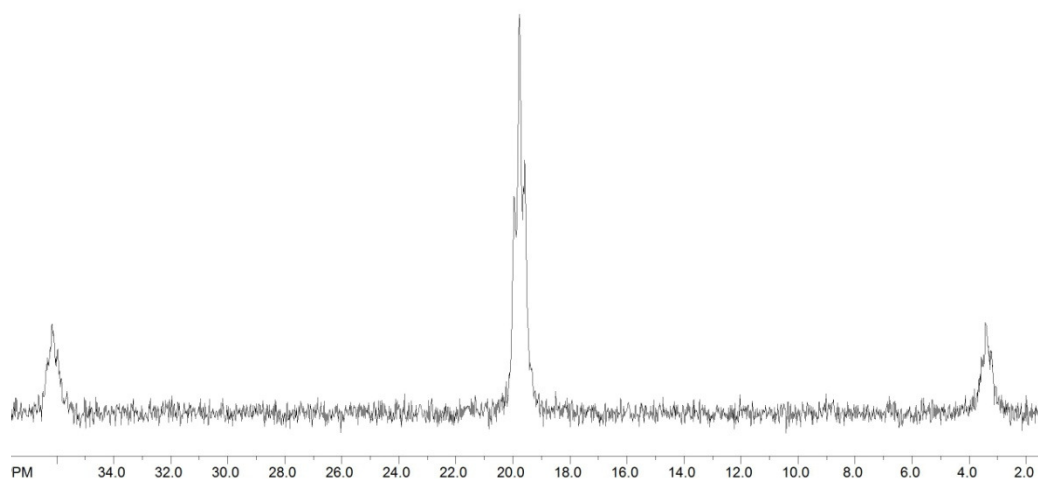
Figure 2.13: Expansion of the signal observed at δ 19.8 ppm in the ^{31}P{^{1}H} NMR spectrum of 12.

Crystals suitable for analysis by X-ray diffraction studies were grown from a layered solution of dichloromethane and diethyl ether. Crystallographic data for these complexes is shown in Table 7.1.

A comparison of the unit cell data (shown in Table 7.1), and the molecular structures shown in Figure 2.14 and Figure 2.15 shows that the two complexes are isomorphous. Both **11** and **12** crystallise in the $P\bar{1}$ space group, have the same cell dimensions, contain two molecules in the asymmetric unit and a centre of inversion at the metal centres (Figure 2.14 for M = Pd, Figure 2.15 for M = Pt).
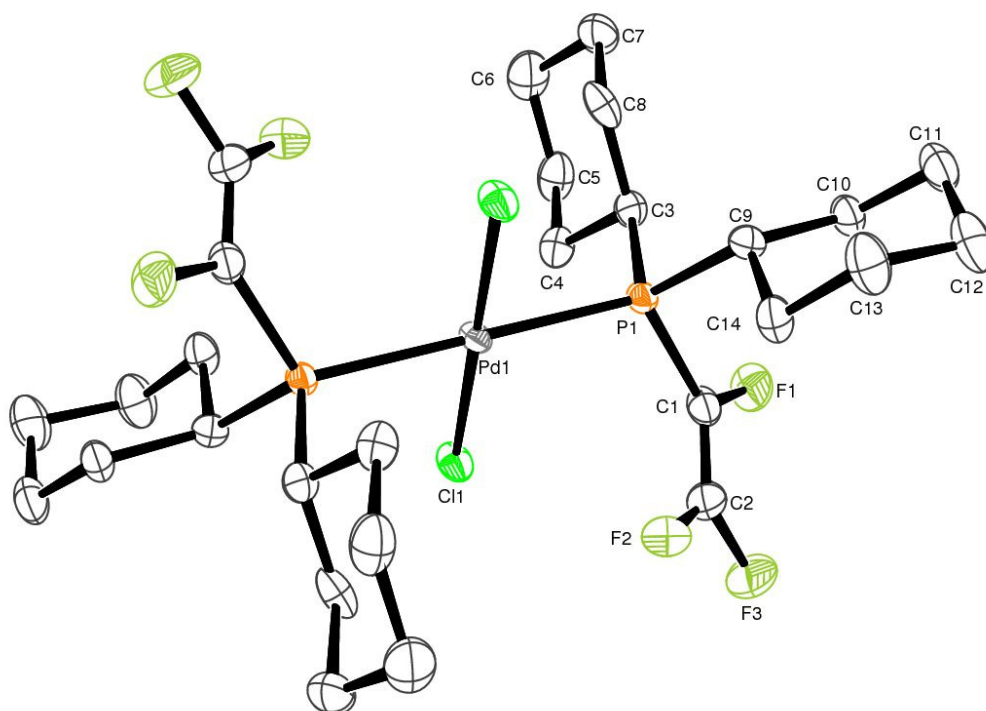
Figure 2.14: ORTEP representation of the molecular structure of 11 (Only one molecule shown and hydrogen atoms omitted for clarity). Thermal ellipsoids are shown at 30%.
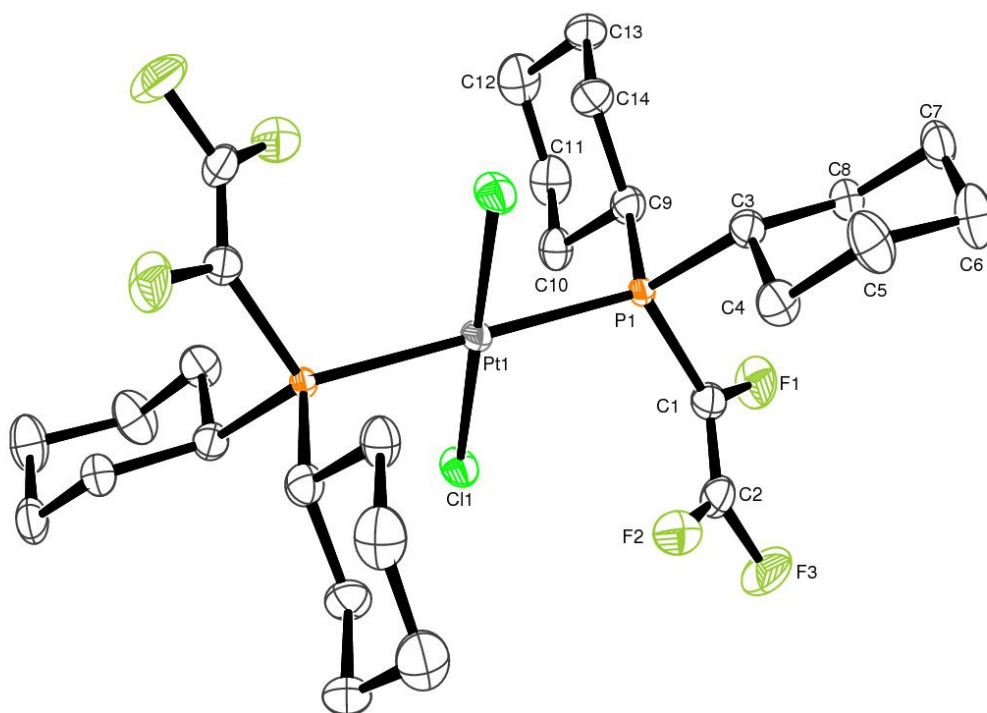
Figure 2.15 : ORTEP representation of the molecular structure of 12 (Hydrogen atoms omitted and only one of the molecules shown for clarity). Thermal ellipsoids are shown at 30%.

The geometry of both molecules is shown to be *trans*-square planar, in agreement with the solution-phase NMR data, and selected bond lengths and angles are given in Table 2.2.

Bond	11 (Å)	12 (Å)	Angle	11 (°)	12 (°)
M−P	2.332(2) 2.317(2)	2.2985(19) 2.3092(16)	M−P−C$_{vin}$	113.5(3) 114.0(4)	113.8(3) 114.8(3)
M−Cl	2.291(2) 2.300(3)	2.310(2) 2.3020(17)	M−P−C$_{cyc}$	111.0(3) 118.7(3) 115.2(3) 110.1(4)	118.8(2) 116.4(3) 112.1(3) 111.1(3)
P−C$_{vin}$	1.807(11) 1.810(12)	1.821(9) 1.824(10)	C$_{vin}$−P−C$_{cyc}$	102.5(5) 103.5(5) 105.4(6) 102.6(6)	103.4(4) 105.2(5) 101.6(4) 101.8(5)
P−C$_{cyc}$	1.830(11) 1.840(9) 1.872(10) 1.838(12)	1.845(8) 1.844(10) 1.836(10) 1.821(10)	C$_{cyc}$−P−C$_{cyc}$	106.2(4) 108.7(5)	105.3(4) 106.2(4)
C=C	1.29(2) 1.291(19)	1.308(17) 1.282(16)			
C−F$_{gem}$	1.390(12) 1.408(15)	1.363(11) 1.384(13)			
C−F$_{cis}$	1.294(16) 1.26(2)	1.288(12) 1.277(15)			
C−F$_{trans}$	1.330(16) 1.353(17)	1.329(12) 1.365(14)			

Table 2.2: Selected bond lengths and angles in 11 and 12.

The M−P and M−Cl bond lengths are comparable to those found in related systems (e.g. [PdCl$_2$\{P^{i}Pr$_2$(CF=CF$_2$)\}$_2$] in which Pd−P = 2.3158(15) Å, Pd−Cl = 2.2856(16) Å, and *trans*-[PtCl$_2$\{P^{i}Pr$_2$(CF=CF$_2$)\}$_2$], Pt−P = 2.290(3) Å and Pt−Cl = 2.292(3) Å). In the palladium complex the C−F$_{gem}$ is the longest C−F bond, whereas in the platinum complex the C−F$_{gem}$ and C−F$_{trans}$ bonds are the same length, within experimental error. In both complexes the C−F$_{cis}$ bond is the shortest C−F bond.

The *cis*-fluorine atoms of each fluorovinyl group make a short contact to the metal centre in both complexes (Pd−F$_{cis}$ = 3.459(8) and 3.493(8) Å, Pt−F$_{cis}$ =

3.470(7) and 3.492(7) Å, all of which are less than the sum of the van der Waals' radii of 3.77 Å), resulting in each metal centre having a pseudo-octahedral geometry (see Figure 2.16).
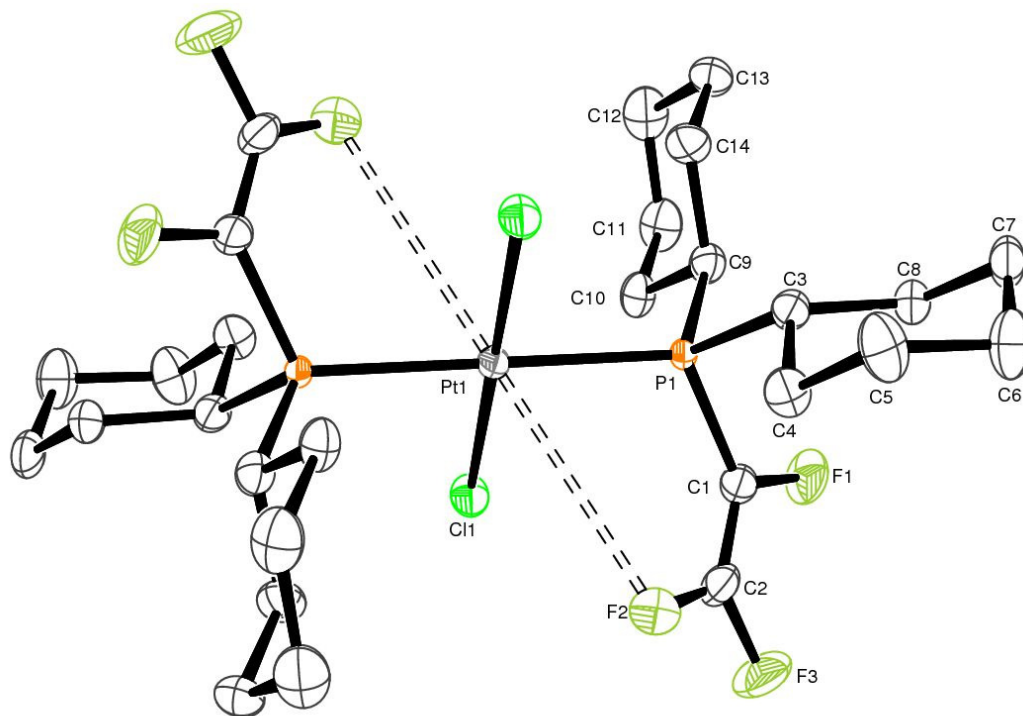
Figure 2.16: ORTEP representation of 12 showing the interaction between the *cis*-fluorine atoms and the metal centre.

From the data obtained for these two complexes the cone angle of **3** can be estimated, and the average of the four values is 169° with similar values for both the palladium and platinum complexes (168° and 170° in **11**, 168° and 170° in **12**). The gold(I) chloride complex of **3** has been synthesised and characterised via X-ray diffraction studies, resulting in the estimation of a cone angle of 173°.[188] These values for the cone angle suggest that the ligand occupies less space in the platinum complex, presumably due to either crystal packing effects or because of the different metal coordination numbers. In any event, based on these data, **3** is the largest perfluorovinyl-containing phosphine to date.

The *trans*-square planar platinum dichloride complex of **5-(Z)**, *trans*-[PtCl$_2$\{PPh$_2$(CF=CF^{t}Bu)\}$_2$], has been previously synthesised,[189] and found to have a cone angle of 165°, making it slightly larger than the parent perfluorovinyl phosphine, Ph$_2$P(CF=CF$_2$) (cone angle = 163°, average of four values).[170]

Phosphine	Cone Angle (°)
PPh$_3$	138
Et$_2$P(CF=CF$_2$)	152
PhP(CF=CF$_2$)$_2$	161
Ph$_2$P(CF=CF$_2$)	163
^{i}Pr$_2$P(CF=CF$_2$)	165
Z-Ph$_2$P(CF=CF^{t}Bu), 5-(*Z*)	165
Cy$_2$P(CF=CF$_2$), 3	170

Table 2.3: Average cone angle for selection of phosphorus(III) compounds.

2.5.2 [Mo(CO)$_5$L] (L = phosphine)

In order to obtain more data regarding the electronic parameter of these ligands, the molybdenum pentacarbonyl phosphine complexes were synthesised (Scheme 2.9). The complexes were isolated as dark green liquid products after column chromatography.

$$[Mo(CO)_6] + Me_3NO \xrightarrow[-CO_2]{MeCN} [Mo(CO)_5(NCMe)]$$

$$\downarrow \textbf{L}$$

$$[Mo(CO)_5L]$$

$$L = Cy_2P(CF=CF_2), \textbf{13}, = PhP(tfp)_2, \textbf{14}$$
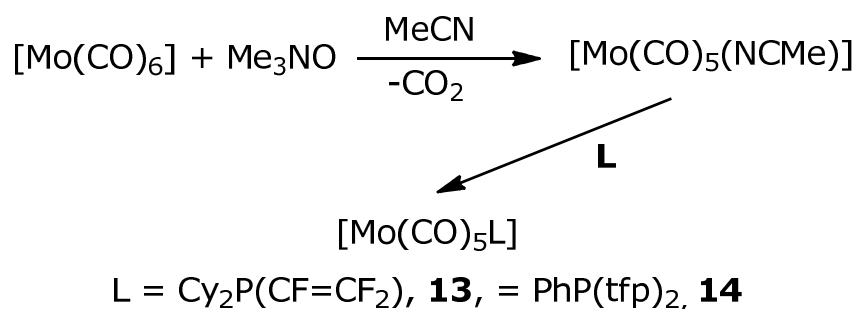
Scheme 2.9: Synthesis of [Mo(CO)$_5$L] complexes.

In the case of **3** the ^{31}P\{^{1}H\} NMR spectrum of the resulting green oil contains a single resonance, at δ 44.0 ppm, shifted +60.3 ppm relative to the starting phosphine **3**. The resonance is observed as a doublet of doublets ($^2J_{PF}$ = 39 Hz, $^3J_{PFtrans}$ = 4.6 Hz). There is no observable coupling between the

phosphorus centre and the *cis*-fluorine atom, unlike in **3**. The ^{19}F NMR spectrum contains the three signals characteristic of the perfluorovinyl moiety, at δ -82.1, -101.2, and -168.9 ppm, all of which are shifted slightly to higher frequency compared with **3**, consistent with that expected on complex formation.
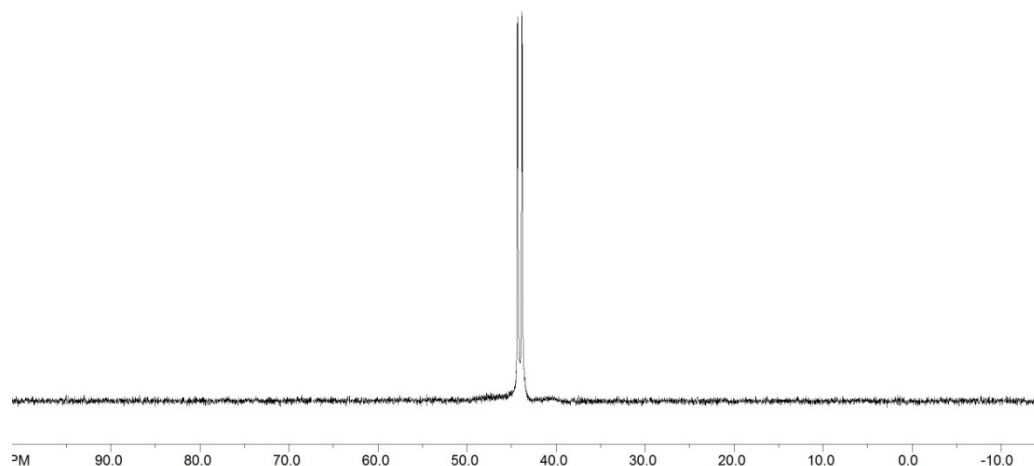
Figure 2.17: ^{31}P{^{1}H} NMR spectrum of [Mo(CO)$_5${PCy$_2$(CF=F$_2$)}], 13.

When L = PhP(tfp)$_2$, the ^{31}P{^{1}H} NMR spectrum of the complex contains a single resonance at δ -13.6 ppm; Δδ of +53.8 ppm compared to the uncoordinated phosphine. This is comparable with the only other molybdenum complex of a tfp-containing phosphine, [Mo(CO)$_5${P^{t}Bu(tfp)$_2$}], the ^{31}P{^{1}H} NMR signal of which occurs at δ 18.7 ppm, a Δδ of +60.5 ppm relative to the free ligand, and is also very similar to the Δδ observed between **3** and **13**. The ^{31}P{^{1}H} NMR signal of **14** is observed as a singlet (as observed for [Mo(CO)$_5${P^{t}Bu(tfp)$_2$}]).[186]

As discussed in Section 1.2, the infra-red stretching frequency of molybdenum pentacarbonyl phosphine complexes is one of the measures of the electronic properties of phosphorus(III) compounds. The [Mo(CO)$_5$L] (L = phosphine) complexes have C_{4v} symmetry, therefore three symmetry allowed

carbonyl absorptions in the infra-red region are expected, of which two are non-degenerate and the other doubly degenerate. These are the A_1^1, A_1^2, and E modes respectively. The infra-red spectra of **13** and **14** display peaks consistent with these expectations. The broadest, most intense peaks at around 1900 cm^{-1} is assigned to the E mode, in accordance with related systems.[33,36] Consequently, the two remaining modes are assigned to the sharper, weaker absorptions. The higher frequency A_1^1 mode is normally taken as the measure of the electronic properties of the ligand, and for [Mo(CO)$_5${PCy$_2$(CF=CF$_2$)}] this is observed at 2073 cm^{-1}; the corresponding absorption for [Mo(CO)$_5${PPh(tfp)$_2$}] is observed at 2081 cm^{-1}. The molybdenum pentacarbonyl complex of **5-(Z)** has been synthesised previously, and the higher frequency A_1^1 mode was observed at 2074 cm^{-1}.[189]

L	v/cm^{-1}	Ref
PPh$_3$	2072	190
Cy$_2$P(CF=CF$_2$), 3	2073	This work
Ph$_2$P(CF=CF^{t}Bu), 5-(Z)	2074	189
Ph$_2$P(CF=CF$_2$)	2076	36
^{t}BuP(tfp)$_2$	2079	186
PhP(tfp)$_2$, 7	2081	This work
PhP(CF=CF$_2$)$_2$	2084	36
PF$_3$	2104	190

Table 2.4: Selection of A_1 CO stretching frequencies in [Mo(CO)$_5$L] complexes.

A comparison of the electronic properties of compound **3** with similar systems suggests that **3** appears to be less electron-withdrawing than Ph$_2$P(CF=CF$_2$), as expected based on the comparative inductive effects of cyclohexyl and phenyl rings.

The data obtained for **5-(Z)** suggests that the substitution of the *trans*-fluorine atom makes the phosphine less electron withdrawing, in agreement with the observations made based on the $^1J_{PSe}$ coupling constant.

These data suggest that **7** is less electron rich than ^{t}BuP(tfp)$_2$, as expected based on the inductive effect of a Ph group *vs*. a ^{t}Bu moiety. Also, the tfp unit appears to confer less electron-withdrawing effect to the phosphorus centre than the perfluorovinyl unit. However, as currently no other sources of stereoelectronic data are available for tfp-containing phosphines, these conclusions should be considered as being preliminary in nature.

3. Saturated Fluoro-organo Containing Phosphines

Though fluorovinyl-containing phosphines have a reasonable electron-withdrawing effect, and it is possible to modify their steric demand, it would be preferable to have access to more sterically demanding systems. One manner in which this could be achieved is via the synthesis of fluoroalkyl phosphines. The report by Clarke et al.[103] in 2003 that Ph_2PCF_2Br could be prepared by the reaction of Ph_2PSiMe_3 with CF_2Br_2 (Scheme 3.1) led us to investigate the potential of this chemistry for introducing perfluoroalkyl substituents into phosphorus(III) systems.

$$Ph_2PSiMe_3 + CF_2Br_2 \longrightarrow Ph_2PCF_2Br + Me_3SiBr$$
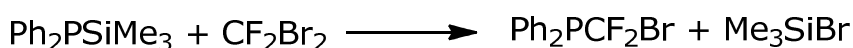
Scheme 3.1: Reaction between CF_2Br_2 and Ph_2PSiMe_3 reported by Clarke et al.[103]

The reaction between Ph_2PSiMe_3 and $(CF_3)_2CFI$ was selected to test whether a new, more versatile synthetic route to fluoroalkyl-substituted phosphines was possible based on the reaction of silyl phosphines and perfluoroalkyl iodides. This was chosen because it has been shown that Ph_2PLi reacts with $(CF_3)_2CFI$ to yield $Ph_2PCF(CF_3)_2$ and LiI,[137] and also because both materials are commercially readily available.

3.1 $Ph_2PCF(CF_3)_2$ (15)

Ph_2PSiMe_3 was dissolved in $CDCl_3$ in an NMR tube, an equimolar quantity of $(CF_3)_2CFI$ was added, and the reaction monitored via $^{31}P\{^1H\}$ and ^{19}F NMR spectroscopy.

$$Ph_2PSiMe_3 + (CF_3)_2CFI \longrightarrow Ph_2PCF(CF_3)_2 + Me_3SiI$$
$$\mathbf{15}$$
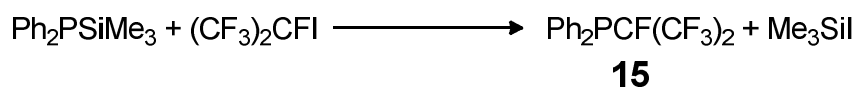
Scheme 3.2: Reaction of $(CF_3)_2CFI$ with Ph_2PSiMe_3.

The resulting $^{31}P\{^1H\}$ NMR spectrum (Figure 3.1) shows no signal corresponding to Ph_2PSiMe_3 (lit: δ −56.4 ppm);[191] instead, a single resonance at δ -0.8 ppm is observed. This signal is an overlapping doublet of septets, as would be expected for coupling to a perfluoroisopropyl group, such as in **15**. As a result, the coupling constants are assigned as $^2J_{PF}$ = 74.0 Hz and $^3J_{PF}$ = 18.0 Hz.
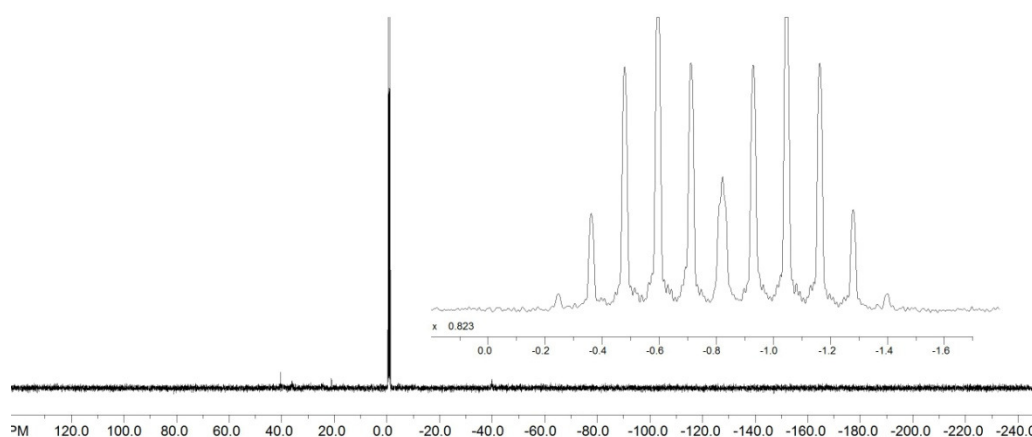
Figure 3.1: $^{31}P\{^1H\}$ NMR spectrum of the reaction between Ph_2PSiMe_3 and $(CF_3)_2CFI$. *Inset:* Expansion of the signal observed at δ -0.8 ppm.

The ^{19}F NMR spectrum no longer contains the two signals corresponding to $(CF_3)_2CFI$, a doublet at δ -74.9 ppm (lit. δ -75.0 ppm)[192] and a septet at δ -148.8 ppm (lit. δ −148.9 ppm);[193] instead two resonances are observed at δ -69.6 and -184.9 ppm (Figure 3.2). The signal at δ -69.6 ppm is a doublet of doublets, with coupling constants of 18.0 and 11.9 Hz, accounts for six fluorine atoms, and is therefore assigned to the fluorine nuclei of the two CF_3 groups. The signal at δ -184.9 ppm is a doublet of septets, with a doublet ($^2J_{PF}$) coupling of 74.0 Hz, a septet ($^3J_{FF}$) coupling of 11.0 Hz, and is assigned to the unique fluorine nucleus on the α-carbon on the basis of its chemical shift and large P−F coupling constant.

90
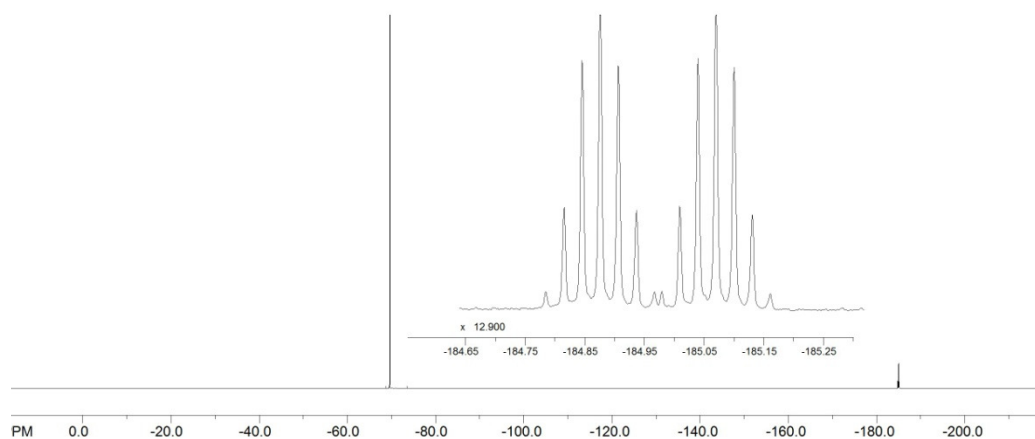
Figure 3.2: ^{19}F NMR spectrum of the reaction between Ph$_2$PSiMe$_3$ and (CF$_3$)$_2$CFI. *Inset:* **Expansion of the signal observed at δ -184.9 ppm, assigned to the unique fluorine on the α-carbon atom of the CF(CF$_3$)$_2$ group.**

The ^{1}H NMR spectrum contains two complex multiplets in the aromatic region of the spectrum, at δ 7.24–7.45 and 7.65–7.85 ppm, consistent with the presence of phenyl rings, and also shows the presence of MeSiI (lit: δ 0.8 ppm).[194] Taken together the spectroscopic data clearly indicates that Ph$_2$PCF(CF$_3$)$_2$, **15**, has been formed, and agrees with the data for this compound published subsequently by Caffyn *et al.* (^{31}P{^{1}H} NMR(C$_6$D$_6$): δ 0.65 ppm, ^{19}F NMR(C$_6$D$_6$): δ -69.8, -185.0 ppm).[195]

3.2 Extension to Other R$_f$I Species

Given the success of this preliminary experiment, a number of other R$_f$I species were reacted in a similar manner, the results of which are summarised in Table 3.1, and subsequently discussed.

R_fI	Product	$^{31}P\{^1H\}$ NMR (δ/ppm)
$(CF_3)_2CFI$	$Ph_2PCF(CF_3)_2$, **15**	-0.8
CF_3I	Ph_2PCF_3, **16**	2.5
C_2F_5I	$Ph_2PC_2F_5$, **17**	-1.9
$^sC_4F_9I$	$Ph_2P(^sC_4F_9)$, **18**	3.6
cyc-$C_6F_{11}I$	$Ph_2P(cyc$-$C_6F_{11})$, **19**	-3.1
$^tC_4F_9I$	$Ph_2P(^tC_4F_9)$, **20**	15.2
$^nC_8F_{17}I$	$Ph_2P(^nC_8F_{17})$, **21**	1.0
$(1$-$CF_3)$-cyc-C_5F_8I	$Ph_2P(pfmcp)$, **22**	-16.1
CF_2=CFI	No reaction	n/a
C_6F_5I	No reaction	n/a

Table 3.1: Summary of Ph_2PR_f compounds (and their ^{31}P NMR chemical shifts) synthesised via reaction of Ph_2PSiMe_3 and corresponding R_fI.

With the exception of compounds **16** and **17** which have been reported previously, though prepared via different routes, six new phosphines have been synthesised, and compounds **18**, **19**, **20** and **22** are the first examples of phosphines bearing these particular fluoroalkyl groups. It is noteworthy that the reaction with pentafluorophenyl iodide with Ph_2PSiMe_3 does not result in the formation of $Ph_2PC_6F_5$. Similarly, the reaction of CF_2=CFI with Ph_2PSiMe_3 does not yield diphenyl perfluorovinyl phosphine, $Ph_2P(CF$=$CF_2)$.

The data obtained for compounds **16** and **17** shows good agreement with literature values. Compound **16** gives the expected quartet in the $^{31}P[^1H]$ NMR spectrum at δ 2.5 ppm with a coupling constant of 73.8 Hz (lit: δ 1.7 ppm, $^2J_{PF}$ = 74.0 Hz),[107] and compound **17** exhibits a doublet of quartets at δ -1.9 ppm in $^{31}P\{^1H\}$ NMR spectrum with coupling constants of 56.8 and 16.9 Hz (lit: δ -1.4 ppm, J = 58.0, 17.0 Hz).[99] Owing to these compounds being previously reported they will not be discussed further.

3.2.1 Ph_2P ($^sC_4F_9$) (18)

The addition of a stoichiometric amount of $^sC_4F_9I$ to Ph_2PSiMe_3 resulted in the evolution of heat and a deepening of the yellow colour of the solution.

$$Ph_2PSiMe_3 + sC_4F_9I \xrightarrow{CDCl_3} Ph_2P(sC_4F_9) + Me_3SiI$$

18
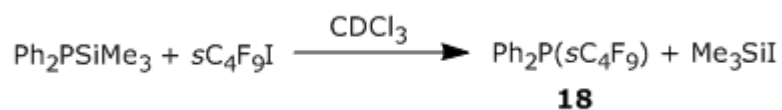
Scheme 3.3: Reaction of $^sC_4F_9I$ with Ph_2PSiMe_3.

The labelling scheme depicted in Figure 3.3 will be used for **18** (and its derivatives, see later).
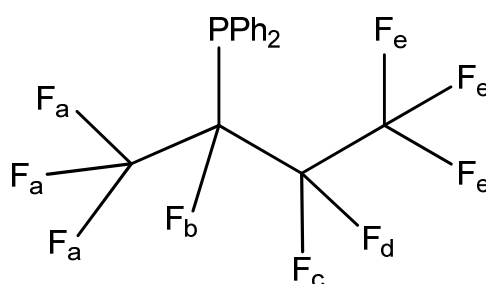
Figure 3.3: Labelling diagram of $Ph_2P(^sC_4F_9)$.

In a similar way to the reaction between Ph_2PSiMe_3 and $(CF_3)_2CFI$, the $^{31}P\{^1H\}$ NMR spectrum recorded immediately following the addition of *sec*-C_4F_9I no longer showed a signal corresponding to Ph_2PSiMe_3, instead a complex multiplet centred at δ 3.6 ppm (Figure 3.4) was observed.
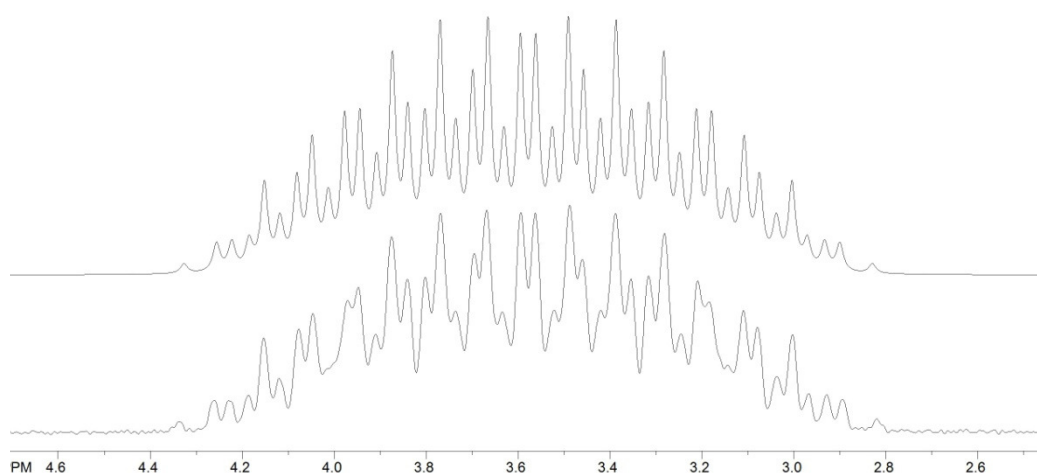
Figure 3.4: Expansion and simulation (top) of the signal observed at δ 3.6 ppm in the $^{31}P\{^1H\}$ NMR spectrum of 18.

93

The signal shown in Figure 3.4 was modelled using the program SpinWorks[200] as an overlapping doublet of quartets of doublets of doublets of quartets (in order of decreasing coupling constant, which are displayed in Table 3.2). The simulated spectrum clearly agrees well with that observed experimentally.

The ^{19}F NMR spectrum of **18** contains five complex signals, centred at δ -67.6, -79.8, -110.5, -114.3 and -183.3 ppm (Figure 3.5–Figure 3.8), with relative intensities of 3:3:1:1:1, and were also simulated using SpinWorks.[196]

The signal shown in Figure 3.5 appears in the region of the spectrum commonly associated with CF$_3$ groups, and corresponds to an overlapping doublet of doublet of doublet of quartets of doublets. It is therefore assigned to F$_a$.

PM   -67.44 -67.46 -67.48 -67.50 -67.52 -67.54 -67.56 -67.58 -67.60 -67.62 -67.64 -67.66 -67.68 -67.70 -67.72 -67.74 -67.76 -67.78 -67.80 -67.82 -67.84 -67.86
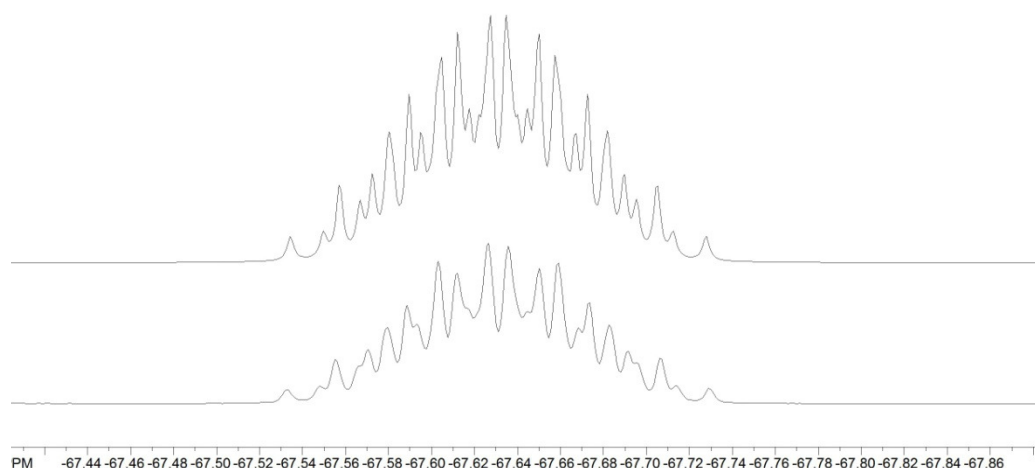
Figure 3.5: Expansion of signal at δ -67.6 ppm in the ^{19}F NMR spectrum of 18, assigned to F$_a$ (top spectrum is simulated spectrum).

The signal shown in Figure 3.6 also corresponds to a CF$_3$ moiety (based on its chemical shift and integration), and is observed as a doublet of doublet of quartets (the remaining doublet are too small to be resolved, but have been determined from the simulated spectra, and these are listed in Table 3.2).

-79.64 -79.66 -79.68 -79.70 -79.72 -79.74 -79.76 -79.78 -79.80 -79.82 -79.84 -79.86 -79.88 -79.90 -79.92 -79.94 -79.96 -79.98 -80.00
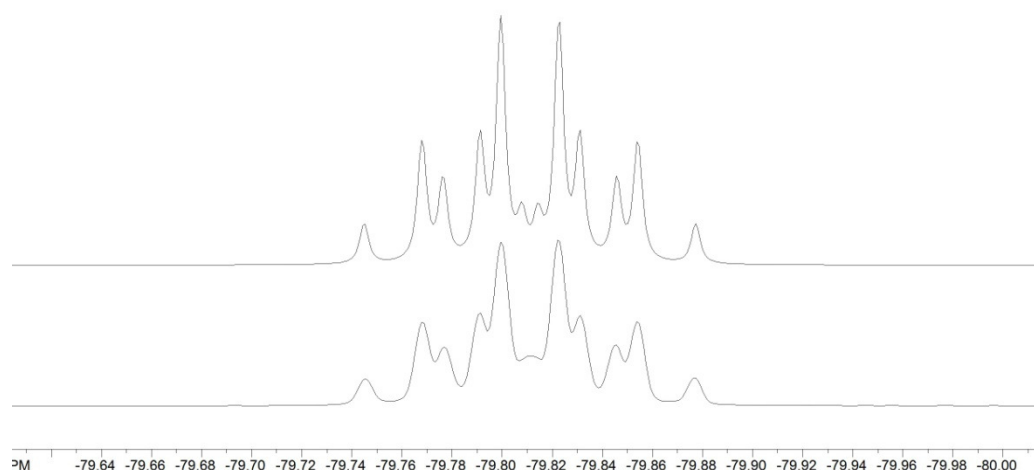
Figure 3.6: Expansion of signal at δ -79.8 ppm in the ^{19}F NMR spectrum of 18, assigned as F_e (top spectrum is simulated spectrum).

The signals at δ -110.5 and -114.3 ppm (Figure 3.7) have a large mutual doublet coupling of 295 Hz, indicative of a vicinal fluorine-fluorine ($^2J_{FF}$) interaction. This can only arise if the fluorine atoms are chemically inequivalent, and in this compound the α-carbon is chiral – thus F_c and F_d are diastereotopic, and consequently chemically inequivalent. The signals also show slight second order effects, as the chemical shift difference between the signals is less than five times the coupling constant (~1450 vs 295 Hz).

PM -109.8 -110.2 -110.6 -111.0 -111.4 -111.8 -112.2 -112.6 -113.0 -113.4 -113.8 -114.2 -114.6 -115.0
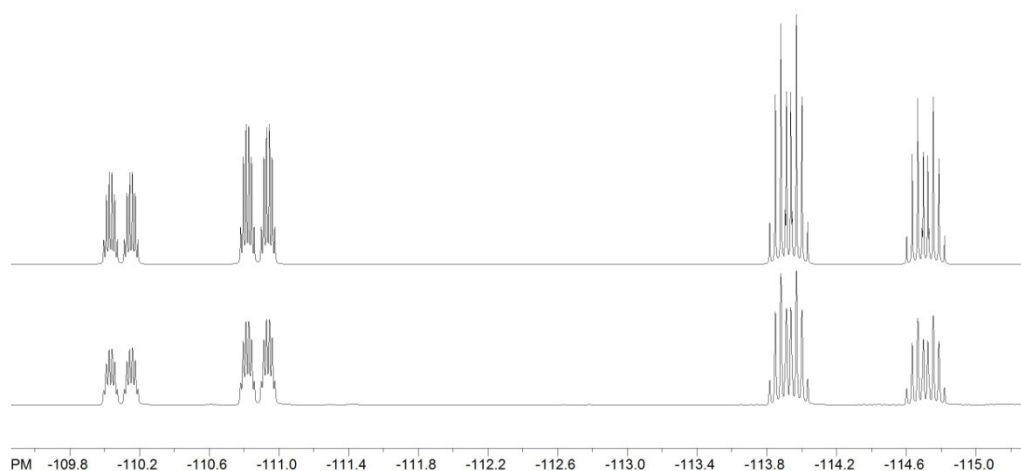
Figure 3.7: Expansion of signals for F_c and F_d in the ^{19}F NMR spectrum of 18, displaying second order effects (top spectrum is the simulated spectrum).

The signal at δ -110.4 is a doublet of doublet of doublet of quartets, whereas the signal occurring at δ -114.3 ppm is a doublet of doublet of quartet of doublets. Both signals show coupling to the phosphorus centre, though the P–F coupling constant found in the signal at δ -110.4 ppm is ~33% larger than in the signal at δ -114.3 ppm (44.6 *vs.* 33.2 Hz), listed in Table 3.2.
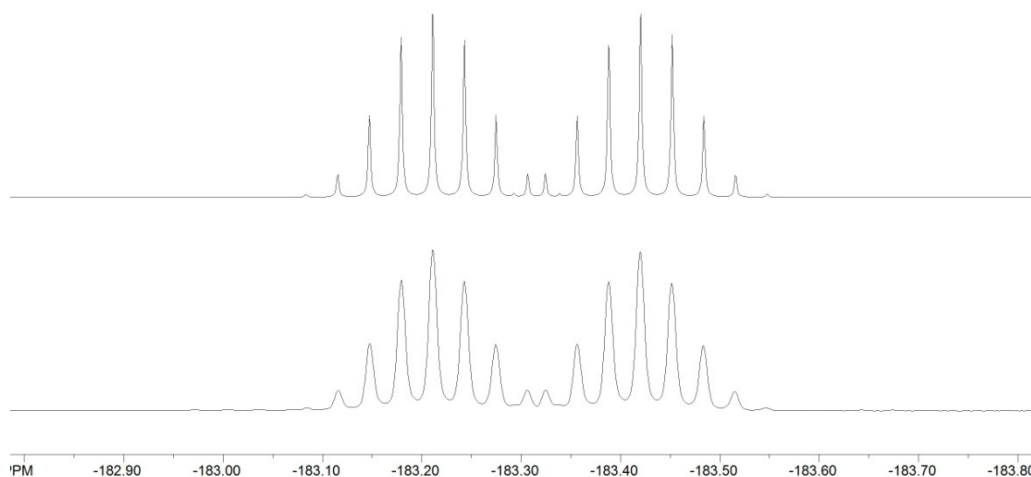
Figure 3.8: Expansion of signal observed at δ -183.3 ppm in the ^{31}P[^{1}H] NMR spectrum of 18 assigned to F$_b$ (top spectrum is simulated spectrum).

The final signal in the ^{19}F NMR spectrum of **18** occurs at δ -183.3 ppm; it is a doublet of quartet of doublet of quartet of doublets (Figure 3.8), and arises from F$_b$.

	F$_e$	F$_d$	F$_c$	F$_b$	F$_a$
P	11.5	33.7	44.6	78.8	16.9
Fa	8.6	12.3	5.7	12.1	
Fb	12.0	12.0	11.9		
Fc	0.6	295.6			
Fd	0.1				

Table 3.2: Summary of coupling constants found in 18 (calculated from the simulated spectrum).

The ^{1}H NMR spectrum contains two complex multiplets, both in the aromatic region of the spectrum, at δ 7.22-7.34 and 7.69-7.79 ppm, confirming the presence of the aromatic groups attached to phosphorus.

The ^{13}C{^{1}H} NMR spectrum of this compound is complicated. In the aromatic region of the spectrum there are eight peaks, instead of the expected four. These eight peaks suggest that the two phenyl rings are inequivalent, and as **18** possesses a chiral centre at the α-carbon, the phenyl rings are diastereotopic, meaning that they will be chemically inequivalent, and therefore giving rise to separate sets of peaks in the ^{13}C{^{1}H} NMR spectrum.

3.2.2 Ph$_2$P(*cyc*-C$_6$F$_{11}$) (19)

The addition of *cyc*-C$_6$F$_{11}$I to a solution of Ph$_2$PSiMe$_3$ in CDCl$_3$ at room temperature resulted in the evolution of heat and a change of the solution to a yellow colour (*cf.* Section 4.3).

$$\text{Ph}_2\text{PSiMe}_3 + cyc\text{-C}_6\text{F}_{11}\text{I} \xrightarrow{\text{CDCl}_3} \text{Ph}_2\text{P}(cyc\text{-C}_6\text{F}_{11}) + \text{Me}_3\text{SiI}$$
19

Scheme 3.4: Reaction of *cyc*-C$_6$F$_{11}$I with Ph$_2$PSiMe$_3$.

The labelling scheme depicted in Figure 3.9 will be used for **19**.
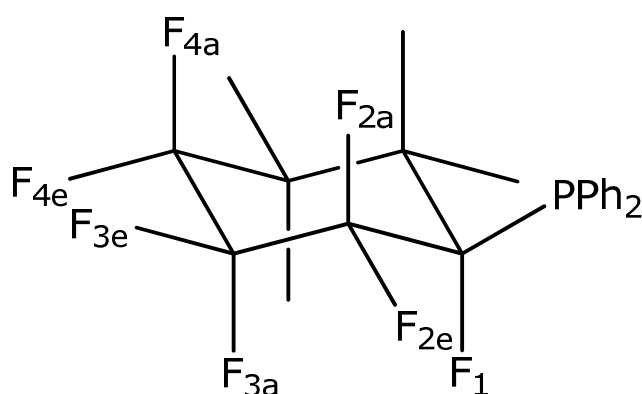
Figure 3.9: Labelling diagram for Ph$_2$P(*cyc*-C$_6$F$_{11}$), 19.

The $^{31}P\{^1H\}$ NMR spectrum of **19** exhibits a resonance at δ -3.1 ppm, and is interpreted as a binomial triplet of doublets (see Figure 3.10).
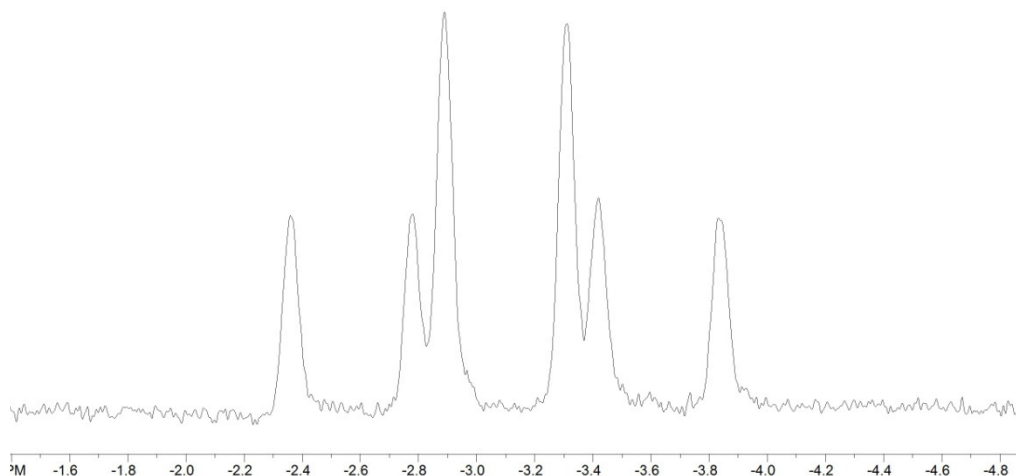
Figure 3.10: Expansion of the signal observed at δ -3.1 ppm in the $^{31}P\{^1H\}$ NMR spectrum of 19.

Given that the diphenylphosphino- moiety is sterically much more demanding than a fluorine atom, it is expected that the $-PPh_2$ group will occupy an equatorial position on the perfluorocyclohexyl ring. The phosphorus nucleus couples to the vicinal fluorine atom giving rise to a doublet based pattern with a similar magnitude ($^2J_{PF}$ = 68.0 Hz) to that observed for compounds **15** and **18**. The triplet coupling arises from the interaction of the phosphorus atom with both F_{2e} nuclei, due to their small dihedral angle resulting in a relatively large ($^3J_{PF}$ = 84.0 Hz) coupling constant. There does not appear to be any measurable coupling between the phosphorus atom and the F_{2a} nuclei.

The ^{19}F NMR spectrum of compound **19** displays seven resonances similar in appearance to the resonances observed for cyc-$C_6F_{11}I$ and therefore assigned in a similar way at δ -110.5 (2F, F_{2e}), -122.6 (2F, F_{3a}), -124.4 (1F, F_{4a}), -

124.5 (2F, F_{2a}), -138.2 (2F, F_{3e}), -142.0 (1F, F_{4e}), and -185.8 (1F, F_1) ppm (Figure 3.11).
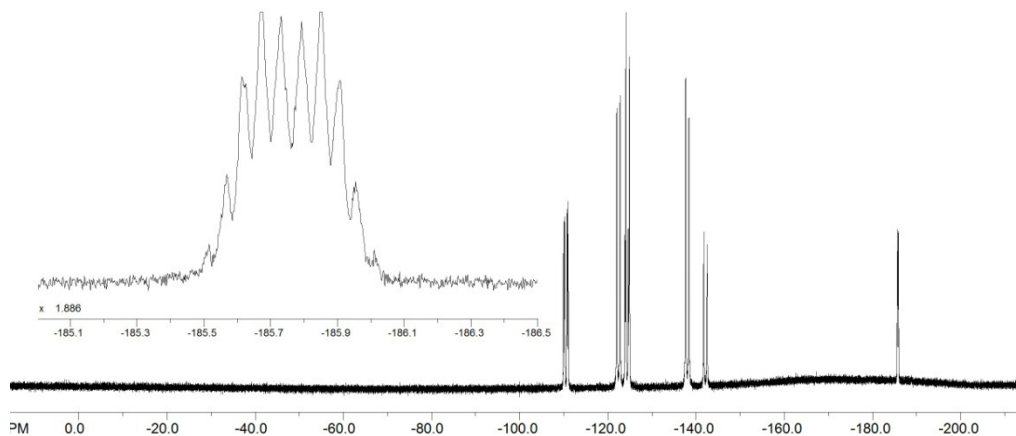
Figure 3.11: ^{19}**F NMR spectrum of 19.** *Inset*: **Expansion of signal occurring at δ -185.8 ppm.**

The signals at δ -110.5 and -185.8 ppm also display additional doublet couplings of 84 and 67 Hz respectively. The signal at δ -185.8 ppm is assigned as F_1, based on its chemical shift and the mutual coupling constant shared with the ^{31}P{^{1}H} NMR spectrum. The signal at δ -110.5 ppm is assigned as F_{2e}, on the assumption that P-F coupling constants follow the Karplus relationship. The geminal coupling constants are all different, therefore the signal at δ -124.5 ppm is assigned as F_{2a} (as this signal shares a $^2J_{FF}$ coupling constant of 298.6 Hz with F_{2e}). The signals at δ -124.4 and -142.0 ppm only correspond to a single fluorine nucleus in each case, and they are therefore assigned as F_{4e} and F_{4a} respectively, leaving the signals at δ -122.6 and δ -138.2 ppm which are assigned as F_{3e} and F_{3a} respectively (the axial/equatorial assignments are made in accordance with related systems).[197,198]

The ^{1}H NMR spectrum, as observed for **15** and **18**, contains two multiplets in the aromatic region of the spectrum, at δ 7.24–7.28 and 7.56–7.62 ppm,

99

consistent with the presence of the phenyl rings. The $^{13}C\{^1H\}$ NMR spectrum also confirms the presence of the aromatic groups, with three doublets centred at δ 128.8 ($^3J_{PC}$ = 6.6 Hz, *meta*), 134.0 ($^1J_{PC}$ = 22.5 Hz, *ipso*) and 136.1 ppm ($^2J_{PC}$ = 27.6 Hz, *ortho*) and a singlet at 130.4 ppm (*para*). The spectrum also contains some extremely complex multiplets between δ 104.0 and 111.0 ppm, as would be expected for a perfluorocyclohexyl group.

These data unequivocally show that **19** has been successfully synthesised, and is the first example of a phosphine containing a perfluorocyclohexyl group.

3.2.3   Ph$_2$P(^{t}C$_4$F$_9$) (20)

The addition of ^{t}C$_4$F$_9$I to a CDCl$_3$ solution of Ph$_2$PSiMe$_3$ in a similar way to those described above results in the evolution of heat, and results in a $^{31}P\{^1H\}$ NMR spectrum that contains a number of unidentifiable species. However, conducting the addition of perfluorotertiarybutyl iodide at low (-30°C) temperature results in a more controllable reaction accompanied by a change in colour of the solution from pale yellow to a slightly darker yellow.

$$Ph_2PSiMe_3 + {}^tC_4F_9I \xrightarrow{\text{CDCl}_3} Ph_2P({}^tC_4F_9) + Me_3SiI$$
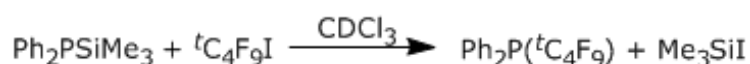
Scheme 3.5: Reaction of ^{t}C$_4$F$_9$I with Ph$_2$PSiMe$_3$.

The $^{31}P\{^1H\}$ NMR spectrum of this solution is less complex than that of the perfluorosecondary butyl derivative. The spectrum displays a resonance at δ 15.2 ppm; it is observed as a binomial dectet (see Figure 3.12; however, the two outside lines are almost indistinguishable above the noise) with $^3J_{PF}$ = 12.3 Hz.

PM 16.8 16.6 16.4 16.2 16.0 15.8 15.6 15.4 15.2 15.0 14.8 14.6 14.4 14.2 14.0 13.8 13.6
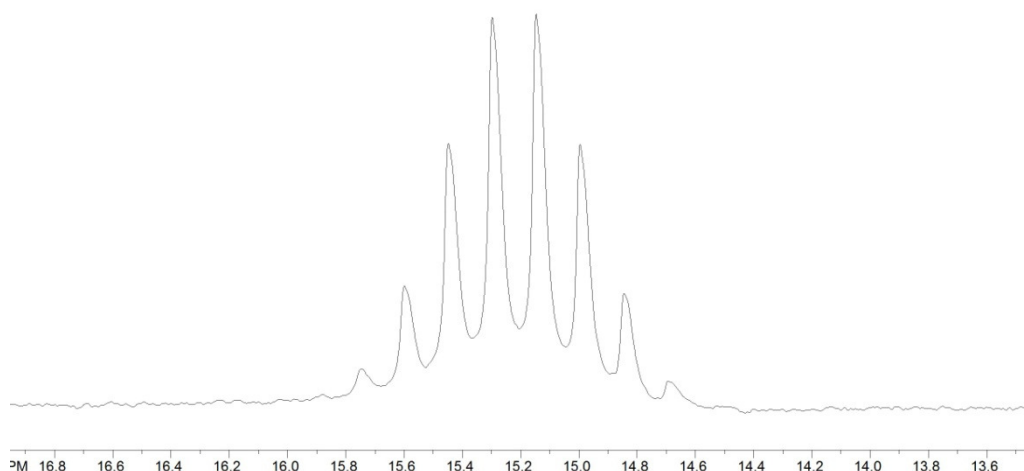
Figure 3.12: Expansion of signal observed at δ 15.2 ppm in the ^{31}P{^{1}H} NMR spectrum of the reaction between Ph$_2$PSiMe$_3$ and ^{t}C$_4$F$_9$I

The ^{19}F NMR spectrum is also much simpler than that of the perfluorosecondary butyl variant **18**, displaying a doublet at δ -59.9 ppm, with $^3J_{PF}$ = 12.3 Hz.

The ^{1}H NMR spectrum confirms the loss of the Me$_3$Si group, by the presence of a singlet at δ 0.81 ppm, with ^{29}Si satellites, corresponding to Me$_3$SiI, and the presence of the aromatic groups with a multiplet observed at δ 7.4–7.7 ppm.

These spectra are consistent with that expected for **20** (in terms of chemical shifts, multiplicities and magnitude of the coupling constant), and is the first example of a perfluorotertiarybutyl-containing phosphine.

3.2.4 Ph$_2$P(^{n}C$_8$F$_{17}$) (21)

Long-chain perfluoro-organo containing compounds have in recent years been of research interest owing to the development of Fluorous Biphase Catalysis.[199-203] Several phosphorus based ligands suitable for Fluorous Biphase Catalysis have been previously synthesised – based on long fluoroalkyl chains which are usually electronically insulated (typically by –

101

CH$_2$CH$_2$– or –C$_6$H$_4$– fragments) to protect the phosphorus centre from the electron withdrawing effect of the fluoro-organo fragment.[199,200]

Therefore, it may be of interest to synthesise phosphorus ligands bearing long-chain perfluorocarbon fragments, as these may have some potential utility in Fluorous Biphase applications but with electronic properties that differ from the usual fluorous ligands.

The addition of $^nC_8F_{17}I$ to a CDCl$_3$ solution of Ph$_2$PSiMe$_3$ in an NMR tube resulted in a slight colour change of the solution over a period of three weeks.

$$Ph_2PSiMe_3 + {}^nC_8F_{17}I \xrightarrow{\text{CDCl}_3} Ph_2P({}^nC_8F_{17}) + Me_3SiI$$
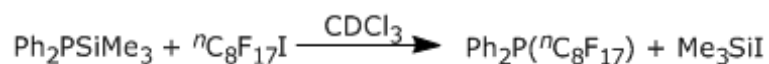
Scheme 3.6: Reaction of Ph$_2$PSiMe$_3$ and $^nC_8F_{17}$I.

The ^{31}P{^{1}H} NMR spectrum (Figure 3.13) of this reaction mixture contains a signal at δ 1.0 ppm which is interpreted as an overlapping binomial triplet of triplets of triplets ($^2J_{PF}$ = 56.2 Hz, $^3J_{PF}$ = 33.4 Hz, $^4J_{PF}$ = 11.5 Hz).
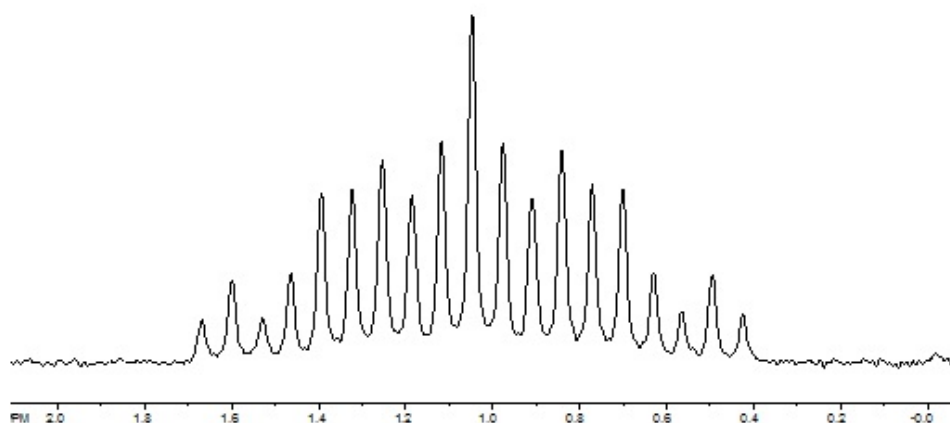
Figure 3.13: Expansion of signal observed at δ 1.0 ppm in the ^{31}P{^{1}H} NMR spectrum of the reaction of Ph$_2$PSiMe$_3$ and $^nC_8F_{17}$I.

The ^{19}F NMR spectrum of this compound displays seven resonances, six of which are observed in the region that would be expected for CF_2 groups, and the remaining signal is observed at δ -81.1 ppm, and accounts for three fluorine nuclei, and so is assigned as the CF_3 group. The signal at δ -108.9 ppm is a complex doublet based pattern ($^2J_{PF}$ = 56.1 Hz), and is therefore assigned as the CF_2 directly attached to the phosphorus centre. The remaining five signals account for the other twelve fluorine atoms; they are all complex multiplets. The ^{1}H NMR spectrum displays a complex multiplet at δ 7.4–7.7 ppm, confirming the presence of the aromatic moieties.

Taken together the multinuclear NMR data confirms the formation of the desired compound, $Ph_2P^nC_8F_{17}$, **21**.

3.2.5 Ph$_2$P(pfmcp) (pfmcp = perfluoromethylcyclopentyl) (22)

The addition of one equivalent of perfluoro-1-iodo-1-methylcyclopentane to a $CDCl_3$ solution of Ph_2PSiMe_3 (Scheme 3.7) results in a colour change of the solution to yellow, and the evolution of a moderate amount of heat.

$$Ph_2PSiMe_3 + (pfcmp)I \xrightarrow{CDCl_3} Ph_2P(pfmcp) + Me_3SiI$$

Scheme 3.7: Reaction of Ph$_2$PSiMe$_3$ with (pfmcp)I.

The ^{31}P{^{1}H} NMR spectrum of the product of this reaction displays a single complex resonance at δ -16.1 ppm; it is a quartet of triplets of triplets (see Figure 3.14; $^3J_{PF}$ = 39.0 Hz, $^3J_{PF}$ = 11.8 Hz, $^3J_{PF}$ = 4.2 Hz).
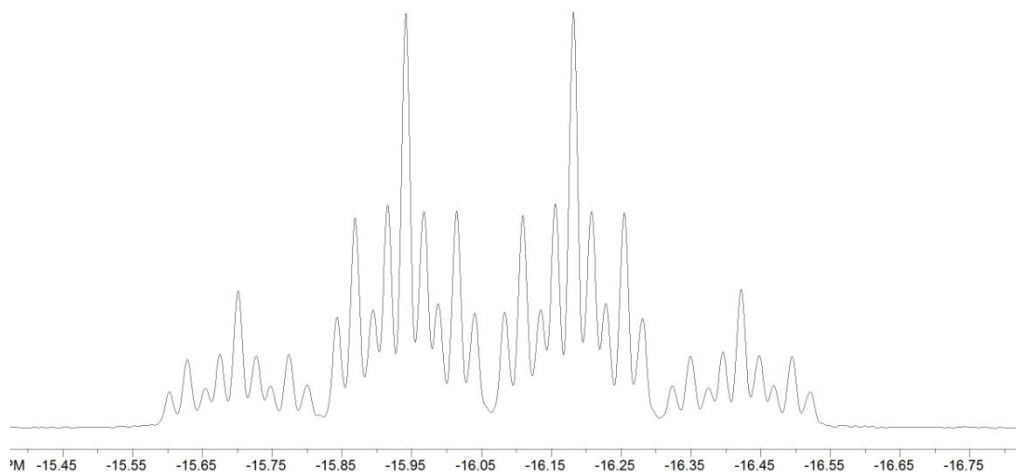
Figure 3.14: Expansion of the signal occurring at δ -16.1 ppm in the ^{31}P{^{1}H} NMR spectrum of the reaction between Ph$_2$PSiMe$_3$ with perfluoro-1-iodo-1-methylcyclopentane.

The observed pattern in Figure 3.14 can be explained by the phosphorus nuclei coupling to a CF$_3$ unit, and two equivalent pairs of fluorine atoms (that is, coupling to the fluorine nuclei circled in orange, red, and blue in Figure 3.15), as would be expected in the desired compound.
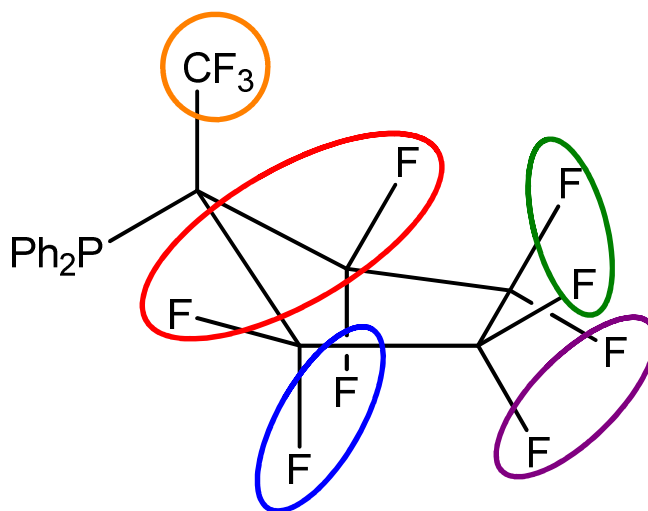
Figure 3.15: Representation of expected environments in 22.

The ^{19}F NMR spectrum of Ph$_2$P(pfmcp) is complex. The spectrum displays resonances at δ -59.6, -106.0, -111.6, and -132.1 ppm (see Figure 3.16),

and a further signal at δ -157.6; this last resonance is a dectet (J = 7.5 Hz) with ^{29}Si satellites (4.7%, I = ½, J = 274.5 Hz) indicating the presence of Me$_3$SiF in the reaction mixture (see Section 3.7 for further discussion of the mechanism of this reaction).
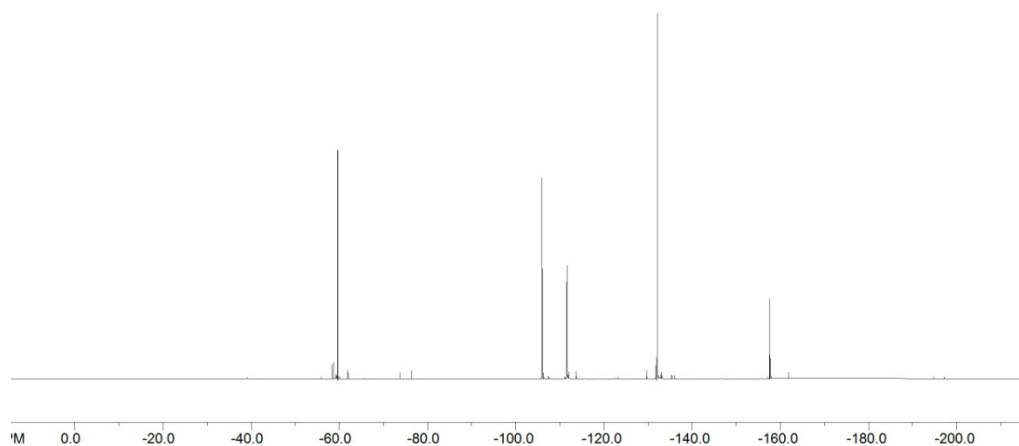
Figure 3.16: ^{19}F NMR spectrum after the reaction between Ph$_2$PSiMe$_3$ and perfluoro-1-iodo-1-methylcyclopentane.

The signal observed at δ -59.6 ppm (see Figure 3.17) appears to be a doublet of septets, with the doublet coupling of 39.0 Hz, shared with the quartet resonance in the ^{31}P{^{1}H} NMR spectrum. On the basis of these data, the signal at δ -59.6 ppm is assigned to the CF$_3$ group. The apparent septet is, however, not binomial, with relative intensities of 1:2:3:4:3:2:1. The couplings that give rise to this splitting pattern are unclear.
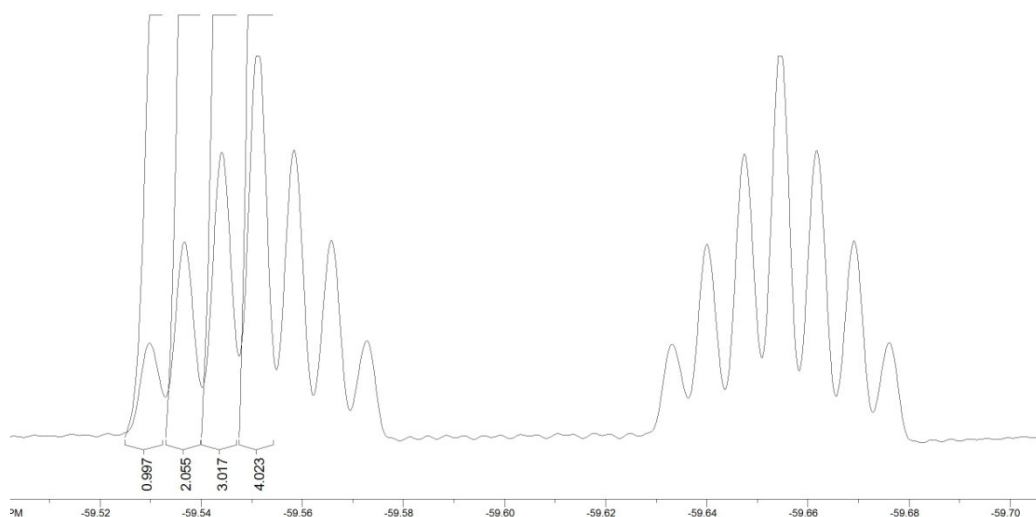
Figure 3.17: Expansion of the resonance observed at δ -59.6 ppm in the ^{19}F NMR spectrum of 22 showing relative intensities of the multiplet.

The signals at δ -106.0 and -111.6 ppm are both complex multiplets (see Figure 3.18), and as such cannot be assigned with absolute certainty.
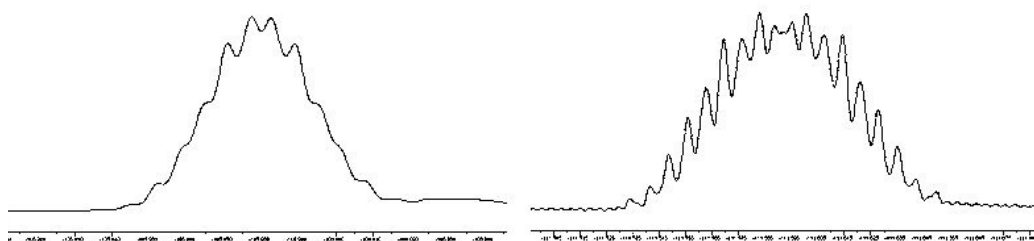
Figure 3.18: Expansion of the signals occurring at δ -106.0 ppm (left) and δ - 111.6 ppm (right) in the ^{19}F NMR spectrum of 22.

The remaining signal at δ -132.1 ppm (see Figure 3.19) appears to be a binomial pentet, though slightly broadened, with an apparent coupling of 4.4 Hz.
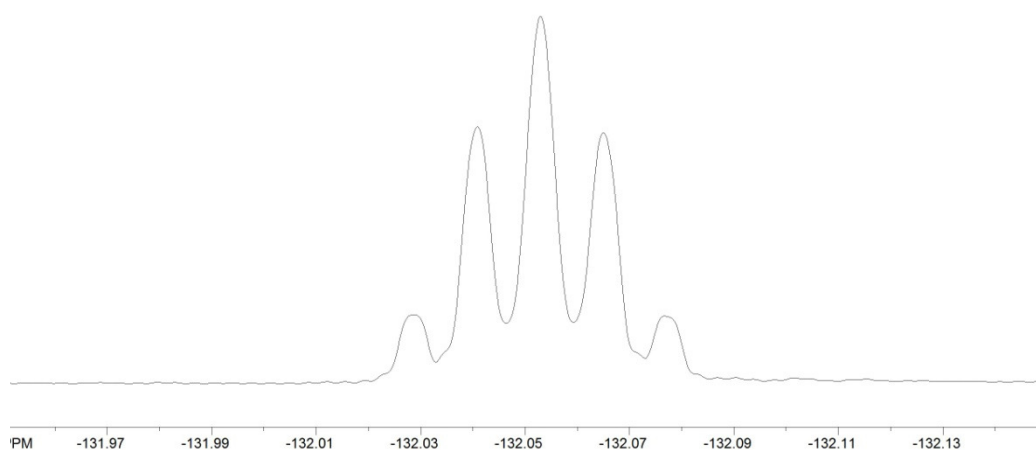
Figure 3.19: Expansion of signal occurring at δ -132.1 ppm in the ^{19}F NMR spectrum of 22.

From the data obtained via the ^{31}P{^{1}H} NMR spectrum, it appears that there are three distinct fluorine environments which couple to the phosphorus centre – the CF_3 group, and the four fluorine atoms on the β-carbons. This would suggest that the remaining signal in the ^{19}F NMR spectrum should be equivalent to the remaining four fluorine nuclei present in the molecule.

It might be anticipated that the pfmcp group should contain five distinct resonances, from the five different environments shown in Figure 3.15. However, the ^{19}F NMR spectrum (Figure 3.17) shows only four signals.

Further, the integrals of the signals do not fit with those expected. If the resonance assigned to the CF_3 group is calibrated as three, the remaining three signals each integrate to 2.7 fluorine nuclei – thus accounting for the remaining eight fluorine nuclei.

Cyclopentane is known to exist in a number of conformations, which are of similar energy,[204] with the two extremes being known as the envelope and the half-chair (see Figure 3.20).

Envelope   Half-Chair
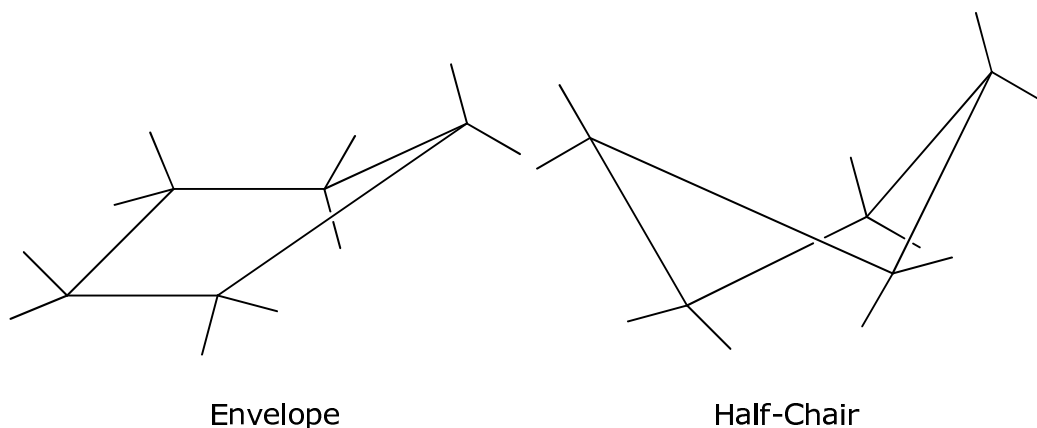
Figure 3.20: The two "extreme" conformations of cyclopentane.

It has been determined that in solution cyclopentane changes between these forms, in what is known as a pseudorotation circuit.[205] This pseudorotation circuit consists of twenty distinctly different conformations. Adding substituents to the ring can alter this pseudorotation circuit, as it would be expected to cause changes in the energy required to obtain particular conformations,[206] but the compound will still exist in several different, yet similar (at least energetically) states.

It is expected that the $-PPh_2$ moiety will occupy the equatorial position preferentially (although strictly speaking the positions of the substituents are only approximately comparable to those of cyclohexanes, the terms axial and equatorial being applied for simplicity),[204] owing to it being sterically more demanding than a CF_3 group. This will limit the number of conformers available. There are reports in the literature of the pfmcp compounds *cyclo-*$C_5F_8XCF_3$ (X = F,[207] Cl,[208] I,[209] CF_3,[210] SCN)[211] – though none of the ^{19}F NMR spectra of these compounds exhibit the complexities seen in the spectrum of $Ph_2P(pfmcp)$. There are also no reports on the nature of phosphorus-fluorine coupling constants in ring systems such as these, and consequently whether or not they follow a Karplus-type relationship, and anyway, the Karplus relationship in the case of cyclopentanes is more complex than that of

cyclohexanes.[212] In this compound the phosphorus centre appears to couple to both the "axial" and "equatorial" fluorine nuclei, unlike in Ph$_2$P(F-Cy), **21** (in which the phosphorus atom only couples to the equatorial fluorine atoms (85 Hz) – the dihedral angle being comparatively small), and both coupling constants are relatively small. The apparent "scrambling" of the eight fluorine nuclei into three signals has not been noted before in the literature, and is presumably due to there being a limited number of conformers of similar energies available in the pseudorotation circuit.

3.3 Partially Fluorinated Substituents

3.3.1 Ph$_2$PCHFCF$_3$ (23)

Having shown that the reaction between Ph$_2$PSiMe$_3$ and iodoperfluoroalkanes generates Ph$_2$PR$_f$ compounds, a similar reaction with CF$_3$CFHI was attempted (see Scheme 3.8), in order to see if this methodology could be extended to partially fluorinated systems.

$$Ph_2PSiMe_3 + CF_3CFHI \xrightarrow{CDCl_3} Ph_2PCFHCF_3 + Me_3SiI$$
$$\textbf{23}$$
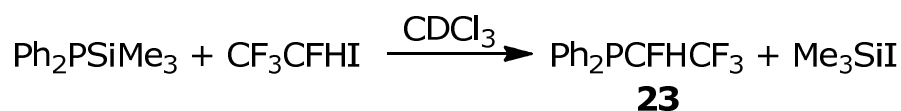
Scheme 3.8: Reaction between Ph$_2$PSiMe$_3$ and CF$_3$CFHI.

The addition of CF$_3$CFHI to a CDCl$_3$ solution of Ph$_2$PSiMe$_3$ results in a slight colour change of the solution from colourless to pale yellow. The ^{31}P{^{1}H} NMR spectrum shows the appearance of a signal at δ -13.0 ppm which is a binomial doublet of quartets ($^2J_{PF}$ = 71.0 Hz, $^3J_{PF}$ = 20.7 Hz), as shown in Figure 3.21.
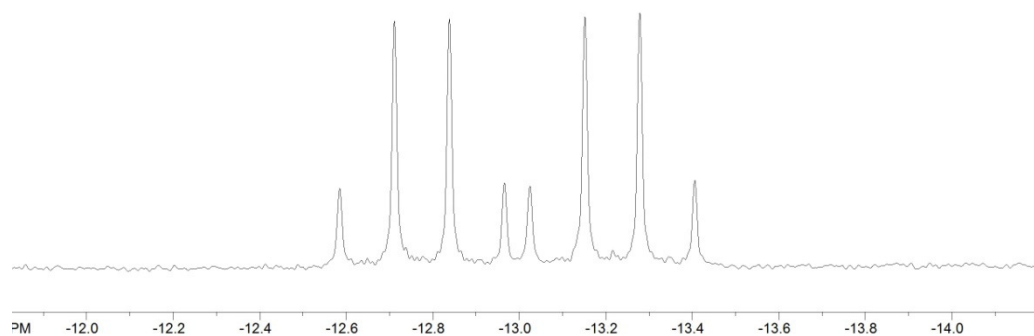
Figure 3.21: Expansion of the signal observed at δ -13.0 ppm in the ^{31}P{^{1}H} NMR spectrum of 23.

The ^{19}F NMR spectrum of **23** contains two peaks corresponding to the target compound. There is a signal observed in the CF$_3$ region of the spectrum, at δ -72.3 ppm which is a binomial doublet of doublet of doublets ($^3J_{PF}$ = 20.7 Hz, $^3J_{FF}$ = 16.8 Hz, and $^3J_{FH}$ = 8.4 Hz).

The other signal is centred at δ -206.4 ppm (see Figure 3.22) and is a binomial doublet of doublet of quartets ($^2J_{PF}$ = 71.0 Hz, $^2J_{FH}$ = 46.5 Hz, $^3J_{FF}$ = 16.8 Hz). This assignment of the fluorine-proton coupling constants is confirmed from the ^{19}F{^{1}H} NMR spectrum, where both signals lose the appropriate doublet coupling.

110

-206.06 -206.10 -206.14 -206.18 -206.22 -206.26 -206.30 -206.34 -206.38 -206.42 -206.46 -206.50 -206.54 -206.58 -206.62 -206.66 -206.70
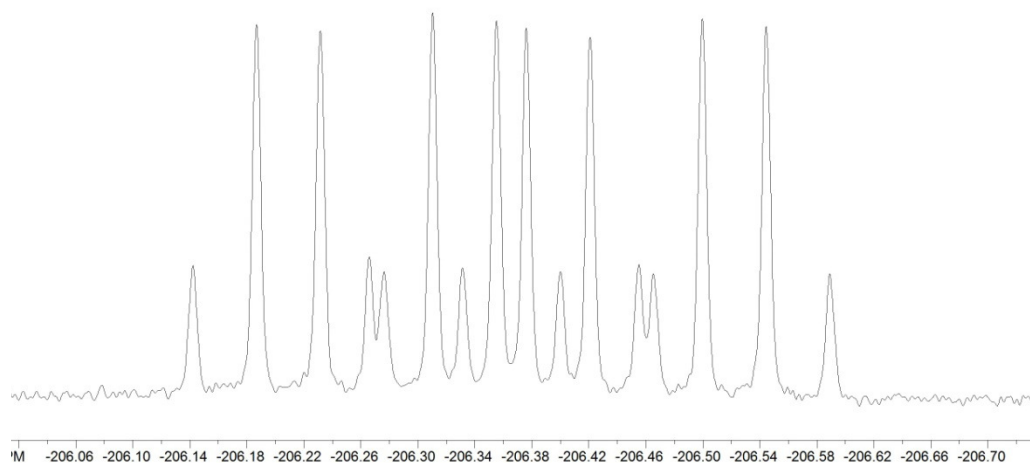
Figure 3.22: Expansion of the signal observed at δ -206.4 ppm in the ^{19}F NMR spectrum of 23.

Further support for this assignment comes from the quaternary salt $[Ph_2BzPCFHCF_3]^+Br^-$ formed serendipitously in the reaction between $Ph_2P(CF=CF_2)$ and BzBr,[137] the spectra of which show similar chemical shifts, multiplicities and magnitude of coupling constants to those observed for **23**.

The ^{1}H NMR spectrum contains a complex multiplet in the aromatic region, as expected owing to the presence of the two phenyl rings. There is also a signal centred at δ 6.66 ppm; the signal is observed as a doublet of quartets ($^2J_{HF}$ = 46.4 Hz, $^3J_{HF}$ = 8.3 Hz).

Taken together these data confirm the successful synthesis of compound **23**.

3.4 Variation of Non-fluorinated Groups

All of the new phosphines reported thus far contain the same non-fluorinated groups. If such a route is to be widely applicable then it should be capable of being used for other related systems. To this end other trimethylsilyl-containing phosphorus(III) starting materials have been prepared, and their reactions with perfluoroalkyl iodides investigated.

111

3.4.1 ^{i}Pr$_2$P(C$_2$F$_5$) (24)

The synthesis of ^{i}Pr$_2$PSiMe$_3$ was achieved by stirring an equimolar mixture of ^{i}Pr$_2$PCl and Me$_3$SiCl in THF with an excess of lithium. The generation of ^{i}Pr$_2$PSiMe$_3$ was confirmed by ^{31}P{^{1}H} NMR spectroscopy (δ -43.2 ppm, lit. δ -42.7 ppm).[213]
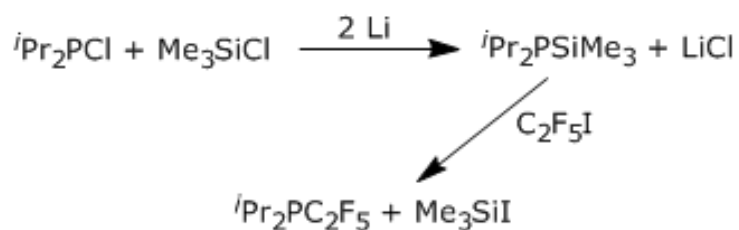
Scheme 3.9: Formation of ^{i}Pr$_2$P(C$_2$F$_5$).

The careful addition of C$_2$F$_5$I to a CDCl$_3$ solution of ^{i}Pr$_2$PSiMe$_3$ resulted in a change in colour of the solution from colourless to yellow.

The ^{31}P{^{1}H} NMR spectrum of the resultant yellow solution showed that the signal corresponding to ^{i}Pr$_2$PSiMe$_3$ had been replaced by a new peak, centred at δ 24.4 ppm. This signal is a triplet of quartets (see Figure 3.23, $^2J_{PF}$ = 41.6 Hz, $^3J_{PF}$ = 14.6 Hz), similar in appearance to that observed for **17**.
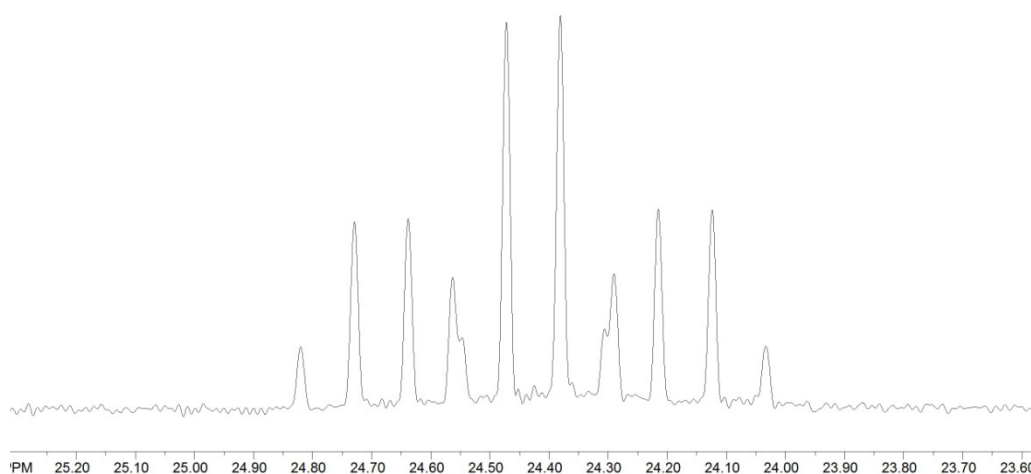
Figure 3.23: Expansion of signal observed at δ 24.4 ppm in the ^{31}P{^{1}H} NMR spectrum of ^{i}Pr$_2$PC$_2$F$_5$.

112

The ^{19}F NMR spectrum of the same solution displays a pair of signals, a doublet of triplets centred at δ −82.4 ppm, and a doublet of quartets at δ −111.7 ppm. The doublet coupling constant in both of these signals matches those observed in the ^{31}P{^{1}H} NMR spectrum, confirming that the C_2F_5 group is bound to the phosphorus centre. They also share a mutual $^3J_{FF}$ coupling constant of 2.8 Hz.

The ^{1}H NMR spectrum contains the expected two signals for an isopropyl group, at δ 2.19 ppm (septet of doublets) and δ 1.15 ppm (doublet of quartets). The unexpected observation of a quartet coupling arising from the CF_3 group on the CH_3 signal at δ 1.15 ppm despite there being six bonds in between these atoms, is assumed to arise from through-space coupling.

3.4.2 $^iPr_2P(^nC_3F_7)$ (25)

In the manner described for the synthesis of compound **24**, $^iPr_2PSiMe_3$ was reacted with a stoichiometric quantity of $^nC_3F_7I$ which resulted in a colour change of the solution from pale yellow to a much deeper yellow, and the evolution of heat (Scheme 3.10).

$$^iPr_2PSiMe_3 + {}^nC_3F_7I \xrightarrow{CDCl_3} {}^iPr_2P^nC_3F_7 + Me_3SiI$$
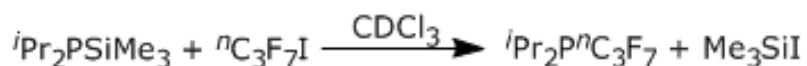
Scheme 3.10: Formation of $^iPr_2P(^nC_3F_7)$.

The ^{31}P{^{1}H} NMR spectrum of the resulting solution shows a triplet of triplet of quartets at δ 27.2 ppm (see Figure 3.24), as expected for this system, with $^2J_{PF}$ = 36.5, $^3J_{PF}$ = 29.6, and $^4J_{PF}$ = 6.9 Hz.
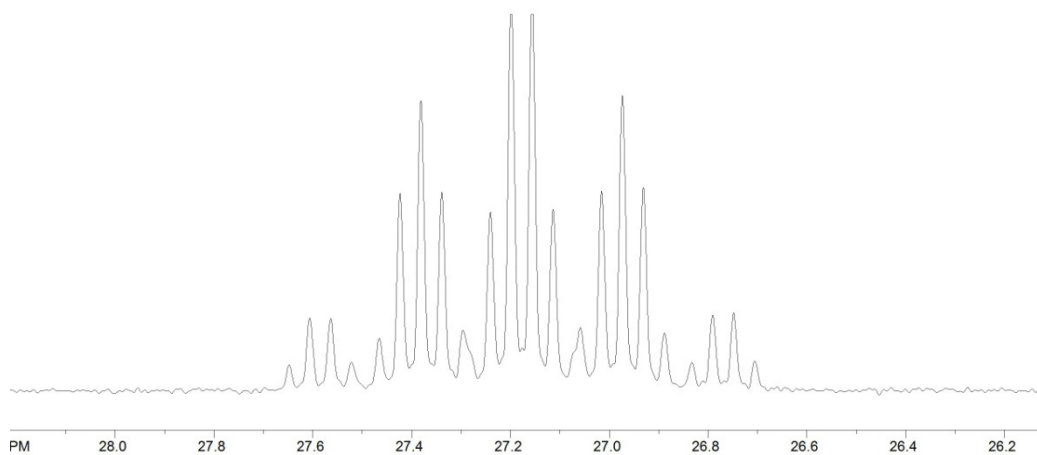
Figure 3.24: Expansion of signal at δ 27.2 ppm in the ^{31}P{^{1}H} NMR spectrum of the reaction between ^{i}Pr$_2$PSiMe$_3$ and ^{n}C$_3$F$_7$I.

The ^{19}F NMR spectrum of this compound contains three major signals, at δ -79.9, -109.4 and -123.3 ppm. The resonance occurring at δ -79.9 ppm (Figure 3.25) is observed as a triplet of doublets ($^{2}J_{FF}$ = 10.4, $^{4}J_{PF}$ = 6.8 Hz), and shares the doublet coupling with the quartet coupling seen in the ^{31}P{^{1}H} NMR spectrum, and as such the signal is assigned to the CF$_3$ fluorine nuclei.
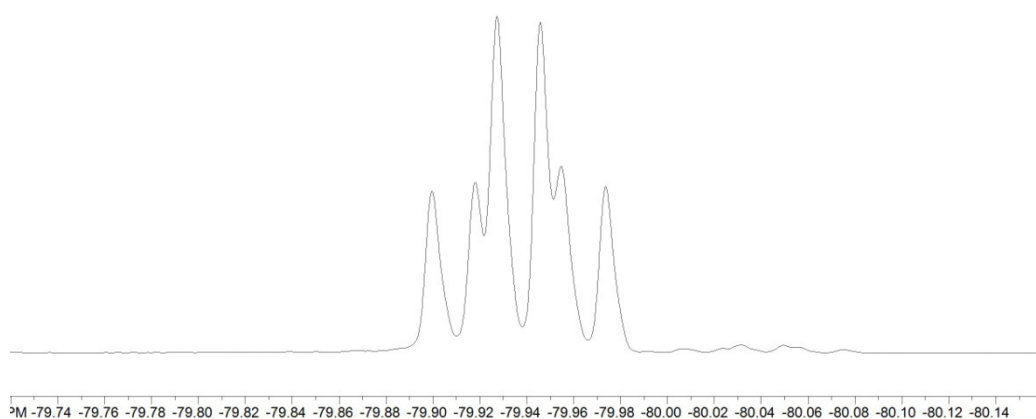
Figure 3.25: Expansion of signal occurring at δ -79.9 ppm in the ^{19}F NMR spectrum of 24.

The signal at δ -109.4 ppm (see Figure 3.26) is observed to be a doublet of quartets ($^2J_{FP}$ = 36.4, $^4J_{FF}$ = 10.5 Hz), though there appears to be some additional fine structure. Based on the magnitude of the coupling constant shared with the resonance observed in the $^{31}P\{^1H\}$ NMR spectrum, this signal is assigned to the CF$_2$ group closest to the phosphorus centre.
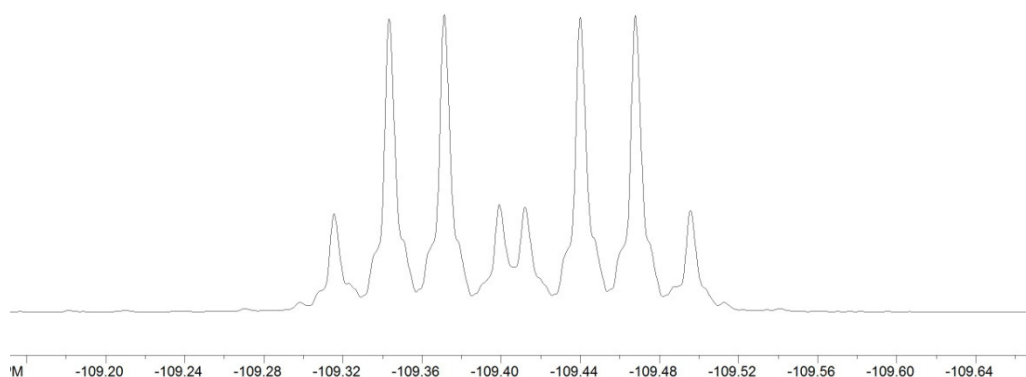
Figure 3.26: Expansion of the signal observed at δ -109.4 ppm in the $^{19}F\{^1H\}$ NMR spectrum of 24.

The remaining signal at δ -123.3 ppm is observed as a doublet ($^3J_{PF}$ = 29.7 Hz). This signal corresponds to the remaining CF$_2$ group in the compound. Interestingly, the fluorine nuclei do not exhibit a detectable coupling to the other fluorine nuclei in the molecule, despite the CF$_3$ fluorine atoms coupling to the distant CF$_2$ fluorine centre. This particular property of *n*-heptafluoropropyl compounds has been noted previously, in CF$_3$CF$_2$CF$_2$X (X = Cl, H)[214,215] though there is no explanation given for the apparent lack of coupling in these cases.

3.4.3 PhMePCF(CF$_3$)$_2$ (26)

The synthesis of this compound was pursued because the resulting compound would provide a rare example of a P-chiral phosphine which possessed a perfluoroalkyl group.

On addition of $(CF_3)_2CFI$ to a solution of $PhMePSiMe_3$ (formed from the reaction of Ph_2PMe with an excess of Li wire, and subsequent addition of two equivalents of Me_3SiCl; Scheme 3.11) in THF there is a colour change of the solution from colourless to yellow. The removal of the solvent results in the isolation of an off-white solid.

$$Ph_2PMe + 2\ Li \longrightarrow PhMePLi + PhLi$$

$$\downarrow 2\ Me_3SiCl$$

$$PhMePCF(CF_3)_2 \xleftarrow{(CF_3)_2CFI} PhMePSiMe_3 + Me_3SiPh$$
$$\textbf{25}$$
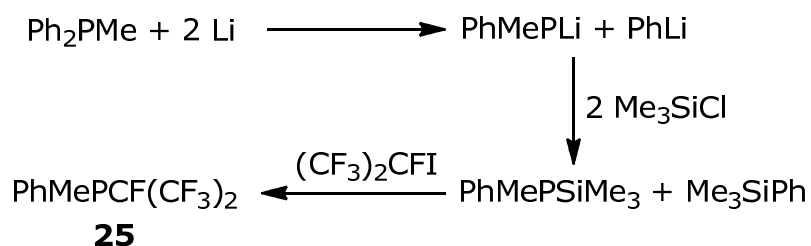
Scheme 3.11: Synthesis of 26.

The $^{31}P\{^1H\}$ NMR spectrum of this solid in $CDCl_3$ (see Figure 3.27) contains a signal that is similar in appearance to the signal observed for **15**; it is an overlapping doublet of septets ($^2J_{PF}$ = 61.1 Hz, $^3J_{PF}$ = 16.4 Hz) at δ -12.0 ppm.

PM -10.6   -10.8   -11.0   -11.2   -11.4   -11.6   -11.8   -12.0   -12.2   -12.4   -12.6   -12.8   -13.0   -13.2   -13.4
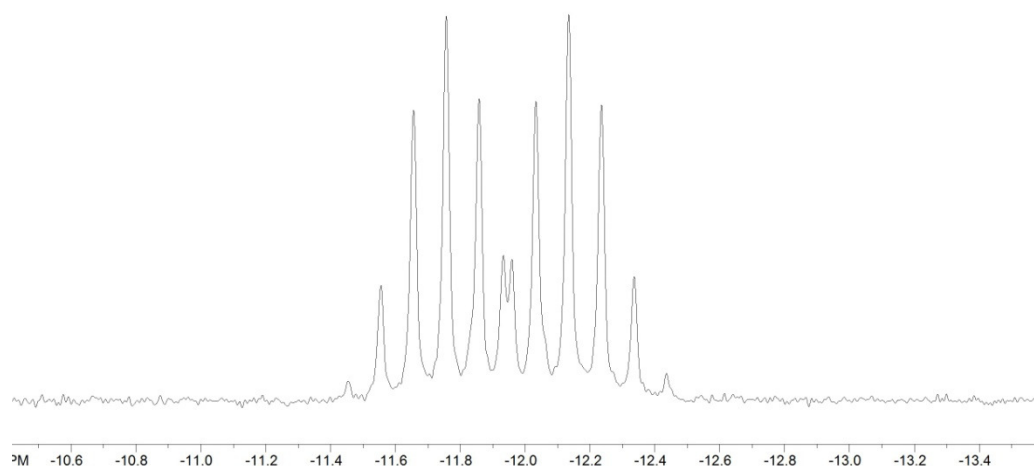
Figure 3.27: Expansion of signal observed at δ -12.0 ppm in the $^{31}P\{^1H\}$ NMR spectrum of 26.

The ^{19}F NMR spectrum of the white solid is interesting. The resonance for the unique fluorine nuclei is observed at δ -190.3 ppm, further downfield than **15** (δ -184.9 ppm). The resonance appears as a doublet of septets, as expected ($^2J_{PF}$ = 61.1 Hz, $^3J_{FF}$ = 11.2 Hz). The CF$_3$ region is more complicated, with two CF$_3$ signals present in the spectrum. Both signals are three times as intense as the signal at δ -190.3 ppm, suggesting that the two CF$_3$ groups are chemically inequivalent. Owing to the chirality of the molecule, the fluorine atoms within the CF$_3$ moieties are diastereotopic (as opposed to enantiotopic in **15**), and consequently chemically inequivalent, giving rise to two CF$_3$ groups which couple to one another as shown in Figure 3.28.
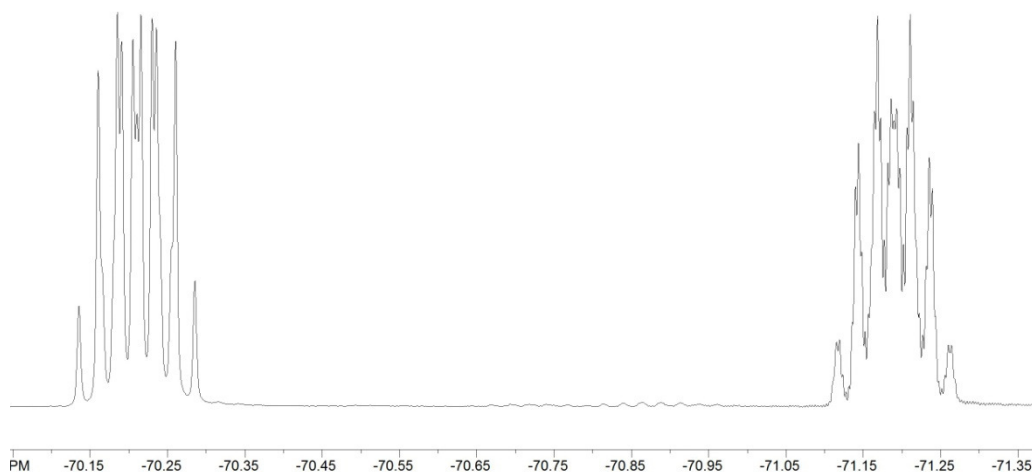
Figure 3.28: CF$_3$ region of the ^{19}F NMR spectrum of 26.

Also, one of the CF$_3$ signals exhibits an extra quartet coupling (J = 1.5 Hz) (see Figure 3.29), which is not present in the ^{19}F{^{1}H} NMR spectrum, and is presumably due to through-space coupling of the fluorine nuclei with the protons of the methyl group.
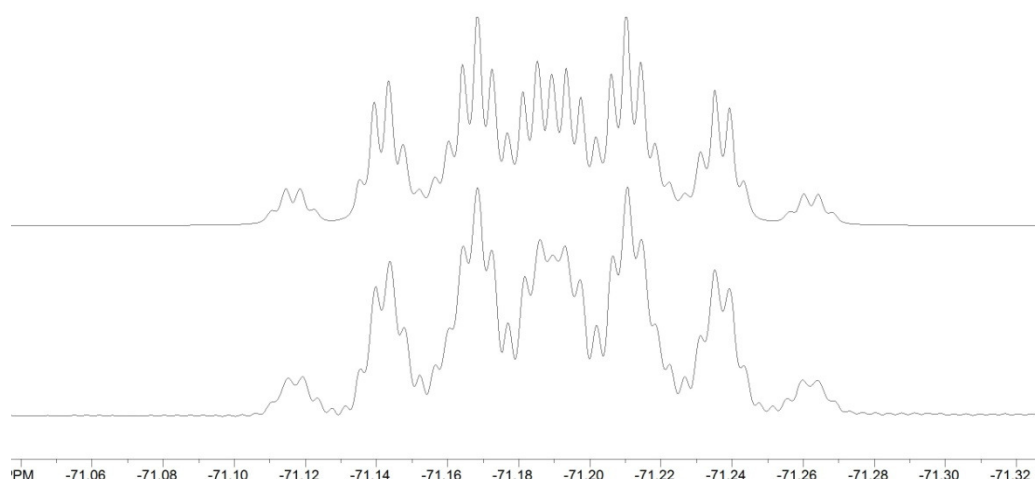
Figure 3.29: Expansion (bottom) and simulation (top) of the CF$_3$ signal observed at δ -71.2 ppm in the ^{19}F NMR spectrum of 26, displaying the quartet coupling to the CH$_3$ group.

Based on the multinuclear NMR data, in particular the presence of two CF$_3$ signals, and the chemical shift in the phosphorus NMR spectrum (δ -12.0 ppm, Grim's Law predicts a chemical shift of δ -16 ppm for **26**), it is concluded that the desired compound has been formed.

3.5 Scale-Up

Given the success of these preliminary, small-scale experiments synthesis on a preparative scale was undertaken, so as to be able to further characterise and investigate the chemistry of these compounds.

3.5.1 Ph$_2$PCF(CF$_3$)$_2$ (15)

As outlined above, due to cost and ease of handling, preliminary large-scale reactions involving Ph$_2$PSiMe$_3$ and (CF$_3$)$_2$CFI were chosen as the starting point.

The reaction of these two compounds in a variety of reaction conditions/temperatures/work-up procedures was evaluated. The most successful method was found to be the slow addition of a stoichiometric

118

amount of $(CF_3)_2CFI$ to a solution of Ph_2PSiMe_3 in hexane (prepared in a glovebox) under an atmosphere of dinitrogen or argon at -0°C, and then allowing the mixture to slowly warm to room temperature. The volatiles were removed under a high vacuum to afford spectroscopically pure **15**, which, if necessary, was distilled under vacuum (98°C/1.0 mmHg). It appears that temperature control is important, as allowing the mixture to warm too quickly results in the formation of other phosphorus containing species, which are as yet unidentified.

$$Ph_2PSiMe_3 + (CF_3)_2CFI \xrightarrow[\text{-30°C}]{\text{Hexane}} Ph_2PCF(CF_3)_2 + Me_3SiI$$

Figure 3.30: Scale-up procedure for synthesis of 15.

Compound **15** is a low melting (m.p. 48°C) white solid, with a distinct but not unpleasant odour. The solid appears stable to air, but if left in solution (pentane) it converts (quantitatively inside 72 hours at 4°C) to the phosphine oxide, **29**, $O=PPh_2CF(CF_3)_2$ (see section 4.3.1 for details of this compound).

Upon slow cooling of a heated sample of **15** needle-like single crystals formed which were suitable for X-ray diffraction studies. Solution of the data obtained resulted in the molecular structure shown in Figure 3.31.
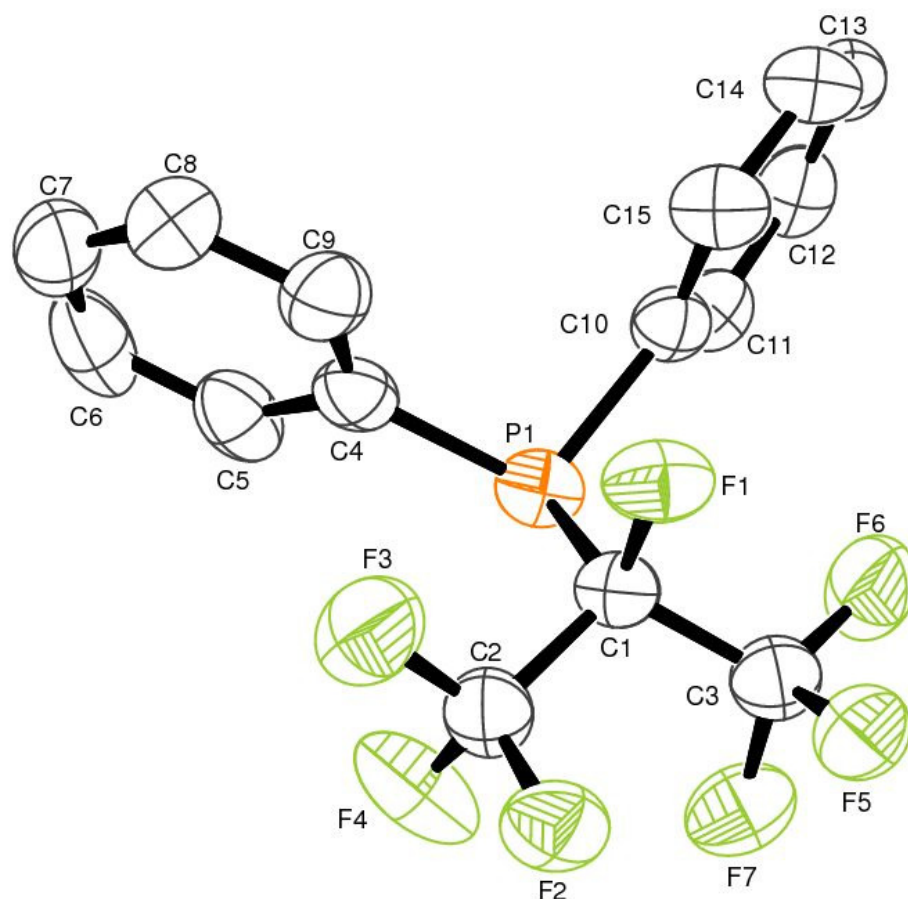
Figure 3.31: ORTEP[174] (Oak Ridge Thermal Ellipsoid Program) representation of the molecular structure of 15, with thermal ellipsoids at 50%. Hydrogen atoms are omitted for clarity.

Compound **15** crystallises in the monoclinic space group $P2_1$/c and contains four molecules in the unit cell. The P–C_F bond length is slightly longer than the average P–C_{Ar} distance (1.899(5) Å vs. 1.830(5) Å). There are few datasets with which to directly compare these distances, as only two X-ray diffraction studies of fluorinated phosphines are available in the Cambridge Structural Database (CSD). However, in both cases, very similar P–CF distances are observed (*cf*. PhP(CF=CF$_2$)$_2$ d(P-C_F) = 1.830(3) Å, Ph$_2$PCF$_2$CF$_3$ d(P-C_F) = 1.891(3) Å).[36,100] The C2–F4 bond is shorter at 1.296(6) Å than the other C–F bonds (see Table 3.3 for a selection of bond lengths). There are no particularly noteworthy intermolecular contacts, though the distances between P1···F4 and P1···F6 are 0.31 Å shorter (on average) than the sum of

the van der Waals radii for phosphorus and fluorine. The unique fluorine F1 also has two short contacts, to fluorine atoms on both CF_3 groups (F3 = 2.571(4) Å, F5 = 2.590(4) Å). This is presumably due to the size of the perfluorisopropyl fragment.

Bond	Distance (Å)	Bond	Distance (Å)
P1−C1	1.899(5)	C2−F3	1.341(6)
P1−C4	1.828(5)	C3−F5	1.328(5)
P1−C10	1.831(5)	C3−F6	1.314(6)
C1−F1	1.400(5)	C3−F7	1.351(6)
C2−F4	1.296(6)	C1−C2	1.539(6)
C2−F2	1.331(5)	C1−C3	1.531(7)

Table 3.3: Selected bond lengths in 15.

The sum of the C-P-C bond angles around the phosphorus centre is larger at 309.6° in **15** (see Table 3.4 for a selection of bond angles) than in either $Ph_2P(CF=CF_2)_2$ (299.6°)[36] or **17** (304.2°),[100] which suggests that it is the largest perfluoroalkyl-containing phosphine to be structurally characterised.

Bond Angle	Angle (Å)
C1−P1−C4	102.9(2)
C1−P1−C10	103.6(2)
C4−P1−C10	103.1(2)
P1−C1−F1	114.8(3)

Table 3.4: Selection of bond angles in 15.

As shown in Figure 3.32 in the extended structure the molecules stack in the z-direction. There is also some offset π-stacking in the x-direction, with a centroid to centroid distance of 3.914(3) Å.
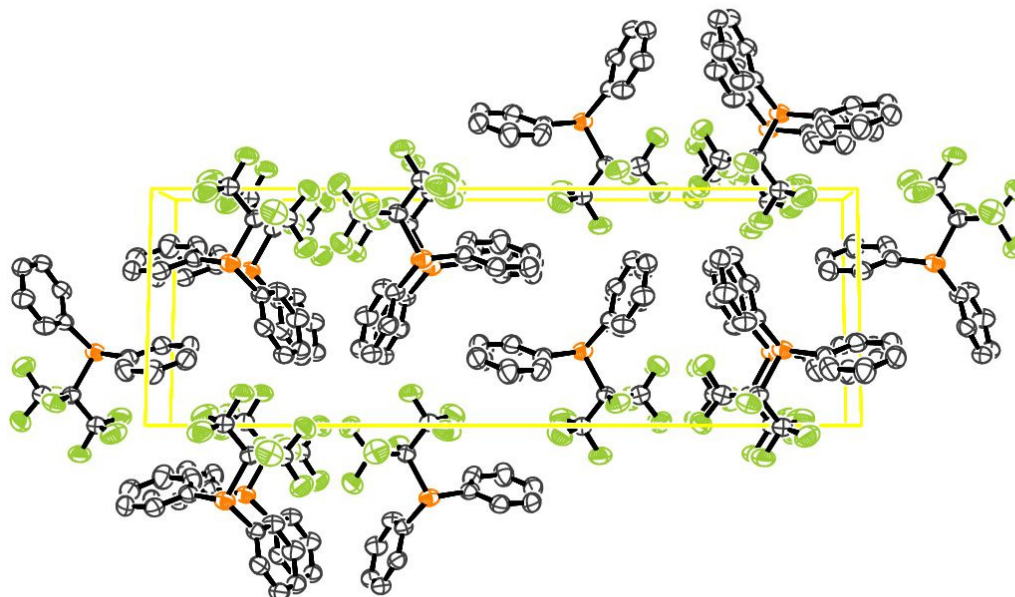
Figure 3.32: Diagram showing the stacking of 15 in the z-direction.

3.5.2   Ph$_2$P (^{s}C$_4$F$_9$) (18)

In a similar fashion to compound **15**, **18** was also prepared on a multi-gram scale, to afford the title compound as a colourless liquid after vacuum distillation. Multinuclear NMR data consistent with the small-scale experiment was obtained (Section 3.2.1) and the compound was characterised by elemental analysis. Compound **18** also has a strong but not unpleasant odour.

3.5.3   Other Perfluoroalkyl Phosphines

Currently the preparative scale reactions in the case of the perfluorocyclohexyl and perfluorotertiarybutyl derivatives results in the formation of the desired compound, however, separation and purification has proven unsuccessful thus far. However, some chemistry of the perfluorocyclohexyl derivative **19** (e.g. oxidation, see later sections) has been accomplished on the crude phosphine.

3.6 Reaction of (CF$_3$)$_2$CFI with PhP(SiMe$_3$)$_2$

The reaction of PhP(SiMe$_3$)$_2$ and iodoperfluoroalkanes was investigated, in the hope that this would result in the synthesis of *bis*-perfluoroalkyl phosphines. Unfortunately, *bis*-trimethylsilyl phosphines are not commercially available, so PhP(SiMe$_3$)$_2$ was synthesised from PhPH$_2$, ^{n}BuLi and Me$_3$SiCl (see Scheme 3.12) and its structure confirmed via multinuclear NMR studies.

$$PhPH_2 + 2\ n\text{BuLi} \xrightarrow{\text{THF}} PhPLi_2 + 2\ BuH \xrightarrow{2\ Me_3SiCl} PhP(SiMe_3)_2 + 2\ LiCl$$
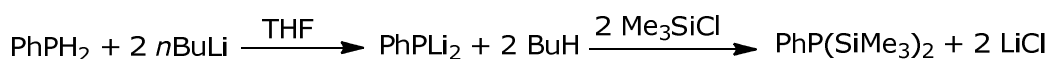
Scheme 3.12: Formation of PhP(SiMe$_3$)$_2$.

The reaction of (CF$_3$)$_2$CFI with PhP(SiMe$_3$)$_2$ was undertaken in a similar manner to the large scale formation of **15**, with work-up affording a colourless liquid. The ^{31}P{^{1}H} NMR spectrum of PhP(CF(CF$_3$)$_2$)$_2$ is expected to be a complex triplet based multiplet centred at approximately δ +5 – 10 ppm (*cf.* PhP(CF$_2$CF$_3$)$_2$ δ +3.5 ppm);[99] however the major resonance observed in the ^{31}P{^{1}H} NMR spectrum of the liquid obtained from this reaction was found at δ -42.3 ppm (see Figure 3.33).
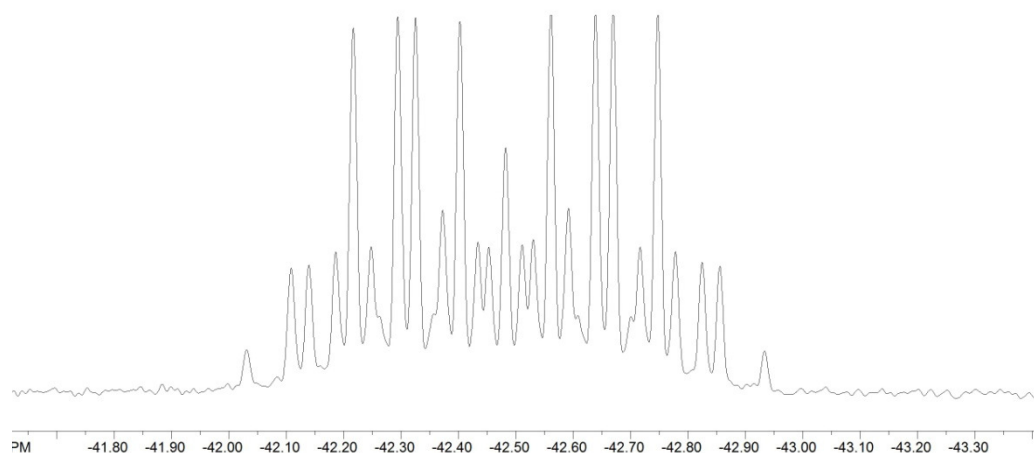
Figure 3.33: Expansion of the signal at δ -42.3 ppm in the ^{31}P{^{1}H} NMR spectrum of the product from the reaction between PhP(SiMe$_3$)$_2$ and (CF$_3$)$_2$CFI.

The multiplet shown in Figure 3.33 can be interpreted as an overlapping doublet of quartet of quartets ($^2J_{PF}$ = 53.1 Hz, $^3J_{PF}$ = 17.8 Hz, and $^3J_{PF}$ = 12.6 Hz).

The ^{19}F NMR spectrum of the liquid has three major peaks, at δ -72.6 (Figure 3.34), -73.4 (Figure 3.35) and -178.3 ppm (Figure 3.36). They integrate in the ratio 3:3:1, indicating that the CF$_3$ groups of the perfluoroisopropyl group are chemically inequivalent. Based on the appearance of the CF$_3$ signals, this suggests that the compound formed is chiral, as in **26**, which also has chemically inequivalent CF$_3$ groups.
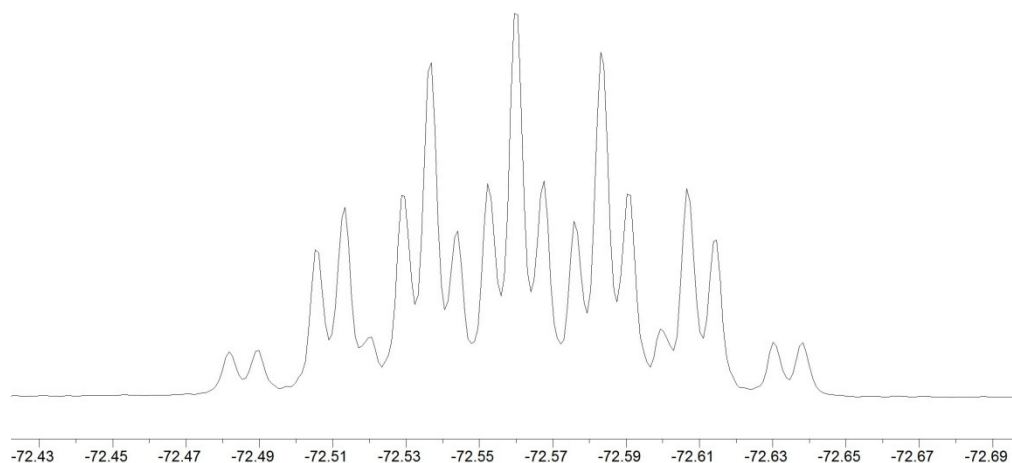
Figure 3.34: Expansion of the peak at δ -72.6 ppm in the ^{19}F NMR spectrum of the of the product from the reaction between PhP(SiMe₃)₂ and (CF₃)₂CFI.
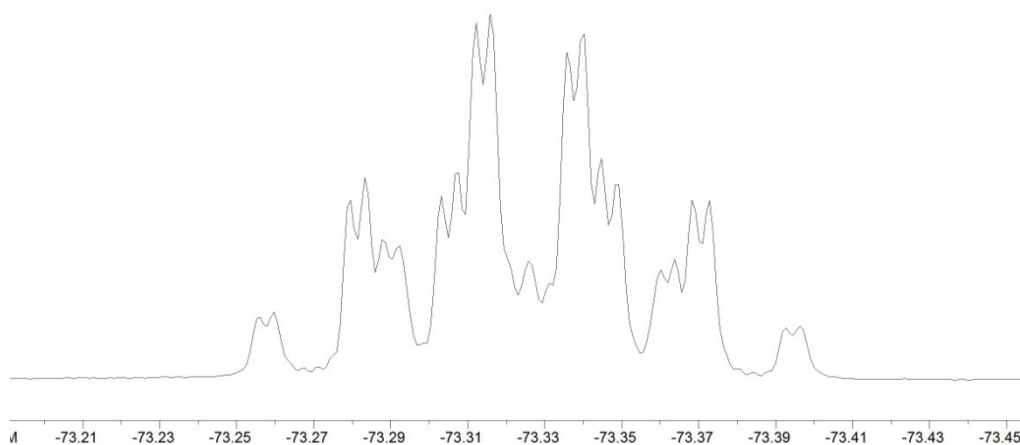
Figure 3.35: Expansion of the signal at δ -73.4 ppm in the ^{19}F NMR spectrum of the reaction between PhP(SiMe₃)₂ and (CF₃)₂CFI.
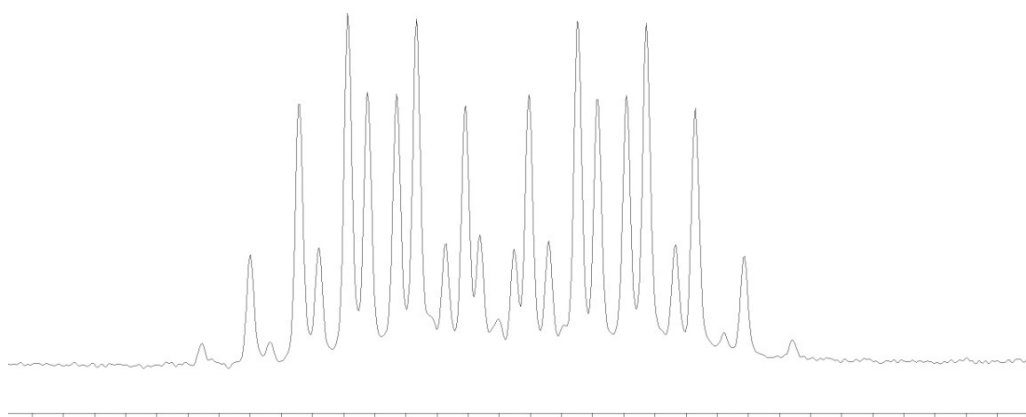
Figure 3.36: Expansion of the signal at δ -178.3 ppm in the ¹⁹F NMR spectrum of the product from the reaction between PhP(SiMe₃)₂ and (CF₃)₂CFI.

The presence of two CF_3 signals is unexpected, and means that the multiplicity of the signal for the fluorine attached to the α-carbon would be expected to be a doublet of quartets of quartets (similar in appearance to the phosphorus signal) or a doublet of septets if the two quartet couplings are similar. However, as shown in Figure 3.36, the pattern observed is an overlapping doublet of doublet of septets. There appears to be an additional doublet coupling (J = 16.4 Hz) than would be expected in the desired product. Both CF_3 signals appear to have a small "extra" doublet coupling.

A ¹⁹F{¹H} NMR spectrum confirms that additional coupling is due to the the presence of a proton, as all three signals were reduced in multiplicity (see Figure 3.37, Figure 3.38, and Figure 3.39).
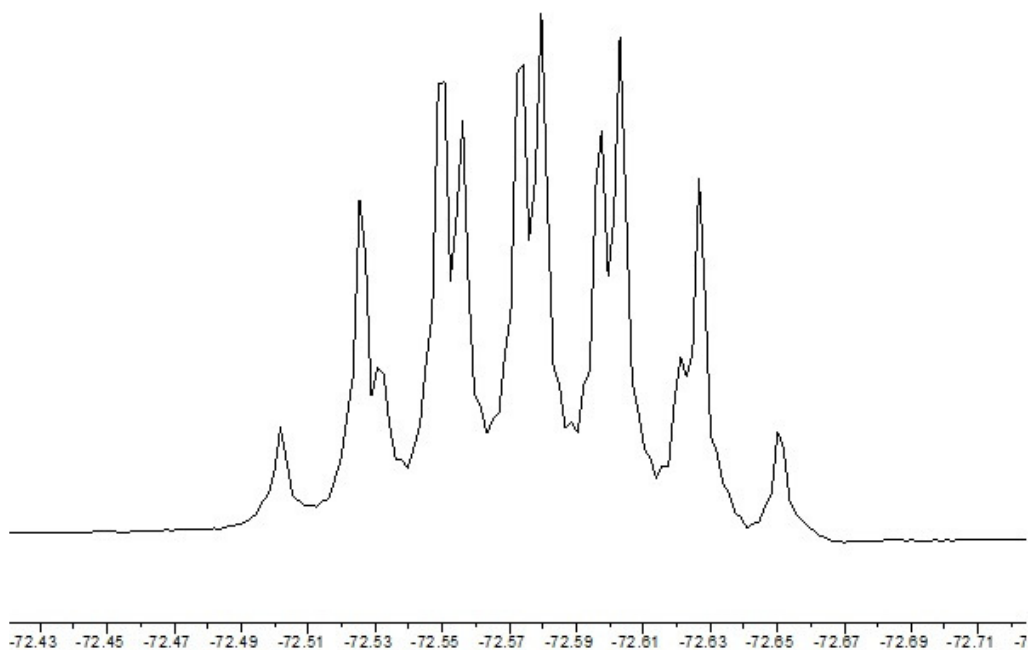
Figure 3.37: Expansion of one of the CF$_3$ signals in the ^{19}F{^{1}H} NMR spectrum of the liquid from the reaction between PhP(SiMe$_3$)$_2$ and (CF$_3$)$_2$CFI.
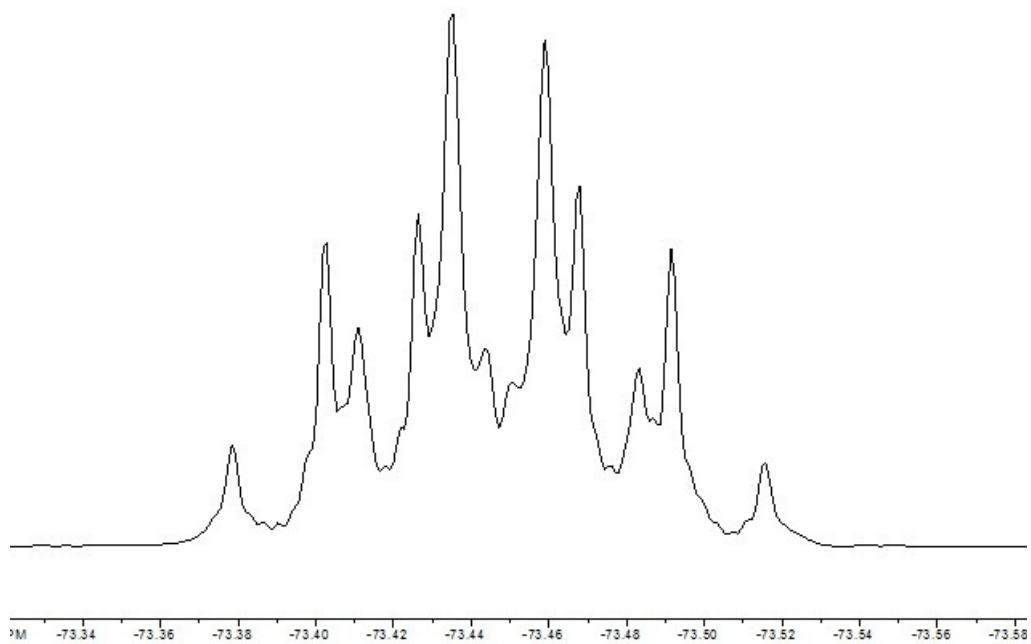
Figure 3.38: Expansion of the signal at δ -73.4 ppm in the ^{19}F{^{1}H} NMR spectrum of the reaction between PhP(SiMe$_3$)$_2$ and (CF$_3$)$_2$CFI.
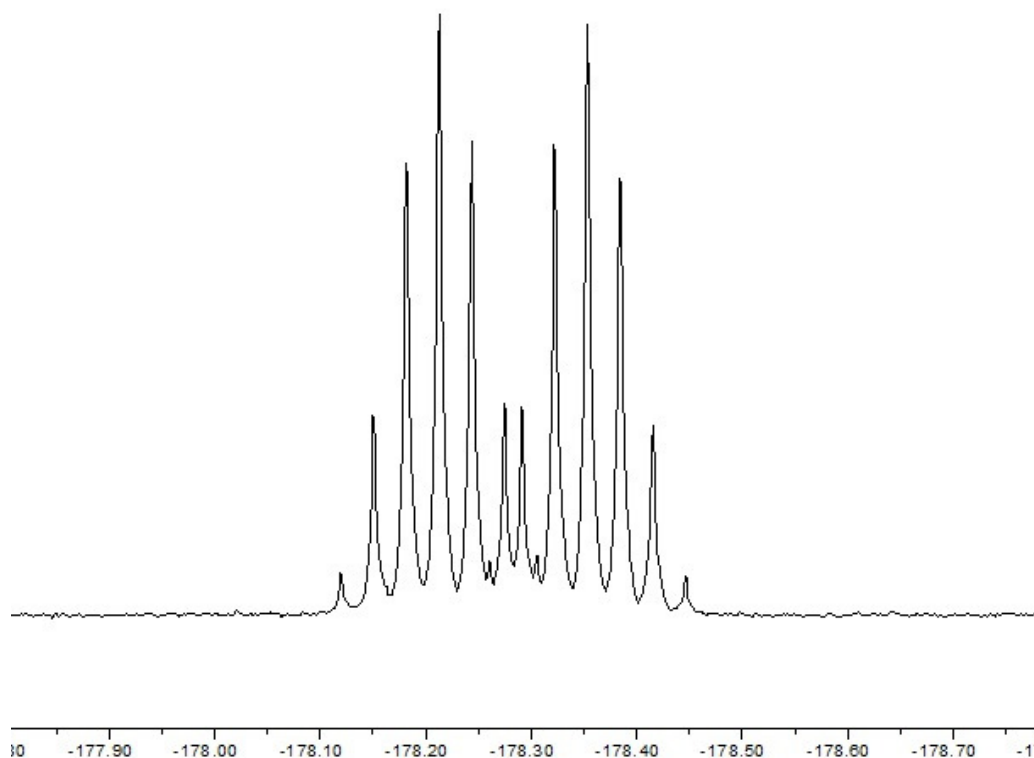
Figure 3.39: Expansion of signal at δ -178.3 ppm in the ^{19}F{^{1}H} NMR spectrum of the reaction between PhP(SiMe$_3$)$_2$ and (CF$_3$)$_2$CFI.

The signal at δ -178.3 ppm in the ^{19}F{^{1}H} NMR spectrum is an overlapping doublet of septets – thus the additional doublet coupling is due to a single proton.

The ^{31}P NMR spectrum displays a broad doublet at δ -42.3 ppm, with a coupling constant of ~230 Hz, which is typical of $^1J_{PH}$ coupling constants, suggesting that a P–H bond has been formed. The $^1J_{PH}$ coupling constant and the chemical shift are very similar to the trifluoromethyl-containing analogue, Ph(H)PCF$_3$, reported by Togni *et al.* (δ -40.4 ppm, $^1J_{PH}$ = 222 Hz).[108] The ^{1}H NMR shows the resonances expected for a phenyl ring, with complex multiplets observed at δ 7.26–7.31, 7.34–7.41 and 7.54–7.60 ppm and a complex doublet based signal centred at δ 4.56 ppm with a doublet coupling constant of 229.1 Hz, indicative of the presence of P–H bond. The ^{13}C{^{1}H}

NMR spectrum has the four expected resonances for the phenyl ring, at δ 136.5, 134.9, 129.9 and 127.5 ppm.

These data are consistent with the formation of a new compound, the previously unknown secondary fluoroalkyl phosphine, $PhP(H)CF(CF_3)_2$, **27**. The source of the hydrogen is currently unclear. If the same reaction is carried out in a solution of $CDCl_3$ then the same product is formed, not $PhPDCF(CF_3)_2$, which suggests that the solvent is not the source of the proton.

3.7 Mechanistic Considerations

At first glance it would appear as though there is a straightforward exchange occurring between the trimethylsilyl-containing phosphine, R_2PSiMe_3 and the perfluoroalkyl iodide, R_fI, to generate R_2PR_f as shown in Scheme 3.13.

$$R_2PSiMe_3 + R_fI \longrightarrow R_2PR_f + Me_3SiI$$
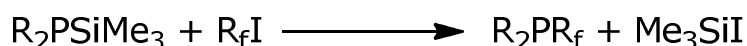
Scheme 3.13: Reaction of silyl-phosphines with R_fI.

Indeed, a peak corresponding to Me_3SiI is observed in the ^1H NMR spectrum at δ 0.81 ppm (lit. δ 0.8 ppm)[194] of the preliminary reactions.

However, on closer investigation it is clear that such a simplistic representation of the reaction is insufficient. The $^{31}P\{^1H\}$ NMR spectrum recorded immediately (<10 mins) after the addition of the perfluoroalkyl iodide to Ph_2PSiMe_3 shows the disappearance of the peak corresponding to Ph_2PSiMe_3 (δ -56.3 ppm, lit. δ -56.7 ppm), and the growth of a new, often somewhat broad, peak at δ -15.0 ppm (see Figure 3.40 for example).
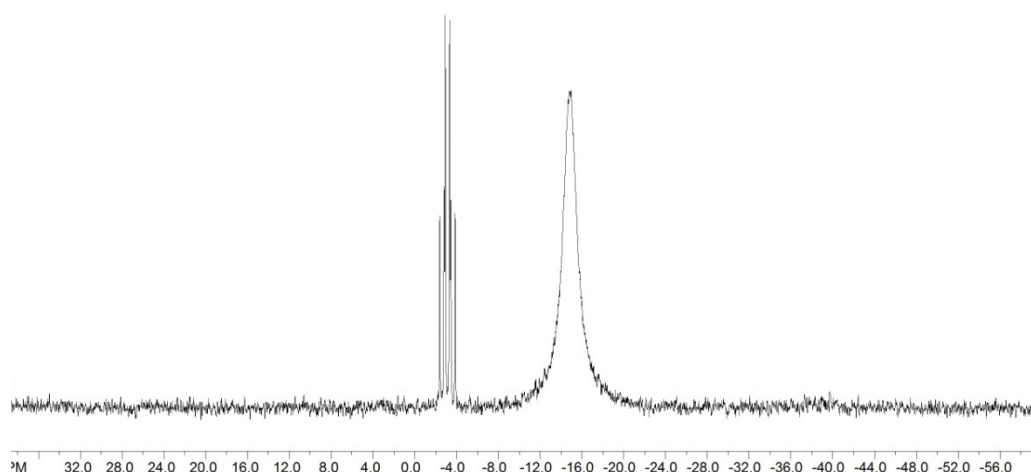
Figure 3.40: $^{31}P[^1H]$ NMR spectrum of reaction between Ph$_2$PSiMe$_3$ and *cyc-*C$_6$F$_{11}$I after approx. 30 minutes.

Recording the $^{31}P\{^1H\}$ NMR spectrum periodically shows a decrease in the intensity of the peak at δ -15.0 ppm and a growth of the signal corresponding to the desired R$_2$PR$_f$ product. This appearance and subsequent disappearance of the peak at δ -15 ppm indicates that it is an intermediate in the formation of Ph$_2$PR$_f$. We postulated that the identity of this species could be Ph$_2$P-PPh$_2$ (lit: δ -14.8 ppm).[216] In an attempt to confirm this a reaction was undertaken where Ph$_2$P-PPh$_2$ was added to one equivalent of (CF$_3$)$_2$CFI and the $^{31}P\{^1H\}$ NMR spectrum recorded, shown in Figure 3.41. It is clear from this spectrum that the formation of **15** results, suggesting that the intermediate observed in the reactions between Ph$_2$PSiMe$_3$ and R$_f$I is tetraphenyldiphosphine, Ph$_2$P-PPh$_2$.
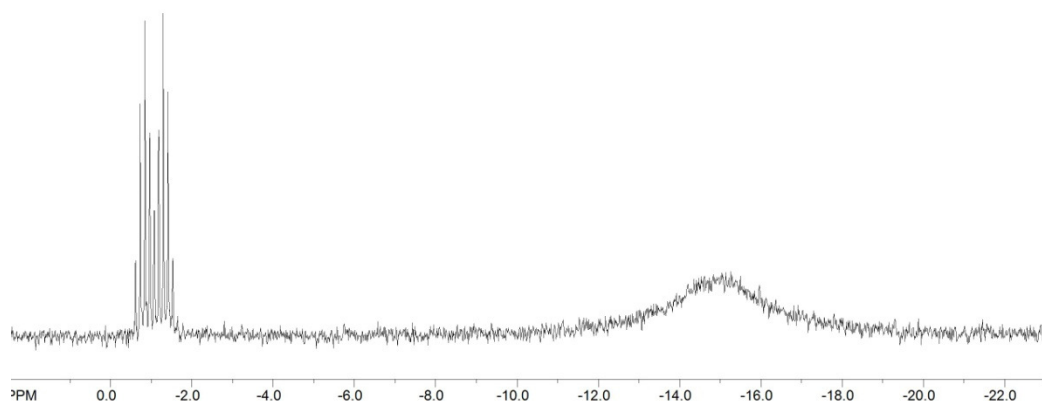
Figure 3.41: $^{31}P\{^1H\}$ NMR spectrum of the reaction between Ph$_2$PPPh$_2$ and (CF$_3$)$_2$CFI.

Further support for this was obtained from the reaction involving $^iPr_2PSiMe_3$, in which an intermediate is observed with a resonance at δ -11.0. This can be compared with the reported phosphorus chemical shift for $^iPr_2P$-P$^iPr_2$ which is δ -11.6 ppm.[217]

A number of factors suggested that a radical mechanism should be considered. These include the known propensity for perfluoroalkylhalides to undergo radical cleavage of the R$_f$-I bond and the fact that a similar reaction is reported to be radical in nature.[104] The broadness of the R$_2$P-PR$_2$ peak might indicate that a radical intermediate is generated. This may explain the presence of varying quantities of Ph$_2$PI (δ 40.2, lit. δ 38.0 ppm),[218] and, in some cases (especially the reaction involving *cyc*-C$_6$F$_{11}$I, see Figure 3.42) a fluoroalkene corresponding to the formal elimination of IF from the perfluoroalkyl iodide. In the case of *cyc*-C$_6$F$_{11}$I, the alkene formed is perfluorocyclohexene, with three signals in the ^{19}F NMR spectrum observed at δ -118.4, -133.3, and -150.5 (lit: δ -118, -133, -151 ppm),[219] as shown in Figure 3.42.

PM   -108.0 -112.0 -116.0 -120.0 -124.0 -128.0 -132.0 -136.0 -140.0 -144.0 -148.0 -152.0 -156.0 -160.0 -164.0 -168.0 -172.0 -176.0 -180.0 -184.0 -188.0
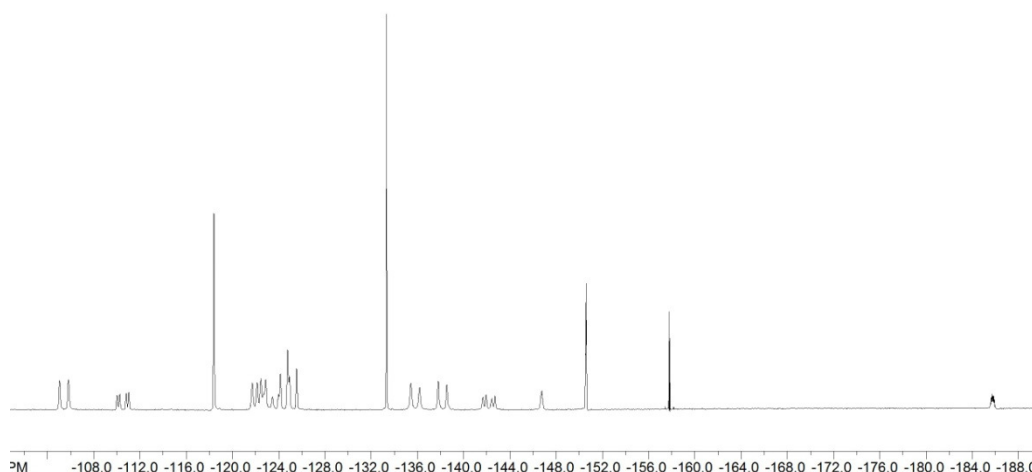
Figure 3.42: ^{19}F NMR spectrum of the reaction between Ph$_2$PSiMe$_3$ and *cyc*-C$_6$F$_{11}$I recorded after approx. 30 minutes.

However, the formation of this alkene could also be accounted for by the elimination of Me$_3$SiF from Me$_3$Si(*cyc*-C$_6$F$_{11}$). Indeed, signals due to Me$_3$SiF are also observed in the ^{19}F NMR spectrum (Figure 3.42) at δ -157.3 ppm (dectet, $^3J_{HF}$ = 10 Hz, with ^{29}Si satellites, $^1J_{SiF}$ = 274.2 Hz, lit: δ -157 ppm, dectet, $^3J_{HF}$ = 8.0 Hz);[220] the formation of Me$_3$SiF being favoured by the strength of the Si–F bond (553 kJ mol^{-1}).[221] Alternatively, the fluoroalkene could be formed by elimination from the perfluoroalkyl phosphorus(III) compound with formation of a P–F bond (439 kJ mol^{-1}).[221]

However, *in situ* EPR (Electron Paramagnetic Resonance) spectroscopic studies of a reaction carried out in the cavity of an EPR spectrometer showed no evidence of the presence of any radical species, although this does not completely exclude the possibility of a radical process, it does suggest that alternative mechanisms should be investigated

An interesting observation was made in reactions involving (CF$_3$)$_2$CFI and Ph$_2$PSiMe$_3$; on addition of the two reactants and before the formation of the product, Ph$_2$PCF(CF$_3$)$_2$, the chemical shift position of the unique fluorine atom

132

changes by several ppm relative to that recorded for a solution of $(CF_3)_2CFI$ alone. The chemical shift of this fluorine nucleus in $(CF_3)_2CFI$ is δ -148.8 ppm (lit. δ −148.9 ppm),[193] but when added to Ph_2PSiMe_3 in an NMR tube scale as described above the chemical shift changes and is observed at around δ -153.0 (dependent on the concentration; when a large excess of $(CF_3)_2CFI$ is used, the signal appears at ca. δ -149.5). When the reaction is conducted with perfluoroalkyl iodide is cyc-$C_6F_{11}I$, the signal corresponding to the fluorine atom attached to the α-carbon is observed at -146.8 ppm (lit. δ -144.6 ppm for cyc-$C_6F_{11}I$ alone),[222] a change of over two ppm. This is similar to that noted during the reaction with $^sC_4F_9I$, where the fluorine atom attached to the α-carbon is observed at δ -148.7 ppm, whereas when recorded alone it is observed at -146.2 ppm (lit. δ -146.9 (C_6D_{12})).[223] This, combined with the broadness of the peak observed at δ -15.0 ppm in the $^{31}P\{^1H\}$ NMR spectrum, suggests that there may be some interaction between one or both of the lone pairs of Ph_2P-PPh_2 and the iodine atom of the perfluoroalkyl iodide. Similar interactions, including observation of comparable changes in chemical shift have been reported in halogen-bond systems by Resnati and others,[224-227] typically involving primary perfluoroalkyl iodides and N, S, or O-heteroatom donors. In such systems the chemical shift differences between the R_fI and the halogen-bonded systems are in the order N>S≥O, and the effect can be as much as 10 ppm.[225]

It is possible that a similar interaction between Ph_2PSiMe_3 and the iodine atom of the perfluoroalkyl iodide results in the formation of Ph_2P-PPh_2. Such coordination will create a greater positive charge at the phosphorus centre. This could then be attacked by the lone pair of another molecule of Ph_2PSiMe_3, generating Ph_2P-PPh_2, and presumably Me_3Si-$SiMe_3$, although this process is not thermodynamically favoured.

To date, these halogen bonding interactions have been used to explain structural motifs, but not reaction pathways. However, this is similar to a charge-transfer mechanism (see Scheme 3.14), promoted by the lone pair(s) on the phosphorus species, allowing the R_f group to become a nucleophile, effectively, although not necessarily formally, as R_f^-.
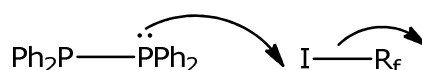
Scheme 3.14: Possible mechanism for interaction of diphosphines with R_fI.

Such an interaction would be consistent with the reactivity trend of the perfluoroalkyl iodides (tertiary > secondary >>> primary), as the strength of the C–I bond increases along the above series (Table 3.5). The considerably greater strength of the C–I bond in C_6F_5I may explain why this does not react with Ph_2PSiMe_3 under these conditions.

Perfluoroalkyl Iodide	C–I Bond Strength (kJ mol^{-1})
CF_3I	224
C_2F_5I	219
$(CF_3)_2CFI$	215
$^tC_4F_9I$	206
C_6F_5I	277

Table 3.5: Bond strengths in selected R_fI compounds.

This means that the R_f^- could potentially attack an electrophile, such as another molecule of Ph_2P-PPh_2, or more likely that an intramolecular reaction occurs, generating the desired product and Ph_2PI. However, this would result in a 50:50 mixture of Ph_2PI and Ph_2PR_f, which is not observed. This suggests that either the resulting Ph_2PI reacts further or that the mechanism is more complicated. So, while an interaction between Ph_2P-PPh_2 and R_fI accounts for the observed rates of reactivity, it does not explain the distribution of products observed.

3.7.1 Investigation of Effect of Lone Pair

The interactions described above involve one or more of the lone pairs of the phosphorus centres, therefore further investigation was undertaken to confirm, or otherwise, this. Firstly, the most obvious method would be to attempt the reaction with phosphorus(V) species, where the lone pairs are unavailable due to their involvement in bonding.

The synthesis of $(Me_2PS)_2$ was accomplished via standard literature methods from $S=PCl_3$ and MeMgBr.[228] The compound was subsequently dissolved in $CDCl_3$ and one equivalent of $(CF_3)_2CFI$ added (Scheme 3.15). Whereas the reaction between Ph_2PSiMe_3 (or Ph_2P-PPh_2) and $(CF_3)_2CFI$ occurs rapidly, no reaction between $(Me_2PS)_2$ and $(CF_3)_2CFI$ was observed under the same conditions over a period of several weeks.
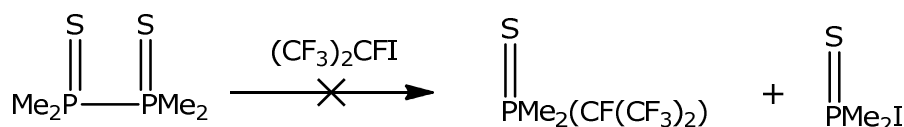
Scheme 3.15: Attempted reaction of $(Me_2PS)_2$ with $(CF_3)_2CFI$.

Based on the lack of success of the reaction between $(Me_2PS)_2$ and $(CF_3)_2CFI$, another reaction was attempted, this time with a mixed phosphorus(III)/phosphorus(V) compound.

Heating $(Me_2PS)_2$ with 0.95 equivalents of P^nBu_3 at 140°C for 20 hours results in the formation of $Me_2P-P(S)Me_2$,[229] (with one phosphorus(III) centre and one phosphorus(V) centre), and $S=P^nBu_3$ as a by-product (Scheme 3.16). The $^{31}P\{^1H\}$ NMR spectrum displays a singlet at δ 48.7 ppm corresponding to $S=P^nBu_3$ (lit. δ 48.7 ppm)[230] and two doublets, centred at δ 37.3 ppm and δ -56.5 ppm with a shared coupling constant of 221.1 Hz, corresponding to the phosphorus(V) and phosphorus(III) centres of $Me_2P-P(S)Me_2$ respectively (lit. δ 35.6 and -57.5 ppm respectively).[231]

135
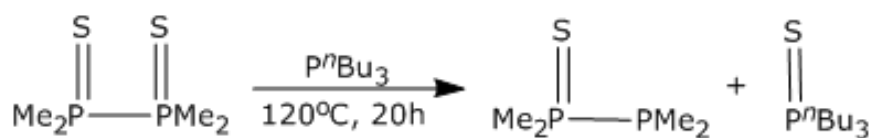
Scheme 3.16: Synthesis of the mixed phosphorus(III)/phosphorus(V) compounds.

Reaction of Me_2P-$P(S)Me_2$ with $(CF_3)_2CFI$ is extremely slow, with the growth of a new peak occurring (<10% after two weeks), at δ -18.2 ppm in the $^{31}P\{^1H\}$ NMR spectrum and as such this compound has only been identified and characterised via $^{31}P\{^1H\}$ and ^{19}F NMR spectroscopy.

The new peak observed in the $^{31}P\{^1H\}$ NMR spectrum of this reaction is similar in appearance to that of **15** and **26**; displaying a doublet of septets ($^2J_{PF}$ = 53.3 Hz, $^3J_{PF}$ = 16.4 Hz), shown in Figure 3.43.
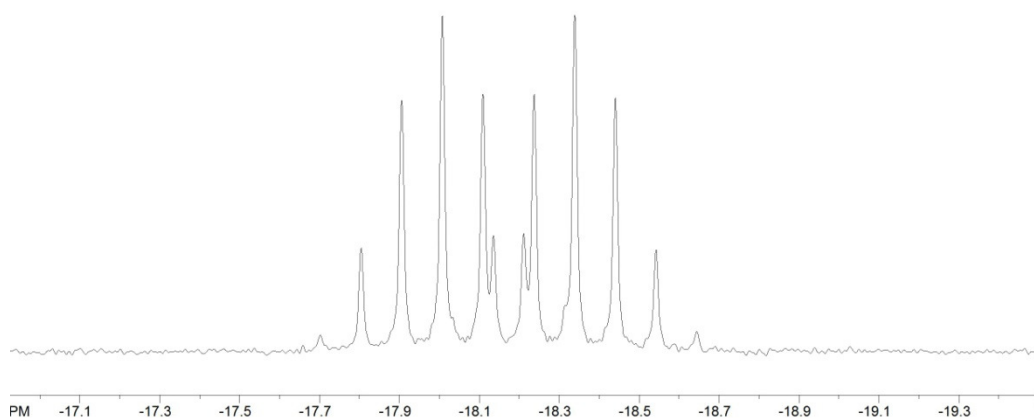
Figure 3.43: Expansion of the peak observed at δ -18.2 ppm in the $^{31}P\{^1H\}$ NMR spectrum of the reaction between Me_2P-$P(S)Me_2$ and $(CF_3)_2CFI$.

The ^{19}F NMR spectrum is also very similar to that observed for **15**, with a doublet of septets observed at δ -195.5 ppm ($^2J_{PF}$ = 53.3 Hz, $^3J_{FF}$ = 10.4 Hz), and a doublet of doublets occurring at δ -71.6 ppm ($^3J_{PF}$ = 16.4 Hz, $^3J_{FF}$ = 10.4 Hz). These data suggest that a perfluoroisopropyl-containing phosphine has been formed. Taken together, both the $^{31}P\{^1H\}$ and ^{19}F NMR data

136

indicate the formation of the expected new compound, $Me_2PCF(CF_3)_2$, **27**. Unfortunately, due to the sluggish nature of the reaction, this material has not yet been prepared on a large scale, nor has it been successfully isolated free of $(CF_3)_2CFI$ for complete characterisation.

Both of these experiments suggest that either one or both of the lone pairs of the diphosphine play an important role in the reaction mechanism.

Indeed, the suggestion of Ph_2P-PPh_2 acting as an electron donor to the iodine centre to facilitate the formation of "R_f^-" is similar to that proposed for the mechanism of the reaction between $P(NEt_2)_3$, CF_3X (X = Br, I) and chlorophosphines, e.g. $Cl_2PCH_2CH_2PCl_2$, to generate $(CF_3)_2PCH_2CH_2P(CF_3)_2$.[77] To investigate this hypothesis, *(CF_3)_2CFI* was added to a mixture of Ph_2P-PPh_2 and $(o$-tol$)_2PCl$. *Bis*-orthotolylchlorophosphine was chosen as it is commercially available, has a reasonably similar stereoelectronic profile to Ph_2PCl, and the expected product $(o$-tol$)_2PCF(CF_3)_2$ should be distinguishable from **15** in the $^{31}P\{^1H\}$ NMR spectrum. However, the only perfluoroisopropyl-containing phosphine observed in this reaction is **15**, meaning that either Ph_2P-PPh_2 is a better electrophile than $(o$-tol$)_2PCl$, or more likely that the reaction occurs via an intramolecular route, rather than liberating "R_f^-".

A number of experiments involving mono-phosphines and fluoroalkyl iodides have shown that mono-phosphines can also be used as a "charge-transfer" reagent, although not particularly cleanly.[232] The addition of $(CF_3)_2CFI$ to a mixture of P^nBu_3 and Ph_2PCl resulted in an extremely exothermic reaction, and a number of products, according to multi-nuclear NMR data, whilst the analogous reaction of $(CF_3)_2CFI$ with PPh_3 resulted in no reaction at all. At first, it was thought that the basicity of the phosphine was important, but the report by Caffyn *et al.*[195] of the room temperature reaction of $P(NEt_2)_3$ with $(CF_3)_2CFI$ and Ph_2PCl resulting in the formation of **15** suggests otherwise as

P(NEt$_2$)$_3$ is more basic than P^{n}Bu$_3$. They propose that this reaction proceeds via a charge-transfer procedure, with the lone-pair of the phosphorus of P(NEt$_2$)$_3$ donating electron density to the iodine nucleus, allowing R$_f^-$ to effectively act as a nucleophile and attack Ph$_2$PCl, resulting in **15** and (Et$_2$N)$_3$PX$_2$ (X = Cl and I).

On switching from mono-phosphine additives to bidentate phosphines, the reaction is observed to be more controllable. The bidentate phosphines Ph$_2$PCH$_2$PPh$_2$ (dppm), Ph$_2$PCH$_2$CH$_2$PPh$_2$ (dppe), Ph$_2$P(CH$_2$)$_3$PPh$_2$ (dppp), Ph$_2$P(CH$_2$)$_4$PPh$_2$ (dppb), Ph$_2$P(CH$_2$)$_6$PPh$_2$ (dpph) and (1,4-diphenylphosphino)benzene all facilitate the reaction between Ph$_2$PCl and (CF$_3$)$_2$CFI. For example, the reaction of dppe, (CF$_3$)$_2$CFI and Ph$_2$PCl results in the formation of **15** and Ph$_2$PCH$_2$CH$_2$PPh$_2$.X$_4$ (X = Cl or I), as shown in the ^{31}P{^{1}H} NMR spectrum of the reaction by singlets observed at δ 75.0 (X = Cl, lit. δ 75.2 ppm)[233] and 50.5 ppm (X = I, lit. δ 51.0 ppm).[234] There does not appear to be formation of mixed halo-*bis*phosphines, based on comparison with literature data.

Dppe has been shown to react with PX$_3$ (X = Br, I)[235] in the presence of a halogen-scavenger (cyclohexene) resulting in the formation of the unusual species shown in Scheme 3.17.
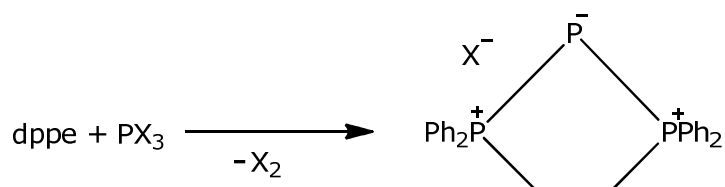
Scheme 3.17: Reaction of dppe with PX$_3$, adapted from Ref. 235.

The reaction is postulated to occur via nucleophilic attack of one of the phosphorus centres of dppe on the halophosphine, forming a quaternary salt. Subsequently, attack of the other phosphorus centre of dppe at the resulting

X_2P centre results in the displacement of X_2, leading to the formation of the species shown in Scheme 3.17.

It is possible that a similar process is occurring in this work, resulting in the formation of a phosphorus – phosphorus bond (see Scheme 3.18)
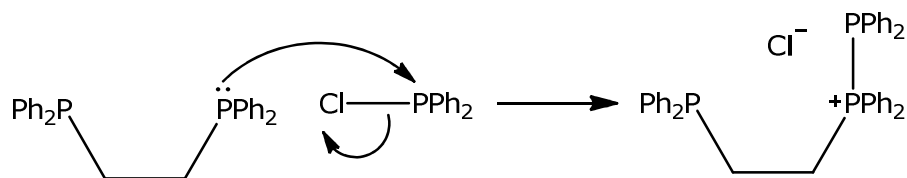
Scheme 3.18: Potential reaction between dppe and Ph$_2$PCl.

This phosphorus – phosphorus bond could then react with $(CF_3)_2CFI$, leading to the formation of dppe.I$_4$ and dppe.Cl$_4$ (via disproportionation) and the fluoroalkyl containing phosphine, **15**.

3.8 Summary

The reaction of perfluoroalkyl iodides with trimethylsilyl-containing phosphines has been explored, resulting in the synthesis of six previously unknown compounds. The methodology has been shown to be suitable for primary, secondary and tertiary fluoro-organo iodides, and to tolerate partially fluorinated substituents. The route has also been extended by varying R groups at the phosphorus centre, and has been used to synthesise a chiral perfluoroalkyl-containing phosphine.

The mechanism of the reaction remains unclear. It is apparent that the first step involves the transformation of Ph_2PSiMe_3 into $Ph_2P\text{-}PPh_2$, in the presence of R_fI, although exactly how the addition of R_fI facilitates this is currently unknown. $Ph_2P\text{-}PPh_2$ then appears to undergo a halogen-bond interaction with the R_fI species, which then undergoes an intramolecular reaction to form Ph_2PR_f and presumably Ph_2PI. The lack of Ph_2PI observed in these

reactions clearly shows that the full picture has not yet been elucidated – Ph_2PI could presumably undergo a similar reaction as Ph_2PCl does when mixed with $P(NEt_2)_3$ and R_fX, or as described above, dppe and R_fI.

The reaction of the diphosphinemonosulfide, $Me_2P-P(S)Me_2$ with R_fI is also interesting, and appears to give a potentially viable, albeit slow alternative strategy for synthesising these compounds.

4. Chemistry of Perfluoroalkyl Phosphines

4.1 Quaternisation

The reaction of **15** with RX was investigated, since the quaternisation of phosphorus(III) compounds is well established.[236]

The reaction of **15** with either MeI or $C_6H_5CH_2Br$ failed to result in the formation of the corresponding quaternary phosphonium salt. This is presumably because of the reduced nucleophilicity of the phosphorus centre due to the strong negative inductive effect of the perfluoroisopropyl group, and also possibly due to the steric bulk of **15**. This observation agrees with previously reported data which found that aryl and alkoxy-containing phosphines quaternise less readily than alkyl-containing phosphines.[236]

4.2 Oxidation Chemistry

Of particular importance for the use of phosphines in catalysis/synthesis is their ease of (or more often, stability towards) oxidation. This is particularly true in catalytic processes where phosphine-oxide formation can significantly reduce the turn-over of a reaction.

4.3 Synthesis of $E=PR_2R_f$ (E = O, S, Se)

4.3.1 $O=PPh_2CF(CF_3)_2$ (29)

As mentioned above in Section 3.5.1, the serendipitous discovery of the formation of the phosphine oxide, $O=PPh_2CF(CF_3)_2$, **29**, upon dissolution of **15** in pentane and allowing it to stand at 4°C for 72 hours, affording a near quantitative yield of white needles.

$$Ph_2PCF(CF_3)_2 + 1/2 \ O_2 \longrightarrow O{=}PPh_2(CF(CF_3)_2)$$

15   **29**
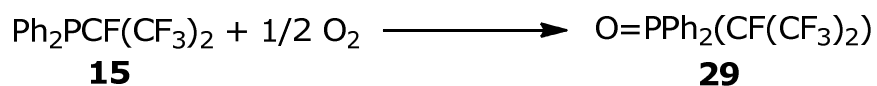
Scheme 4.1: Oxidation of 15.

The $^{31}P\{^1H\}$ NMR spectrum of the needles dissolved in $CDCl_3$ contains a single resonance at δ 20.8 ppm which is a doublet with J = 51.4 Hz (see Figure 4.1).
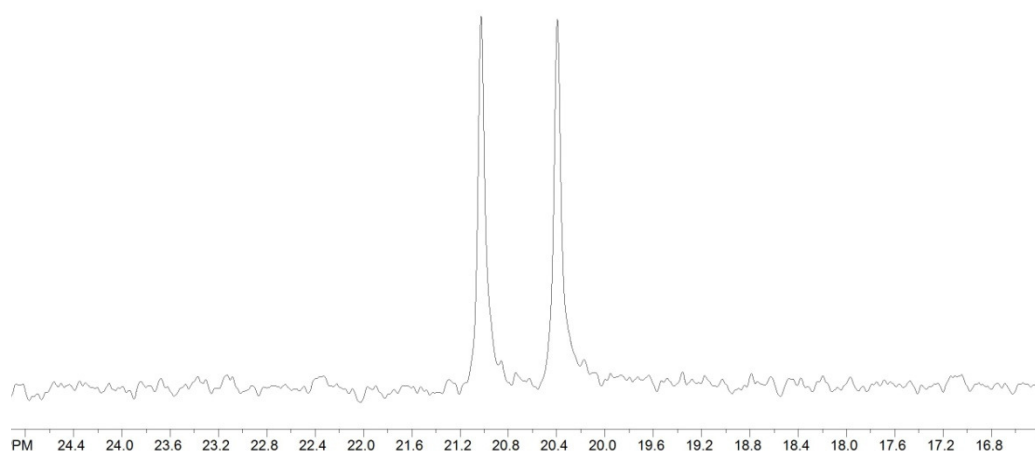
Figure 4.1: Expansion of the signal observed at δ 20.8 ppm in the $^{31}P\{^1H\}$ NMR spectrum of 29.

The ^{19}F NMR spectrum contains two signals, a doublet centred at δ -69.1 ppm ($^3J_{FF}$ = 10.7 Hz) and binomial doublet of septets, centred at δ -188.6 ppm ($^2J_{PF}$ = 51.4, $^3J_{FF}$ = 10.7 Hz).

The ^{19}F NMR spectrum is consistent with the presence of a perfluoroisopropyl group attached to a phosphorus centre (shown by the chemical shift of the unique fluorine atom and the mutual J_{PF} coupling shared with the signal in the $^{31}P\{^1H\}$ NMR spectrum). Interestingly, there is a loss of coupling from the phosphorus centre to the fluorine nuclei on the CF_3 groups, and a (slight) reduction in magnitude of the other coupling constants relative to those observed in **15**. This suggests that lone-pair assisted through-space coupling

142

is more significant than through-bond coupling, at least to the more distant CF_3 groups. The signal observed for **29** in the $^{31}P\{^1H\}$ NMR spectrum is shifted 21.6 ppm upfield, a change comparable to other species on increasing the oxidation state from phosphorus(III) to phosphorus(V) (*cf.* $PPh_3 \rightarrow O=PPh_3$ $\Delta\delta$ +34.2 ppm).[237,238] The data also compares favourably with that reported by Vaillard *et al.*, who reported the formation of $O=PPh_2(n\text{-}C_4F_9)$ (δ +24.4 ppm, t, $^2J_{PF}$ = 7.0 Hz) and $O=PPh_2(n\text{-}C_6F_{13})$ (δ +24.6 ppm, t, $^2J_{PF}$ = 7.1 Hz).[104] Taken together this suggests the formation of the phosphorus(V) species, $O=PPh_2CF(CF_3)_2$, **29**.

The needles of **29** obtained from the pentane solution of **15** were of sufficient quality to be structurally characterised via single crystal X-ray diffraction studies; solution of the data resulted in the molecular structure depicted in Figure 4.2.
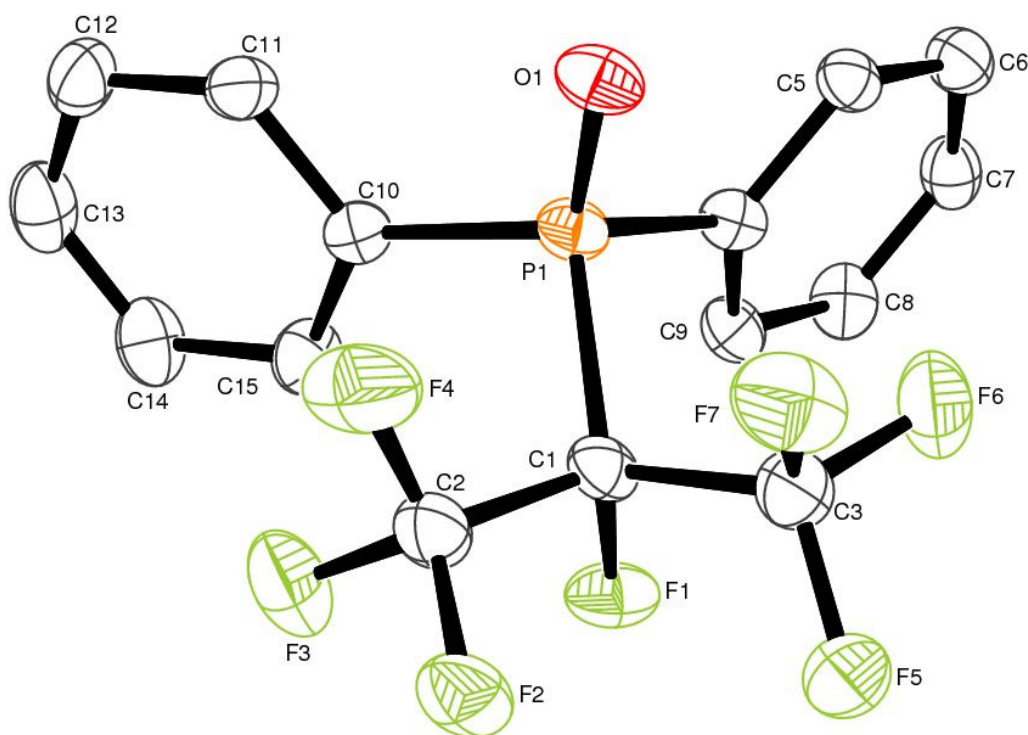
Figure 4.2: ORTEP[174] representation of the molecular structure of 29. Thermal ellipsoids are shown at 50%, and hydrogen atoms have been omitted for clarity.

Compound **29** crystallises in the $P\bar{1}$ space group, with two molecules in the unit cell, and the molecular geometry is consistent with that expected for this compound. A search of the CSD shows that only two phosphine oxides of fluoroalkyl-containing phosphines have previously been characterised by X-ray crystallographic studies; $(^iC_4F_9)_3P=O$ and $Ph_2P(O)CF_2Br$. The P1–O1 bond in **29** is 1.477(4) Å, very similar to those reported for $(^iC_4F_9)_3P=O$ (d (P–O) 1.447(2) Å) and $Ph_2P(O)CF_2Br$ (d(P–O) 1.471(4) Å). The phosphorus – carbon distance to the fluorinated group is longer than the distances to the phenyl rings (1.896(5) Å *vs.* 1.794(6)/1.779(6) Å), as observed in both the molecular structure of compound **15**, and of $Ph_2P(O)CF_2Br$ (P-C$_F$ = 1.893(5) Å, PC$_{Ar}$ = 1.799(6) and 1.796(6) Å). Both the C-C bond lengths in the perfluoroisopropyl moiety are identical within experimental error, again as observed in **15**. Similarly to $(^iC_4F_9)_3P=O$, the C-F bond on the methine carbon is the longest C-F bond, at 1.390(7) Å in **29** (average 1.370(1) Å in $(^iC_4F_9)_3P=O$). The C1–F1 bond is anti to the P1–O1 bond, with an O1–P1–C1–F1 torsion angle of 169.1(3)°, similar to **15**, where the C1-F1 bond is *anti* to the lone pair of the phosphorus centre. In contrast to **15**, one of the C-F bond lengths is markedly shorter than the others (See Table 4.1 for a selection of bond lengths). F1 also shows short intramolecular contacts to F3 and F5 (2.543(6) and 2.608(3) Å respectively, twice the sum of the van der Waals' radii of fluorine = 2.94 Å), as does **15**.

Bond	Distance (Å)	Bond	Distance (Å)
P1–O1	1.477(4)	C2–F2	1.322(7)
P1–C1	1.896(5)	C2–F3	1.360(8)
P1–C4	1.794(6)	C2–F4	1.286(9)
P1–C10	1.779(6)	C3–F5	1.323(7)
C1–C2	1.522(8)	C3–F6	1.320(8)
C1–C3	1.519(9)	C3–F7	1.360 (9)
C1–F1	1.390(7)		

Table 4.1: Selected bond lengths in 29.

Molecules of **29** stack in the x-direction in the solid state, as shown in Figure 4.3. There also appears to be some offset π-stacking in the y-direction, though the centroid to centroid distance is rather long (4.669(3) Å) to be considered a genuine interaction.
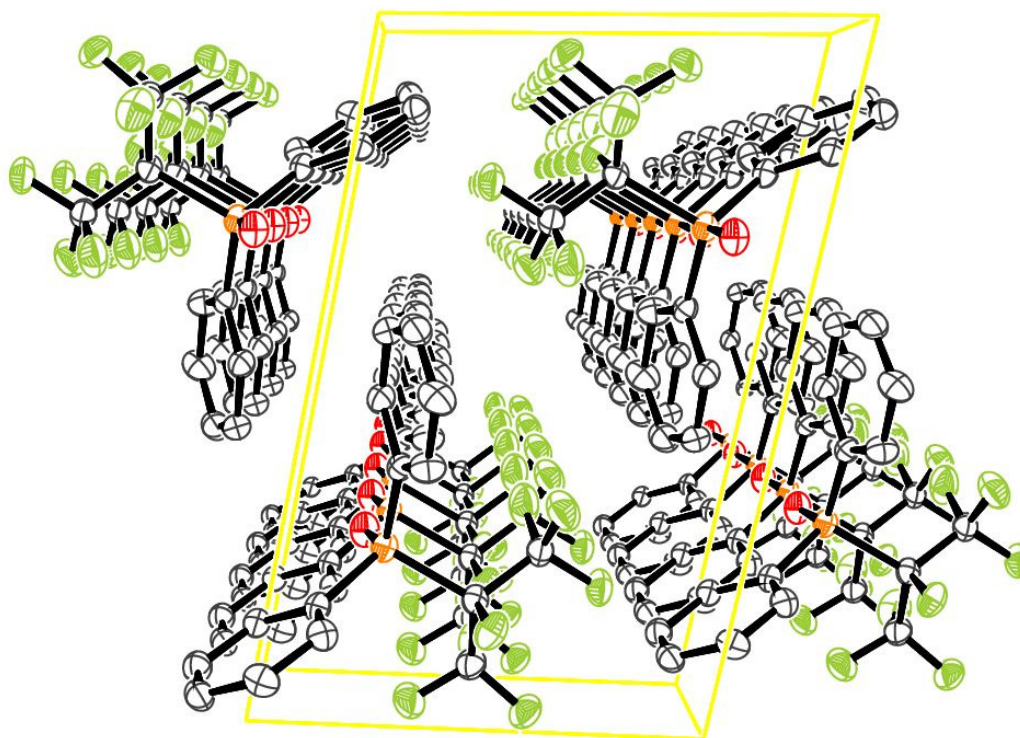
Figure 4.3: Crystal packing of 29 looking in the x-direction.

As can be seen in Figure 4.3, there appears to be regions of fluorous domains running in the x-direction in the crystal packing of **29**. The data also allows for the estimation of the cone angle of **15**, calculated to be 215°.

4.3.2   O=PPh$_2$(*cyc*-C$_6$F$_{11}$) (30)

The reaction of **19** with H$_2$O$_2$ was investigated in an attempt to deliberately oxidise the phosphorus centre (see Scheme 4.2).

$$Ph_2P(cyc\text{-}C_6F_{11}) + H_2O_2 \longrightarrow O=PPh_2(cyc\text{-}C_6F_{11}) + H_2O$$
$$\textbf{19} \qquad\qquad\qquad\qquad\qquad\qquad \textbf{30}$$
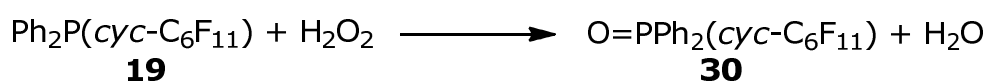
Scheme 4.2: Oxidation of 19 with H$_2$O$_2$.

The $^{31}P\{^1H\}$ NMR spectrum of the white solid resulting from the reaction shown in Scheme 4.2 displays a doublet centred at δ 20.9 ppm, with $^2J_{PF}$ = 54.4 Hz. The changes in chemical shift and reduction in magnitude of the $^2J_{PF}$ coupling constant are consistent with that observed for **29**.

The ^{19}F NMR spectrum displays the expected seven resonances, and as in the free phosphine **19**, they are all complex multiplets. The chemical shift of the fluorine nucleus attached to the α-carbon is at δ -190.4 ppm; it is shifted to lower frequency relative to **19**, as is observed for **15** and **29**. The recovered yield of this reaction was rather low, suggesting that the method described for the formation of **29** is of greater synthetic utility.

Based on the apparent ease of formation of **29** from **15**, the deliberate oxidation of **15** was attempted with other chalcogens.

4.3.3 $S=PPh_2CF(CF_3)_2$ (31)

A solution of **15** in toluene was refluxed in the presence of a slight excess of sulfur, and after work up afforded an orange solid.

$$Ph_2PCF(CF_3)_2 + 1/8\ S_8 \xrightarrow[\text{Toluene}]{\triangle} S=PPh_2CF(CF_3)_2$$
$$\textbf{15} \qquad\qquad\qquad\qquad\qquad\qquad \textbf{31}$$
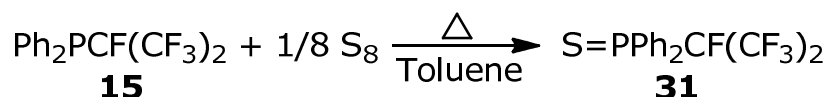
Scheme 4.3: Synthesis of compound 31.

The $^{31}P\{^1H\}$ and ^{19}F NMR spectra of this compound are similar in appearance to that of the phosphine oxide **29**; the $^{31}P\{^1H\}$ spectrum displays a resonance centred at δ 39.6 ppm, which is a doublet ($^2J_{PF}$ = 43.4 Hz). The ^{19}F NMR spectrum displays two resonances, a doublet centred at δ -66.7 ppm ($^3J_{FF}$ = 8.7 Hz) and a doublet of septets centred at δ -176.3 ppm ($^2J_{PF}$ = 43.4 Hz, $^3J_{FF}$ = 8.7 Hz). These data (along with the elemental analysis) confirm the identity of the compound. Further confirmation was obtained from X-ray

diffraction studies of a crystal grown by the slow evaporation of a solution of **31** in DCM. Unfortunately, the crystals were of poor quality, resulting in an R factor of 8.94%. Solution of the data yielded the molecular structure shown in Figure 4.4.
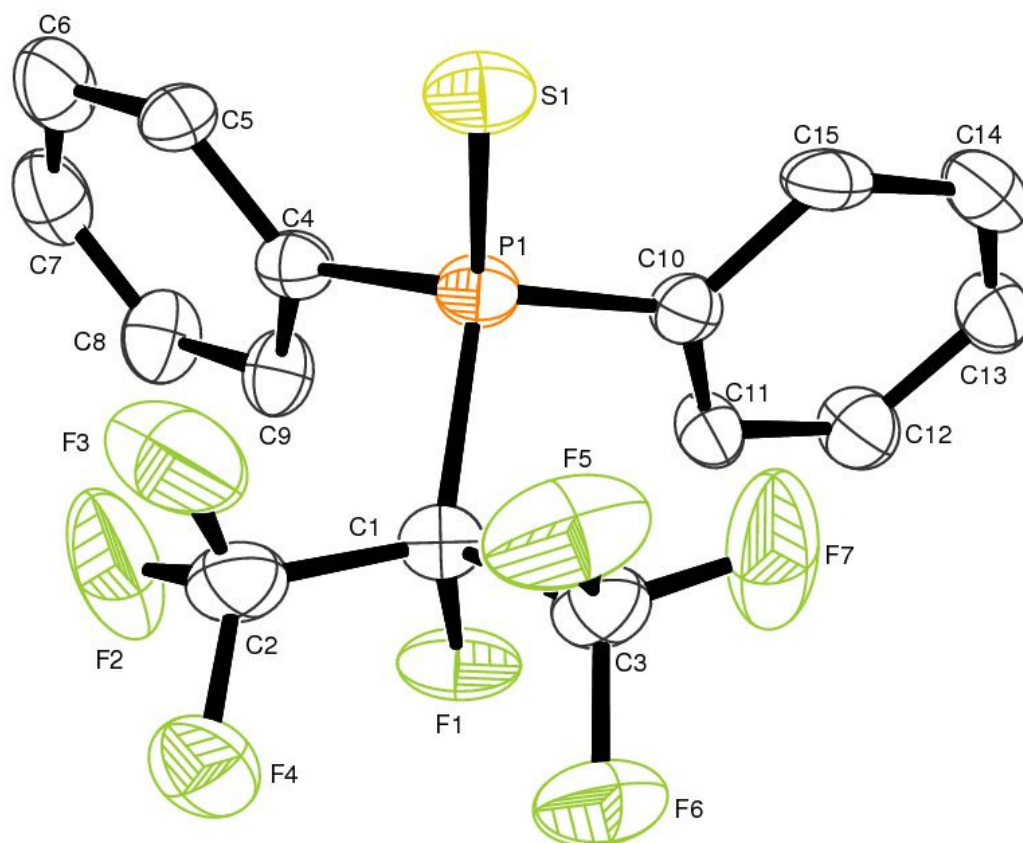
Figure 4.4: ORTEP[174] representation of the molecular structure of 31. Hydrogen atoms omitted for clarity, and thermal ellipsoids shown at 30%.

There are six reported fluoro-organo containing phosphine sulfides which have been characterised by X-ray crystallography (not including fluoro-aryl containing species), none of which contains a perfluoro-organo group.

Compound **31** crystallises in the triclinic $P\bar{1}$ space group and contains two molecules in the asymmetric unit. Similar to **29**, the C1–F1 bond is *anti* to the phosphorus–chalcogen bond, with an S1–P1–C1–F1 torsion angle of 174.5°. The P1–S1 bond length is 1.935(4) Å, which is very similar to the P–

S distance of 1.9364(13) Å in S=PPh$_2$CF$_2$CF$_2$Br,[239] and is shorter than in triaryl –containing phosphine sulfides, such as S=PPh$_3$ (d(P–S) 1.952(1) Å)[240] and S=P(2-CH$_3$C$_6$H$_5$)$_3$ (d(P–S) = 1.953(4) Å).[241] The P–C$_F$ bond distance is longer at 1.913(11) Å than the distances in the P–C$_{Ar}$ bonds (1.785(12) and 1.816(11) Å), as seen in compounds **15** and **29**. This is also the case in S=PPh$_2$CF$_2$CF$_2$Br, where the P–C$_F$ bond is longer (1.901(4) Å) than the P–C$_{Ar}$ bonds (1.807(3) and 1.809(3) Å).[239] The longest C–F distance in the molecule is between C1 and F1, at 1.387(13) Å, as observed in **15** and **29**, though within experimental error it is the same length as the C2–F2 bond.

Bond	Length (Å)	Bond	Length (Å)
P1–S1	1.935(4)	C2–F2	1.359(19)
P1–C1	1.913(11)	C2–F3	1.29(2)
P1–C4	1.816(11)	C2–F4	1.301(15)
P1–C10	1.785(12)	C3–F5	1.337(17)
C1–C2	1.525(18)	C3–F6	1.308(15)
C1–C3	1.523(18)	C3–F7	1.264(17)
C1–F1	1.387(13)		

Table 4.2: Selected bond lengths in 31.

The S–P–C angle is smallest to the fluorinated fragment, at 110.3(4)° (compared to 114.1(4) and 114.4(4)° to the phenyl rings), as is observed in **15** and **29**. A selection of bond angles is given in Table 4.3.

Bond	Angle (°)	Bond	Angle (°)
S1–P1–C1	110.3(4)	C1–P1–C4	104.7(5)
S1–P1–C4	114.1(4)	C1–P1–C10	104.1(5)
S1–P1–C10	114.4(4)	C4–P1–C10	108.4(5)
P1–C1–F1	109.0(7)		

Table 4.3: Selected bond angles in 31.

Molecules of **31** stack in the x-direction (Figure 4.5), due to the π-stacking of adjacent residues in both the y- and z-directions (Figure 4.6 and Figure 4.7). When viewed down the z-direction a fluorous domain becomes apparent.
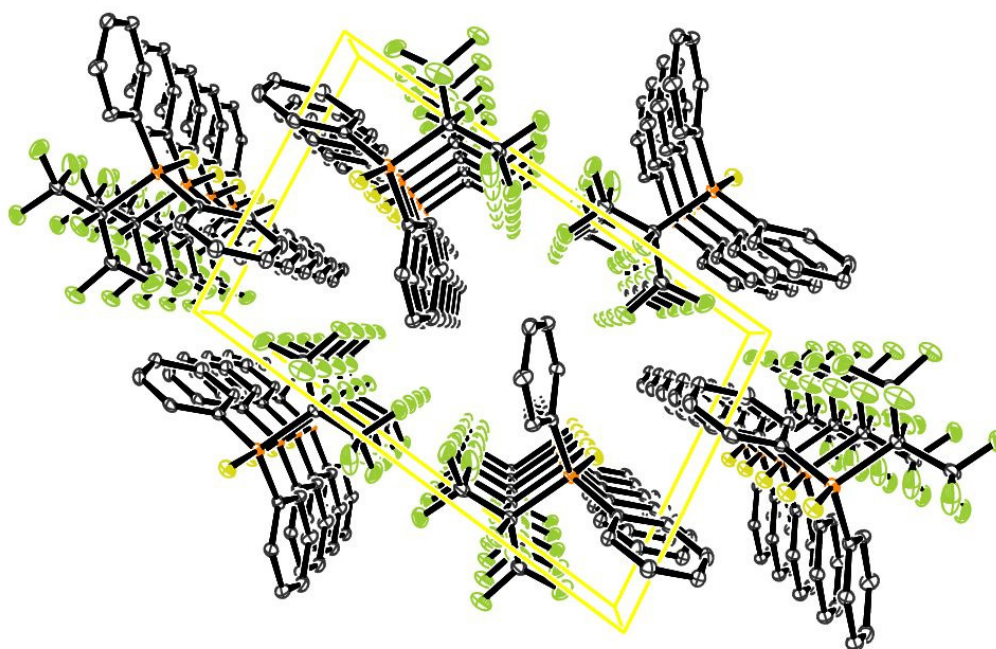
Figure 4.5: ORTEP[174] representation of the packing of 31 looking down the x-direction.
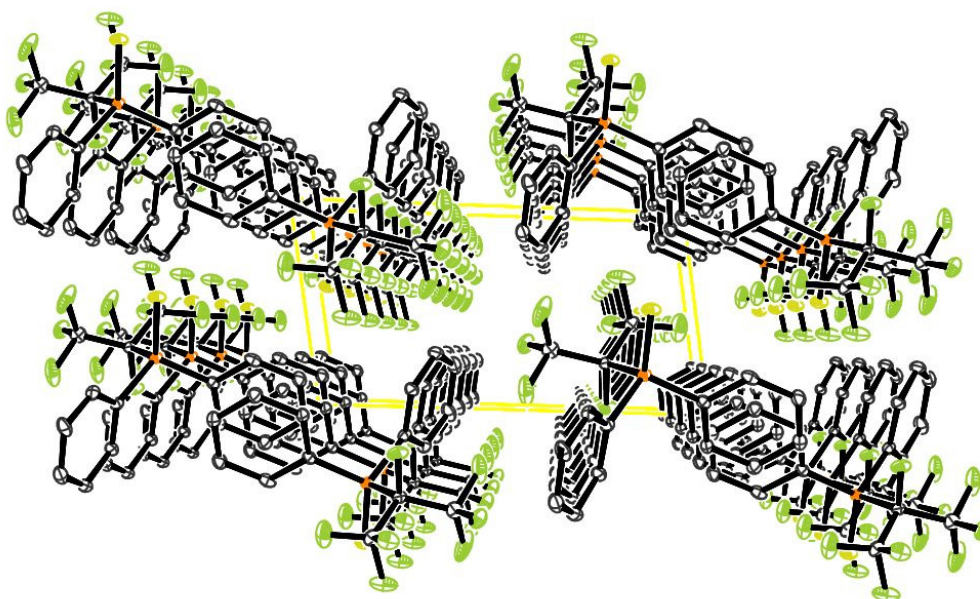
Figure 4.6: ORTEP[174] representation of the crystal packing of 31 looking down the y-direction, showing the π-stacking interaction.
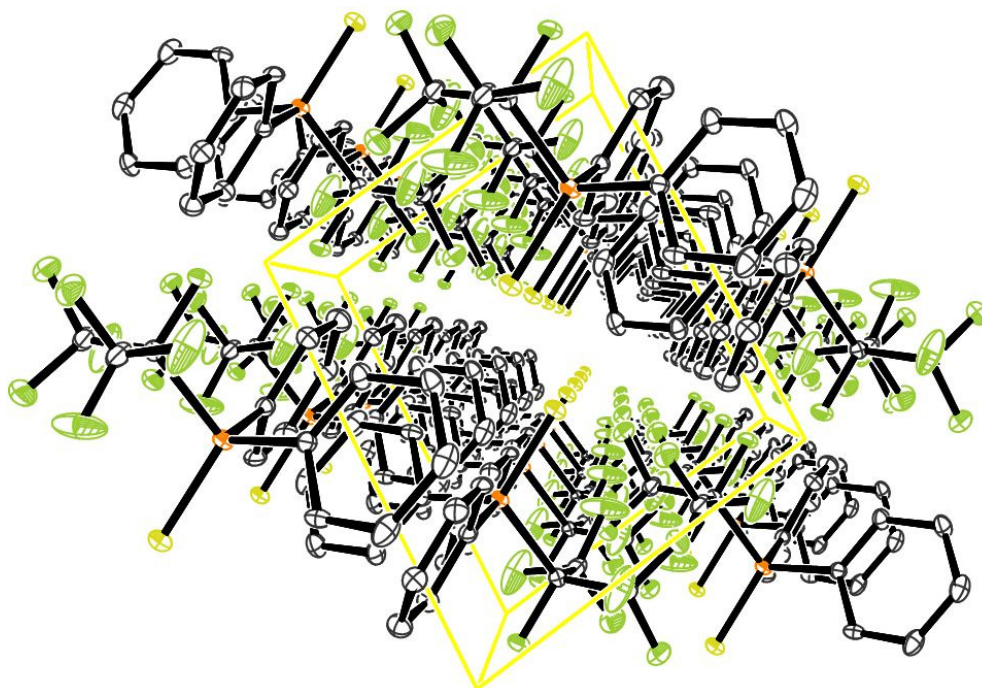
Figure 4.7: ORTEP[174] representation of the crystal packing of 31 looking down the z-direction, showing both π-stacking interactions and fluorous regions.

The data allows for an estimation of the steric demand of **15**, and the cone angle is calculated to be 190°, somewhat smaller than calculated for the oxide, **29**.

4.3.4   Se=PPh₂CF(CF₃)₂ (32)

In a procedure similar to that described for the preparation of **31**, a toluene solution of **15** was refluxed gently in the presence of an excess of elemental selenium for two hours, affording large colourless crystals.

$$Ph_2PCF(CF_3)_2 + Se \xrightarrow[\text{Toluene}]{\triangle} Se=PPh_2CF(CF_3)_2$$

15   **32**
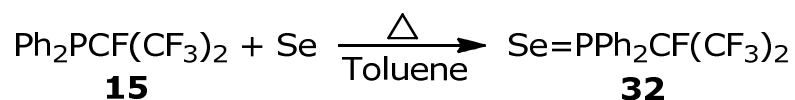
Scheme 4.4: Synthesis of compound 32.

^{31}P{^{1}H} NMR studies showed the presence of a doublet centred at δ 35.2 ppm, which exhibits ^{77}Se (I = ½, 7.6%) satellites, with $^1J_{Pse}$ = 828 Hz (see Figure 4.8).

PM 42.5 41.5 40.5 39.5 38.5 37.5 36.5 35.5 34.5 33.5 32.5 31.5 30.5 29.5 28.5 27.5
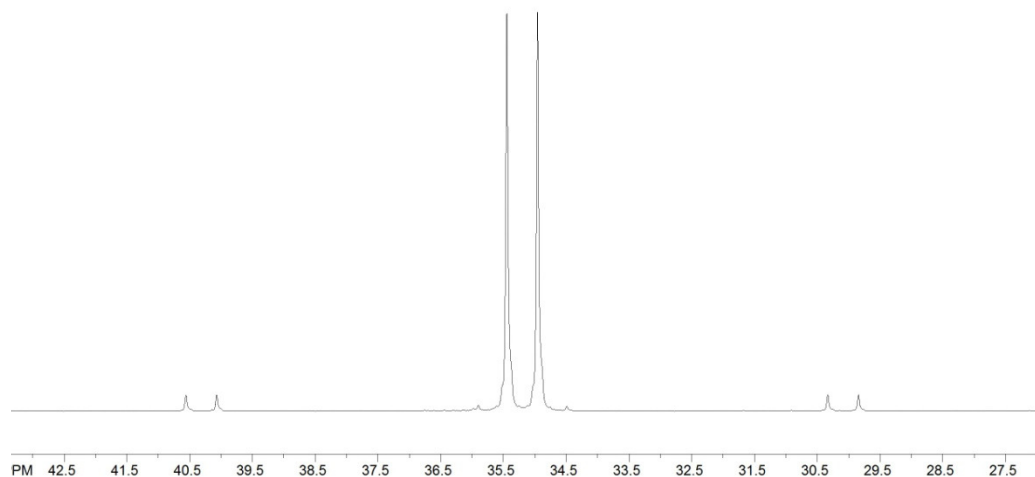
Figure 4.8: Expansion of the signal observed at δ 35.2 ppm in the ^{31}P{^{1}H} NMR spectrum of 32.

A reduction in multiplicity of the ^{31}P{^{1}H} NMR signal is observed (compared to **15**), as it was for **29** and **31,** there being no observable coupling to the fluorine nuclei attached to the β-carbon atoms of the perfluoroisopropyl unit.

The ^{19}F NMR spectrum is also similar in appearance to the spectra observed for **29** and **31**; it contains two resonances, a doublet (δ -66.0 ppm, $^3J_{FF}$ = 8.8 Hz) and a doublet of septets (δ -173.1 ppm, $^2J_{PF}$ = 39.4 Hz, $^3J_{FF}$ = 8.8.Hz), confirming the presence of a perfluoroisopropyl group. The ^{77}Se{^{1}H} NMR spectrum displays a doublet centred at δ -372.5 ppm ($^1J_{PSe}$ = 828 Hz). All of this data is consistent with the formation of Se=PPh$_2$CF(CF$_3$)$_2$, **32**.

It was noted that the chemical shift of the unique fluorine atom alters depending on the nature of the chalcogen (see Table 4.4).

Chalcogen	Unique F δ/ppm	$^2J_{PF}$/Hz
O	-188.6	50.8
None	-184.9	74.0
S	-176.3	43.6
Se	-173.1	39.4

Table 4.4: Chemical shifts of the unique fluorine nuclei and $^2J_{PF}$ coupling constants in compounds 15, 29, 31 and 32.

The effect of the chalcogen on the phosphorus centre will depend on several things, not least of which is the electronegativity of the chalcogen (O>>S>Se) and the efficiency of the orbital overlap (and the consequences that this will have on the nature of the bonds to the other substituents). The greater the electronegativity of the chalcogen, the lower the electron density should be around the phosphorus centre. This, coupled with the loss of the lone pair, may explain why there is a loss of coupling to the CF_3 group (which is exhibited by the starting phosphorus(III) compound, **15**) and the reduction in the $^2J_{PF}$ coupling constant, however the magnitude of the effect on the chemical shift of the unique fluorine is surprising.

Crystals of **32** obtained by the slow evaporation of DCM were suitable for analysis by single crystal X-ray diffraction studies. Solution of the data obtained provided further confirmation of the formation of Se=PPh$_2$CF(CF$_3$)$_2$, **32**, and the molecular structure is shown in Figure 4.9.
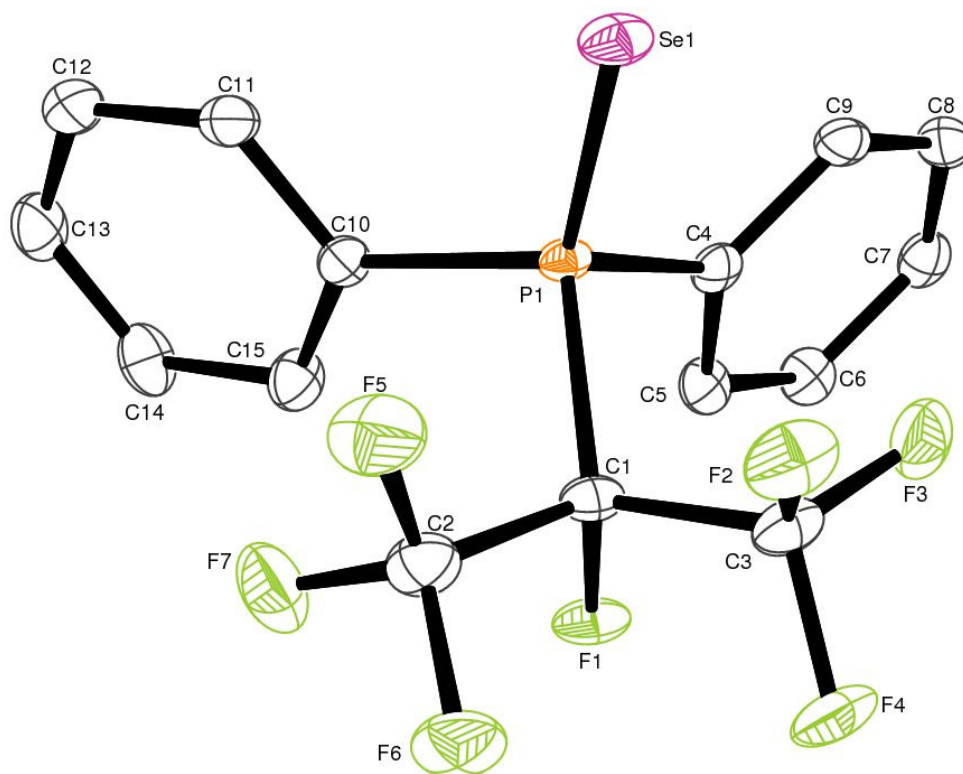
Figure 4.9: ORTEP[174] representation of the molecular structure of 32. Thermal ellipsoids are shown at 50% probability. Hydrogen atoms are omitted for clarity.

Compound **32** crystallises in the triclinic $P\bar{1}$ space group, and contains two molecules in the asymmetric unit. As in compound **29** (where the P=O bond is *anti* to the C1-F1 bond), the C1-F1 bond is also *anti* to the P–Se bond, with an Se1–P1–C1–F1 torsion angle of 169.25(14)°. The P–Se bond length is 2.0834(7) Å, which according to searches of the CCDC is the shortest P=Se bond distance known in non-cyclic Se=PR_3 compounds (the same, within experimental error, as observed in Se=P(3,5-$(CF_3)_2C_6H_3)_3$, where the P=Se distance is 2.085(1) Å),[242] The P-C_F distance is longer at 1.908(3) Å than the P-C_{aryl} distances (average 1.817(5) Å), a trend also seen for compounds **15** and **29.** The C-F bond distance for the fluorine atom attached to the α-carbon is the longest C-F bond in the molecule – however, unlike **15** and **29** (where one of the C-F bonds is noticeably shorter) all of the remaining six C-F bonds are very similar in length (see Table 4.5). The unique fluorine atom

153

has short contacts of 2.54 and 2.60 Å to F4 and F7 (0.40(2) Å and 0.34(2) shorter than the sum of the van der Waals' radii respectively), as previously noted in compounds **15** and **29.**

Bond	Distance (Å)	Bond Angle	Angle (°)
P1–Se1	2.0834(7)	Se1–P1–C1	110.28(10)
P1–C1	1.908(3)	Se1–P1–C4	114.61(10)
P1–C4	1.813(3)	Se1–P1–C10	114.39(9)
P1–C10	1.821(3)	C1–P1–C4	103.52(12)
C1–C2	1.547(4)	C1–P1–C10	104.74(12)
C1–C3	1.547(4)	C4–P1–C10	108.31(13)
C1–F1	1.389(3)	P1–C1–F1	109.06(18)
C2–F5	1.317(4)		
C2–F6	1.337(3)		
C2–F7	1.327(3)		
C3–F2	1.329(3)		
C3–F3	1.322(3)		
C3–F4	1.336(3)		

Table 4.5: Selected bond lengths and angles in compound 32.

Molecules of **32** stack in the x-direction (see Figure 4.10) and also exhibits some π-stacking in the y-direction (see Figure 4.11) with a centroid to centroid distance of 3.8737(15) Å between neighbouring residues. There is no obvious hydrogen bonding present in the molecule. Also, when looking down the x-direction, it is clear that there is a fluorous region in the crystal packing (Figure 4.10).
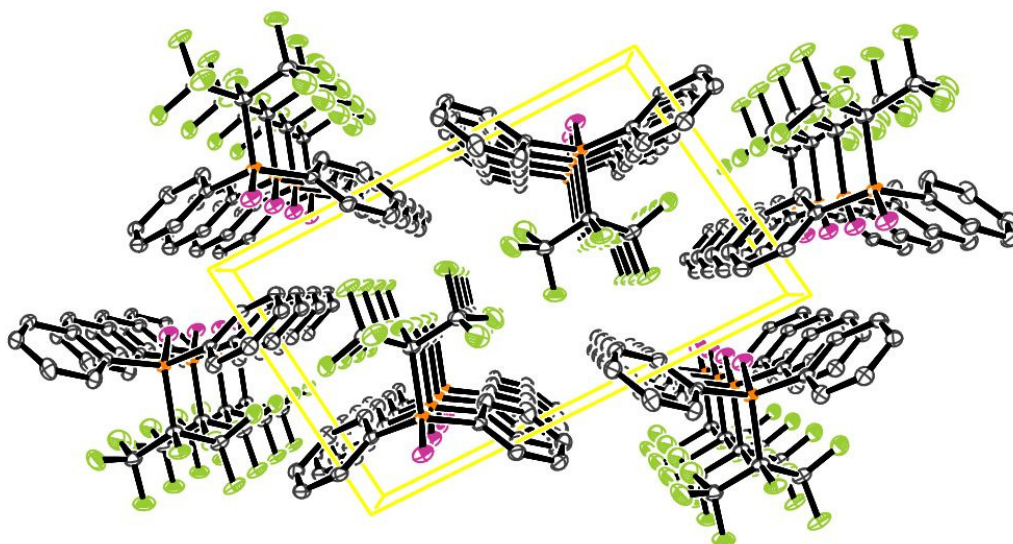
Figure 4.10: ORTEP[174] representation of the packing of compound 32 looking down the x-direction.
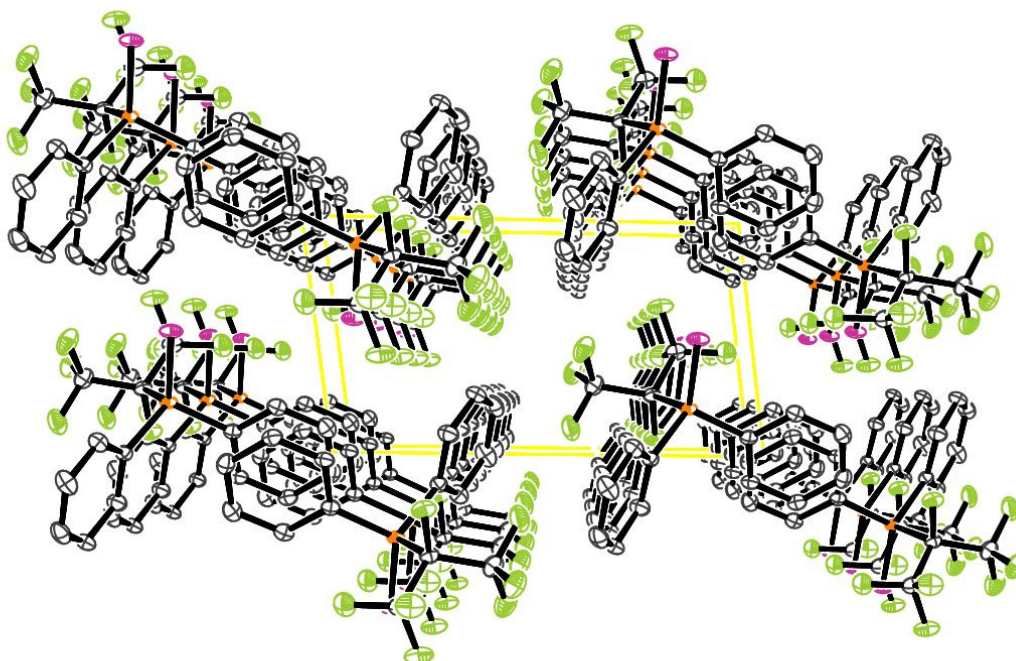
Figure 4.11: ORTEP[174] representation of the packing of compound 32 looking down the y-direction.

The cone angle of **15** can be estimated from the data obtained from compounds **29**, **31**, and **32**, and they are found to give cone angles of 215°, 190° and 184.5° respectively. The reason for the disparity in these values is

the P=E (E = O, S, Se) distance (the shorter the distance, the larger the crystallographically determined cone angle will be).

As the formation of the phosphorus(V) selenides from the perfluoroalkyl-containing phosphines proceeds smoothly, several more have been synthesised as the electronic properties of the phosphine can be quantified from the magnitude of the $^1J_{PSe}$ coupling constant.

4.3.5   Se=PPh$_2$($^sC_4F_9$) (33)

The reaction of **18** with elemental selenium was performed similarly to that described in Section 4.3.4 (see Scheme 4.5).

$$Ph_2P(^sC_4F_9) + Se \xrightarrow[\text{Toluene}]{\triangle} Se=PPh_2(^sC_4F_9)$$
$$\mathbf{18} \qquad\qquad\qquad\qquad\qquad\qquad \mathbf{33}$$
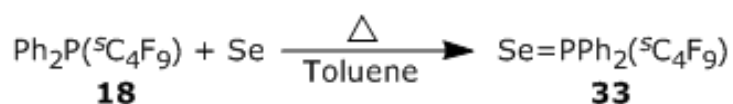
Scheme 4.5: Oxidation of 18 with elemental selenium.

The $^{31}P\{^1H\}$ NMR spectrum of the resultant solid in CDCl$_3$ (see Figure 4.12) displays a a doublet of doublet based resonance at δ 37.7 ppm (J = 41.3, 10.6 Hz), and also contains ^{77}Se satellites (I = ½, 7.6%) with $^1J_{PSe}$ = 831 Hz. Similarly to **32**, there is a reduction in multiplicity (there is no observable coupling between the phosphorus nucleus and any fluorine atom other than the fluorine nuclei attached to the α-carbon) on oxidation from **18** to **33**.
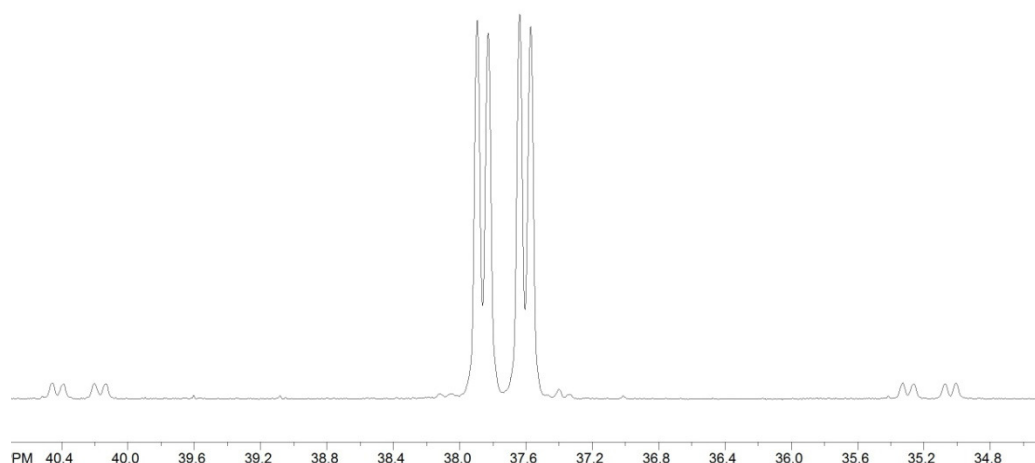
Figure 4.12: Expansion of the signal at δ 37.7 ppm in the ^{31}P{^{1}H} NMR spectrum of 33.

The following labelling scheme will be applied for this compound, similar to that used for **19** (Figure 4.13).
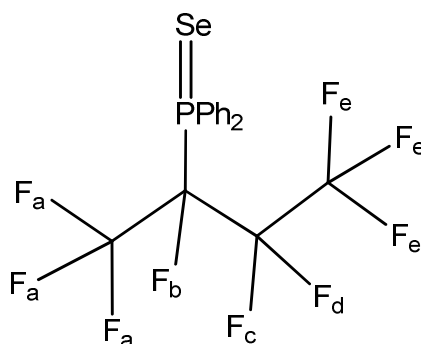
Figure 4.13: Labelling of fluorine atoms in compound 33.

The ^{19}F NMR spectrum of **33** contains five signals, as expected (and analogous to **18**), at δ -64.4, -80.2, -108.6, -109.6 and -172.1 ppm. All show a reduction in multiplicity compared to **18** (apart from the signal at -172.1 ppm).

PPM   -64.20   -64.24   -64.28   -64.32   -64.36   -64.40   -64.44   -64.48   -64.52   -64.56   -64.60   -64.64
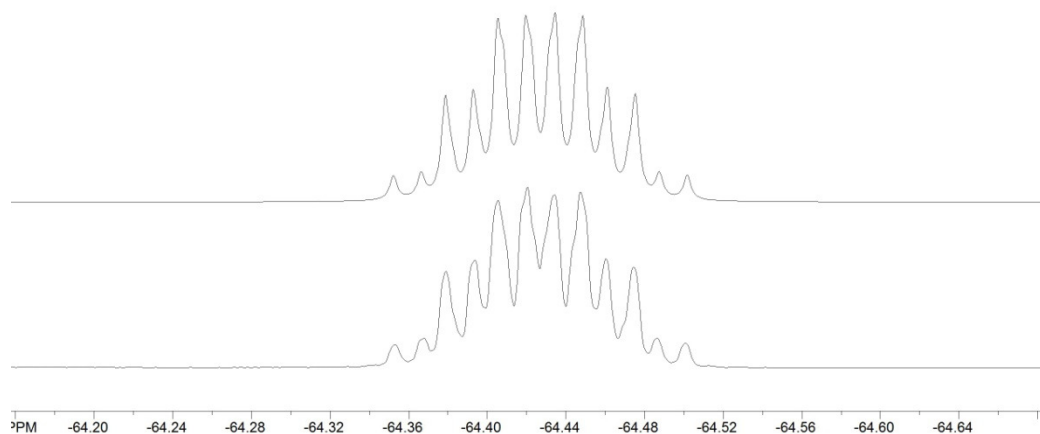
Figure 4.14: Expansion of the ^{19}F NMR signal assigned to F_e.

There are two signals seen in the CF_3 region of the ^{19}F NMR spectrum of **33**; one of these resonances, at δ -64.4 ppm, is an overlapping doublet of doublet of quartet of doublets ($^3J_{FeFd}$ = 13.0 Hz, $^4J_{FeFb}$ = 10.2 Hz, $^5J_{FeFa}$ = 9.9 Hz, $^3J_{FeFc}$ = 3.5 Hz).

PM   -80.01 -80.03 -80.05 -80.07 -80.09 -80.11 -80.13 -80.15 -80.17 -80.19 -80.21 -80.23 -80.25 -80.27 -80.29 -80.31 -80.33 -80.35 -80.37 -80.39
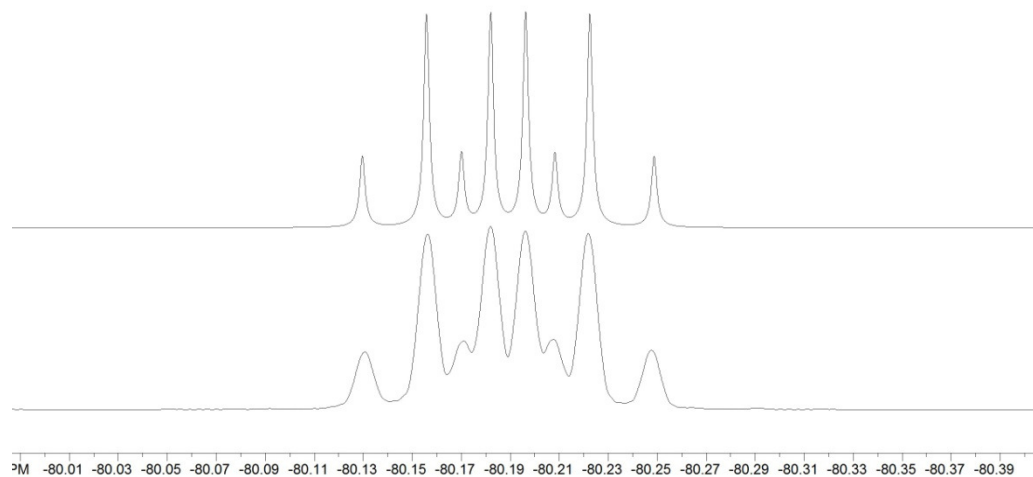
Figure 4.15: Expansion of the ^{19}F NMR signal assigned to F_a.

The second signal observed in the CF_3 region of the spectrum occurs at δ -80.2 ppm and is observed as a (slightly broad) doublet of quartets ($^3J_{FaFb}$ = 15.2 Hz, $^5J_{FaFe}$ = 9.2 Hz). It is perhaps surprising that there appears to be

some coupling between the fluorine nuclei on the CF_3 groups, as they are five bonds apart, and do not appear to be particularly close in space.
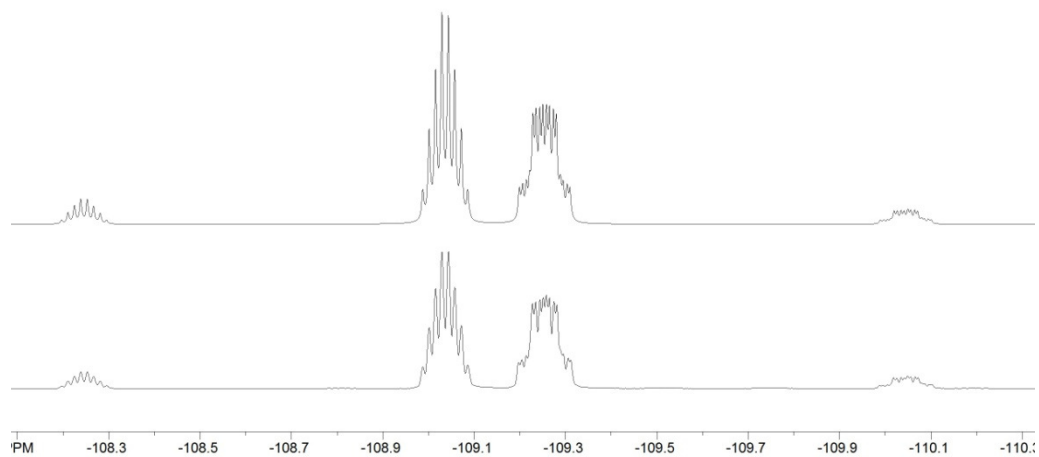
Figure 4.16: Expansions of the ^{19}F NMR signals assigned to F_c and F_d.

The signals due to the diastereotopic fluorine nuclei of the CF_2 group are observed at δ -108.6 and -109.6 ppm, and share a large geminal coupling constant of 297.7 Hz. The chemical shift difference (~380 Hz) is of a similar in magnitude to the coupling constant, giving rise to the large second-order distortion seen here (Figure 4.16). Also of interest is the fact that only one of the two fluorine nuclei displays coupling to the phosphorus centre (signal centred at δ -108.6 ppm), despite being the same number of bonds and a similar distance apart in space.

PM -171.80 -171.84 -171.88 -171.92 -171.96 -172.00 -172.04 -172.08 -172.12 -172.16 -172.20 -172.24 -172.28 -172.32
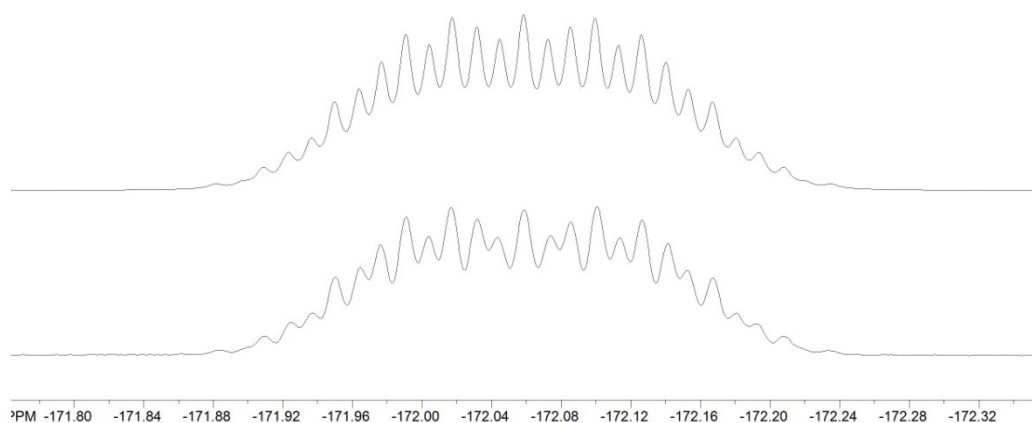
Figure 4.17: Expansion of the ^{19}F NMR signal assigned to F$_b$.

The remaining peak at δ -172.0 ppm corresponds to the fluorine nucleus attached to the α-carbon. The signal is an overlapping doublet of quartet of doublet of quartet of doublets ($^2J_{PFb}$ = 41.0 Hz, $^3J_{FbFa}$ = 15.2 Hz, $^3J_{FbFc}$ = 11.8 Hz, $^4J_{FbFe}$ = 10.2 Hz, $^3J_{FbFd}$ = 4.3 Hz), and, as is clear from the figures above, in all cases the simulated spectrum agrees well with that obtained experimentally.

A single crystal of **33** suitable for analysis via X-ray diffraction was grown by the slow evaporation of a solution of **33** in DCM and hexane (1:1), and resulted in the molecular structure shown in Figure 4.18 (selected bond lengths are given in Table 4.6, and selected bond angles are listed in Table 4.7) .
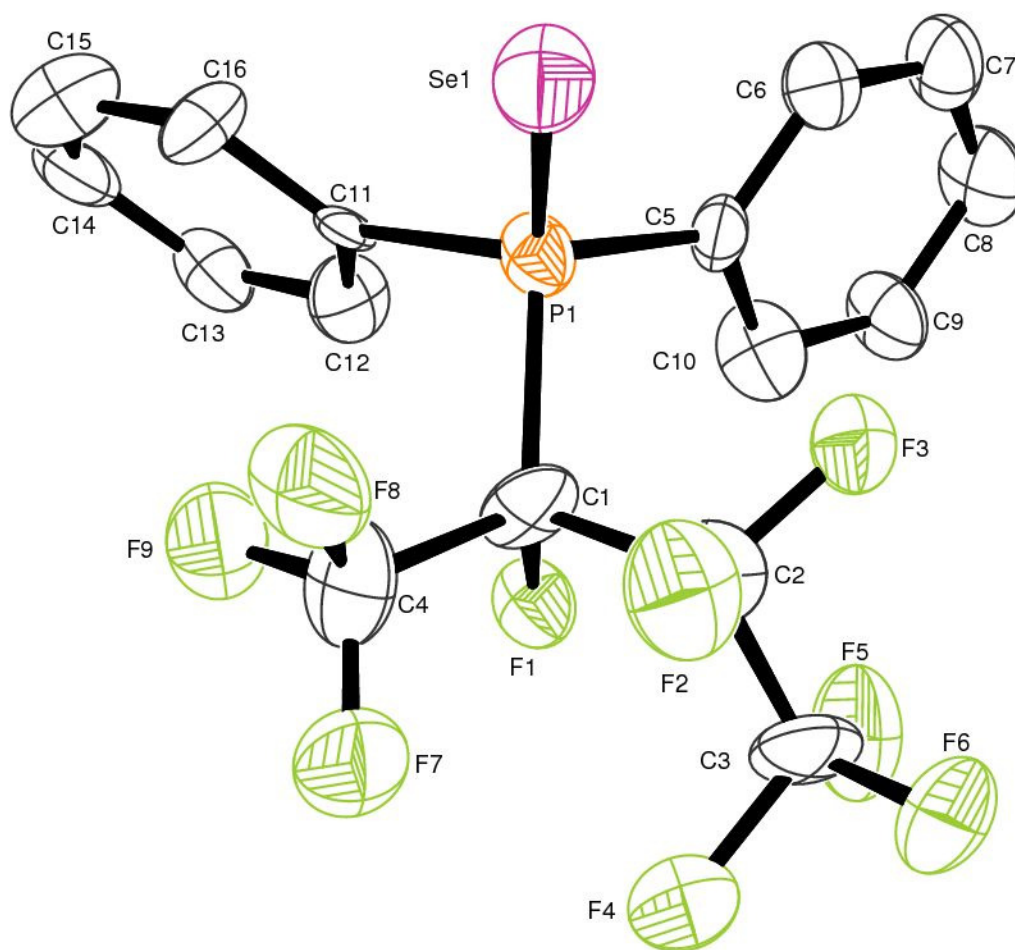
Figure 4.18: ORTEP[174] representation of the molecular structure of 33. Thermal ellipsoids shown at 30% and hydrogen atoms have been omitted for clarity.

Compound **33** crystallises in the monoclinic space group $P2_1/c$, and there are four molecules in the unit cell, all of which are the (*S*)-enantiomer. As in **29** and **32**, the C1-F1 bond is again *anti* to the phosphorus–chalcogen bond (the Se1–P1–C1–F1 torsion angle is 177.2(11)°). The P–Se bond length is 2.077(6) Å, which is, within experimental error, the same length as in **32**. The P–C$_F$ distance (1.90(3) Å) is longer than the P–C$_{Ar}$ distances (1.789(18) and 1.818(17) Å), as previously noted for **15**, **29**, and **32**. The C–F distances vary from 1.26(3) Å to 1.41(4) Å, but no one bond is significantly shorter or longer than the remainder.

Bond	Length (Å)	Bond	Length (Å)
P1-Se1	2.077(6)	C2-F2	1.39(3)
P1-C1	1.90(3)	C2-F3	1.37(4)
P1-C5	1.789(18)	C3-F4	1.41(4)
P1-C11	1.818(17)	C3-F5	1.26(3)
C1-C2	1.55(4)	C3-F6	1.31(3)
C1-C4	1.56(4)	C4-F7	1.28(4)
C2-C3	1.51(5)	C4-F8	1.34(3)
C1-F1	1.41(2)	C4-F9	1.32(3)

Table 4.6: Selected bond lengths in 33.

The smallest Se–P–C angle is to the fluorinated group (110.8(7)° vs 115.4(8)° and 114.9(7)°), as it is in **32** and a selection of bond angles is given in Table 4.7. The αC–F bond is anti to the P–Se bond, with an Se1–P1–C1–F1 of 177.2(11)°, as observed in **32**.

Bond	Angle (°)	Bond	Angle (°)
Se1-P1-C1	110.8(7)	C1-P1-C5	105.8(10)
Se1-P1-C5	115.4(8)	C1-P1-C11	103.2(10)
Se1-P1-C11	114.9(7)	C5-P1-C11	105.8(9)
P1-C1-F1	110.2(14)	P1-C1-C2	111.3(9)
P1-C1-C4	117.1(8)		

Table 4.7: Selected bond angles in 33.

There is a large number of F⋯F intramolecular contacts within the *sec*-C_4F_9 group, all of which are shorter than twice the van der Waals radius of fluorine (2.94 Å). F1 makes four intramolecular short contacts, to F4 (2.849(19) Å), F5 (2.629(17) Å), F7 (2.728(19) Å) and F9 (2.619(17) Å). F2 also makes four short intramolecular contacts, to F4 (2.84(2) Å), F6 (2.63(2) Å), F7 (2.83(2) Å), and F8 (2.626(18) Å). F3 makes short contacts to F5 (2.65(2) Å) and F6 (2.70(2) Å). F4 makes a short contact to F7 (2.64(2) Å).

There are also a several intermolecular F⋯F contacts, resulting in the presence of a fluorous domain within the crystal structure (Figure 4.19). F1 makes a short contact to F5 (3.062(17) Å), as does F2 (2.97(2) Å) on different neighbouring residues. F6 makes short contacts to F7 (3.08(2) Å) and F9 (2.83(2) Å), again on different residues.
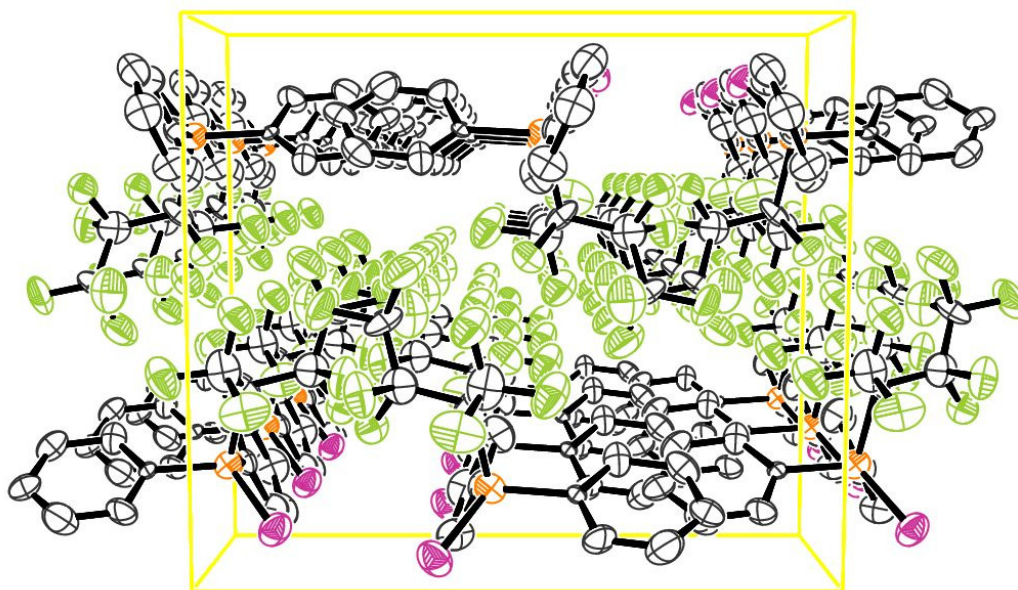
Figure 4.19: ORTEP[174] representation of the crystal packing on the z-direction, showing the fluorous region and offset π-stacking in 33.

The data allows for estimation of the cone angle of the phosphine, and it is calculated to be 179.5°, suggesting that this phosphine has a large steric demand, and appears to be very similar in size to the perfluoroisopropyl group.

4.3.6 Se=PPh₂(*cyc*-C₆F₁₁) (34)

Refluxing **19** in toluene in the presence of elemental selenium (Scheme 4.6) in a manner analogous to that described above results in the formation of a white solid after work-up.

$$\text{Ph}_2\text{P}(cyc\text{-C}_6\text{F}_{11}) + \text{Se} \xrightarrow[\text{Toluene}]{\triangle} \text{Se=PPh}_2(cyc\text{-C}_6\text{F}_{11})$$
$$\mathbf{19} \qquad\qquad\qquad\qquad\qquad \mathbf{34}$$
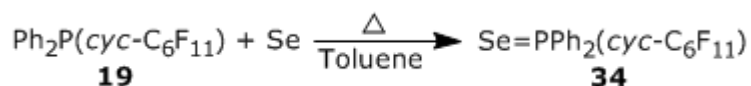
Scheme 4.6: Reaction of 19 with elemental selenium.

The $^{31}\text{P}\{^1\text{H}\}$ NMR spectrum (Figure 4.20) of the resulting white solid displays a doublet centred at δ 34.3 ppm ($^2J_{PF}$ = 41.6 Hz), with characteristic ^{77}Se satellites ($^1J_{PSe}$ = 836.7 Hz).
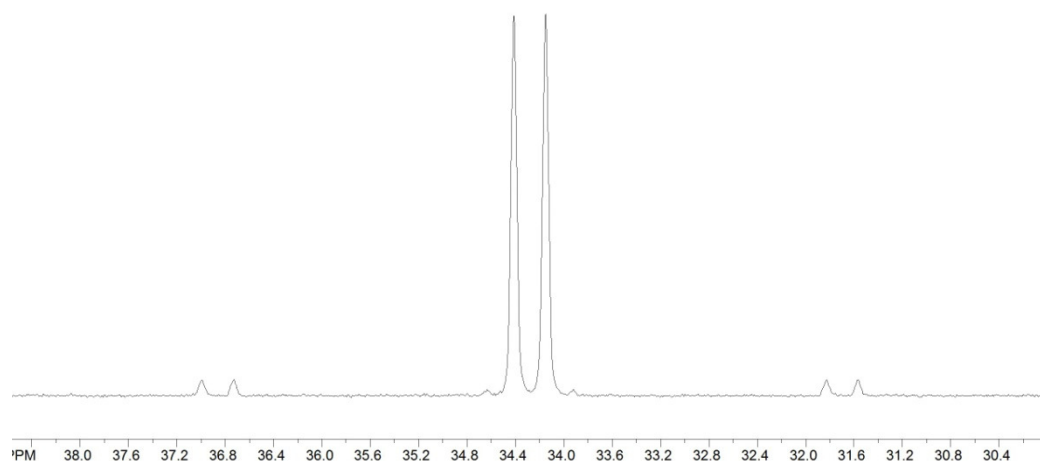
Figure 4.20: Expansion of the signal observed at δ 34.3 ppm in the ^{31}P{^{1}H} NMR spectrum of 34.

The ^{19}F NMR spectrum (Figure 4.21) of **34** displays the expected seven resonances; these are observed at δ -110.3, -121.8, -123.6, -124.5, -138.4, -141.8, and -175.2 ppm.
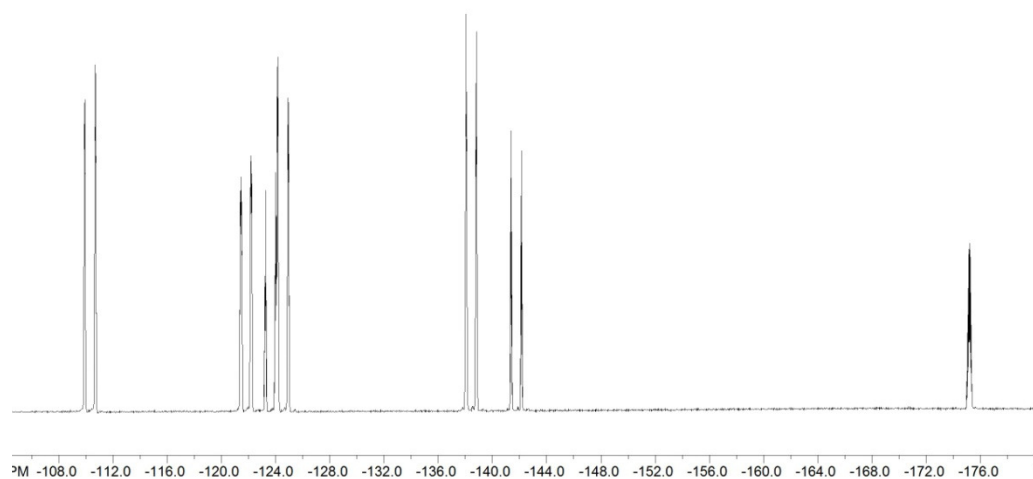
Figure 4.21: ^{19}F NMR spectrum of 34.

All of the resonances are complex multiplets, and six of them occur at very similar chemical shifts to those observed for the free phosphine, **19**, with only the fluorine atom bonded to the α-carbon altering by a significant amount, a shift of δ +10.6 ppm. This is comparable to the shift of the

164

equivalent fluorine atoms in **32** and **33**, where the resonance moves 11.8 ppm to higher frequency in both compounds.

Crystals suitable for analysis by X-ray diffraction studies were grown by the slow evaporation of a solution of **34** in Et$_2$O and hexane (1:1). Unfortunately, the crystals were of poor quality, resulting in a slightly high R factor of 9.07%. Solution of the data resulted in the molecular structure shown in Figure 4.22.
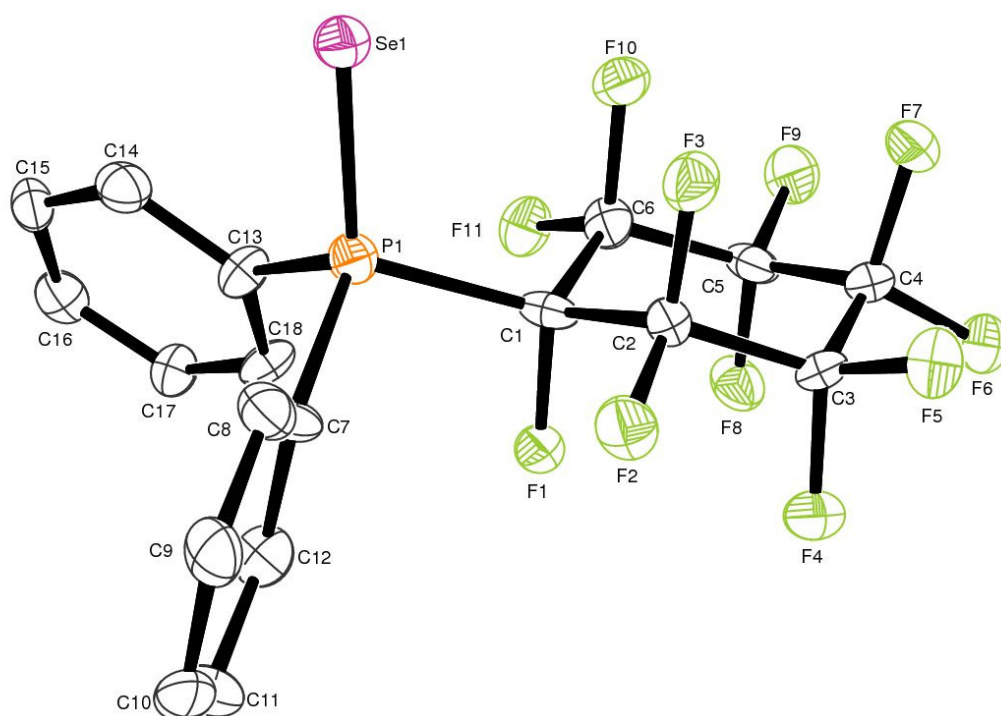
Figure 4.22: ORTEP[174] representation of the molecular structure of 34. Thermal ellipsoids are shown at 30%, and hydrogen atoms omitted for clarity.

This is only the fourth structure containing a perfluorcyclohexyl group to be characterised by X-ray diffraction according to searches of the CCDC database. The others being C$_6$F$_{11}$H,[243] C$_6$F$_{12}$,[243] *bis*((m$_2$-1,5-*bis*(C$_6$F$_{11}$)pentane-2,4-dionato-O-O-O′,F)-(m$_2$-1,5-*bis*(C$_6$F$_{11}$)pentane-2,4-dionato-O-O′,F)-lead(II)[244] (Figure 4.23) and 2-(1-(C$_6$F$_{11}$)ethoxy)-2,5-dioxo-4,4-*bis*(CF$_3$)-6,7-benzo-1,3,2-dooxaphosphepine[245] (Figure 4.23), though

only the latter contains coordinates. This structure therefore represents the first where it is bound to phosphorus.
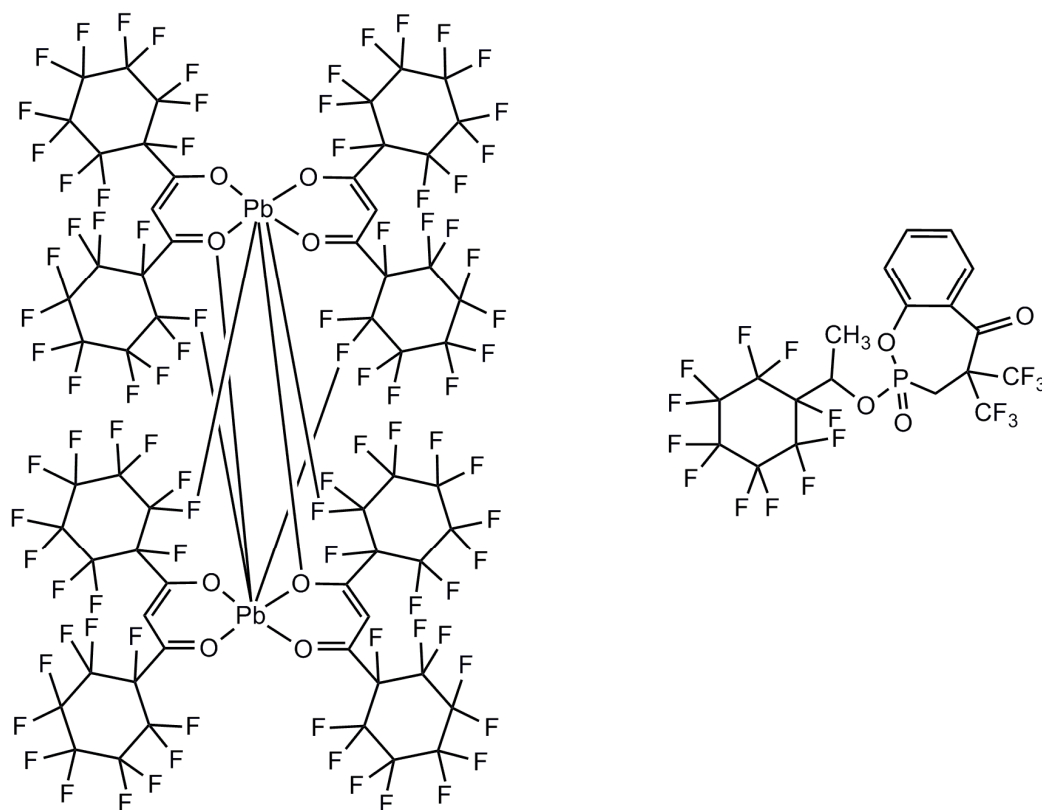
Figure 4.23: Representation of *bis*((m$_2$-1,5-*bis*(C$_6$F$_{11}$)pentane-2,4-dionato-O-O-O',F)-(m$_2$-1,5-*bis*(C$_6$F$_{11}$)pentane-2,4-dionato-O-O',F)-lead(II) (left) and 2-(1-(C$_6$F$_{11}$)ethoxy)-2,5-dioxo-4,4-*bis*(CF$_3$)-6,7-benzo-1,3,2-dioxaphosphepine (right).

As can clearly be seen in Figure 4.22, the –P(Se)Ph$_2$ group occupies an equatorial position on the ring, as expected based on its size relative to a fluorine atom. Compound **34** crystallises in the monoclinic space group $P2_1/c$, and there are two asymmetric molecules in the unit cell, and eight in total.

The Se–P distances are identical, within experimental error (2.87(4) and 2.91(4) Å), and are slightly longer than observed in **32** and **33**. The P–C$_F$ distances (1.906(13) and 1.908(14) Å) are again longer than the P–C$_{Ar}$ distances (1.819(13), 1.807(12), 1.814(12), and 1.815(13) Å) as observed in **15**, **29**, **31**, and **32**. The longest C–F bonds in both molecules are from

the α-carbon to F1 and F12 (1.403(13) and 1.398(14) Å). The low accuracy of the C–F bonds is due to the poor quality of the crystal and makes further comparison of the C–F distances meaningless, as many of them are the same within experimental error. The longest C–F bond in 2-(1-(C_6F_{11})ethoxy)-2,5-dioxo-4,4-*bis*(CF_3)-6,7-benzo-1,3,2-dooxaphosphepine is also the αC–F bond, and the remainder are all very similar in length.[245]

Bond	Length (Å)	Bond	Length (Å)
Se1–P1	2.091(4)	Se2–P2	2.087(4)
P1–C1	1.906(13)	P2–C19	1.908(13)
P1–C7	1.807(12)	P2–C25	1.814(12)
P1–C13	1.819(13)	P2–C31	1.815(13)
C1–F1	1.403(13)	C19–F12	1.398(14)
C2–F2	1.338(13)	C20–F13	1.355(15)
C2–F3	1.325(13)	C20–F14	1.337(14)
C3–F4	1.358(15)	C21–F15	1.359(14)
C3–F5	1.376(16)	C21–F16	1.352(14)
C4–F6	1.352(15)	C22–F17	1.361(15)
C4–F7	1.370(15)	C22–F18	1.323(14)
C5–F8	1.366(15)	C23–F19	1.327(15)
C5–F9	1.336(14)	C23–F20	1.363(15)
C6–F10	1.382(14)	C24–F21	1.368(14)
C6–F11	1.339(14)	C24–F22	1.325(15)

Table 4.8: Selected bond lengths in compound 34.

The torsion angles of the Se–P–C–F bonds are 174.1(6) and 174.7(6)°, with the C–F bond being *anti* to the P–chalcogen bond, as observed in **29**, **31**, **32** and **33**. The Se–P–C angles are smallest to the fluorinated fragment (112.1(4) and 112.6(4)°), though they are much closer to the Se–P–C_{Ar} angles in this compound than in **32** and **33**.

Bond	Angle(°)	Bond	Angle(°)
Se1–P1–C1	112.1(4)	Se2–P2–C19	112.6(4)
Se1–P1–C7	114.4(4)	Se2–P2–C25	114.1(4)
Se1–P1–C13	114.3(4)	Se2–P2–C31	113.4(4)

Table 4.9: Selected bond angles in compound 34.

There are twenty intramolecular fluorine–fluorine contacts within residue one, and twenty four F···F interactions in residue two that are shorter than the sum of the van der Waals' radii (there are several more that are slightly

greater than the sum of the van der Waals' radii). These interactions are likely due to the geometry of the perfluorocyclohexyl group.

Atom Se1 makes two short intermolecular contacts to hydrogen atoms (H10 and H11) on a neighbouring residue (2.99 and 3.27 Å respectively, sum of van der Waals' radii is 3.10 Å). Se1 makes a contact to a neighbouring Se1 atom of 3.3747(19) Å (sum of van der Waals' radii is 3.80 Å). There are three F···H intermolecular interactions less than the sum of the van der Waals' radius, at 2.55 (1), 2.56(1) and 2.64(1) Å from residue one.

Atom Se2 also makes two intermolecular contacts to hydrogen atoms (H30 and H36) on a neighbouring residue (2.78 and 2.75 Å respectively), but does not make a contact to another Se atom. Atoms H28, H30 and H33 make short contacts to neighbouring fluorine atoms of 2.64(1), 2.55(1), and 2.56(1) Å.

There are fluorous domains within the crystal packing, as can be seen in Figure 4.24. Residue 1 makes a total of nine F···F interactions to four neighbouring residues (the shortest of which is 2.719(10) Å) whereas residue two makes a total of eight intermolecular F···F contacts to five different residues (the shortest being 2.968(11) Å). There are also some π-stacking interactions in the z-direction (Figure 4.24). There are a variety of interactions within the crystal packing of **34**, with no particular interaction dominating.
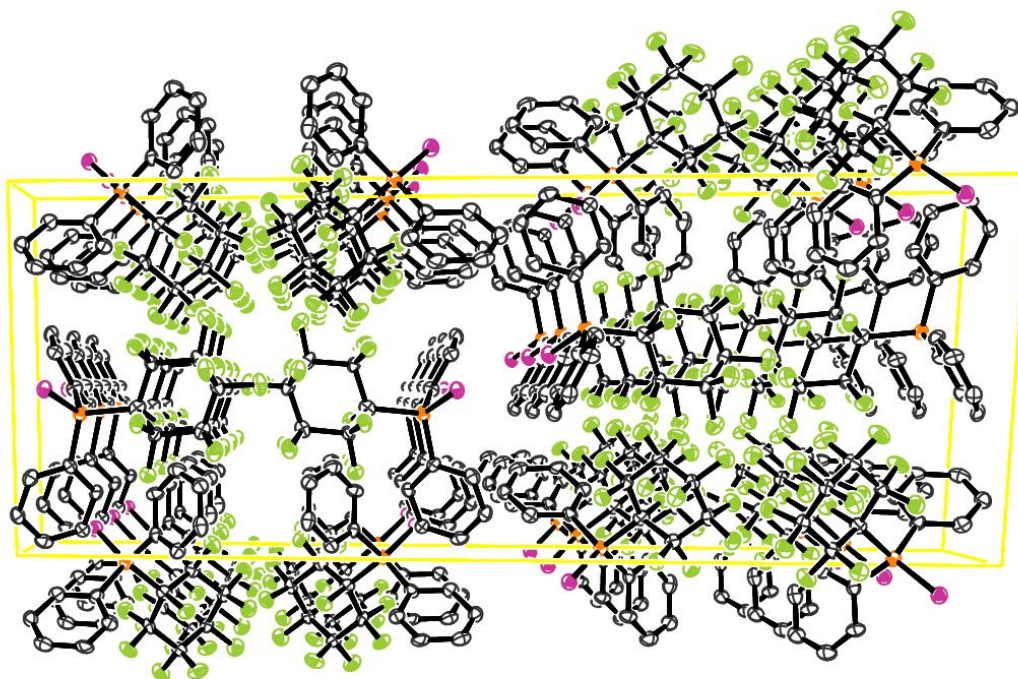
Figure 4.24: ORTEP[174] representation of the crystal packing of 34 looking in the z-direction.

The cone angle of $Ph_2P(cyc\text{-}C_6F_{11})$ derived from the selenide is estimated to be 183°, which suggests that the perfluorocyclohexyl group imparts a similar steric demand to the $-CF(CF_3)_2$ and $sec\text{-}(C_4F_9)$ moieties. Compared with the cone angle calculated from the non-fluorinated analogue, $Ph_2P(Se)Cy$, of 168.4°[246] the perfluorocyclohexyl group is sterically more demanding than a cyclohexyl group.

4.3.7 Se=PPh$_2$CF$_3$ (35)

The phosphine Ph_2PCF_3, was oxidised to the phosphorus(V) selenide in a manner analogous to that described above (Scheme 4.7).

$$Ph_2PCF_3 + Se \xrightarrow[\triangle]{Toluene} Se=PPh_2CF_3$$
$$\mathbf{16} \qquad\qquad\qquad\qquad \mathbf{35}$$
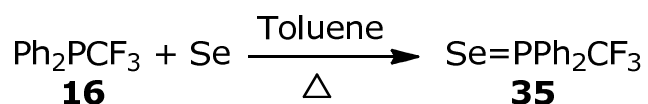
Scheme 4.7: Reaction of 16 with elemental selenium.

The ^{31}P{^{1}H} NMR spectrum of **35** (see Figure 4.25) displays a binomial quartet at δ 39.3 ppm ($^{2}J_{PF}$ = 84.4 Hz), with ^{77}Se satellites ($^{1}J_{PSe}$ = 816.0 Hz). The chemical shift difference between the free phosphine and its selenide is *ca*. 37 ppm, comparable to the Δδ observed in compounds **32-34**.
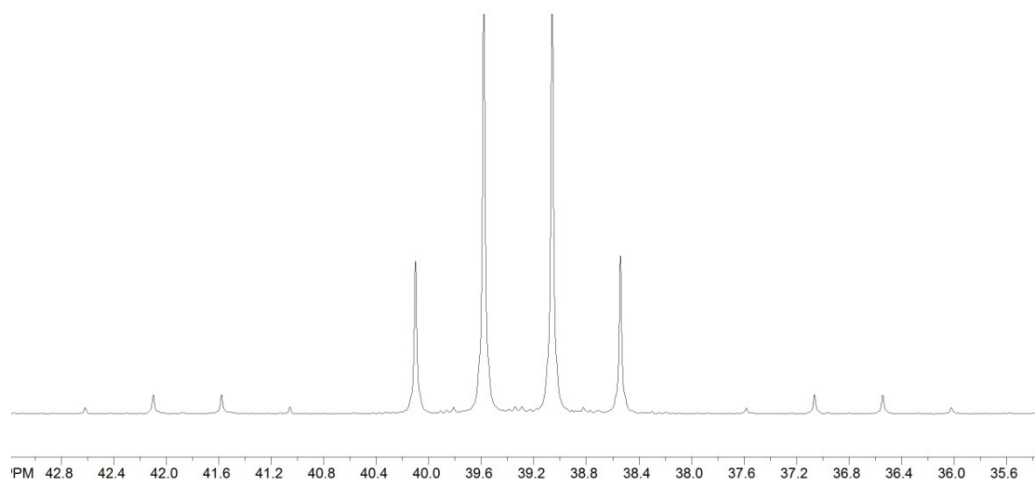
Figure 4.25: Expansion of the signal observed at δ 39.3 ppm in the ^{31}P{^{1}H} NMR spectrum of 35, with ^{77}Se satellites.

The ^{19}F NMR spectrum displays a doublet in the CF$_3$ region, centred at δ -66.6 ppm ($^{2}J_{PF}$ = 84.5 Hz), as would be expected for **35**. The ^{77}Se{^{1}H} NMR spectrum displays a doublet, at δ -364.2 ppm ($^{1}J_{PSe}$ = 816.0 Hz). Unlike in the secondary fluoroalkyl-containing compounds, the fluorine chemical shift has moved in the opposite direction relative to the free ligand, Δδ of -11.6 ppm.

4.4   Comparison of $^{1}J_{PSe}$ Coupling Constants

As discussed earlier, the magnitude of P-Se coupling constants can be used as a measure of the electronic properties of a phosphine, with a good correlation with the carbonyl stretching frequency of [Ni(CO)$_3$L] systems that have been used historically. Large $^{1}J_{PSe}$ coupling constants correspond to electron-poor phosphines, as shown Table 4.10, which lists $^{1}J_{PSe}$ coupling

170

constants for the phosphine selenides described above and some related examples.

Se=PR$_3$	$^1J_{PSe}$/Hz	Ref.
Se=PMe$_3$	684	39
Se=PPh$_3$	732	37
Z-Ph$_2$P(Se)(CF=CF^{t}Bu), 6	764	This work
Ph$_2$P(Se)(CF=CF$_2$)	785	121
Ph$_2$P(Se)OMe	788	247
Ph$_2$P(Se)OEt	796	248
Ph$_2$P(Se)CF$_3$, 35	816	This work
Ph$_2$P(Se)CF(CF$_3$)$_2$, 32	828	"
Ph$_2$P(Se)CF(CF$_3$)(C$_2$F$_5$), 33	831	"
Ph$_2$P(Se)(C$_6$F$_{11}$), 34	837	"
PhP(Se)(CF=CF$_2$)$_2$	848	121
PhP(Se)(OMe)$_2$	881	247
Se=P(OMe)$_3$	955	249

Table 4.10: Selected $^1J_{PSe}$ coupling constants in a series of phosphine selenides.

The $^1J_{PSe}$ coupling constants for the perfluoroalkyl containing phosphines **15**, **16**, **18**, and **19** are quite similar – suggesting that despite altering the bulk of the R$_f$ group the electronic effect does not change significantly. Interestingly, the $^1J_{PSe}$ coupling constant for all of the secondary fluoroalkyl groups is greater than for the CF$_3$-containing analogue. These data suggest that the presence of an R$_f$ group on the α-carbon has a more profound electron withdrawing effect than a fluorine atom in the same position – though the added bulk may significantly influence the change in the magnitude of the coupling constant, as this will alter the s character of the phosphorus centre, and hence the effect on the P=Se bond. As expected, the perfluoroalkyl groups appear to be far more electron withdrawing than perprotio groups, and decidedly more electron-withdrawing than the

perfluorovinyl groups. They also appear to have a greater effect on the $^1J_{PSe}$ coupling constant than alkoxy moieties.

4.5 $F_2PPh_2R_f$ Compounds

As part of the investigation into the chemistry and properties of perfluoroalkyl-containing phosphines, the reaction of them with XeF_2 was studied in an NMR tube under an inert atmosphere (Scheme 4.8).

$$Ph_2PR_f + XeF_2 \xrightarrow[Ar]{CDCl_3} F_2PPh_2R_f + Xe$$
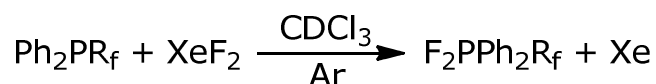
Scheme 4.8: Oxidation of fluoroalkyl phosphines with XeF_2.

4.5.1 $F_2PPh_2CF(CF_3)_2$ (36)

The $^{31}P\{^1H\}$ NMR spectrum recorded after the addition of approx. 0.25 equivalents of XeF_2 to a $CDCl_3$ solution of **15** contained two resonances; a doublet of septets at δ -0.8 ppm corresponding to unreacted **15**, and a new signal at δ -58.4 ppm. Further portions of XeF_2 crystals were added until the signal corresponding to **15** could no longer be detected. The $^{31}P\{^1H\}$ NMR spectrum (Figure 4.26 and Figure 4.27) only contained the resonance at δ -58.4 ppm which is observed as a binomial triplet of doublet of septets (see Figure 4.26), consistent with the formation of **36**, and has the coupling constants $^1J_{PF}$ = 805.2 Hz, $^2J_{PF}$ = 82.6 Hz and $^3J_{PF}$ = 4.7 Hz.
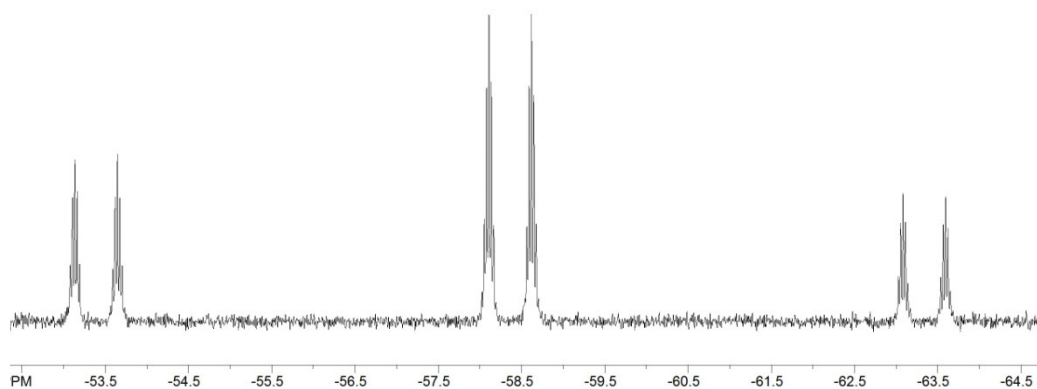
Figure 4.26: Expansion of the signal observed at δ -58.4 ppm in the ^{31}P{^{1}H} NMR spectrum of 36.
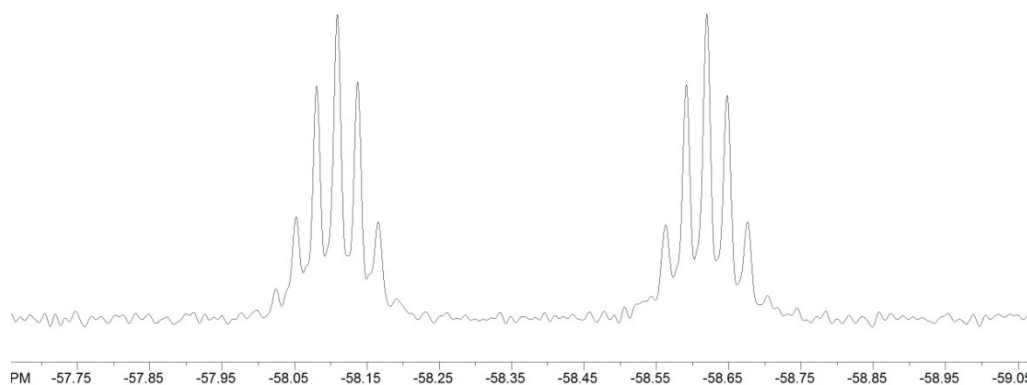
Figure 4.27: Expansion of the major triplet signal in the ^{31}P{^{1}H} NMR spectrum of 36.

The ^{19}F NMR spectrum also confirms the formation of **36**, with the expected three resonances present in the spectrum; these are observed as multiplets at δ -53.8, -69.8, and -173.1 ppm.

The signal observed at δ -173.1 ppm in the ^{19}F NMR spectrum is a binomial doublet of triplet of septets, with coupling constants of $^2J_{PF}$ = 82.6 Hz, $^3J_{FF}$ = 20.7, and $^3J_{FF}$ = 7.5 Hz (see Figure 4.28), and on the basis of the chemical

shift position and coupling constants is therefore assigned as the unique fluorine nucleus attached to the α-carbon.

PM -172.86 -172.90 -172.94 -172.98 -173.02 -173.06 -173.10 -173.14 -173.18 -173.22 -173.26 -173.30 -173.34 -173.38 -173.42 -173.46
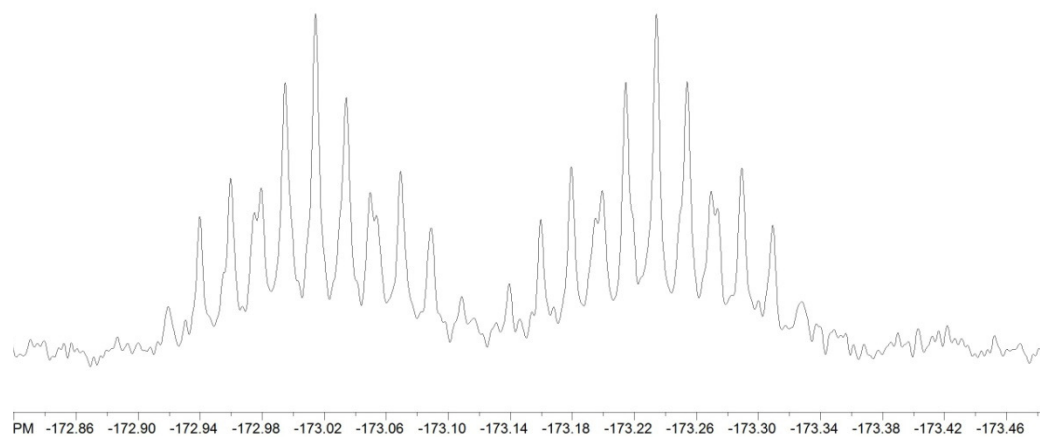
Figure 4.28: Expansion of the signal observed at δ -173.1 ppm in the ^{19}F NMR spectrum of the reaction between 15 and XeF$_2$.

The signal observed at δ -69.8 ppm (see Figure 4.29) is a triplet of doublet of doublets (with coupling constants of $^4J_{FF}$ = 10.4, $^3J_{FF}$ = 7.5, and $^3J_{PF}$ = 4.7 Hz) with six times the relative intensity of the signal at δ -173.1 ppm, and as such is assigned as the signal corresponding to the CF$_3$ groups.

PPM   -69.74   -69.76   -69.78   -69.80   -69.82   -69.84   -69.86   -69.88   -69.90   -69.92
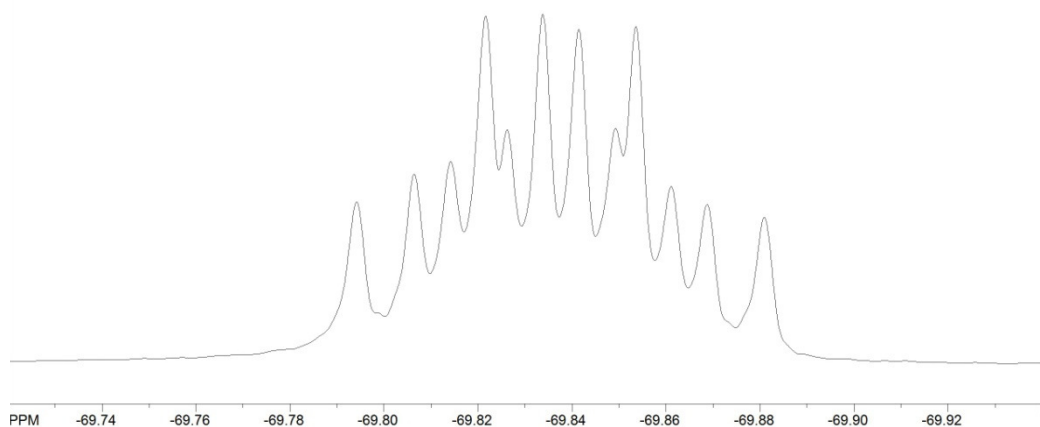
Figure 4.29: Expansion of signal observed at δ -69.8 ppm in the ^{19}F NMR spectrum of 36.

174

The remaining resonance in the ^{19}F NMR spectrum occurs at δ -53.8 ppm, and is a widely separated overlapping doublet of doublet of septets (see Figure 4.30) with $^1J_{FP}$ = 805.9, $^3J_{FF}$ = 20.7, $^4J_{FF}$ = 10.4 Hz and this is assigned to the two fluorine nuclei bonded directly to the phosphorus centre.
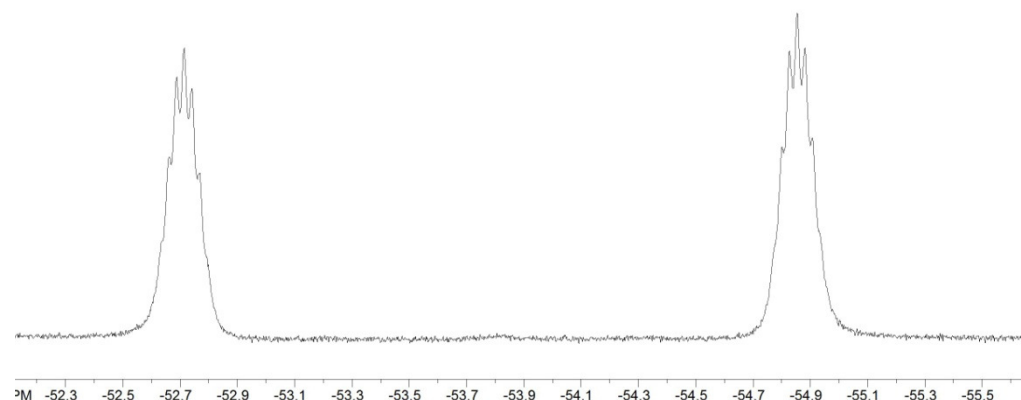
Figure 4.30: Expansion of the signal occurring at δ -53.8 ppm in the ^{19}F NMR spectrum of 36.

There is also a very small peak observed at δ -69.1 ppm, which is in exactly the same position as the CF$_3$ resonance of **29**, suggesting that some O=PPh$_2$CF(CF$_3$)$_2$ is also formed, which most likely arises from the hydrolysis of **36** with adventitious moisture.

4.5.2 F$_2$PPh$_2$(^{s}C$_4$F$_9$) (37)

In the same manner as that described in Section 4.5.1, XeF$_2$ was added to a CDCl$_3$ solution of **18** (Scheme 4.9) until no signals corresponding to the starting phosphine could be detected.

$$Ph_2P(^sC_4F_9) + XeF_2 \xrightarrow{CDCl_3} F_2PPh_2(^sC_4F_9) + Xe$$
$$\textbf{18} \qquad\qquad\qquad\qquad\qquad \textbf{37}$$
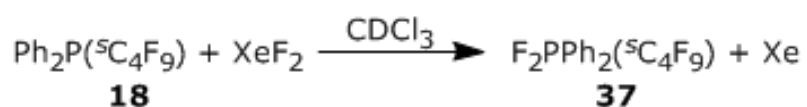
Scheme 4.9: Reaction between XeF$_2$ and 18.

The $^{31}P\{^1H\}$ NMR spectrum recorded after the addition of XeF_2 to **18** shows the growth of a new signal centred at δ -56.3 ppm, similar to that observed in the spectrum to **36**; it is a very complex triplet of doublets of multiplets, with $^1J_{PF}$ = 821.5 Hz, and $^2J_{PF}$ = 84.5 Hz.
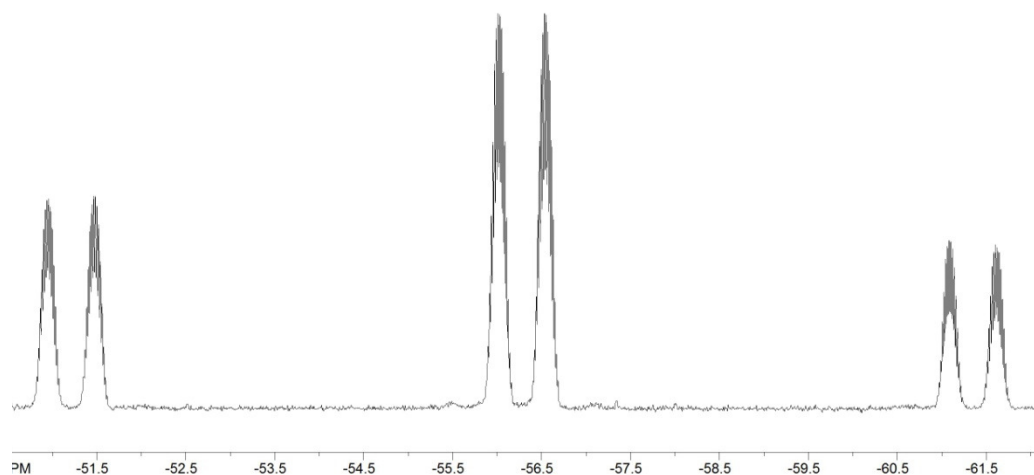
Figure 4.31: Expansion of the signal at δ -56.3 ppm in the $^{31}P\{^1H\}$ NMR spectrum of $F_2PPh_2(^sC_4F_9)$, 37.

The ^{19}F NMR spectrum of this compound contains six complex resonances, centred at δ -53.0, -67.8, -80.2, -112.8, -116.1 and -171.0 ppm. The signals centred at δ -112.8, and -116.1 ppm both show slight second order signposting, as the chemical shift difference (~1240 Hz) is less than five times the coupling constant ($^2J_{FF}$ = 300.1 Hz). The effect is similar to that observed for the "free" phosphine, **18** and decidedly less than in the phosphorus(V) selenide, **33**. The signal for the unique fluorine is observed at δ -171.0 ppm (see Figure 4.32); it is a complex doublet-based pattern.

PM   -170.68 -170.72 -170.76 -170.80 -170.84 -170.88 -170.92 -170.96 -171.00 -171.04 -171.08 -171.12 -171.16 -171.20 -171.24 -171.28 -171.32 -171.36
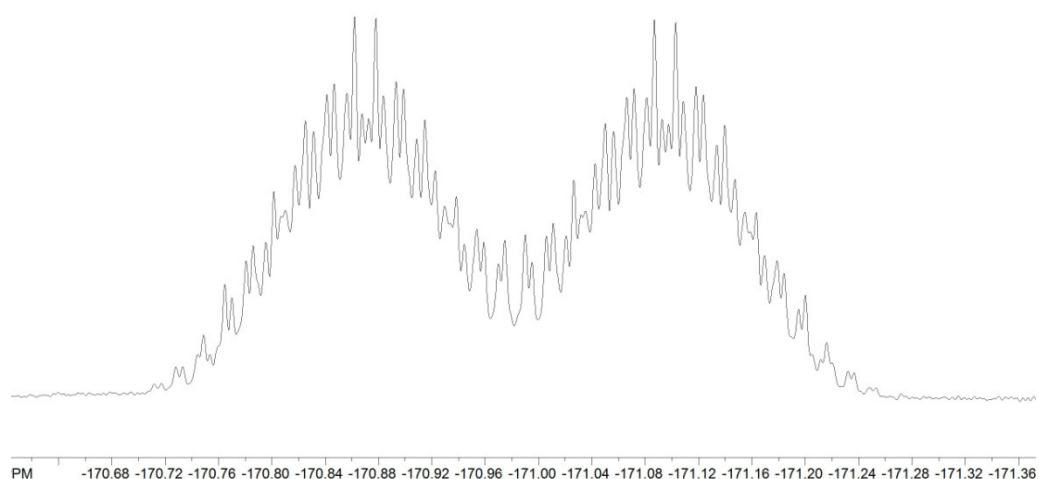
Figure 4.32: Expansion of the signal observed at δ -171.0 ppm in the ^{19}F NMR spectrum of 37, assigned to the unique fluorine.

The signal observed at δ -53.0 ppm in the ^{19}F NMR spectrum of **37** is a broad doublet, with a coupling constant of 821.5 Hz which is shared with the signal in the ^{31}P{^{1}H} NMR spectrum. The ^{19}F NMR chemical shift and magnitude of the coupling constant are indicative of fluorine nuclei directly bound to a phosphorus centre, and thus it is assigned to the P–F fluorine atoms.

Taken together, the multinuclear NMR data confirms the successful synthesis of **37**.

Interestingly, the magnitude of the $^2J_{PF}$ coupling constant has increased in the $F_2PPh_2R_f$ relative to the "free" phosphines, unlike those observed for the chalcogenides, where it has decreased (~85 Hz *vs.* ~70 Hz *vs.* ~50 Hz respectively). This suggests that oxidation state of the phosphorus centre is not the only factor influencing the P–F coupling constants, with the geometry of the molecule and the effect that this has on the % s character of the P–C bond appearing also to have a significant effect.

5. Coordination Chemistry of Fluoroalkyl Phosphines

This chapter is concerned with the coordination chemistry of the newly prepared phosphines described in Chapter 4. It also deals with data derived from those complexes, such as the most common method of quantifying the steric parameters of phosphines, the cone angle.

5.1 Platinum(II) Complexes

5.1.1 *trans*-[PtCl$_2$\{PPh$_2$CF(CF$_3$)$_2$\}$_2$] (38)

The reaction of two equivalents of phosphine with K$_2$[PtCl$_4$] in an ethanol-water mixture (see Scheme 5.1) afforded a yellow solid after work-up.

$$K_2[PtCl_4] + 2\ Ph_2PCF(CF_3)_2 \xrightarrow{\text{EtOH, H}_2\text{O}} [PtCl_2\{PPh_2CF(CF)_2\}] + 2\ KCl$$
$$\mathbf{15} \qquad\qquad\qquad\qquad\qquad\qquad\qquad \mathbf{38}$$
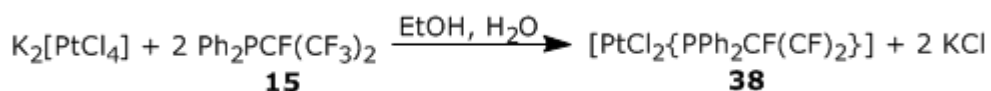
Scheme 5.1: Reaction of 15 with K$_2$[PtCl$_4$].

The ^{31}P\{^{1}H\} NMR spectrum of the yellow solid in CDCl$_3$ isolated from the reaction showed the presence of some unreacted **15**, and a new resonance at δ 24.0 ppm, which appears as a "virtual" triplet (J = 29.5 Hz). This phenomenon is observed in *trans*-isomers of such complexes, and arises where both phosphorus nuclei interact strongly, resulting in the measurement of an apparent coupling constant, corresponding to ½|$^2J_{PF}$ + $^4J_{PF}$|. The signal also displays ^{195}Pt satellites (I = ½, 33%, $^1J_{PtP}$ = 2986 Hz); the magnitude of which also suggests the formation of the *trans*-isomer (*cis*-isomers typically have $^1J_{PtP}$ coupling constants between 3200–3500 Hz, whereas the *trans*-isomers are typically quoted to have $^1J_{PtP}$ values between 2000–2500 Hz;[250] however, this upper limit is not especially accurate, given the number of *trans*-complexes that are known to have a larger $^1J_{PtP}$ coupling constant, and a better range would be 2000–3000 Hz). The value obtained is

rather larger than those found in analogous complexes bearing electron rich species (see Table 5.1), but very similar to that reported for the *trans*-complex of $Ph_2PC_2F_5$.[100]

Phosphine	$^1J_{PtP}$	Reference
$Ph_2PCF(CF_3)_2$, **15**	2986	This work
PPh_3	2637	251
P^iPr_3	2415	252
$Ph_2PC_2F_5$, **17**	2945	100

Table 5.1: Comparison of $^1J_{PtP}$ coupling constants for *trans*-[PtCl$_2$L$_2$].

The ^{19}F NMR spectrum of **38** displays two resonances, at δ -172.0 and -66.5 ppm. Integration of these peaks shows that they have a relative intensity of 6:1, consistent with the perfluoroisopropyl moiety. The signal at δ -172.0 ppm is observed as a "virtual" triplet of septets, where the triplet coupling is ½|$^2J_{PF}$ + $^4J_{PF}$| = 29.5 Hz, and the septet coupling is 9.5 Hz (see Figure 5.1). These data are consistent with the formation of *trans*-[PtCl$_2$\{PPh$_2$CF(CF$_3$)$_2$\}$_2$], **38**.
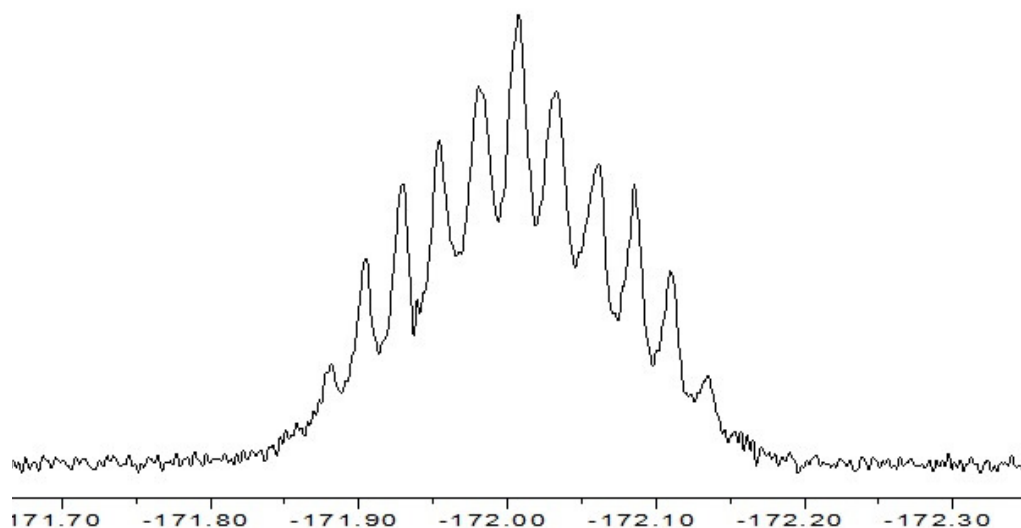
Figure 5.1: Expansion of the signal corresponding to the unique fluorine in the ^{19}F NMR spectrum of 38.

Confirmation of the geometry of **38** was obtained when crystals suitable for analysis by X-ray diffraction studies were grown via the slow evaporation of a mixture of dichloromethane and hexane. Solution of the data yielded the molecular structure shown in Figure 5.2, and selected bond lengths and angles are given in Table 5.2 and Table 5.3 respectively.
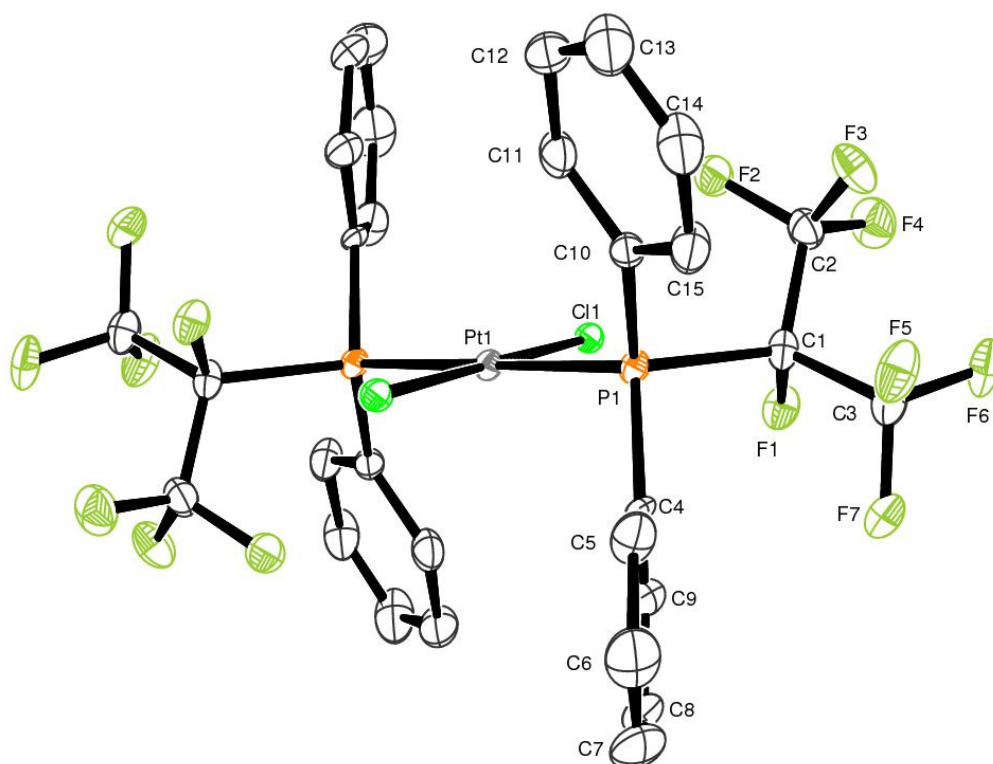
Figure 5.2: ORTEP[174] representation of the molecular structure of 38. Thermal ellipsoids are shown at 50% (hydrogen atoms have been omitted for clarity).

$[PtCl_2\{PPh_2CF(CF_3)_2\}_2]$ crystallises in the $P\overline{1}$ space group, and there are two molecules in the asymmetric unit (see Figure 5.3) both of which have a centre of inversion about the metal.
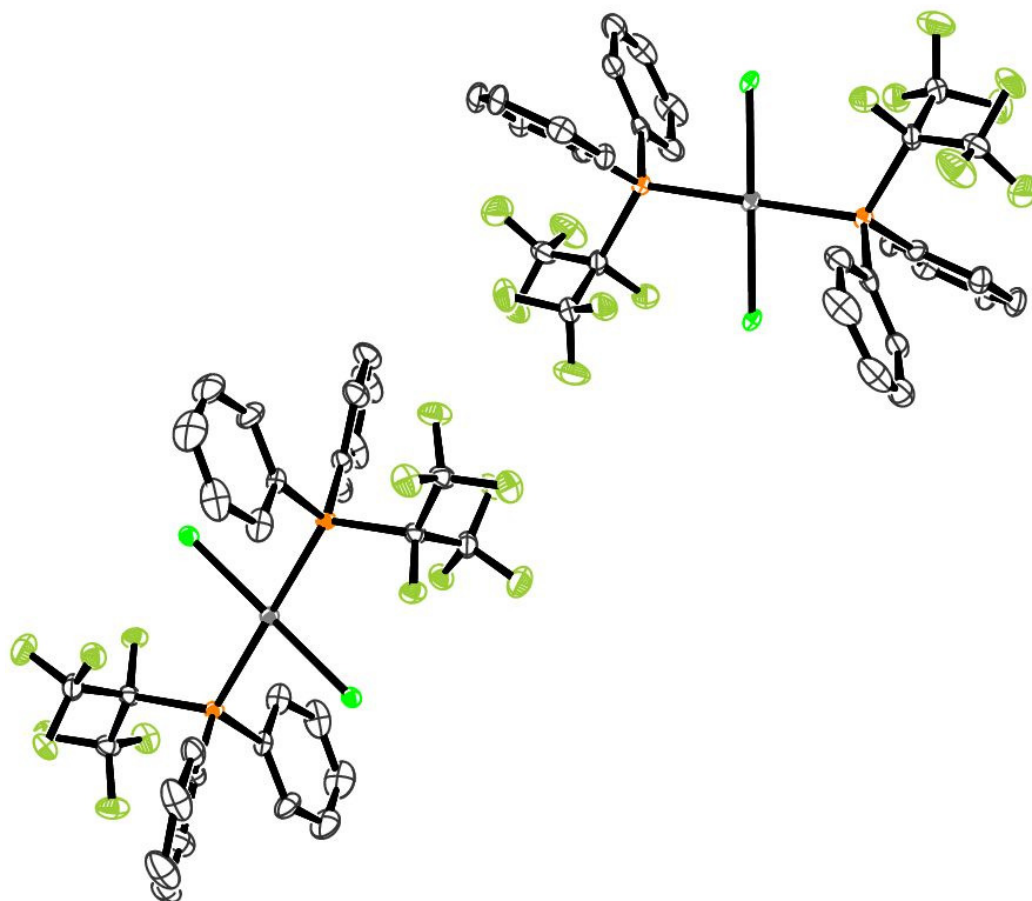
Figure 5.3: ORTEP[174] representation of the contents of the unit cell of compound 38. Thermal ellipsoids shown at 50% (hydrogen atoms have been omitted for clarity).

The Pt–P bond distances are different within the two molecules (2.3223(16) Å and 2.3417(16) Å), but the Pt–Cl distances are the same, within experimental error (2.3422(16) Å and 2.3448(16) Å). These bond distances are comparable to those found in the closest structural analogues of this compound, which are the *trans*-dichloroplatinum complexes of $Ph_2PC_2F_5$, **17**, (Pt–P and P–Cl distances of 2.2961(13) and 2.3070(12) Å respectively),[100] and $PhP(CF_2CF_3)_2$ (Pt–P and P–Cl distances of 2.2916(12) and 2.3002(12) Å respectively).[100] The P–C_F distances are identical between the molecules, whilst the other P–C distances differ slightly between the two molecules in **38**. As observed in the molecular structure of the free phosphine **15**, and the chalcogenides **29**, **31**, **32**, the longest C–F bond in the molecule is from the

α-carbon to the unique fluorine (average dist. 1.376(11) Å). As was observed in the **32** (the selenide of **15)**, the carbon-fluorine bond lengths in the CF_3 groups are very similar, and do not show the variation seen in **15** and the oxide, **29**.

Bond	Length (Å)	Bond	Length (Å)
Pt1-Cl1	2.3422(14)	Pt2-Cl2	2.3448(14)
Pt1-P1	2.3223(16)	Pt2-P2	2.3417(16)
P1-C1	1.933(7)	P2-C16	1.927(7)
P1-C4	1.808(6)	P2-C19	1.822(5)
P1-C10	1.809(5)	P2-C25	1.823(6)
C1-C2	1.521(9)	C16-C17	1.563(11)
C1-C3	1.559(9)	C16-C18	1.547(10)
C1-F1	1.372(8)	C16-F8	1.381(8)
C2-F2	1.336(8)	C17-F9	1.345(9)
C2-F3	1.341(8)	C17-F10	1.308(9)
C2-F4	1.340(7)	C17-F11	1.339(8)
C3-F5	1.326(8)	C18-F12	1.332(9)
C3-F6	1.329(8)	C18-F13	1.335(8)
C3-F7	1.338(7)	C18-F14	1.318(9)

Table 5.2: Selected bond lengths in compound 38.

The Cl-Pt-P bond angles (98.78(5)° and 82.29(5)°) show that both of the unique molecules have a distorted square planar arrangement. Unlike in the solid state structures of **15** and its chalcogenides, in **38** the α C–F is not anti to the Pt – P bond, having torsion angles of 40.4(8)° and 38.7(5)°.

Bond	Angle (°)	Bond	Angle (°)
Cl1-Pt1-P1	98.78(5)	Cl2-Pt2-P2	82.29(5)
Pt1-P1-C1	116.5(2)	Pt2-P2-C16	115.9(2)
Pt1-P1-C4	113.38(19)	Pt2-P2-C19	111.4(2)
Pt1-P1-C10	108.0(2)	Pt2-P2-C25	111.75(18)
P1-C1-F1	107.8(4)	P2-C16-F8	106.2(4)

Table 5.3: Selected bond angles in compound 38.

Short intramolecular contacts are observed within the perfluoroisopropyl unit, from F1 to F3 and F7 (2.549(5) Å and 2.538(5) Å respectively); atom F8 also has short distances to F10 and F14 (2.580(6) Å and 2.546(5) respectively). These are consistent with the structures of the free phosphine **15**, and the chalcogenides **29**, **31**, and **32**.

There are intermolecular contacts between the two residues, notably F4-F14 (2.794(6) Å), F3-F11 (2.708(6) Å), F12-H14 (2.39 Å) and Cl2-H14 (2.73 Å). None of these are particularly short compared with the sum of their respective van der Waals' radii, and are probably a result of the crystal packing, rather than any particular interaction. Compound **38** stacks in the x-direction, with a π-stacking interaction (see Figure 5.4, with the shortest centroid to centroid distance being 4.132(4) Å.
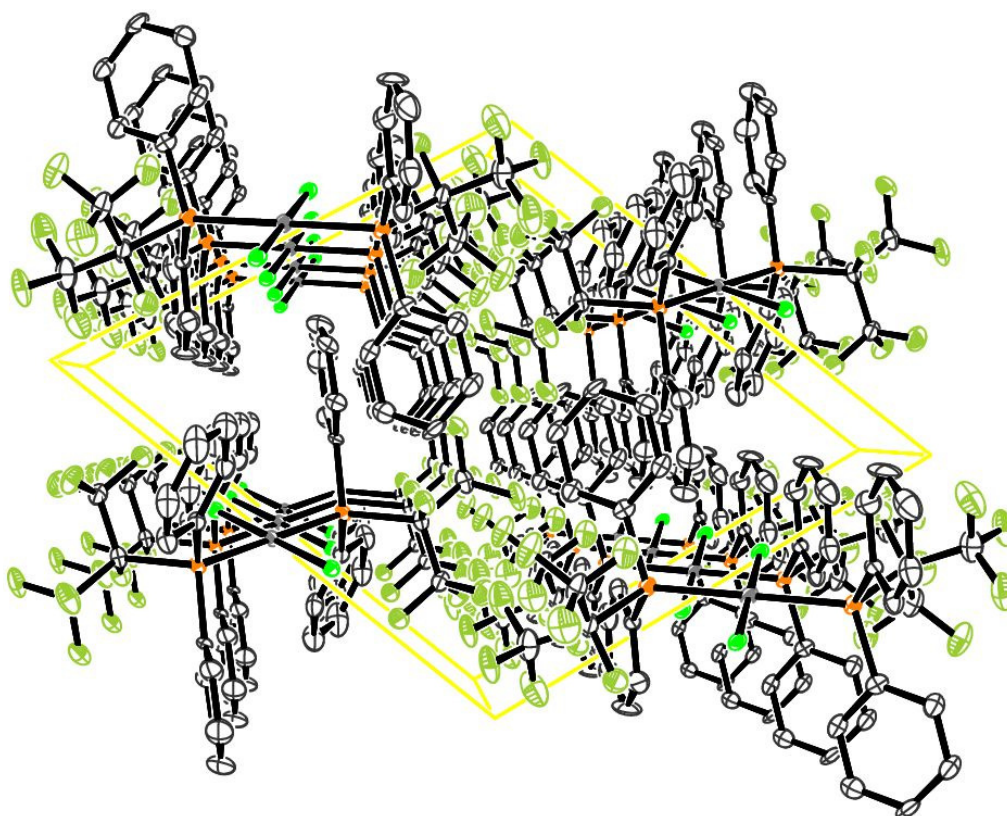
Figure 5.4: ORTEP[174] representation showing the π-stacking interaction in the crystal lattice in the x-direction of 38.

Estimates of the cone angle of $Ph_2PCF(CF_3)_2$ have been obtained from this data using the program STERIC,[162] which calculates that the two molecules in the unit cell have slightly differing values of 163.5° and 158.9°, giving an average cone angle value of 161.2°.

5.2 Gold(I) Complexes

The synthesis of a series of gold(I) phosphine complexes was investigated, by the reduction of the gold(III) salt, $K[AuCl_4]$ with two equivalents of tetrahydrothiophene (tht) in an ethanol/water mix, to afford [AuCl(tht)]. The labile tht ligand is then readily replaced by one equivalent of the phosphine in DCM solution (see Scheme 5.2). The linear gold(I) complexes should allow the phosphine to occupy the largest possible volume of space, thus giving an estimate of the upper limit of its steric bulk.

$$K[AuCl_4] + 2\ tht + H_2O \xrightarrow{\text{Ethanol}} [AuCl(tht)] + 2\ HCl + KCl + C_4H_8SO$$

$$\text{DCM} \diagdown \text{Ph}_2PR_f$$

$$[AuCl(PPh_2R_f)]$$

$$R_f = CF_3,\ \textbf{39},\ CF(CF_3)_2,\ \textbf{40},\ {}^sC_4F_9,\ \textbf{41}$$
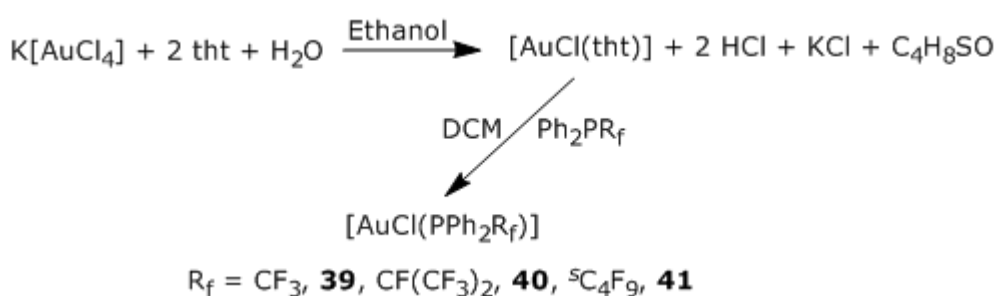
Scheme 5.2: Formation of gold(I) phosphine complexes.

All three complexes, **39**-**41**, were readily isolated as white solids following the removal of the volatiles *in vacuo*, and the resulting $^{31}P\{^1H\}$ NMR spectroscopic data is summarised in Table 5.4.

Compound	δP/ppm	ΔδP/ppm	J/Hz
[AuCl{PPh$_2$(CF$_3$)}], 39	30.6	+28.1	q, $^2J_{PF}$ = 83.6
[AuCl{PPh$_2$CF(CF$_3$)$_2$}], 40	37.3	+38.1	dm, $^2J_{PF}$ = 39.5
[AuCl{PPh$_2$(*sec*-C$_4$F$_9$)}], 41	39.9	+36.7	m

Table 5.4: $^{31}P\{^1H\}$ NMR spectroscopic data and coupling constants for complexes 39-41.

The signals observed for complexes **40** and **41** are complex multiplets. However, for **39** the P–F coupling constant is resolved. Interestingly, the magnitude of the $^2J_{PF}$ coupling constant in **39** is larger than that observed in the free ligand (83.1 Hz *vs* 74.0 Hz). However, in the secondary fluoroalkyl-

containing phosphines the $^2J_{PF}$ coupling constant has decreased (from ~70 to ~40 Hz). The phosphorus signals of all three complexes have shifted to a higher frequency compared with the starting phosphines, consistent with that observed for other complexes of this nature, for example, when the phosphine is $Ph_2P(CF=CF)_2$ or $PhP(CF=CF_2)_2$, the changes in δ upon coordination to gold are 38.6 and 43.7 ppm respectively.[36]

The ^{19}F NMR spectra of these complexes are consistent with expectations, and are summarized in Table 5.5.

Compound	δ_F/ppm	J/Hz
$[AuCl\{PPh_2(CF_3)\}]$, 39	-57.6	d, 83.1
$[AuCl\{PPh_2CF(CF_3)_2\}]$, 40	-67.4 -180.9	dd, 8.5, 8.5 br. d, 39.5
$[AuCl\{PPh_2(sec\text{-}C_4F_9)\}]$, 41	-65.7 -79.9 -107.3 -111.6 -179.8	m m m m m

Table 5.5: ^{19}F NMR spectral data for compounds 39-41.

All three compounds produced crystals of sufficient quality to be analysed by X-ray diffraction studies, and these data provided further confirmation of the formation of the title compounds.

5.2.1 $[AuCl\{PPh_2(CF_3)\}]$ (39)

This compound crystallises in the orthorhombic space group Pna2$_1$, with a total of four molecules in the unit cell. The asymmetric unit is shown in Figure 5.5, and a selection of bond lengths and angles are listed in Table 5.6 and Table 5.7 respectively.
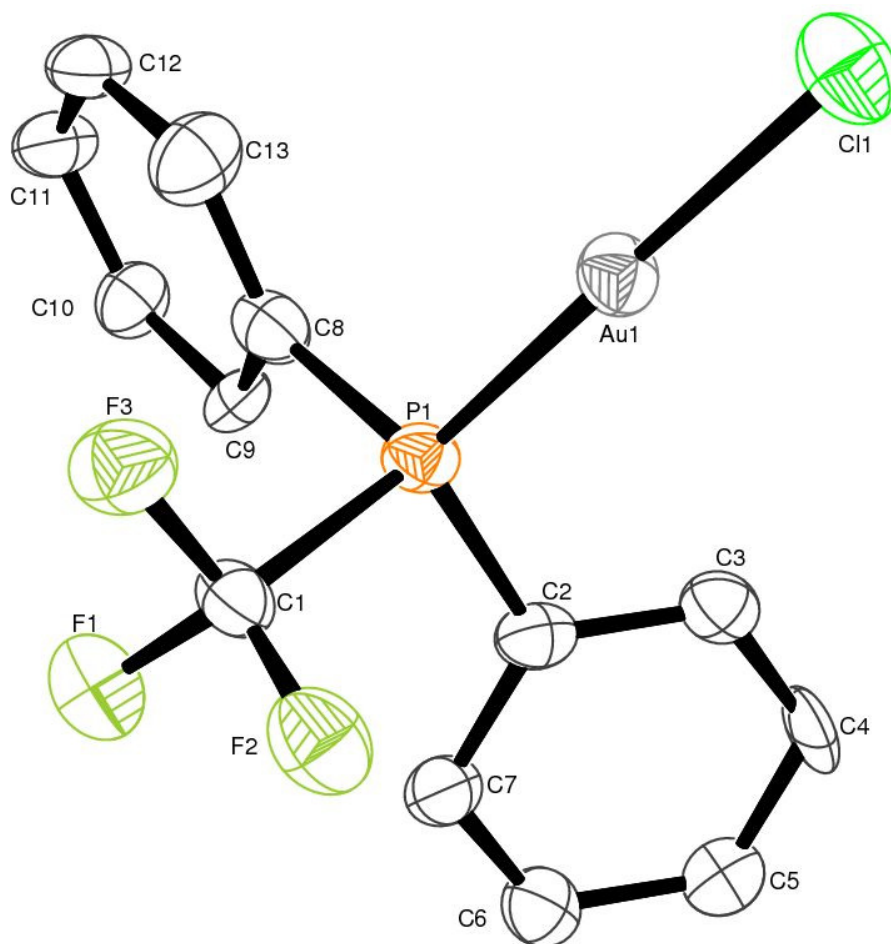
Figure 5.5: ORTEP[174] representation of the asymmetric unit of 39. Hydrogen atoms are omitted for clarity with thermal ellipsoids shown at 50%.

The Au1–P1 bond length is 2.216(6) Å which is similar to that reported for the complex [AuC{PPh(CF=CF$_2$)$_2$}], which has Au–P distances of 2.216(2) Å and 2.218(2) Å (there are two residues in the unit cell). The distance is shorter than is observed in [AuCl(PPh$_3$)] (d(Au-P) = 2.235(3) Å, which is typical of the average Au–P distance of 2.236 Å observed for all structures containing trialkyl- and triaryl- phosphines.[253,254] The distance, although short, is not quite as short as observed in phosphite and fluorophosphine complexes, such as [AuCl{P(OPh)$_3$}] (d(Au-P) = 2.195(5) Å, and in the air-sensitive chloro[(2,5-dimethylphenyl)difluorophosphine]gold(I) complex (d(Au-P) = 2.188(2) Å). The Au–Cl distance in **39** at 2.273(6) Å is very similar to those reported for [AuCl{PPh(CF=CF$_2$)$_2$}], [AuCl(PPh$_3$)],

[AuCl{P(OPh)$_3$}] and chloro[(2,5-dimethylphenyl)difluorophosphine]gold(I) complex (d(Au-Cl) = 2.282(2) Å, 2.279(3) Å, 2.273(5) Å, and 2.281(3) Å respectively).[36,253,255]

Bond	Distance (Å)	Bond	Distance (Å)
Au1-Cl1	2.273(6)	P1-C8	1.798(18)
Au1-P1	2.216(6)	C1-F1	1.34(2)
P1-C1	1.87(2)	C1-F2	1.32(2)
P1-C2	1.793(19)	C1-F3	1.39(2)

Table 5.6 Selected bond lengths in 39.

The angle created by the Au-P-C bonds is smallest to the fluorinated fragment, as can be seen from the data in Table 5.7.

Bonds	Angle (°)	Bond	Angle(°)
Cl1-Au1-P1	178.9(2)	P1-C1-F1	115.3(13)
Au1-P1-C1	107.7(6)	P1-C1-F2	112.5(13)
Au1-P1-C2	116.1(7)	P1-C1-F3	110.4(13)
Au1-P1-C8	115.6(7)		

Table 5.7: Selected bond angles observed in 39.

There is a short contact of 2.42 Å between F7 and H1 (0.25 Å shorter than the sum of the van der Waals' radii), and the chlorine atom appears to form a bifurcated H-bond to H5 and H13 of a neighbouring residue, though these contacts at 3.09 and 2.98 Å are very close to the sum of the van der Waals' radii (2.95 Å). There are no classical hydrogen bonds present. There also appears to be some offset face-to-face aryl interactions, and these interactions appear to be responsible for the crystal packing. No significant gold-gold interactions are apparent in this complex (the shortest gold-gold distance is 5.196 Å), though looking down the x-direction pairs of **39** adopt a "crossed swords" packing motif (Figure 5.6), which is commonly observed in systems which exhibit aurophilic interactions.
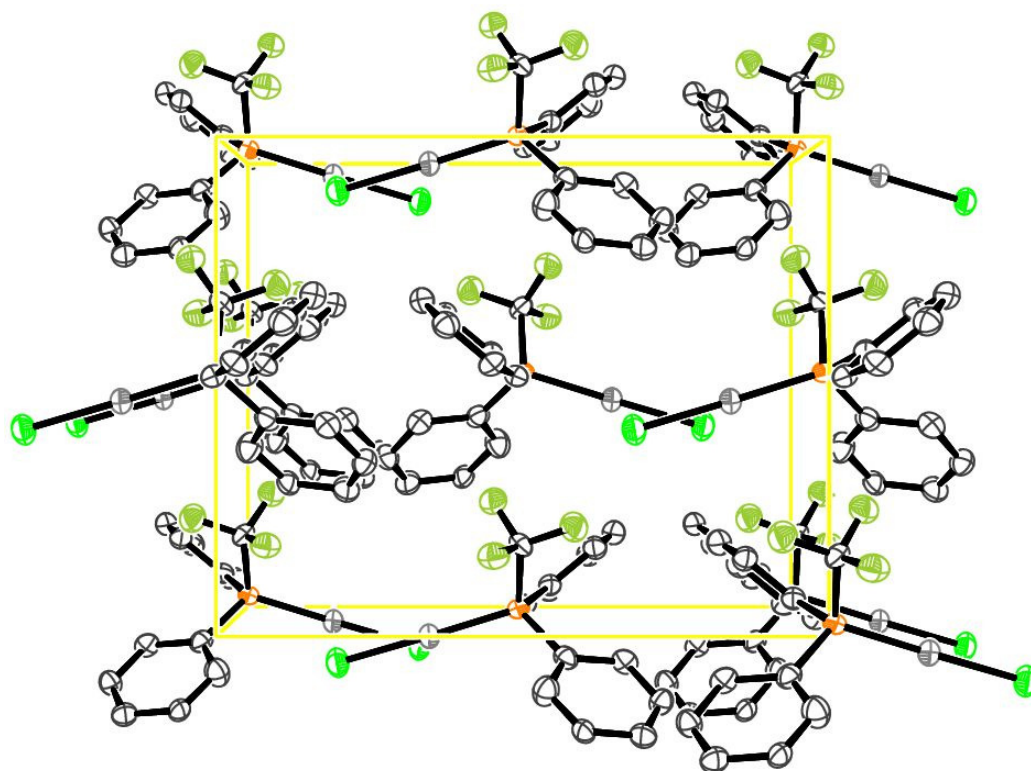
Figure 5.6: Crystal packing looking in down the x-direction in the solid state structure of 39.

From the X-ray structural data, it is possible to estimate the size of the cone angle of the ligand, which is calculated to be 105°. This is significantly smaller than the value of 142° that was reported by Tolman,[40] derived from the measurement of space-filling models. However, later work suggests that the size of CF_3-containing phosphines may have been overestimated.[52]

5.2.2   [AuCl{PPh$_2$CF(CF$_3$)$_2$}] (40)

Crystals of **40** were grown via the slow evaporation of the solvent from a DCM solution of **40**. Solving the X-ray diffraction data for **40** yielded the molecular structure shown in Figure 5.7, selected bond lengths/angles are given in Table 5.8 and Table 5.9 respectively and the X-ray collection parameters can be found in Section 7.
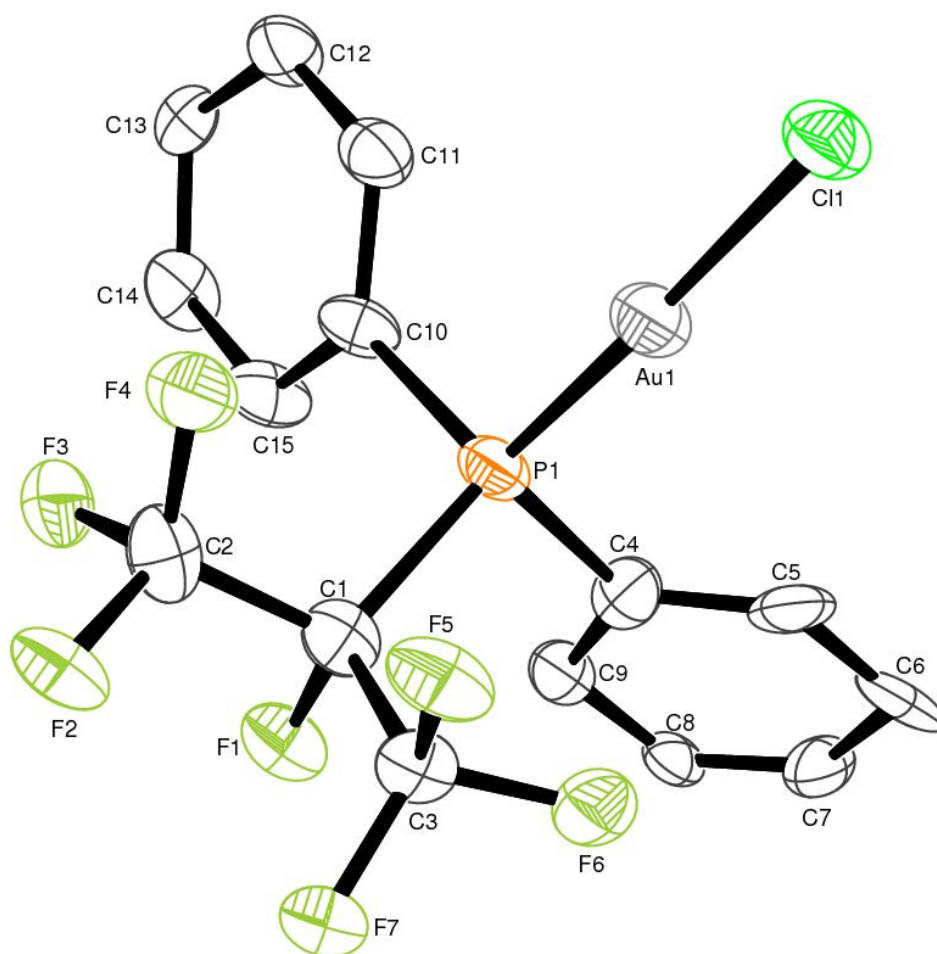
Figure 5.7: ORTEP[174] representation of the molecular structure of 40 Hydrogen atoms have been omitted for clarity and thermal ellipsoids are shown at 30%.

This complex crystallises in the monoclinic space group C2/c, and contains eight molecules in the unit cell. Unfortunately, the quality of the crystal was poor, resulting in an R factor of 10.65%. The Au1-P1 distance is somewhat longer than in **39** at 2.243(5) Å, and also longer than the average bond observed in trialkyl- and triaryl- phosphines (2.236 Å, see above). Similarly, the Au1-Cl1 distance at 2.301(5) Å is longer than that found on average for the gold(I) phosphine chlorides. The poor quality crystal means that the precision on the C–F bonds is rather low, and as such apart from the C3–F7, bond, which is significantly shorter at 1.295(19) Å, the remainder are all the same within experimental error, 1.36(3) Å.

Bond	Distance	Bond	Distance
Au1-P1	2.243(5)	C1-F1	1.37(2)
Au1-Cl1	2.301(5)	C2-F2	1.36(2)
P1-C1	1.880(18)	C2-F3	1.33(3)
P1-C4	1.82(2)	C2-F4	1.39(2)
P1-C10	1.82(2)	C3-F5	1.38(2)
C1-F1	1.37(2)	C3-F6	1.39(2)
C1-C2	1.54(3)	C3-F7	1.295(19)
C1-C3	1.49(3)		

Table 5.8: Selected bond lengths in 40.

There are several short intramolecular interactions between the fluorine atoms. F1 displays short contacts of 2.900(18) and 2.885(17) Å to F2 and F6 respectively which are slightly shorter than twice the van der Waals' radius of fluorine (2.94 Å), and also to F3 and F7 (2.582(17) and 2.539(16) Å respectively) which are considerably shorter than twice the van der Waals' radius of fluorine. This is expected as intramolecular F⋯F interactions have been noted for compounds **15**, **29**, **32**, and **38**, and are presumably due to the size of the perfluoroisopropyl unit.

Bonds	Angle(°)	Bond	Angle(°)
Cl1-Au1-P1	178.3(2)	Au1-P1-C10	113.6(6)
Au1-P1-C1	109.5(6)	P1-C1-F1	110.6(12)
Au1-P1-C4	113.4(7)		

Table 5.9: Selected bond angles in 40

As Table 5.9 shows, the Cl-Au-P bond is practically linear, as expected, and as in **39** the smallest Au-P-C angle is to the fluorinated fragment at 109.5°. The α C–F bond is anti to the Au–P bond, with an Au1–P1–C1–F1 torsion angle of 167.1(11)°, a feature similar to those observed in **15**, **29**, **31**, and **32**.

The shortest Au⋯Au interaction is 4.501 Å, and whilst this is rather long, the crystal packing in the z-direction (Figure 5.8) suggests that pairs of molecules of **40** adopt a "crossed swords" motif, as previously observed in **39**.
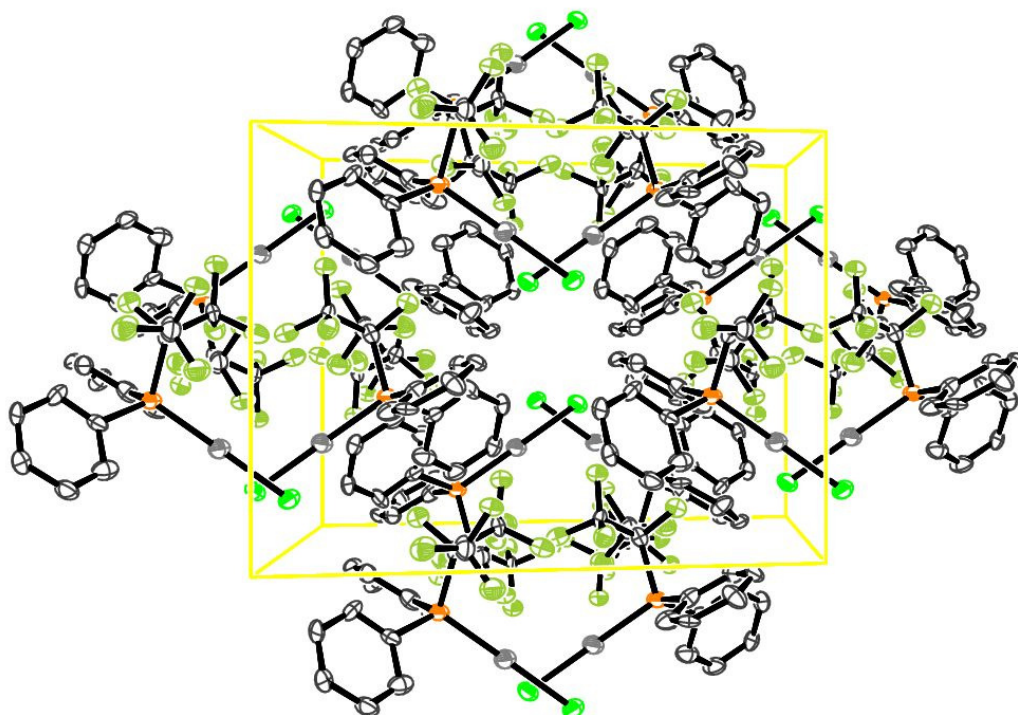
Figure 5.8: Crystal packing in the z-direction of 40.

There are some intermolecular interactions between the chlorine atom and two hydrogen atoms on neighbouring residues, H7 and H15 (2.86 and 3.01 Å respectively). There are also some fluorous domains within the crystal structure, though the shortest of the intermolecular F···F distances at 3.250 Å is 0.31 Å longer than twice the van der Waals' radius of fluorine (see Figure 5.9).
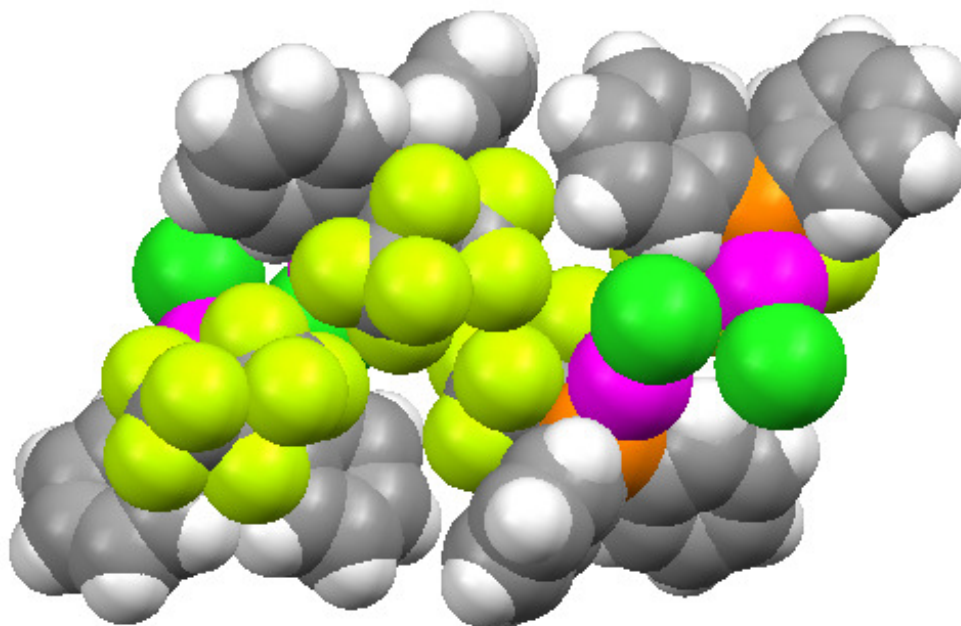
Figure 5.9: Space-filling diagram showing the packing in 40. Carbon = grey, hydrogen = white, chlorine = green, fluorine = yellow-green, gold = purple, phosphorus = orange.

The data gathered allows the cone angle for $Ph_2PCF(CF_3)_2$ to be estimated; this is calculated to be 186°. This is a marked increase on the values calculated from the structural data gathered for **38** (avg. 161°), most likely due to less crowding of the coordination sphere in **40**. The value is also larger than estimated from **31** (177.9°) and **32** (172.3°), though smaller than calculated from the phosphine oxide, **29** (201.9°). Compound **15** has a much larger cone angle than is estimated for **16** (105°), as might be expected when replacing two fluorine atoms for CF_3 groups.

5.2.3 [AuCl{PPh$_2$($^sC_4F_9$)}] (41)

Solution of the X-ray diffraction data recorded for a crystal of **41** grown by slow evaporation of a mixed DCM/Et_2O solution resulted in the molecular structure shown in Figure 5.10.
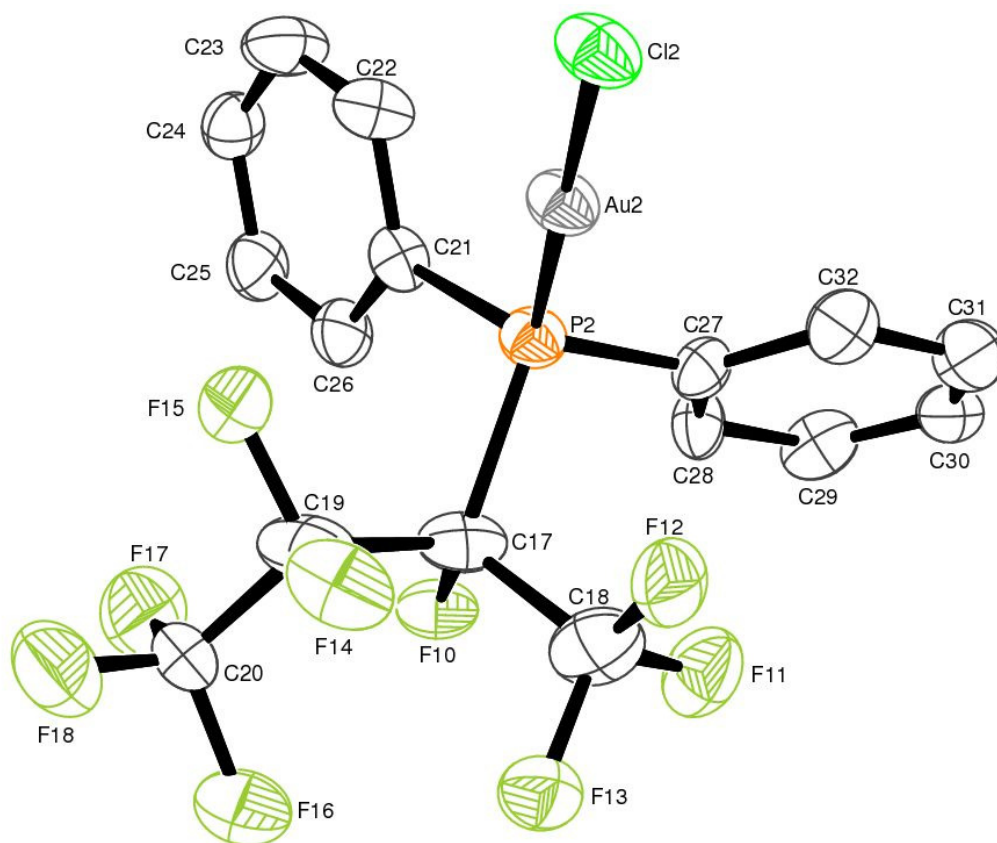
Figure 5.10: ORTEP[174] representation of the molecular structure of 41. Hydrogen atoms omitted for clarity and thermal ellipsoids are shown at 50%.

This complex crystallises in the monoclinic space group $P2_1/c$, and like **40** contains eight molecules in the unit cell, with two molecules in the asymmetric unit. One of these molecules has a disordered perfluorosecondarybutyl group (Figure 5.11), whilst the other does not and is the (*R*)-enantiomer of the phosphine (Figure 5.10).
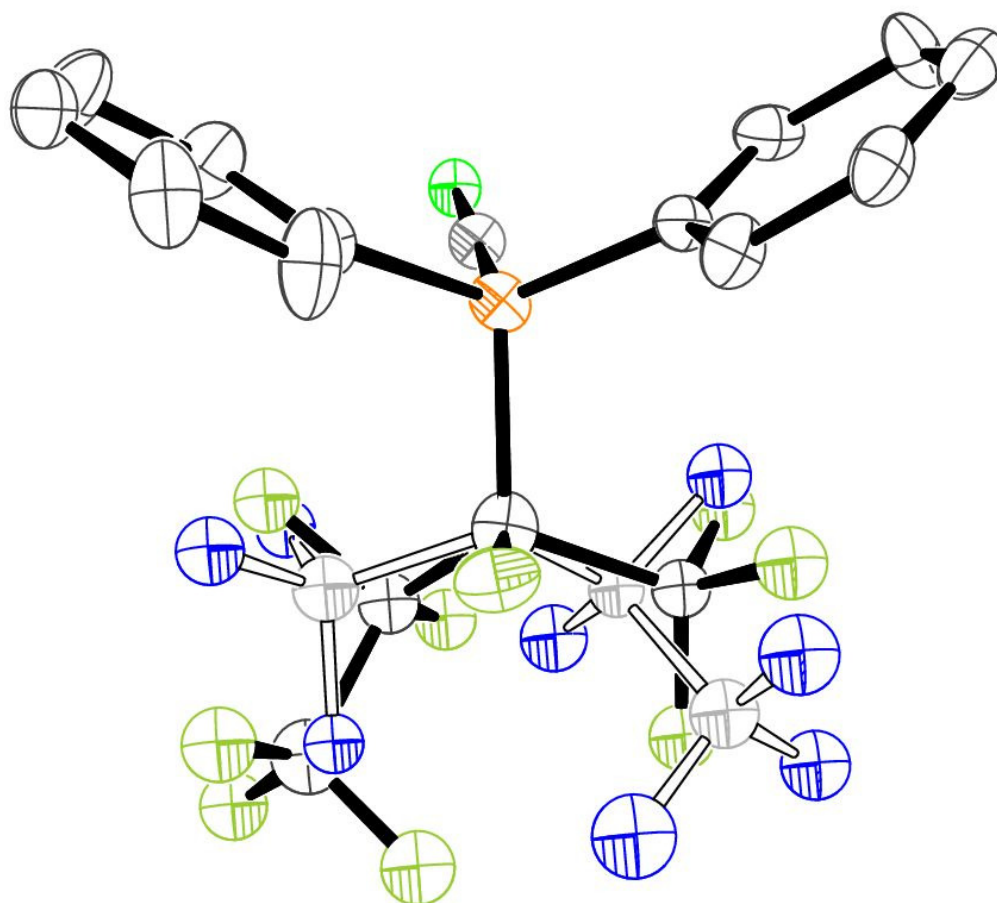
Figure 5.11: ORTEP[174] representation of the disordered molecule in the asmmetric unit of 41, showing both the (*R*)-(white bond, grey carbon atoms, blue fluorine atoms) and (*S*)-enantiomers. Hydrogen atoms omitted for clarity and thermal ellipsoids shown at 40%.

Figure 5.11 shows the modelling of the disordered perfluorosecondary butyl group across two sites, effectively showing both enantiomers of the phosphine (they are synthesised as a racemic mixture, and are C-chiral at the α-carbon). The black bonds correspond to the (*S*)-enantiomer, and accounts for approximately 2/3 of the crystal, whereas the white bonds show the (*R*)-enantiomer, and accounts for the remaining 1/3 of the crystal. Selected bond lengths for both the ordered and disordered molecules are listed in Table 5.10.

Disordered		Ordered	
Bond	**Distance**	**Bond**	**Distance**
Au1-Cl1	2.3126(17)	**Au2-Cl2**	2.2790(19)
Au1-P1	2.233(2)	**Au2-P2**	2.226(2)
P1-C1	1.936(10)	**P2-C17**	1.910(8)
P1-C5	1.823(8)	**P2-C21**	1.826(8)
P1-C11	1.822(8)	**P2-C27**	1.790(8)
C1-F1	1.348(10)	**C17-F10**	1.392(9)
C2-F2 C2b-F2b	1.327(12) 1.334(18)	**C18-F11**	1.335(12)
C2-F3 C2b-F3b	1.339(12) 1.34(2)	**C18-F12**	1.269(12)
C2-F4 C2b-F4b	1.324(13) 1.32(2)	**C18-F13**	1.343(12)
C3-F5 C3b-F5b	1.346(13) 1.341(19)	**C19-F14**	1.372(12)
C3-F6 C3b-F6b	1.407(13) 1.41(2)	**C19-F15**	1.340(12)
C4-F7 C4b-F7b	1.314(14) 1.31(2)	**C20-F16**	1.398(12)
C4-F8 C4b-F8b	1.303(14) 1.30(2)	**C20-F17**	1.393(13)
C5-F9 C5B-F9b	1.362(14) 1.35(2)	**C20-F18**	1.267(13)

Table 5.10: Selected bond lengths in complex 41. The atoms labelled b are from the lower occupancy sites within the disordered molecule.

The Au–P and Au-Cl bonds are slightly shorter in the ordered molecule than the disordered one. The P-C_F bonds are longer than the P-C_{Ar} bonds, as seen in Table 5.10 above. Also, the two bond lengths for each C-F bond in the disordered molecule are identical (within experimental error), and are very similar to those observed in the ordered molecule, with the exceptions of C18-F12 and C20-F18, which are substantially shorter than the other C-F bonds. F18 makes two short contacts to two fluorine atoms in neighbouring residues (2.643 and 2.931 Å), though F12 only has a short intramolecular contact to F14 (2.710 Å).

Disordered		Ordered	
Bond	Angle (°)	Bond	Angle (°)
Cl1-Au1-P1	179.50(7)	Cl2-Au2-P2	178.18(7)
Au1-P1-C1	110.3(3)	Au2-P2-C17	108.4(3)
Au1-P1-C5	113.7(3)	Au2-P2-C21	115.2(3)
Au1-P1-C11	114.4(3)	Au2-P2-C27	114.8(3)
P1-C1-F1	109.8(5)	P2-C17-F10	109.4(5)
P1-C1-C2	108.8(8)		
P1-C1-C2b	106.6(7)		
P1-C1-C3	113.0(6)		
P1-C1-C3b	112.3(8)		

Table 5.11: Selected bond angles in 41. The atoms labelled b are from the lower occupancy sites within the disordered molecule.

The P-Au-Cl bonds are almost linear in both of the molecules in the asymmetric unit, as expected for this compound, and as seen in **39** and **40**. Similarly, the smallest Au-P-C angle again involves the fluorinated fragment. The angles close to the metal centre show little variation between the ordered and disordered molecules. However, there appears to be some variation between the enantiomers observed in the disordered molecule, although it is generally small and probably due to crystal packing interactions.

As in **40**, the α C–F bond is *anti* to the P–Au bond, with torsion angles of 175.8(4)° and 171.3(5)°, averaging 173.6(6)°.

There are several intermolecular F···F interactions in the structure that are less than twice the van der Waals' radius of fluorine, resulting in fluorous domains within the crystal (see Figure 5.12). There also appears to be a pair of bifurcated Cl-H interactions (2.824 and 2.857 Å) to hydrogen atoms on a neighbouring residue, and a Cl-F interaction (3.080 Å, sum of the van der Waals' radii = 3.22 Å). As in **39** and **40** there are no significant aurophilic interactions, as the shortest Au-Au distance is 5.624 Å.
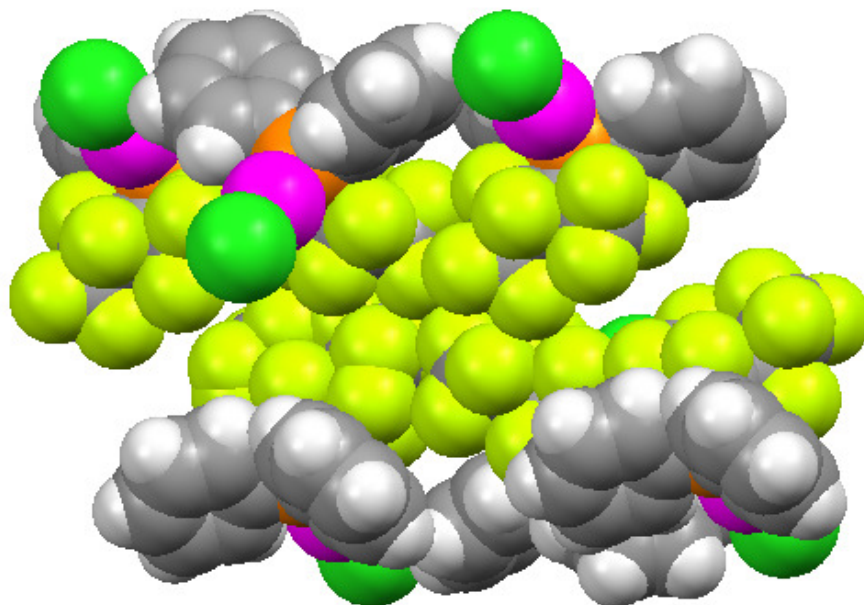
Figure 5.12: Space-filling diagram of the crystal packing of 41, illustrating the fluorous domains.

The data collected also allows for an estimate of the steric bulk of these ligands, and from this data the cone angle of $Ph_2P(sec$-$C_4F_9)$, **18**, is calculated to be 187°, slightly larger than $Ph_2PCF(CF_3)_2$, **15**, as would be expected based on the differences in the ligands. This value is larger than that estimated from the phosphine selenide, **33** (179.5°). Compounds **39**, **40**, and **41** are the first tertiary perfluoroalkyl-containing phosphine gold(I) complexes to be structurally characterised, and **41** is the first structural determination of any complex bearing the $Ph_2P(sec$-$C_4F_9)$ ligand.

5.3   Molydenum(0) complexes

As discussed above, the IR stretching frequency of carbonyl complexes of a variety of metals have been used as an estimate of the electronic parameter of an array of ligands. Thus, the synthesis of $[Mo(CO)_5\{PPh_2(CF(CF_3)_2)\}]$, **42**, was undertaken, so as to have more data with which to determine the properties of **15**.

5.3.1 [Mo(CO)$_5${PPh$_2$(CF(CF$_3$)$_2$)}] (42)

The reaction of **15** with [Mo(CO)$_5$NCMe] (generated via the reaction of [Mo(CO)$_6$] with Me$_3$NO.2H$_2$O), results in the formation of a brown oil. The ^{31}P{^{1}H} NMR spectrum of this oil shows the growth of a new peak centred at δ 57.0 ppm, a shift of +57.8 ppm from **15**. The signal is a binomial doublet of septets, and the coupling constants are slightly different in magnitude than observed for **15** (for example, the $^2J_{PF}$ coupling constant has increased slightly to 79.3 Hz from 74.0 Hz, whilst the $^3J_{PF}$ coupling has reduced from 18.0 Hz to 3.1 Hz). The ^{19}F NMR spectrum contains two new peaks compared with **15** (but of the same multiplicity), a doublet of doublets centred at δ -65.7 ppm and a doublet of septets centred at δ -174.0 ppm. These data are consistent with the formation of [Mo(CO)$_5${PPh$_2$CF(CF$_3$)$_2$}], **42**. The IR data recorded for this compound shows that the A$_1$ C≡O stretching frequency is 2081 cm^{-1}. This value can be compared with other, related phosphines (Table 5.12)

Phosphine	v/cm^{-1}	Ref
PPh$_3$	2072	190
Cy$_2$P(CF=CF$_2$), 3	2073	This work
Ph$_2$P(CF=CF$_2$)	2076	36
^{t}BuP(tfp)$_2$	2079	186
PhP(tfp)$_2$, 7	2081	This work
Ph$_2$PCF(CF$_3$)$_2$, 15	2081	This work
PhP(CF=CF$_2$)$_2$	2084	36
PF$_3$	2104	190

Table 5.12: v(CO) of [Mo(CO)$_5$L] complexes.

These data suggest that the CF(CF$_3$)$_2$ group is more electron withdrawing than the perfluorovinyl unit and the trifluoropropynyl unit, as expected since it is saturated with electron withdrawing fluorine atoms. The position of the v(CO) frequency is as expected based on the magnitude of the $^1J_{PSe}$ coupling

constant observed for compound **32**. Since the v(CO) in [Mo(CO)$_5$L] complexes can be estimated from the $^1J_{PSe}$ coupling constant. This suggests that both sets of data are reliable methods for assessing the electronic profile of phosphines.

5.4 Stereoelectronic Profile

The data described above allows us to place **3**, **5-(Z)**, **15**, **16**, **18** and **19** on a stereoelectronic plot, as shown below in Figure 5.13.
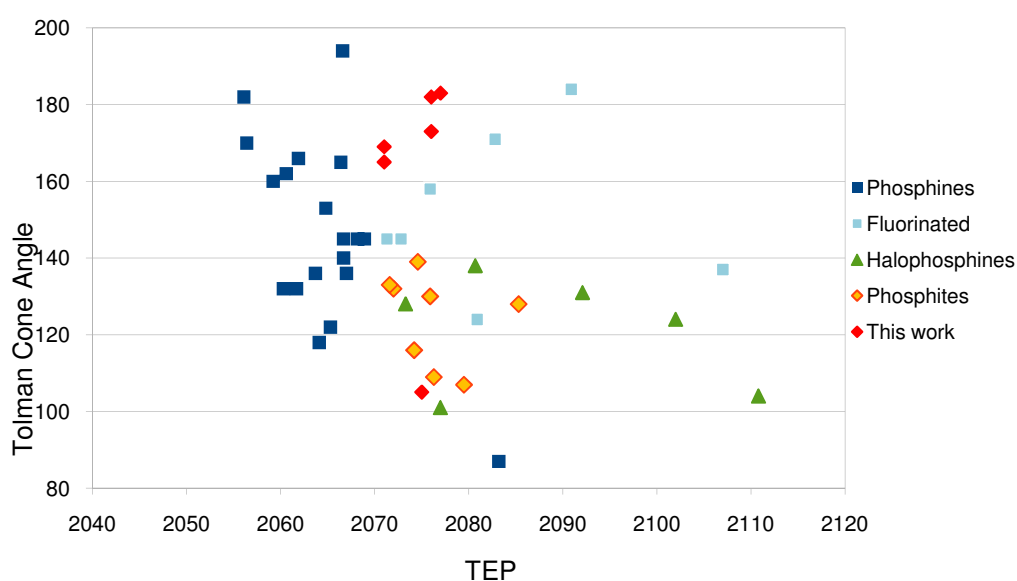
Figure 5.13: Stereoelectronic plot of PR$_3$ compounds (TEP = Tolman Electronic Parameter).

The chart shown in Figure 5.13 plots the cone angle versus the Tolman Electronic Parameter (TEP; the v(CO) observed in the corresponding [Ni(CO)$_3$L] complex). The TEP for the compounds shown in Figure 5.13 have been either taken directly from [Ni(CO)$_3$L] data where available or calculated from one or more of the following datasets; v(CO) in [Mo(CO)$_5$L], [RhL$_2$(CO)Cl], or $^1J_{PtP}$, $^1J_{PSe}$, and $^1J_{RhP}$ coupling constants.

The lack of compounds found in the upper right quadrant of the chart correlates very well with that reported by Cooney *et al*.,[35] shown in Figure

1.8. The few compounds found in that region are fluoroaryl-containing phosphines, which were not considered in the report by Cundari and co-workers.[35]

The red points in Figure 5.13 correspond to the phosphines in this work – and as can be seen, phosphines **3** and **5-(*Z*)** are shown to possess near identical electronic properties, with **3** having a slightly larger steric demand. Compounds **15**, **18** and **19** are in the gap noted previously.[35] The data also shows that altering the perfluoroalkyl fragment does not have a particularly marked effect on the electronic properties of the phosphine, but can alter its steric profile considerably. This illustrates the potential tunability of phosphorus(III) ligands.

Further alteration of the R groups at the phosphorus centre, and the development of a widely applicable methodology to *bis*-perfluoroalkyl containing phosphines will allow the chemistry and potential utility of ligands with these stereoelectronic properties to be explored in detail.

6. Conclusions and Further Work

This thesis describes the synthesis and properties of some sterically demanding fluorine-containing phosphines. The synthesis of $Cy_2P(CF=CF_2)$ was accomplished followed by the subsequent coordination of this phosphine to palladium and platinum, and as a result shown to be the bulkiest perfluorovinyl phosphine known.

The reaction of $Ph_2P(CF=CF_2)$ with ^tBuLi results in the synthesis of both the *cis* and *trans* isomers of $Ph_2P(CF=CF^tBu)$, contrary to previous reports. The electronic properties of which has been further investigated via the synthesis of the phosphorus(V) selenide, and it is found to be less electron-withdrawing than the starting phosphine $Ph_2P(CF=CF_2)$, and very similar to **3**.

The development of a new methodology to perfluoroalkyl phosphines has been achieved, utilising trimethylsilyl phosphines as a starting material. This synthetic procedure has resulted in the preparation of nine new and three known perfluoroalkyl-phosphines. These have all been fully characterised, including multinuclear NMR spectroscopy. The large scale synthesis of $Ph_2PCF(CF_3)_2$, **15**, and $Ph_2P(^sC_4F_9)$, **18**, has shown that this route is capable of generating significant quantities of these new phosphorus(III) compounds. Compound **15** has also been characterised by x-ray diffraction studies, and is only the second perfluoroalkyl phosphine to be characterised in this manner. The sum of the C–P–C angles in **15** identifies it as the largest structurally characterised perfluoroalkyl phosphine.

The mechanism by which this reaction proceeds has also been investigated. $Ph_2P–PPh_2$ has been shown to be the key intermediate formed in the first step, though precisely how this occurs remains unknown. The intermediate reacts with the perfluoroalkyl iodide at a rate which depends on the identity

of the perfluoroalkyl iodide (tertiary>secondary>>primary), forming the desired compounds and Ph_2PI, but not in a 50:50 ratio, since Ph_2PI is capable of reacting to generate further product. This interesting transformation deserves further investigation so as to elucidate exactly what is happening in this reaction.

In the process of the mechanistic investigation, $Me_2P-P(S)Me_2$ was prepared and has been shown to have the potential as a starting material for the synthesis of Me_2PR_f compounds. This can be extended to a variety of $R_2P-P(S)R_2$ compounds, and has been used for the formation of $Me_2PCF(CF_3)_2$, **28**, another hitherto unknown compound. However, the Me_2P- group imparts a similar volatility onto the R_f group as an iodine atom, making it very difficult to separate **28** from $(CF_3)_2CFI$. This has been noted by others in earlier syntheses of Me_2PCF_3.[68]

The oxidative properties of these compounds has been investigated, and it was found that they oxidise readily, despite the presence of the electron withdrawing group. Oxidation with selenium resulted in several phosphorus(V) selenides being produced, and the electronic profile of the phosphines were estimated via the $^1J_{PSe}$ coupling constants. The perfluoroalkyldiphenylphosphines **15, 16, 18,** and **19** have been shown to be markedly more electron deficient than unsaturated fluoro-organo containing phosphines, and phosphines bearing an alkoxy group. Cone angles estimated from the phosphine selenides suggest that the steric demand of the fluoroalkyl fragments increases along the series $CF(CF_3)_2<(^sC_4F_9)<(cyc-C_6F_{11})$.

The coordination chemistry of the perfluoroalkyldiphenylphosphines **15**, **16**, and **18** has been investigated, resulting in the formation of complexes of the type $[PtCl_2L_2]$, $[ClAuL]$, and $[Mo(CO)_5L]$ (where L = phosphine). From these

more information regarding the electronic properties has been obtained. Furthermore, X-ray structural data of these complexes have been used to gain an insight into their steric parameters, alongside the data from the chalcogenides. Compound **16** has been shown to have a particularly small cone angle at 105°, whilst **15**, **18** and **19** are much more sterically demanding, with average cone angles of 173°, 182°, and 183° respectively.

The phosphines **15**, **18** and **19** are located in the bulky electron-withdrawing void shown on the stereoelectronic plot of Cundari *et al*,[35] as illustrated in Figure 5.13, whereas **16** has been shown to possess very similar electronic properties yet occupy a much smaller volume.

Further investigation into these interesting ligands is clearly required, particularly with regard to their potential utility in catalysis.

7. Experimental

All syntheses were carried out using standard Schlenk techniques under inert (N_2) atmospheres unless otherwise stated. Air/moisture sensitive compounds were handled under argon in a glove box (Belle Technology, UK). Low temperature reactions were carried out using an ethanol bath with a closed cycle dip chiller (L.P. Technology, Leeds, UK), liquid nitrogen/ethanol slush, or solid carbon dioxide/acetone bath.

Diethyl ether and THF (Fisher Scientific/Sigma-Aldrich) were dried over sodium/benzophenone for *ca*. 1 day and then freshly distilled prior to use, or dried over activated alumina columns on a specially designed Solvent Purification System (Innovative Technology, Inc., USA). Hexane (Fisher Scientific/Sigma-Aldrich) was dried over sodium wire for *ca*. 1 day and then freshly distilled prior to use. CF_3I, C_2F_5I, $^nC_3F_7I$, $(CF_3)_2CFI$, $^sC_4F_9I$, $^tC_4F_9I$, *cyc*-$C_6F_{11}I$, and CF_3CHFI (all Apollo Scientific), $K[AuCl_4]$, $K_2[PdCl_4]$ and $K_2[PtCl_4]$ (Johnson-Matthey), $PhPH_2$ (Strem), P^nBu_3, Li (3.2 mm diam. wire), ^nBuLi (2.5 M in hexanes), ^tBuLi (1.5M in pentanes), MeLi (1.6 M in Et_2O) (all Acros), $[Mo(CO)_6]$, Ph_2PCl, $PhPCl_2$, Ph_2PMe, $^iPr_2PCl$, PPh_3, $PSCl_3$, Me_3SiCl, CH_3I, magnesium turnings, $CDCl_3$, and d_6-benzene (all Sigma-Aldrich) were purchased from commercial vendors and used as supplied.

$MesPCl_2$,[256] Mes_2PCl,[257] $Ph_2P(CF=CF_2)$,[36] $^iPr_2P(CF=CF_2)$,[121] $Cy_2P(CF=CF_2)$,[121] Ph_2PSiMe_3,[191] $PhP(SiMe_3)_2$,[258] and $(Me_2PS)_2$[228] were synthesized via literature methods.

NMR data were recorded in $CDCl_3$ unless stated otherwise. $^{31}P\{^1H\}$, ^{31}P, and ^1H NMR spectra were recorded on a Bruker Avance III 400 MHz or a Bruker DPX200 spectrometer operating at 161.967 or 81.013 MHz, and 400.130 or 200.131 MHz respectively. The chemical shifts quoted are referenced to external 85% H_3PO_4 and $SiMe_4$. ^{19}F, $^{13}C\{^1H\}$ and $^{77}Se\{^1H\}$ NMR spectra were

recorded using a Bruker AVANCE III 400MHz spectrometer operating at 376.461, 100.622, and 76.349 MHz and referenced externally to $CFCl_3$, $SiMe_4$, or selenophene respectively. IR spectra were recorded as nujol mulls on a Nicolet instrument, or as neat samples on Bruker Alpha-P or Perkin Elmer Spectrum-BX FT-IR spectrometers. Elemental analyses were performed by the school's microanalsyis department.

X-ray diffraction data was collected on a Bruker Nonius κ-CCD 4-circle or on an Oxford Excalibur 2 diffractometer, and were corrected for Lorentz, polarisation and absorption using the multi-scan method. The X-ray structural data were solved by direct methods, with full-matrix least-squares refinement of F^2 using the SHELXL[259] or SHELXTL[259] programs. Non-hydrogen atoms were refined with anisotropic thermal parameters; hydrogen atoms were placed in idealised locations. The programs MERCURY[260] and ORTEP[174] were used to investigate the structures and generate the graphical representations.

Table 7.1: Crystallographic data for compounds 11, 12, 15, 29, 31, 32, 33, 34, 38, 39, 40, 41.

	11	12	15	29	31	32
Formula	$C_{28}Cl_2F_6H_{44}P_2Pd$	$C_{28}Cl_2F_6H_{44}P_2Pt$	$C_{15}F_7H_{10}P$	$C_{15}F_7H_{10}OP$	$C_{15}F_7H_{10}PS$	$C_{15}F_7H_{10}PSe$
Formula Weight	733.87	822.20	354.12	370.12	386.26	433.16
Crystal System	Triclinic	Triclinic	Monoclinic	Triclinic	Triclinic	Triclinic
Space Group	$P\bar{1}$	$P\bar{1}$	$P2_1/c$	$P\bar{1}$	$P\bar{1}$	$P\bar{1}$
a (Å)	11.2691(6)	11.2760(2)	8.9091(2)	6.5888(3)	7.1885(17)	7.2941(4)
b (Å)	11.6674(6)	11.6583(2)	26.2430(6)	8.7148(5)	8.3926(18)	8.2588(4)
c (Å)	14.9514(9)	14.9767(3)	6.3928(1)	13.8123(10)	13.682(4)	13.3659(7)
α (°)	74.405(2)	74.5780(10)	90	77.966(2)	79.515(7)	80.973(4)
β (°)	70.092(3)	70.0010(10)	99.406(1)	76.548(2)	79.362(9)	81.111(4)
γ (°)	63.955(3)	63.9810(10)	90	81.291(2)	79.662(15)	79.561(4)
Z	2	2	4	2	2	2
V (Å^3)	1644.00(16)	1646.86(5)	1474.55(5)	749.97(8)	788.6(3)	775.20(7)
T/K	150(2)	150(2)	150(2)	150(2)	100	100
D_c (g cm^{-3})	1.483	1.659	1.595	1.639	1.627	1.856
Crystal Size (mm)	0.25 x 0.04 x 0.01	0.07 x 0.18 x 0.18	0.15 x 0.15 x 0.15	0.14 x 0.14 x 0.20	0.10 x 0.10 x 0.12	0.08 x 0.4 x 0.8
μ (mm^{-1})	0.875	4.570	0.257	0.262	0.376	2.595
2θ Range (°)	4.52 → 49.96	6.0 → 55.0	6.2 → 51.0	6.4 → 50	5.8 → 51.0	5.6 → 52.8
Total Reflections	22106	7530	2736	2437	1366	5833
Unique Reflections (R_{int})	5820(0.091)	7530 (0.085)	2736 (0.047)	2437 (0.074)	1366 (0.056)	3145 (0.040)
Obs. Reflections [I > 2σ(I)]	4101	5104	1979	1594	770	2753
Parameters	357	355	208	217	217	217
Final R Indices [I > 2σ(I)]	R_1 0.0792 wR_2 0.1758	R_1 0.0531 wR_2 0.1407	R_1 0.0796 wR_2 0.2488	R_1 0.0847 wR_2 0.1860	R_1 0.0894 wR_2 0.2523	R_1 0.0384 wR_2 0.1014
Max., Min. Δρ (eÅ^{-3})	1.313, -1.011	3.04, -3.02	0.92, -0.42	0.85, - 0.41	-0.31, 0.42	0.73, -0.94
Goodness of Fit on F^2	1.069	1.09	1.08	1.16	1.01	1.01

	33	34	38	39	40	41
Formula	$C_{16}F_9H_{10}PSe$	$C_{18}F_{11}H_{10}PSe$	$C_{30}Cl_2F_{14}H_{20}P_2Pt$	$AuC_{13}ClF_3H_{10}P$	$Au_1C_{15}ClF_7H_{10}P$	$Au_1C_{16}ClF_9H_{10}P$
Formula Weight	483.17	545.11	974.38	486.60	586.82	636.55
Crystal System	Monoclinic	Monoclinic	Triclinic	Orthorhombic	Monoclinic	Monoclinic
Space Group	$P2_1/c$	$P2_1/c$	$P\bar{1}$	$P_{na}2_1$	$C2/c$	$P2_1/c$
a (Å)	12.550(4)	13.1301(4)	10.5189(5)	9.1057(3)	16.0370(16)	14.8800(4)
b (Å)	14.116(3)	32.6404(10)	13.1905(7)	13.7198(5)	11.7410(9)	15.7970(4)
c (Å)	10.057(3)	9.1970(2)	13.2821(6)	11.2174(5)	19.3340(18)	15.9240(4)
α (°)	90	90	109.012(4)	90	90	90
β (°)	97.946(6)	105.187(1)	95.970(4)	90	109.717(4)	95.226(1)
γ (°)	90	90	108.774(4)	90	90	90
Z	4	8	2	4	8	8
V (Å^3)	1764.6(8)	3803.92(18)	1604.13(16)	1401.37(9)	3427.0(5)	3727.53
T/K	100	100	100	100	100	100
D_c (g cm^{-3})	1.819	1.904	2.017	2.306	2.274	2.269
Crystal Size (mm)	0.08 x 0.08 x 0.12	0.08 x 0.08 x 0.20	0.10 x 0.25 x 0.40	0.13 x 0.18 x 0.18	0.04 x 0.1 x 0.14	0.10 x 0.10 x 0.18
μ (mm^{-1})	2.306	2.166	4.745	10.484	8.628	8.207
2θ Range (°)	6.2 → 41.8	6 → 50.8	5.6 → 52.8	6 → 50.8	7 → 50.8	6 → 50.8
Total Reflections	5287	29344	15167	2415	2861	77002
Unique Reflections (R_{int})	1663 (0.304)	6944 (0.140)	6517 (0.052)	2415 (0.000)	2861 (0.000)	6827 (0.079)
Obs. Reflections [I > 2σ(I)]	538	3240	4332	1908	1619	5075
Parameters	244	559	445	174	226	495
Final R Indices [I > 2σ(I)]	R_1 0.0775 wR_2 0.2095	R_1 0.0907 wR_2 0.2510	R_1 0.0334 wR_2 0.0698	R_1 0.0631 wR_2 0.1507	R_1 01065 wR_2 0.2475	R_1 0.0580 wR_2 0.1688
Max., Min. Δρ (eÅ^{-3})	-0.47, 0.45	-1.21, 1.03	1.43, -0.93	5.19, -2.65	5.39, -2.77	2.12, -2.62
Goodness of Fit on F^2	0.85	1.17	0.96	1.15	1.27	1.03

7.1 Unsaturated Fluoroorgano-Containing Phosphines

7.1.1 Fluorovinyl Phosphines

MesP(CF=CF$_2$)$_2$, 1

HFC-134a (4.5 cm^3, 52.9 mmol) was dissolved in Et$_2$O (150 cm^3) at -85°C, followed by the addition of ^{n}BuLi (16 cm^3, 40 mmol) drop-wise over ca. 30 minutes, ensuring that the internal reaction temperature remained below 80°C. The reaction was then allowed to warm to -60°C and maintained between -60°C and -65°C for 2h during which time the solution turned golden coloured. The solution was then cooled to ca. -100°C and a solution of MesPCl$_2$ (1.99 g, 9.0 mmol) in Et$_2$O (20 cm^3) was added over ca. 45 minutes. The solution was maintained at -70°C overnight, and then allowed to warm to room temperature. Hexane (100 cm^3) was added, the mixture filtered and the volatiles removed *in vacuo* affording **1** as an impure dark brown oil (0.6 g, 22%): ^{31}P{^{1}H} δ -63.3 ppm (m); ^{19}F NMR: δ_{Ftrans} -84.6 ppm (ddd, $^3J_{PFb}$ = 8.5 Hz, $^3J_{FbFa}$ = 30.5 Hz, $^3J_{FbFc}$ = 46.0 Hz) δ_{Fcis} -106.8 ppm (ddd, $^2J_{FcFb}$ = 46.5 Hz, $^3J_{FcP}$ = 54.6 Hz, $^3J_{FcFa}$ = 120.8 Hz) δ_{Fgem} -170.7 ppm (ddd, $^2J_{PFa}$ = 18.0 Hz, $^3J_{FaFb}$ = 29.9 Hz, $^3J_{FaFc}$ = 121.0 Hz), ^{1}H NMR: δ 6.97 ppm (s, Ar-*H*, 2H), 2.44 ppm (s, *o*-C*H*$_3$, 6H), 2.29 ppm (s, *p*-C*H*$_3$, 3H).

Mes$_2$P(CF=CF$_2$), 2

In a typical procedure, HFC-134a (4.5 cm^3, 52.9 mmol) was dissolved in Et$_2$O (200 cm^3) at -85°C, then ^{n}BuLi (12.8 cm^3, 32 mmol) was added drop-wise over ca. 30 minutes to ensure that the temperature remained below -80°C. Upon completion of this addition, the internal reaction temperature was allowed to rise to ca. -60°C and maintained between -60°C and -65°C for 2h, during which time the solution became golden coloured. The reaction mixture was then cooled to ca. -100°C, and a solution of Mes$_2$PCl (4.00 g, 13.0

mmol) in Et$_2$O (15 cm^3) was added slowly over ca. 45 minutes. The solution was maintained at -70°C overnight, and allowed to warm to room temperature. Hexane (100 cm^3) was added, and the mixture filtered through Celite®, and the volatiles removed *in vacuo* to yield a brown oil, which was shown to only contain Mes$_2$PCl in the ^{31}P{^{1}H} NMR spectrum.

E/Z-^{i}Pr$_2$P(CF=CF^{t}Bu), 4-(*E*)/4-(*Z*)

^{i}Pr$_2$P(CF=CF$_2$) (0.68 g, 3.44 mmol) was dissolved in Et$_2$O (100 cm^3), and cooled to -78°C. ^{t}BuLi (11.5 cm^3, 17.25 mmol) was then added drop-wise over ca. 15 minutes, and the mixture allowed to attain room temperature overnight. Hexane (50 cm^3) was added, the mixture filtered through Celite® and the volatiles removed *in vacuo*. Flash chromatography (hexane/diethyl ether, 50:50) afforded the title compound as a mixture of *E/Z*-isomers (0.31 g, 38%) **4-(*Z*)**: ^{31}P{^{1}H} NMR δ -4.9 ppm (dd, $^2J_{PFgem}$ = 6.3 Hz, $^3J_{PFcis}$ = 95.5 Hz), ^{19}F NMR: δ -136.9 ppm (dd, $^3J_{PF}$ = 95.5 Hz, $^3J_{FF}$ = 144.1 Hz, 1F, F$_{cis}$), δ -156.2 ppm (dd, $^3J_{PF}$ = 4 Hz, $^3J_{FF}$ = 144.1 Hz, 1F, F$_{gem}$) **4-(*E*)**: ^{31}P{^{1}H} NMR: δ -2.3 ppm (dd, $^2J_{PFgem}$ = 10.5 Hz, $^3J_{PFtrans}$ = 2.9 Hz), ^{19}F NMR: δ -112.2 (d, $^2J_{PFa}$ = 11.0 Hz), δ -139.3 ppm (d, $^3J_{PFb}$ = 3 Hz).

E/Z-Ph$_2$P(CF=CF^{t}Bu), 5-(*E*)/5-(*Z*)

Ph$_2$P(CF=CF$_2$) (1.0 g, 3.8 mmol) was dissolved in Et$_2$O (100 cm^3), and cooled to -78°C. ^{t}BuLi (2.6 cm^3, 3.9 mmol) was then added drop-wise over ca. 15 minutes, and the mixture allowed to attain room temperature overnight. Hexane (50 cm^3) was added, the mixture filtered through Celite® and the volatiles removed *in vacuo*. Column chromatography (hexane/diethyl ether, 50:50) afforded the title compound as a mixture of *E/Z*-isomers (0.71 g, 68%). **5-(*Z*)**: ^{31}P{^{1}H} NMR: δ -23.6 ppm (dd, $^3J_{PFcis}$ = 112.1 Hz, $^2J_{PFgem}$ = 5.5 Hz), ^{19}F NMR δ -134.1 ppm (dd of dectets, $^3J_{FF}$ = 143.4 Hz, $^3J_{PF}$ = 112.2 Hz, $^4J_{FH}$ = 2.0 Hz, 1F, F$_{cis}$), -156.3 ppm (dd of dectets, =$^3J_{FF}$ = 143.4 Hz, $^3J_{PF}$ =

5.6 Hz, $^5J_{FH}$ = 2.0 Hz, 1F, F_{gem}), ^1H NMR: δ 1.19 ppm (dd, $^4J_{FH}$ = 2.0 Hz, $^5J_{FH}$ = 2.0 Hz, C(CH_3)$_3$), 7.24-7.30 ppm (m, Ar-H, 6H), 7.33-7.43 ppm (m, Ar-H, 4H). **5-(E)**: $^{31}P\{^1H\}$ NMR: δ -19.6 ppm (dd, $^2J_{PF}$ = 16.3 Hz, $^3J_{PF}$ = 3.4 Hz), ^{19}F NMR: -108.3 ppm (dm, $^2J_{PF}$ = 16.3 Hz, 1F, F_{gem}), -139.5 (d, $^3J_{PF}$ = 3.5 Hz, 1F, F_{trans}), ^1H NMR: 1.30 ppm (s, 9H, C(CH_3)$_3$), 7.65-7.72 ppm (m, Ar-H, 6H), 7.84-7.91 ppm (m, Ar-H, 4H).

7.1.2 Oxidation of Fluorovinyl-Containing Phosphines

Se=PPh$_2$(CF=CF^{t}Bu), 6

Powdered elemental selenium (0.52 g, 6.6 mmol) was added to a solution of **5-(Z)** (1.0 g, 3.3 mmol) in toluene (60 cm^3). The solution was refluxed for *ca*. 2 hours, and then allowed to cool to room temperature. The excess of selenium was removed by filtration, and the volatiles removed *in vacuo*. The residue was purified by flash column chromatography (DCM) to yield the title compound as a yellow solid. (0.62 g, 50%). $^{31}P\{^1H\}$ NMR: δ 24.4 ppm (dd, $^3J_{PFcis}$ = 70.9 Hz, $^2J_{PFgem}$ = 4.4 Hz, $^1J_{PSe}$ = 764.0 Hz), ^{19}F NMR: -126.1 ppm (d of dectets, $^3J_{FF}$ = 141.4 Hz, $^5J_{FH}$ = 2.0 Hz, 1F, F_{gem}), -156.8 ppm (dd of dectets, $^3J_{FF}$ = 141.4 Hz, $^3J_{PF}$ = 70.8 Hz, $^4J_{FH}$ = 2.2 Hz, 1F, F_{cis}). $^{77}Se\{^1H\}$ NMR: δ -294.8 ppm (ddd, $^1J_{PSe}$ = 764.0 Hz, $^3J_{SeF}$ = 5.0 Hz, $^4J_{SeF}$ = 5.0 Hz). ^1H NMR: δ 1.17 ppm (dd, $^4J_{FH}$ = 2.2 Hz, $^5J_{FH}$ = 2.0 Hz, 9H, C(CH_3)$_3$) 7.37–7.44 ppm (m, 6H, Ar-H), 7.74–7.82 ppm (m, 4H, Ar-H).

7.1.3 Fluroalkynyl-Containing Phosphines

PhP(tfp)$_2$, 7

A three necked flask was charged with Et$_2$O (200 cm^3) and cooled to -20°C. HFC-245fa (6 cm^3, 59.0 mmol) was introduced. ^{n}BuLi (61.2 cm^3, 153 mmol) was then added drop wise (over *ca*. 1h), whilst maintaining the temperature below -15°C. Once the addition was complete, the reaction was allowed to

stir for 1h at -15°C. The temperature was then lowered to -70°C, and a solution of PPh$_2$Cl (2.31 cm^3, 17 mmol) in Et$_2$O (15 cm^3) was added slowly ensuring that the temperature remained below -70°C. The reaction was then left to warm to room temperature overnight. Hexane (150 cm^3) was added, and the mixture stirred for 15 minutes, then filtered through Celite® and the solvent removed *in vacuo* to yield a dark brown liquid. Distillation at 88°C (10 mmHg) gave the title compound as a pale yellow oil (2.98 g, 59.7%). PC$_{12}$H$_5$F$_6$ requires C = 48.95, H = 1.71, P = 10.54 found C = 49.16, H = 1.41, P = 10.17. ^{31}P{^{1}H} NMR: δ -67.2 ppm (septet, $^4J_{PF}$ = 6.4 Hz) ^{19}F NMR: δ –51.9 ppm (d, $^4J_{FP}$ = 6.4 Hz), ^{1}H NMR: δ 7.50–7.60 ppm (m, Ar–*H*, 3H), 7.75–7.90 ppm (m, Ar–*H*, 2H), ^{13}C{^{1}H} NMR: δ 134.3 (d, $^2J_{PC}$ = 24.8 Hz, *ortho*), 132.0 (s, *para*), 130.0 (d, $^3J_{PC}$ = 9.9 Hz, *meta*), 126.5 (s, *ipso*), δ 113.7 (q, $^1J_{CF}$ = 259.4 Hz), 92.4 ppm (q, $^2J_{CF}$ = 53.0 Hz), δ 81.7 ppm (dm, $^2J_{PC}$ = 21.8 Hz).

7.1.4 Chemistry of Fluoroalkynyl Phosphines

Reaction of PhP(tfp)$_2$ with ^{t}BuLi (Synthesis of Ph^{t}BuP(dfcp), 8, *Z*-Ph^{t}BuP(CH=C(^{t}Bu)CF$_3$), 9, and Ph^{t}BuP(tfp), 10)

PhP(tfp)$_2$ (1.0g, 3.4 mmol) was dissolved in Et$_2$O (80 cm^3) and cooled to -78°C. ^{t}BuLi (4.6 cm^3, 6.9 mmol) was added slowly and the mixture allowed to attain room temperature overnight. Hexane (50 cm^3) was added, the mixture filtered through Celite® and the volatiles removed *in vacuo* to yield a brown oil that contained a mixture of products. **Ph^{t}BuP(dfcp), 8**: ^{31}P{^{1}H} NMR: δ -1.6 ppm (dd, $^3J_{PF}$ = 14.6 Hz, $^3J_{PF}$ = 4.9 Hz), ^{19}F NMR: δ -99.1 ppm (dd, $^2J_{FF}$ = 122.0 Hz, $^3J_{PF}$ = 14.5 Hz, 1F), -101.9 ppm (dd, $^2J_{FF}$ = 122.0 Hz, $^3J_{PF}$ = 4.9 Hz, 1F). **Z-Ph^{t}BuP(CH=C(^{t}Bu)CF$_3$), 9**: ^{31}P{^{1}H} NMR: δ -6.0 ppm (q, $^4J_{PF}$ = 54.4 Hz), ^{19}F NMR: δ -54.2 ppm (d, $^4J_{PF}$ = 54.4 Hz). **Ph^{t}BuP(tfp),**

10: $^{31}P\{^1H\}$ NMR: δ -14.4 ppm (q, $^4J_{PF}$ = 6.5 Hz), ^{19}F NMR: δ -50.2 ppm (d, $^4J_{PF}$ = 6.5 Hz).

7.1.5 Complexes of Unsaturated Fluoro-organo Phosphines

trans-[PdCl$_2$\{PCy$_2$(CF=CF$_2$)\}$_2$], 11

PCy$_2$(CF=CF$_2$) (0.27 g, 0.97 mmol) was dissolved in ethanol (4 cm^3), and added dropwise to a solution of K$_2$[PdCl$_4$] (0.2 g, 0.48 mmol) in water (4 cm^3) and stirred for ~30 minutes. The mixture was filtered, and the filtrate washed with ethanol (2 x 5 cm^3) to yield a yellow solid (0.27 g, 77%). C$_{28}$Cl$_2$F$_6$H$_{22}$P$_2$Pd requires C 45.8, H 5.9, Cl 9.3 found C 46.0, H 6.0 Cl 9.7%. Raman (cm^{-1}): 302 v(Pd-Cl). IR (Nujol, cm^{-1}): 1738 v(C=C), 1308, 1152, 1047 v(C-F). $^{31}P\{^1H\}$ NMR: δ 24.1 ppm (vt, ½ |$^2J_{PF}$ + $^4J_{PF}$| = 15.0 Hz). ^{19}F NMR: δ -83.9 ppm (dd, $^2J_{FF}$ = 49 Hz, $^3J_{FF}$ = 32 Hz, 1F, *trans*), -97.1 ppm (dd, $^2J_{FF}$ = 49 Hz, $^3J_{FF}$ = 116 Hz, 1F, *cis*), -175.0 ppm (ddvt, ½ |$^2J_{PF}$ + $^4J_{PF}$| = 15.0 Hz, $^3J_{FF}$ = 32.0 Hz, $^3J_{FF}$ = 118.0 Hz, 1F, *gem*).

trans-[PtCl$_2$\{PCy$_2$(CF=CF$_2$)\}$_2$], 12

PCy$_2$(CF=CF$_2$) (0.27 g, 0.97 mmol) was dissolved in ethanol (4 cm^3), and added dropwise to a solution of K$_2$[PtCl$_4$] (0.2 g, 0.48 mmol) in water (4 cm^3) and stirred for ~30 minutes. The mixture was filtered, and the filtrate washed with ethanol (2 x 5 cm^3) to yield a white solid. Yield = 0.12 g, 50%. Raman (cm^{-1}): 333 v(Pt-Cl). IR (Nujol, cm^{-1}): 1736 v(C=C) 1312, 1147, 1049 v(C-F). $^{31}P\{^1H\}$ NMR: δ + 19.8 ppm (vt, ½|$^2J_{PF}$ + $^4J_{PF}$| = 16 Hz, $^1J_{PtP}$ = 2654 Hz) ^{19}F NMR: δ$_{Fb}$ –83.9 ppm (dd, $^2J_{FF}$ = 43 Hz, $^3J_{FF}$ = 31 Hz, $^4J_{PtF}$ = 16 Hz), δ$_{Fc}$ - 98.3 ppm (dd, $^2J_{FF}$ = 48 Hz, $^3J_{FF}$ = 116 Hz, $^4J_{PtF}$ = 43 Hz) δ$_{Fa}$ – 182.2 ppm (ddvt, ½($^2J_{PF}$ + $^4J_{PF}$) = 15 Hz, $^3J_{FF}$ = 31 Hz, $^3J_{FF}$ = 116 Hz, $^3J_{PtF}$ = 70 Hz.

[Mo(CO)₅{PCy₂(CF=CF₂)}], 13

[Mo(CO)$_6$] (0.25 g, 0.95 mmol) was dissolved in toluene (~25 cm^3) and PCy$_2$(CF=CF$_2$) (0.3 g, 1.07 mmol) was added. The mixture was refluxed for 3 hours, allowed to cool, and the solvent removed *in vacuo* to yield a black liquid. This was purified via column chromatography (toluene) to yield the title compound as a dark green oil (0.26 g, 53%). ^{31}P{^{1}H} NMR: + 44.0 ppm (dd, $^2J_{PFgem}$ = 39.3 Hz, $^3J_{PFc}$ = 4.6 Hz), ^{19}F NMR: δ -82.1 ppm (ddd, $^2J_{FtransFcis}$ = 49.7 Hz, $^3J_{FtransFgem}$ = 32.6 Hz, $^3J_{PFtrans}$ = 4.9 Hz, 1F, F$_{trans}$), δ -101.2 ppm (dd, $^3J_{FcisFgem}$ = 116.3 Hz, $^2J_{FtransFcis}$ = 49.7 Hz, 1F, F$_{cis}$), δ -168.9 ppm (ddd, $^3J_{FgemFcis}$ = 116.5 Hz, $^2J_{PFgem}$ = 40.5 Hz, $^3J_{FgemFtrans}$ = 32.6 Hz, 1F, F$_{gem}$) v(cm^{-1}): 2073 (C≡O), 1990, 1942.

[Mo(CO)₅{PPh(tfp)₂}], 14

[Mo(CO)$_6$] (0.31 g, 1.17 mmol) was dissolved in MeCN (25 cm^3), and Me$_3$NO.2H$_2$O (0.13 g, 1.17 mmol) was added. This was stirred under a static vacuum for 1 hour. A solution of **7** (0.35 g, 1.2 mmol) in MeCN (5 cm^3) was then added and the mixture allowed to stir overnight. The mixture was then passed down a short silica column (toluene) affording the title compound as a viscous dark brown oil (0.13 g, 21%). IR (cm^{-1}): 2081 (C≡O), 2032, 1947, 1585, 1245. ^{31}P{^{1}H} NMR: δ -13.6 ppm (s), ^{19}F NMR: -52.0 ppm (s).

7.2 Fluoroalkyl-Containing Phosphines

7.2.1 Evaluation of Reaction of R₂SiMe₃ with R$_f$I on Small Scale

R$_2$PSiMe$_3$ (0.1 cm^3, 0.39 mmol) was dissolved in CDCl$_3$ (0.75 cm^3) in an NMR tube in a glove box. One equivalent of perfluoroalkyl iodide was then added, and the tube sealed. Spectra were recorded immediately and periodically until no further signs of reaction could be observed. The products were identified on the basis of their multinuclear NMR spectra.

^{i}Pr$_2$PSiMe$_3$

A mixture of Me$_3$SiCl (4.3 cm^3, 33.6 mmol) and ^{i}Pr$_2$PCl (5.2 cm^3, 32.8 mmol) were dissolved in THF (100 cm^3). Lithium (0.58 g, 83 mmol) was added, and the mixture stirred for 72 hours. The excess lithium was removed, and hexane (50 cm^3) added. The mixture was filtered, and the volatiles removed *in vacuo*. The residue was distilled to afford the title compound (with *ca*. 5% ^{i}Pr$_2$PCl) as a clear liquid. ^{31}P$\{^1$H$\}$ NMR: δ -43.2 ppm (s), ^{1}H NMR: 0.65 ppm (m, 9H, Si(CH_3)$_3$) 1.05 ppm (m, 12H, PCH(CH_3)$_2$), 1.85 ppm (m, 2H, PCH).

Ph$_2$PCF(CF$_3$)$_2$, 15

^{31}P$\{^1$H$\}$ NMR: δ -0.8 ppm (dsept, $^2J_{PF}$ = 74.0 Hz, $^3J_{PF}$ = 18.0 Hz). ^{19}F NMR: δ -69.6 ppm (6F, dd, $^3J_{PF}$ = 18.0 Hz, $^3J_{FF}$ = 11.9 Hz, CF_3), -184.9 ppm (1F, dsept, $^2J_{PF}$ = 73.9 Hz, $^3J_{FF}$ = 11.9 Hz, PCF). ^{1}H NMR: δ 7.24-7.45 ppm (6H, m), 7.65-7.85 (4H, m). ^{13}C$\{^1$H$\}$ NMR: δ 135.8 ppm (d, $^2J_{PC}$ = 26.0 Hz, *ortho*), 131.2 ppm (s, *para*), 130.0 ppm (dd, $^1J_{PC}$ = 12.3 Hz, $^3J_{CF}$ = 6.8 Hz, *ipso*), 128.9 (d, $^3J_{PC}$ = 10.3 Hz, *meta*).

Ph$_2$PCF$_3$, 16

^{31}P$\{^1$H$\}$ NMR: δ 2.5 ppm (q, $^2J_{PF}$ = 73.8 Hz) [lit.[107] δ 1.7 ppm (q, $^2J_{PF}$ = 74.0 Hz)]. ^{19}F NMR: δ -55.1 ppm (d, $^2J_{PF}$ = 73.9 Hz [lit.[107] δ -56.8 ppm (d, $^2J_{PF}$ = 74.0 Hz)]. ^{1}H NMR: δ 7.4-7.7 ppm (m, Ar-H, 10H).

Ph$_2$PC$_2$F$_5$, 17

^{31}P$\{^1$H$\}$ NMR: δ -1.9 ppm (tq, $^2J_{PF}$ = 56.8 Hz, $^3J_{PF}$ = 16.9 Hz) [lit.[99](C$_6$D$_6$) δ -1.4 ppm (tq, J = 58.0, 17.0)]. ^{19}F NMR: δ -113.0 ppm (2F, dq, $^2J_{PF}$ = 56.8 Hz, $^3J_{FF}$ = 3.0, CF_2), -81.0 ppm (3F, dt, $^3J_{PF}$ = 16.5 Hz, $^3J_{FF}$ = 3.0 Hz, CF_3) [lit.[99] (C$_6$D$_6$): δ -112.6 ppm (dq, $^2J_{PF}$ = 57.0, $^3J_{FF}$ = 3.1 Hz), -80.7 ppm (dt, $^3J_{PF}$ = 16.5 Hz, $^2J_{FF}$ = 3.1 Hz)]. ^{1}H NMR: δ 7.4-7.7 ppm (m, Ar-H, 10H).

Ph$_2$P(^{s}C$_4$F$_9$), 18

^{31}P{^{1}H} NMR δ 3.6 ppm (dddqq, $^2J_{PFb}$ = 78.8 Hz, $^3J_{PFc}$ = 45.0 Hz, $^3J_{PFd}$ = 33.7 Hz, $^3J_{PFa}$ = 16.9 Hz, $^4J_{PFe}$ = 11.5 Hz) ^{19}F NMR: δ -67.6 ppm (dddqd, $^3J_{PFa}$ = 16.9 Hz, $^3J_{FaFd}$ = 12.3 Hz, $^4J_{FaFb}$ = 12.1 Hz, $^5J_{FaFe}$ = 8.6 Hz, $^4J_{FaFc}$ = 5.7 Hz, 3F, F$_a$), -79.8 ppm, (ddqdd, $^4J_{PFe}$ = 12.0 Hz, $^4J_{FeFb}$ = 12.0 Hz, $^5J_{FeFa}$ = 8.6 Hz, $^3J_{FeFc}$ = 0.6 Hz, $^3J_{FeFd}$ = 0.1 Hz, 3F, F$_e$), -110.5 ppm ($^2J_{FcFd}$ = 295.6 Hz, $^3J_{PFc}$ = 44.6 Hz, $^3J_{FcFb}$ = 11.9 Hz, $^4J_{FcFa}$ = 5.7 Hz, $^3J_{FcFe}$ = 0.6 Hz, 1F, F$_c$), -114.3 ppm (ddqdq, $^2J_{FdFc}$ = 295.6 Hz, $^3J_{PFd}$ = 33.2 Hz, $^4J_{FdFa}$ = 12.3 Hz, $^3J_{FdFb}$ = 12.0 Hz, $^3J_{FdFe}$ = 0.1 Hz, 1F, F$_d$), -183.3 ppm (dqdqd, $^2J_{PFb}$ = 78.8 Hz, $^3J_{FbFa}$ = 12.3 Hz, $^3J_{FbFd}$ = 12.0, $^4J_{FbFe}$ = 12.0 Hz, $^3J_{FbFc}$ = 11.9 Hz, 1F, F$_b$). ^{1}H NMR: δ 7.22-7.34 ppm (m, 6H, Ar-H), 7.69-7.79 ppm (m, 4H, Ar-H). ^{13}C{^{1}H} NMR: δ 135.9 ppm (d, $^2J_{PC}$ = 26.2 Hz, $ortho$), 135.3 ppm (d, $^2J_{PC}$ = 26.2 Hz), 130.9 ppm (s, $para$), 130.7 ppm (s, $para$), 130.4 ppm (d, $^1J_{PC}$ = 13.2 Hz, $ipso$), 129.8 ppm (d, $^1J_{PC}$ = 15.0 Hz, $ipso$), 128.7 ppm (d, $^3J_{PC}$ = 9.8 Hz, $meta$), 128.6 ppm (d, $^1J_{PC}$ = 9.7 Hz, $meta$), 121.2 ppm (m, C-F), 118.0 ppm (m, C-F), 112.5 ppm (m, C-F), 100.1 ppm (m, C-F).

Ph$_2$P(cyc-C$_6$F$_{11}$), 19

^{31}P{^{1}H} NMR: δ -3.1 ppm (td, $^3J_{PF2ax}$ = 84.0 Hz, $^2J_{PF1}$ = 68.0 Hz). ^{19}F NMR: δ -110.5 ppm (2F, $^3J_{PF}$ = 84.0 Hz, $^2J_{FF}$ = 297.3 Hz), -122.6 ppm (2F, d, $^2J_{FF}$ = 280.0 Hz), -124.4 ppm (1F, d, $^2J_{FF}$ = 288.8 Hz) -124.5 ppm (2F, d, $^2J_{FF}$ = 298.6 Hz), -138.2 ppm (2F, d, $^2J_{FF}$ = 281.0 Hz), -142.0 ppm (1F, d, $^2J_{FF}$ = 285.5 Hz), and -185.8 ppm (1F, m, $^2J_{PF}$ = 67.0 Hz). ^{1}H NMR: δ 7.24-7.28 ppm (m, 4H), 7.56-7.62 ppm (m, 6H). ^{13}C{^{1}H} NMR: δ 128.8 ppm ($^3J_{PC}$ = 6.6 Hz, $meta$), 130.4 ppm ($para$), 134.0 ppm ($^1J_{PC}$ = 22.5 Hz, $ipso$), 136.1 ppm ($^2J_{PC}$ = 27.6 Hz, $ortho$).

Ph$_2$P(^{t}C$_4$F$_9$), 20

^{31}P{^{1}H} NMR: δ 15.2 ppm (dectet, $^3J_{PF}$ = 12.3 Hz), ^{19}F NMR: δ -59.9 ppm (d, $^3J_{PF}$ = 12.3 Hz). ^{1}H NMR: δ 7.4–7.7 ppm (m, Ar–H, 10H).

Ph$_2$P(^{t}C$_8$F$_{17}$), 21

^{31}P{^{1}H} NMR: δ 1.0 ppm (ttt, $^2J_{PF}$ = 56.2 Hz, $^3J_{PF}$ = 33.4 Hz, $^4J_{PF}$ = 11.5 Hz). ^{19}F NMR: δ -81.1 ppm (ttt, $^3J_{FF}$ = 10.1 Hz, $^4J_{FF}$ = 2.2 Hz, $^5J_{FF}$ = 2.2 Hz, CF_3, 3F), -108.9 ppm (dtm, $^2J_{PF}$ = 56.1 Hz, $^3J_{FF}$ = 14.5 Hz, P-CF_2CF$_2$-, 2F), -117.7 ppm (m, 2F), -121.5 ppm (m, 2F), -122.0 (m, 2F), -122.2 ppm (m, 2F), -123.0 ppm (m, 2F), -126.4 ppm (m, 2F). ^{1}H NMR: δ 7.4-7.7 ppm (m, Ar-H, 10H).

Ph$_2$P((1-CF$_3$)-*cyc*-C$_5$F$_8$), 22

^{31}P{^{1}H} NMR: δ -16.1 ppm (qtt, $^3J_{PF}$ = 39.0 Hz, $^3J_{PF}$ = 11.8 Hz, $^3J_{PF}$ = 4.2 Hz). ^{19}F NMR: δ -59.6 ppm (dm, $^3J_{PF}$ = 39.0 Hz, 3F, PCCF_3), -106.0 ppm (m, 2.33F), -111.6 ppm (m, 2.33F), -132.1 ppm (m, 2.33F). ^{1}H NMR: 7.30-7.40 ppm (m, 6H, Ar-H), 7.55-7.61 ppm (m, 4H, Ar-H).

Ph$_2$P(CHFCF$_3$), 23

^{31}P{^{1}H} NMR: δ -13.0 ppm (dq, $^2J_{PF}$ = 71.0 Hz, $^3J_{PF}$ = 20.7 Hz). ^{19}F NMR: δ -72.3 ppm (ddd, $^3J_{PF}$ = 20.7 Hz, $^3J_{FF}$ = 16.8 Hz, $^3J_{FH}$ = 8.4 Hz, 3F, CF_3), -206.4 ppm (ddq, $^2J_{PF}$ = 71.0 Hz, $^2J_{FH}$ = 46.5 Hz, $^3J_{FF}$ =16.8 Hz, 1F, PCHF). ^{1}H NMR: 6.66 ppm (dq, $^2J_{HF}$ = 46.5 Hz, $^3J_{HF}$ = 8.4 Hz, 1H, PCHF) 7.15-7.25 (m, 6H, Ar-H), 7.33-7.38 ppm (m, 4H, Ar-H).

^{i}Pr$_2$P(C$_2$F$_5$), 24

^{31}P{^{1}H} NMR: δ 24.4 ppm (tq, $^2J_{PF}$ = 41.6 Hz, $^3J_{PF}$ = 14.6 Hz). ^{19}F NMR: δ -82.4 ppm (dt, $^3J_{PF}$ = 14.6 Hz, $^3J_{FF}$ = 2.9 Hz, CF_3, 3F), -111.7 ppm (dq, $^2J_{PF}$ = 41.6 Hz, $^3J_{FF}$ = 2.8 Hz, PCF_2CF$_3$, 2F). ^{1}H NMR: δ 1.15 ppm (qd, $^6J_{FH}$ = 13.9

Hz, $^3J_{HH}$ = 7.2 Hz, 6H, PCH(CH_3)$_2$), 2.19 ppm (septd, $^3J_{HH}$ = 7.2 Hz, $^2J_{PH}$ = 2.5 Hz, 2H, PCH).

$^iPr_2P(^nC_3F_7)$, 25

$^{31}P\{^1H\}$ NMR: δ 27.2 ppm (ttq, $^2J_{PF}$ = 36.5 Hz, $^3J_{PF}$ = 29.6 Hz, $^4J_{PF}$ = 6.9 Hz). ^{19}F NMR: δ -79.9 ppm (td, $^3J_{FF}$ = 10.4 Hz, $^5J_{PF}$ = 6.8 Hz, -CF_2CF_3, 3F), -109.4 ppm (dq, $^2J_{PF}$ = 36.4 Hz, $^4J_{FF}$ = 10.5 Hz, PCF_2CF$_2$CF$_3$, 2F), -123.3 ppm (d, $^3J_{PF}$ = 29.7 Hz, PCF$_2$CF_2CF$_3$, 2F). ^1H NMR: δ 1.16 ppm (ddd, J = 16.2 Hz, J = 8.8 Hz, $^3J_{HH}$ = 7.4 Hz, 6H, CH_3), 2.21 ppm (septet of d, $^3J_{HH}$ = 7.2 Hz, $^2J_{PH}$ = 2.0 Hz, 1H, PCH).

7.2.2 Preparative Scale Chemistry

$Ph_2PCF(CF_3)_2$, 15

Ph_2PSiMe_3 (2.3 cm^3, 8.5 mmol) was dissolved in hexane (30 cm^3), and then cooled to -30°C. (CF$_3$)$_2$CFI (1.26 cm^3, 8.5 mmol) was added slowly over *ca.* 10 minutes. The solution was then allowed to warm to room temperature, and the volatiles removed *in vacuo*. The resultant yellow solid was re-dissolved in hexane (15 cm^3) and DCM (5 cm^3). This was filtered and volatiles were removed under high vacuum, affording the title compound as a white crystalline solid (2.27 g, 72% m.p. 48°C). PC$_{15}$H$_{10}$F$_7$ requires C 50.84, H 2.85, P 8.75, found C 50.88, H 2.71, P 8.04.

$Ph_2P(^sC_4F_9)$, 18

Ph_2PSiMe_3 (2.2 cm^3, 8.5 mmol) was dissolved in hexane (30 cm^3), and cooled to *ca.* -30°C. $^sC_4F_9I$ (1.42 cm^3, 8.6 mmol) was then added drop-wise over *ca.* 10 mins, and the mixture stirred and allowed to attain room temperature overnight. The volatiles were removed and the resulting residue distilled (123°C, 0.1 mmHg) to yield the title compound as a clear liquid (2.3

g, 57.6 %). $PC_{16}H_{10}F_9$ requires C 47.52, H 2.49, P 7.67, found C 48.7, H 3.0, P 7.7.

PhMePCF(CF$_3$)$_2$, 26

Ph_2PMe (2.00 g, 10 mmol) was dissolved in THF (40 cm^3), cooled to 0°C and Li (0.32 g, 46.1 mmol) was added. This was allowed to stir overnight and attain room temperature. The excess lithium wire was removed, the mixture cooled to 0°C and Me_3SiCl (2.387 g, 22.0 mmol) was added. This was allowed to warm to room temperature, then hexane (20 cm^3) was added, and the mixture filtered. The filtrate was then cooled to *ca.* -30°C and $(CF_3)_2CFI$ (1.70 cm^3, 12 mmol) was added, then allowed to warm to room temperature overnight. The volatiles were then removed *in vacuo* to yield an off white solid. (0.72 g, 24%). $^{31}P\{^1H\}$ NMR: δ -12.0 ppm (dsept, $^2J_{PF}$ = 61.1 Hz, 16.4 Hz), ^{19}F NMR: δ -70.2 ppm (ddq, $^3J_{PF}$ = 16.4 Hz, $^3J_{FF}$ = 11.2 Hz, $^4J_{FF}$ = 9.5 Hz, 3F, CF_3), -71.2 ppm (ddqq, $^3J_{PF}$ = 16.4 Hz, $^3J_{FF}$ = 11.2 Hz, $^4J_{FF}$ = 9.5 Hz, $^5J_{FH}$ = 1.5 Hz, 3F, CF_3), -190.3 ppm (dsept, $^2J_{PF}$ = 61.1 Hz, $^3J_{FF}$ = 11.2 Hz, 1F, PCF).

7.2.3 Reaction of PhP(SiMe$_3$)$_2$ with R$_f$I

PhP(H)CF(CF$_3$)$_2$, 27

A Schlenk vessel was charged with $PhP(SiMe_3)_2$ (0.59 g, 2.32 mmol) and hexane (30 cm^3). This was cooled to *ca*. -50°C and $(CF_3)_2CFI$ (0.65 cm^3, 4.64 mmol) added slowly. The solution was allowed to warm to 0°C and stirred overnight. The mixture was then cooled to -10°C, and MeLi (0.9 cm^3, 1.44 mmol) was added drop-wise. The mixture was then filtered, and the solvent removed *in vacuo*, to yield **27** as a clear liquid (0.22 g, 34%) $^{31}P\{^1H\}$ NMR: δ -42.3 ppm (dqq, $^2J_{PF}$ = 53.1 Hz, $^3J_{PF}$ = 17.8, 12.6 Hz), ^{19}F NMR: δ -72.6 ppm (3F, ddqd, $^3J_{PF}$ = 17.9 Hz, $^3J_{FF}$ = 11.9 Hz, $^4J_{FF}$ = 9.0 Hz, $^4J_{FH}$ = 2.8 Hz,

CF_3), -73.4 ppm (3F, ddqd, $^3J_{PF}$ = 12.1 Hz, $^3J_{FF}$ = 12.1 Hz, $^4J_{FF}$ = 9.0 Hz, $^4J_{FH}$ = 1.5 Hz, CF_3) -178.3 ppm (1F, ddqq, $^2J_{PF}$ = 53.0 Hz, $^3J_{FH}$ = 16.4 Hz, $^3J_{FF}$ = 12.0, 11.9 Hz, CF), ^{1}H NMR: δ 7.26-7.31 ppm (2H, m), 7.34-7.41 ppm (1H, m), 7.54-7.60 ppm (2H, m) 4.60 ppm (1H, ddm, $^1J_{PH}$ = 229.1 Hz, $^2J_{HF}$ = 16.3 Hz). ^{13}C{^{1}H} NMR: 127.5 ppm (d, J = 8.0 Hz, *meta*), 129.9 ppm (s, *para*), 134.9 ppm (d, J = 29.0 Hz, *ortho*), 136.5 ppm (d, J = 19.5 Hz, *ipso*).

7.2.4 Mechanistic Studies

NMR Tube Reaction of Ph$_2$P-PPh$_2$ with (CF$_3$)$_2$CFI

Ph$_2$P-PPh$_2$ (0.15 g, 0.4 mmol) was dissolved in d_6-Benzene (1 cm^3), in an NMR tube under argon. (CF$_3$)$_2$CFI (0.06 cm^3, 0.4 mmol) was then added, and the reaction monitored by NMR spectroscopy, which showed the presence of **15**.

Me$_2$P-P(S)Me$_2$

This compound was prepared by a slight modification of a literature procedure.[229] (Me$_2$PS)$_2$ (4.2 g, 22.6 mmol) and P^{n}Bu$_3$ (4.5 cm^3, 22.4 mmol) were placed into a Schlenk vessel which was then sealed. The mixture was heated to 140°C for 20 hours, then allowed to cool to room temperature. The resulting mixture was found to contain the title compound and S=P^{n}Bu$_3$, and was used without further purification. **S=P^{n}Bu$_3$:** ^{31}P{^{1}H} NMR: δ 48.7 ppm (s). **Me$_2$P-P(S)Me$_2$:** ^{31}P{^{1}H} NMR: δ -56.5 ppm (d, $^1J_{PP}$ = 221.1 Hz, Me$_2$$P$-P(S)Me$_2$, 1P), 37.3 ppm (d, $^1J_{PP}$ = 221.1 Hz, Me$_2$P-P(S)Me$_2$,1P).

Me$_2$PCF(CF$_3$)$_2$, 28

Me$_2$P-P(S)Me$_2$ (1.0 g of the mixture formed in the reaction above, max 6.5 mmol), and (CF$_3$)$_2$CFI (1.92 cm^3, 6.5 mmol) were stirred in a sealed Schlenk vessel for 3 weeks. Trap-to-trap condensation resulted in the isolation of a mixture of (CF$_3$)$_2$CFI and **28** in the trap cooled to -196°C. **28:** ^{31}P{^{1}H} NMR:

δ -18.2 ppm (dsept, $^2J_{PF}$ = 53.3 Hz, 16.4 Hz), ^{19}F NMR: δ -71.6 ppm (dd, $^3J_{PF}$ = 16.4 Hz, $^3J_{PF}$ = 10.4 Hz, 6F, CF(CF_3)$_2$), -195.5 ppm (dsept, $^2J_{PF}$ = 53.3 Hz, $^3J_{FF}$ = 10.4 Hz, 1F, PCF). ^{1}H NMR: 1.20 ppm (s, 6H).

7.2.5 Oxidation of Fluoroalkyl-Containing Phosphines

O=PPh$_2$CF(CF$_3$)$_2$, 29

This compound was serendipitously isolated via filtration from a solution of **15** (1.24 g, 3.5 mmol) in pentane (~15 cm^3) that had been left to stand at 4°C for 72 hours. Purification by flash chromatography (DCM) yielded the title compound as a white crystalline solid (0.8 g, 62%). PC$_{15}$H$_{10}$F$_7$O requires 48.64, H 2.72, P 8.37, found C 48.41, H 2.33, P 7.77 ^{31}P{^{1}H} NMR: δ 20.8 ppm (d, $^2J_{PF}$ = 51.4 Hz), ^{19}F NMR: δ -69.1 ppm (PCCF_3, 6F, d, $^3J_{FF}$ = 10.7 Hz), -188.6 ppm (PCF, 1F, dsept, $^2J_{PF}$ = 51.4 Hz, $^3J_{FF}$ = 10.7 Hz), ^{1}H NMR: δ 7.30-7.36 (m, 2H), 7.38-7.44 (m, 1H), 7.80-7.91 (m, 2H), ^{13}C{^{1}H} NMR: δ 133.5 ppm (d, $^4J_{PC}$ = 2.9 Hz, *para*), 132.0 ppm (dd, $^3J_{PC}$ = 9.5 Hz, $^5J_{CF}$ = 2.9 Hz, *ortho*), 128.9 ppm (d $^3J_{PC}$ = 13.0 Hz, *meta*), 127.5 ppm (d, $^1J_{PC}$ = 105.4 Hz, *ipso*), 120.4 ppm (CF$_3$, 2C, qd, $^1J_{CF}$ = 289.0 Hz, $^2J_{CF}$ = 25.8 Hz), 93.2 ppm (PCF, 1C, m).

O=PPh$_2$(*cyc*-C$_6$F$_{11}$), 30

19 (0.50 g, 1.07 mmol) was dissolved in THF (10 cm^3). An aqueous solution of H$_2$O$_2$ (0.25 cm^3, 30%, 2.15 mmol) was added at 0°C. This solution was allowed to stir and warm to room temperature over *ca*. 18 hours. H$_2$O (10 cm^3) was then added, and the mixture extracted with CHCl$_3$ (2 x 25 cm^3), dried over MgSO$_4$, filtered and the volatiles removed *in vacuo* to yield an orange-brown solid (0.12 g, 23%). ^{31}P{^{1}H} NMR: δ 20.9 ppm (d, $^2J_{PF}$ = 54.4 Hz). ^{19}F NMR: -116.3 ppm (dm, $^2J_{FF}$ = 301 Hz, 2F), -122.4 ppm (dm, $^2J_{FF}$ = 280 Hz, 2F), -124.0 ppm (dm, $^2J_{FF}$ = 285 Hz, 1F), -124.4 ppm (dm, $^2J_{FF}$ =

301 Hz, 2F), -138.6 ppm (dm, $^2J_{FF}$ = 281 Hz, 2F), -141.9 ppm (dm, $^2J_{FF}$ = 285 Hz, 1F), -190.4 ppm (m, 1F, PC*F*). ^{1}H NMR: 7.30-7.68 ppm (m, 6H, Ar-*H*), 8.01-8.09 ppm (m, 4H, Ar-*H*).

S=PPh$_2$CF(CF$_3$)$_2$, 31

Sulfur (0.5 g, 15 mmol) was added to a solution of **15** (1.5 g, 4.25 mmol) in toluene (70 cm^3) and refluxed for 4 hours. The solution was then allowed to cool and the excess of sulfur removed by filtration. The volatiles were removed *in vacuo* and the residue purified via flash chromatography (hexane/DCM, 1:1) to yield the product as a yellow-orange solid (0.63 g, 39%). ^{31}P{^{1}H} NMR: δ 39.6 ppm (d, $^2J_{PF}$ = 43.4 Hz). ^{19}F NMR: δ -66.7 ppm (d, $^3J_{FF}$ = 8.7 Hz, CF$_3$, 6F), -176.3 ppm (dsept, $^2J_{PF}$ = 43.0 Hz, $^3J_{FF}$ = 8.7 Hz, PC*F*(CF$_3$)$_2$, 1F). ^{1}H NMR: δ 8.1–8.2 ppm (m, Ar-*H*, 4H), 7.44–7.54 ppm (m, Ar-*H*, 6H).

Se=PPh$_2$CF(CF$_3$)$_2$, 32

Powdered elemental selenium (1.057 g, 13.4 mmol) was added to a solution of **15** (1.941 g, 5.5 mmol) in toluene (50 cm^3) and refluxed for 90 minutes. The mixture was allowed to cool to room temperature, filtered through Celite®, and the volatiles removed *in vacuo*. The resulting brown oil was purified via flash chromatography (DCM), affording **32** as a yellow oil, which crystallised on standing (1.21 g, 51%). C$_{15}$F$_{14}$H$_{10}$PSe requires C 41.57, H 2.33, P 7.15, found C 40.93, H 2.00, P 6.93; v(cm^{-1}): 571 (P=Se); ^{31}P{^{1}H} NMR: δ 35.2 ppm (d, $^2J_{PF}$ = 39.7 Hz, $^1J_{PSe}$ = 828 Hz). ^{19}F NMR: δ -66.0 ppm (PCC*F*$_3$ 6F, d, $^3J_{FF}$ = 8.8 Hz), -173.1 ppm (PC*F*, 1F, dsept, $^2J_{PF}$ = 39.4 Hz, $^3J_{FF}$ = 8.8 Hz). ^{1}H NMR: δ 7.24-7.38 ppm (1H, m), 7.56-7.66 ppm (2H, m), 8.35-8.42 ppm (2H, m). ^{13}C{^{1}H} NMR: δ 92.6 ppm (PC*F*, dds, $^1J_{CF}$ = 235 Hz, $^1J_{PC}$ = 30 Hz, $^2J_{CF}$ = 30 Hz), 119.2 ppm (PCC*F*$_3$ d, $^1J_{CF}$ = 290 Hz). ^{77}Se{^{1}H} NMR: δ -372.5 ppm (d, $^1J_{PSe}$ = 828 Hz).

Se=PPh$_2$(^{s}C$_4$F$_9$), 33

18 (3.64 g, 9.0 mmol) was dissolved in toluene (60 cm^3). Powdered elemental selenium (1.42 g, 18.0 mmol) was added and the mixture refluxed for 2 hours. The excess of selenium was removed by filtration through Celite® and the volatiles removed *in vacuo*. The residue was purified by flash chromatography (DCM) to yield **33** as an off-white solid (1.81 g, 42%). C$_{16}$F$_9$H$_{10}$PSe requires C 39.75, H 2.09, P 6.41; found C 39.82, H 2.15, P 6.08. ^{31}P{^{1}H} NMR: δ 37.7 ppm (dd, $^2J_{PFb}$ = 41.0 Hz, $^3J_{PFc}$ = 10.6 Hz, $^1J_{PSe}$ = 831 Hz); ^{19}F NMR: δ$_{Fa}$ -80.2 ppm (3F, dq, $^3J_{FaFb}$ = 15.2 Hz, $^5J_{FaFe}$ = 9.9 Hz), δ$_{Fb}$ -172.1 ppm (1F, dqdqd, $^2J_{PF}$ = 41.0 Hz, $^3J_{FbFa}$ = 15.2 Hz, $^4J_{FbFc}$ = 11.8 Hz, $^3J_{FbFe}$ = 10.2 Hz, $^3J_{FbFd}$ = 4.3 Hz), δ$_{Fc}$ -108.6 ppm (1F, dddq, $^2J_{FcFd}$ = 297.7 Hz, $^3J_{FcP}$ = 15.2 Hz, $^3J_{FcFb}$ = 11.8 Hz, $^3J_{FcFe}$ = 3.5 Hz), δ$_{Fd}$ = -109.6 ppm (1F, dqd, $^2J_{FdFc}$ = 297.7 Hz, $^3J_{FdFe}$ = 13.0 Hz, $^3J_{FdFb}$ = 4.3 Hz), δ$_{Fe}$ -64.4 ppm (3F, ddqd, $^3J_{FeFd}$ = 13.0 Hz, $^4J_{FeFb}$ = 10.2 Hz, $^5J_{FeFa}$ = 9.9 Hz, $^3J_{FeFc}$ = 3.5 Hz).

Se=PPh$_2$(*cyc*-C$_6$F$_{11}$), 34

19 (0.50 g, 1.07 mmol) was dissolved in toluene (60 cm^3) and powdered elemental selenium (0.2 g, 2.5 mmol) was added. The mixture was refluxed for *ca.* 2 hours, then allowed to cool and the excess of selenium removed by filtration. The volatiles were removed *in vacuo* and the residue purified by column chromatography (hexane/DCM, 7:3) affording the title compound as a white solid (0.22 g, 38%). ^{31}P{^{1}H} NMR: δ 34.3 ppm (d, $^2J_{PF}$ = 42.6 Hz, $^1J_{PSe}$ = 836.7 Hz), ^{19}F NMR: -110.3 ppm (dm, $^2J_{FF}$ = 299.8 Hz, 2F), -121.8 ppm (dm, $^2J_{FF}$ = 284 Hz, 2F), -123.6 (dm, $^2J_{FF}$ = 285.2 Hz, 1F), -124.5 ppm (dm, $^2J_{FF}$ = 300.3 Hz, 2F), -138.4 ppm (dm, $^2J_{FF}$ = 281.2 Hz, 2F), -141.8 ppm (dm, $^2J_{FF}$ = 285.2 Hz, 1F), -175.2 ppm (m, 1F). ^{1}H NMR: δ 7.40-7.50 ppm (m, Ar-H, 3H), 8.25 ppm (dd, 14.1 Hz, 7.5 Hz).

Se=PPh$_2$CF$_3$, 35

Powdered elemental selenium (0.51 g, 6.45 mmol) was added to a solution of **16** (1.01 g, 3.97 mmol) in toluene (60 cm^3) and refluxed for *ca*. 4 hours. The solution was allowed to cool to room temperature, the excess selenium removed via filtration and the volatiles removed *in vacuo* to afford the title compound as a clear liquid (1.15 g, 87.0%). C$_{11}$F$_3$H$_{10}$PSe requires C 46.85, H 3.03, P 9.30, found C 47.52, H 3.15, P 9.17. ^{31}P{^{1}H} NMR: δ 39.3 ppm (q, $^2J_{PF}$ = 84.4 Hz, $^1J_{PSe}$ = 816.0 Hz), ^{19}F NMR: δ -66.6 ppm (d, $^2J_{PF}$ = 84.4 Hz), ^{77}Se{^{1}H} NMR: δ -364.2 ppm (d, $^1J_{PSe}$ = 816.0 Hz), ^{1}H NMR: δ 7.35 – 7.50 ppm (m, Ar-*H*, 6H), 7.75-7.90 ppm (m, Ar-*H*, 4H), ^{13}C{^{1}H} NMR: δ 125.2 ppm (d, *J* = 75.8 Hz, *ipso*) 129.2 ppm (d, *J* = 13.2 Hz, *ortho*), 132.9 ppm (d, *J* = 11.2 Hz, *meta*), 133.5 ppm (d, *J* = 3.0 Hz, *para*), 121.9 ppm (qd, $^1J_{CF}$ = 320.0 Hz, $^1J_{PC}$ = 110.1 Hz, *C*F$_3$).

F$_2$PPh$_2$(CF(CF$_3$)$_2$), 36

15 (0.17 g, 0.5 mmol) was dissolved in CDCl$_3$ (0.75 cm^3) in an NMR tube in the glovebox, then small crystals of XeF$_2$ were added in portions until no starting materials could be observed spectroscopically. ^{31}P{^{1}H} NMR: δ -58.4 ppm (tdsept, $^1J_{PF}$ = 805.2 Hz. $^2J_{PF}$ = 82.6 Hz, $^3J_{PF}$ = 4.7 Hz). ^{19}F NMR: δ -53.8 ppm (P*F*, 2F, ddsept, $^1J_{PF}$ = 805.9 Hz, $^3J_{FF}$ = 20.7 Hz, $^4J_{FF}$ = 10.4 Hz), δ -69.8 ppm (PCC*F*$_3$, 6F, tdd, $^4J_{FF}$ = 10.4 Hz, $^3J_{FF}$ = 7.5 Hz, $^3J_{PF}$ = 4.7 Hz), δ -173.1 ppm (PC*F*, 1F, dtsept, $^2J_{PF}$ = 82.6 Hz, $^3J_{FF}$ = 20.7 Hz, $^3J_{FF}$ = 7.5 Hz).

F$_2$PPh$_2$(^{s}C$_4$F$_9$), 37

18 (0.20 g, 0.5 mmol) was dissolved in CDCl$_3$ (0.75 cm^3), then small crystals of XeF$_2$ were added portion-wise until no starting material could be detected spectroscopically. ^{31}P{^{1}H} NMR: δ -56.3 ppm (tdm, $^1J_{PF}$ = 821.5 Hz, $^2J_{PF}$ = 84.5 Hz). ^{19}F NMR: δ -53.0 ppm (d, 820.7 Hz, 2F, P*F*), -67.8 ppm (m, 3F), -

80.2 ppm (m, 3F), -112.8 ppm (dm, $^2J_{FF}$ = 300.6 Hz, PCF(CF$_3$)CFFCF$_3$, 1F), -116.1 ppm (dm, $^2J_{FF}$ = 300.6 Hz, PCF(CF$_3$)CFFCF$_3$, 1F), -171.0 ppm (dm, 84.6 Hz, PCF, 1F).

7.2.6 Complexes of Fluoroalkyl-Containing Phosphines

trans-[PtCl$_2${PPh$_2$CF(CF$_3$)$_2$}$_2$], 38

A solution of **15** (0.29 g, 0.81 mmol) in ethanol (5 cm^3) was added to K$_2$[PtCl$_4$] (0.1 g, 0.24 mmol) in H$_2$O (1 cm^3), and the mixture allowed to stir for *ca*. 1 hour. The solution changed colour from red to salmon-pink to pale yellow, and a precipitate appeared. This precipitate was removed by filtration, washed with cold water (5 cm^3) and ethanol (5 cm^3) and dried *in vacuo* to give the title compound as a pale yellow powder (0.12 g, 47%). PtCl$_2$P$_2$C$_{30}$H$_{20}$F$_{14}$ requires C 36.96 H 2.07 P 6.36 found C 39.0 H 2.5 P 7.5. ^{31}P{^{1}H} NMR: δ 24.0 ppm (vt, ½(|$^2J_{PF}$ + $^4J_{PF}$| = 29.5 Hz, $^1J_{PtP}$ = 2986 Hz), δ -66.5 ppm (PCCF_3, 12F, d, $^3J_{FF}$ = 9.5 Hz), δ -172.0 ppm (PCF, 2F, vtsept, ½|$^2J_{PF}$ + $^4J_{PF}$| = 29.8 Hz, $^3J_{FF}$ = 9.5 Hz).

[AuCl{PPh$_2$(CF$_3$)}], 39

K[AuCl$_4$] (0.2 g, 0.5 mmol) was dissolved in ethanol (5 cm^3) and water (2 cm^3). Tetrahydrothiophene (0.1 cm^3, 1.1 mmol) was then added drop-wise, and the mixture stirred for 15 minutes, during which time the solution became yellow, then white. The mixture was then filtered and the white solid dried *in vacuo*, then placed in a flask containing DCM (5 cm^3). A solution of Ph$_2$PCF$_3$ (0.12 g, 0.47 mmol) in DCM (1 cm^3) was then added, and the mixture allowed to stir overnight. The volatiles were then removed *in vacuo*, affording a white solid (0.13 g, 56.7 %). AuC$_{13}$ClF$_3$H$_{10}$ requires H 2.07 P 6.37 found H 1.96, P 7.0. ^{31}P{^{1}H} NMR: δ 30.6 (q, $^2J_{PF}$ = 83.6 Hz); ^{19}F NMR: δ -57.6 ppm (d, $^2J_{PF}$ = 83.1 Hz); ^{1}H NMR: δ 7.64-7.72 (*ortho*-CH m, 4H), 7.50-

7.57 (*para*-CH, m, 2H), 7.42-7.48 (*meta*-CH, m, 4H); $^{13}C\{^{1}H\}$ NMR: δ 122.6 ppm (d, $^{1}J_{PC}$ = 41.0 Hz, *ipso*), 125.4 ppm (qd, $^{1}J_{CF}$ = 317.8 Hz, $^{1}J_{PC}$ = 56.6 Hz), 128.6 ppm (d, $^{2}J_{PC}$ = 10.9 Hz, *para*), 132.0 ppm (d, $^{3}J_{PC}$ = 2.1 Hz, *meta*), 133.5 ppm (d, $^{2}J_{PC}$ = 16.3 Hz, *ortho*).

[AuCl{PPh$_2$CF(CF$_3$)$_2$}], 40

In the manner described above, K[AuCl$_4$] (0.3 g, 0.79 mmol) was reacted with tetrahydrothiophene (0.14 cm^3, 1.6 mmol), then the white precipitate isolated by filtration and dried *in vacuo*, then placed in a flask containing DCM (5 cm^3). Ph$_2$PCF(CF$_3$)$_2$ (0.28 g, 0.8 mmol in DCM (2cm^3)) was then added and the mixture allowed to stir for 1 hour, after which the volatiles were removed *in vacuo* to yield the title compound as a white solid (0.27 g, 57.5%). AuC$_{15}$ClF$_7$H$_{10}$P requires C 30.69, H 1.72, P 5.28 found C 29.96, H 1.63, P 5.25. $^{31}P\{^{1}H\}$ NMR: δ 37.3 ppm (dm, $^{2}J_{PF}$ = 39.5 Hz); ^{19}F NMR: δ -67.4 ppm (dd, $^{3}J_{FF}$ = 8.5 Hz, $^{3}J_{PF}$ = 8.5 Hz), -180.9 ppm (br. d, $^{2}J_{PF}$ = 39.5 Hz); ^{1}H NMR: δ 8.04 (dd, *J* = 14.0, 7.5 Hz, 4H), 7.56-7.62 ppm (m, 2H), 7.47-7.52 (m, 4H).

[AuCl{PPh$_2$(^{s}C$_4$F$_9$)}], 41

In a manner analogous to that described above, K[AuCl$_4$] (0.3 g, 0.79 mmol) was reacted with tetrahydrothiophene (0.14 cm^3, 1.6 mmol) to afford a white solid which was placed in DCM (5 cm^3). Ph$_2$P(*sec*-C$_4$F$_9$) (0.32 g, 0.8 mmol in DCM (2 cm^3)) was then added and the mixture stirred for 90 minutes. Then the volatiles were removed *in vacuo* affording the title compound as a white solid (0.24 g, 47.1 %). C$_{16}$H$_{10}$AuClF$_9$P requires C 30.17, H 1.58, P 4.87 found C 31.4, H 1.69, P 5.23. $^{31}P\{^{1}H\}$ NMR: δ 39.9 ppm (m); ^{19}F NMR: -65.7 ppm (m, 3F), -79.9 ppm (m, 3F), -107.3 ppm (dddm, $^{2}J_{FF}$ = 297.8 Hz, *J* = 33.1 Hz, 10.3 Hz, 1F), -111.6 ppm (dm, $^{2}J_{FF}$ = 297.8 Hz, 1F), -179.8 ppm (m,

1F); ^{1}H NMR: δ 8.02-8.10 ppm (m, 4H), 7.56-7.60 ppm (m, 2H), 7.46-7.52 ppm (m, 4H).

[Mo(CO)$_5${PPh$_2$CF(CF$_3$)$_2$}], 42

[Mo(CO)$_6$] (0.31 g, 1.17 mmol) and Me$_3$NO.2H$_2$O (0.13 g, 1.17 mmol) were dissolved in MeCN (40 cm^3) under a static vacuum and allowed to stir for 1 hour. A solution of Ph$_2$PCF(CF$_3$)$_2$ (0.40 g, 1.17 mmol) in MeCN (10 cm^3) was then added and the mixture allowed to stir overnight. This mixture was then passed down a short silica column (toluene) resulting in the title compound as a dark brown oil that still contained some unreacted **15**. IR (cm^{-1}): 2081, 1982, 1957, 1219, 1155, 1087. ^{31}P{^{1}H} NMR: δ 57.0 ppm (dsept, $^2J_{PF}$ = 79.3 Hz, $^3J_{PF}$ = 3.1 Hz). ^{19}F NMR: δ -65.7 ppm (dd, $^3J_{FF}$ = 9.2 Hz, $^3J_{PF}$ = 3.1 Hz, 6F, PCF(CF_3)$_2$), -174.0 ppm (dsept, $^2J_{PF}$ = 79.2 Hz, $^3J_{FF}$ = 9.2 Hz, 1F, PCF).

8. References

(1)   R. H. Crabtree, *The Organometallic Chemistry of the Transition Metals*; 3rd ed.; Wiley, 2000.
(2)   A. C. J. Koeken, M. C. A. van Vliet, L. J. P. van den Broeke, B. J. Deelman, J. T. E. Keurentjes, *Adv. Synth. Catal.*, **2008**, *350*, 179-188.
(3)   P. Cheliatsidou, D. F. S. White, D. J. Cole-Hamilton, *Dalton Trans.,* **2004**, 3425-3427.
(4)   S. Bischoff, M. Kant, In *3rd International Symposium on Catalysis in Multiphase Reactors*; Elsevier Science Bv: Naples, Italy, 2000, p 183-189.
(5)   A. Tenaglia, L. Giordano, *Tetrahedron Lett.* **2004**, *45*, 171-174.
(6)   I. F. Duan, C. H. Cheng, J. S. Shaw, S. S. Cheng, K. F. J. Liou, *Chem. Soc. Chem. Comm.,* **1991**, 1347-1348.
(7)   M. Lautens, W. Klute, W. Tam, *Chem. Rev.* **1996**, *96*, 49-92.
(8)   P. Kuhn, D. Semeril, D. Matt, M. J. Chetcuti, P. Lutz, *Dalton Trans.,* **2007**, 515-528.
(9)   P. Kuhn, D. Semeril, C. Jeunesse, D. Matt, M. Neuburger, A. Mota, *Chem.-Eur. J.,* **2006**, *12*, 5210-5219.
(10)   P. Kuhn, D. Semeril, C. Jeunesse, D. Matt, P. Lutz, R. Welter, R. *Eur. J. Inorg. Chem.,* **2005**, 1477-1481.
(11)   R. A. Baber, M. L. Clarke, K. M. Heslop, A. C. Marr, A. G. Orpen, P. G. Pringle, A. Ward, D. E. Zambrano-Williams, *Dalton Trans.,* **2005**, 1079-1085.
(12)   E. P. Kundig, C. M. Saudan, F. Viton, *Adv. Synth. Cat.,* **2001**, *343*, 51-56.
(13)   E. P. Kundig, C. M. Saudan, F. Viton, *Adv. Synth. Cat.,* **2000**, 2063-2070.
(14)   E. G. Hope, A. M. Stuart, *Handbook of Fluorous Chemistry* **2004**, 272-281.
(15)   E. G. Hope, A. M. Stuart, *Multiphase Homogeneous Catalysis* **2005**, *1*, 354-361.
(16)   M. S. Balakrishna, S. Priya, R. Panda, *Phosphorus Sulfur,* **2004**, *179*, 911-914.
(17)   O. Stelzer, S. Rossenbach, D. Hoff, M. Schreuder-Goedheijt, P. C. J. Kamer, J. N. H. Reek, P. W. N. M. van Leeuwen, *Multiphase Homogeneous Catalysis,* **2005**, *1*, 66-82.
(18)   D. W. Allen, *Organophosphorus Chemistry* **2006**, *35*, 1-91.
(19)   R. Engel, J. I. Rizzo, *Curr. Org. Chem.* **2006**, *10*, 2393-2405.
(20)   C. L. Pollock, G. C. Saunders, E. Smyth, V. I. Sorokin, *J. Fluorine Chem.,* **2008**, *129*, 142-166.
(21)   C. M. Giandomenico, C. T. Lam, S. J. Lippard, *J. Am. Chem. Soc.,* **1982**, *104*, 1263-1271.
(22)   P. T. Wolczanski, J. E. Bercaw, *J. Am. Chem. Soc.,* **1979**, *101*, 6450-6452.
(23)   E. Singleton, H. E. Oosthuizen, *Adv. Organomet. Chem.,* **1983**, *22*, 209-310.
(24)   J. F. Nixon, *Adv. Inorg. Chem.,* **1985**, *29*, 41-141.
(25)   J. S. Dewar, *B. Soc. Chim. Fr.,* **1951**, *18*, C71-C79.
(26)   J. Chatt, L. A. Duncanson, *J. Chem. Soc.,* **1953**, 2939-2947.
(27)   J. Chatt, A. A. Williams, *J. Chem. Soc.,* **1951**, 3061-3067.
(28)   J. Chatt, R. G. Wilkins, *J. Chem. Soc.,* **1952**, 273-278.
(29)   S. X. Xiao, W. C. Trogler, D. E. Ellis, Z. Berkovitchyellin, *J. Am. Chem. Soc.,* **1983**, *105*, 7033-7037.

(30) D. S. Marynick, *J. Am. Chem. Soc.,* **1984**, *106*, 4064-4065.

(31) A. G. Orpen, N. G. Connelly, *J. Chem. Soc. Chem. Comm.,* **1985**, 1310-1311.

(32) G. Pacchioni, P. S. Bagus, *Inorg. Chem.,* **1992**, *31*, 4391-4398.

(33) O. Kuhl, *Coord. Chem. Rev.,* **2005**, *249*, 693-704.

(34) W. Strohmeier, F. J. Müller, *Chem. Ber.,* **1967**, *100*, 2812-2821.

(35) K. K. Banger, R. P. Banham, A. K. Brisdon, W. I. Cross, G. Damant, S. Parsons, R. G. Pritchard, A. Sousa-Pedrares, *J. Chem. Soc., Dalton* **1999**, 427-434.

(36) K. D. Cooney, T. R. Cundari, N. W. Hoffman, K. A. Pittard, M. D. Temple, Y. Zhao, *J. Am. Chem. Soc.,* **2003**, *125*, 4318-4324.

(37) D. W. Allen, B. F. Taylor, *J. Chem. Soc. Dalton,* **1982**, 51-54.

(38) D. J. Adams, J. A. Bennett, D. Duncan, E. G. Hope, J. Hopewell, A. M. Stuart, A. J. West, *Polyhedron,* **2007**, *26*, 1505-1513.

(39) A. Cogne, A. Grand, J. Laugier, J. B. Robert, L. Wiesenfeld, *J. Am. Chem. Soc.,* **1980**, *102*, 2238-2242.

(40) C. A. Tolman, *Chem. Rev.,* **1977**, *77*, 313-48.

(41) A. Immirzi, A. Musco, B. E. Mann, *Inorg. Chim. Acta,* **1977**, *21*, L37-L38.

(42) D. White, B. C. Taverner, N. J. Coville, P. W. Wade, *J. Organomet. Chem.,* **1995**, *495*, 41-51.

(43) D. White, B. C. Taverner, P. G. L. Leach, N. J. Coville, *J. Comput. Chem.,* **1993**, *14*, 1042-1049.

(44) H. Jacobsen, A. Correa, A. Poater, C. Costabile, L. Cavallo, *Coord. Chem. Rev.,* **2009**, *253*, 687-703.

(45) H. Jacobsen, A. Correa, A. Poater, C. Costabile, L. Cavallo, *Coord. Chem. Rev.,* **2009**, *253*, 2784-2784.

(46) A. Poater, F. Ragone, S. Giudice, C. Costabile, R. Dorta, S. P. Nolan, L. Cavallo, *Organometallics,* **2008**, *27*, 2679-2681.

(47) R. A. Kelly, H. Clavier, S. Giudice, N. M. Scott, E. D. Stevens, J. Bordner, I. Samardjiev, C. D. Hoff, L. Cavallo, S. P. Nolan, *Organometallics*, **2008**, *27*, 202-210.

(48) L. Cavallo, A. Correa, C. Costabile, H. Jacobsen, J. *Organomet. Chem.*, **2005**, *690*, 5407-5413.

(49) M. S. Viciu, O. Navarro, R. F. Germaneau, R. A. Kelly, W. Sommer, N. Marion, E. D. Stevens, L. Cavallo, S. P, Nolan, *Organometallics*, **2004**, *23*, 1629-1635.

(50) A. C. Hillier, W. J. Sommer, B. S. Yong, J. L. Petersen, L. Cavallo, S.P. Nolan, *Organometallics*, **2003**, *22*, 4322-4326.

(51) A. Poater, B. Cosenza, A. Correa, S. Giudice, F. Ragone, V. Scarano, L. Cavallo, *Eur. J. Inorg. Chem.*, **2009**, 1759-1766.

(52) B. J. Dunne, R. B. Morris, A. G. Orpen, *J. Chem. Soc. Dalton*, **1991**, 653-661.

(53) D. M. Roddick, R. C. Schnabel, in *Inorganic Fluorine Chemistry - toward the 21st Century*; Edited by J. S. Thrasher, S. H. Strauss, American Chemical Society: Washington, 1994; Vol. 555, 421-437.

(54) F. W. Bennett, G. R. A. Brandt, H. J. Emeleus, R. N. Haszeldine, *Nature*, **1950**, *166*, 225.

(55) H. J. Emeleus, J. D. Smith, *J. Chem. Soc.,* **1958**, 527-528.

(56) B. Hoge,

(57) F. W. Bennett, H. J. Emeleus, R. N. Haszeldine, *J. Chem. Soc.*, **1953**, 1565-71.

(58) H. J. Emeleus, J. D. Smith, *J. Chem. Soc.*, **1959**, 375-381.

(59) A. H. Cowley, T. A. Furtsch, D. S. Dierdorf, *J. Chem. Soc. Chem. Comm.*, **1970**, 523-524.

(60) B. N. Ghose, *J. Indian Chem. Soc.*, **1978**, *55*, 1254-1259.

(61) F. W. Bennett, H. J. Emeleus, R. N. Haszeldine, *J. Chem. Soc.,* **1954**, 3896-3904.
(62) A. B. Burg, W. Mahler, A. J. Bilbo, C. P. Haber, D. L. Herring, *J. Am. Chem. Soc.,* **1957**, *79*, 247.
(63) T. Mahmood, J. M. Shreeve, *Inorg. Chem.,* **1986**, *25*, 3128-3131.
(64) J. F. Nixon, R. G. Cavell, *J. Chem. Soc.,* **1964**, 5983-5990.
(65) I. G. Maslennikov, A. N. Lavrentev, N. V. Khovanskaya, V. B. Lebedev, E. G. Sochilin, *Zh. Obshch. Khim.*, **1979**, *49*, 1498-1501.
(66) V. N. Kulakova, Y. M. Zinovev, L. Z. Soborovskii, *Zh. Obshch. Khim.*, **1959**, *29*, 3957-3959.
(67) A. B. Burg, G. Brendel, *J. Am. Chem. Soc.*, **1958**, *80*, 3198-3202.
(68) R. N. Haszeldine, B. O. West, *J. Chem. Soc.*, **1956**, 3631-3637.
(69) R. N. Haszeldine, B. O. West, *J. Chem. Soc.*, **1957**, 3880-3884.
(70) W. R. Cullen, *Can. J. Chem.*, **1962**, *40*, 426-430.
(71) W. Mahler, A. B. Burg, *J. Am. Chem. Soc.*, **1958**, *80*, 6161-6167.
(72) H. G. Ang, B. O. West, M. E. Redwood, *Aust. J. Chem.*, **1972**, *25*, 493-498.
(73) A. B. Burg, W. Mahler, *J. Am. Chem. Soc.*, **1957**, *79*, 4242.
(74) R. G. Cavell, R. C. Dobbie, *J. Chem. Soc. A.,* **1967**, 1308-1310.
(75) L. R. Grant, PhD Thesis, University of Southern California, 1961.
(76) I. G. Phillips, R. G. Ball, R. G. Cavell, *Inorg. Chem.,* **1988**, *27*, 4038-4045.
(77) L. D. Field, M. P. Wilkinson, *Tetrahedron Lett.*, **1992**, *33*, 7601-7604.
(78) L. D. Field, M. P. Wilkinson, *Tetrahedron Lett.*, **1997**, *38*, 2779-2782.
(79) M. Goerg, G. V. Roeschenthaler, A. A. Kolomeitsev, *J. Fluorine Chem.,* **1996**, *79*, 103-104.
(80) M. A. A. Beg, H. C. Clark, *Can. J. Chem.*, **1961**, *39*, 564-70.
(81) M. A. A. Beg, H. C. Clark, *Can. J. Chem.*, **1962**, *40*, 283-288.
(82) E. Wiberg, M. Van Ghemen, G. Muller-Schiedmayer, *Angew. Chem.*, **1963**, *75*, 814-823.
(83) I. G. Maslennikov, L. N. Kirichenko, S. F. Aleinikov, V. B. Lebedev, A. N. Lavrent'ev, *Zh. Obshch. Khim.*, **1983**, *53*, 939-90.
(84) J. F. Nixon, *J. Chem. Soc.*, **1964**, 2469.
(85) O. Adler, F. Kober, *J. Organomet. Chem.* **1974**, *72*, 351-360.
(86) H. G. Ang, G. Manoussa. Y. O. El-Nigumi, *J. Inorg. Nucl. Chem.*, **1968**, *30*, 1715-1717.
(87) W. Volbach, I. Ruppert, *Tetrahedron Lett.* **1983**, *24*, 5509-5512.
(88) K. Gosling, D. J. Holman, J. D. Smith, B. N. Ghose, *J. Chem. Soc. A.*, **1968**, 1909-1914.
(89) D. K. Kang, A. B. Burg, *Inorg. Chem.*, **1972**, *11*, 902-904.
(90) R. Fields, R. N. Haszeldine, J. Kirman, *J. Chem. Soc. C.*, **1970**, 197-200.
(91) R. Fields, N. F. Wood, *J. Chem. Soc. C.*, **1970**, 744-748.
(92) R. Fields, R. N. Haszeldine, N. F. Wood, *J. Chem. Soc. C.*, **1970**, 1370-1375.
(93) A. N. Lavrentev, I. G. Maslennikov, E. G. Sochilin, *Zh. Obshch. Khim.*, **1975**, *45*, 1702-1704.
(94) E. A. Ganja, C. D. Ontiveros, J. A. Morrison, *Inorg. Chem.*, **1988**, *27*, 4535-4538.
(95) V. Y. Semenii, V. A. Stepanov, N. V. Ignatev, G. G. Furin, L. M. Yagupolskii, *Zh. Obshch. Khim.* **1985**, *55*, 2716-2720.
(96) N. Ignat'ev, P. Sartori, *J. Fluorine Chem.* **2000**, *103*, 57-61.
(97) J. J. Kampa, J. W. Nail, R. J. Lagow, *Angew. Chem. Intl. Ed.*, **1995**, *34*, 1241-1244.
(98) M.F Ernst, D. M. Roddick, *Inorg. Chem.* **1989**, *28*, 1624-1627.

(99) R. G. Peters, B. L. Bennett, R. C. Schnabel, D. M. Roddick, *Inorg. Chem.*, **1997**, *36*, 5962-5965.

(100) J. D. Palcic, P. N. Kapoor, D. M. Roddick, R. G. Peters, *Dalton Trans.*, **2004**, 1644-1647.

(101) J. J. Adams, A. Lau, N. Arulsamy, D. M. Roddick, *Inorg. Chem.*, **2007**, *46*, 11328-11334.

(102) M. Fild, P. G. Jones, K. Ruhnau, K. *J. Fluorine Chem.*, *54*, 387.

(103) M. L. Clarke, A. G. Orpen, P. G. Pringle, E. Turley, *Dalton Trans.*, **2003**, 4393-4394.

(104) S. E. Vaillard, A. Postigo, R. A. Rossi, *Organometallics*, **2004**, *23*, 3003-3007.

(105) M. N. Lanteri, R. A. Rossi, S. E. Martín, *J. Organomet. Chem.* **2009**, *694*, 3425-3430.

(106) I. Tworowska, W. Dabkowski, J. Michalski, *Angew. Chem. Intl. Ed.* **2001**, *40*, 2898-2900.

(107) M. B. Murphy-Jolly, L. C. Lewis, A. J. M. Caffyn, *Chem. Commun.* **2005**, 4479-4480.

(108) P. Eisenberger, I. Kieltsch, N. Armanino, A. Togni, *Chem. Commun.* **2008**, 1575-1577.

(109) J. D. Park, R. J. Seffl, J. R. Lacher, *J. Am. Chem. Soc.* **1956**, *78*, 59-62.

(110) I. L. Knunyants, R. N. Sterlin, R. D. Yatsenko, L. N. Pinkina, *Izv. Akad. Nauk. SSSR, Ser. Khim.*, **1958**, 1345-1347.

(111) R. N. Sterlin, I. L. Knunyants, L. N. Pinkina, R. D. Yatsenko, *Izv. Akad. Nauk. SSSR, Ser. Khim.*, **1959**, 1492-1493.

(112) R. N. Sterlin, V. G. Li, I. L. Knunyants, *Izv. Akad. Nauk. SSSR, Ser. Khim.*, ***1959,*** 1506.

(113) H. D. Kaesz, S. L. Stafford, F. G. A. Stone, *J. Am. Chem. Soc.* **1960**, *82*, 6232-6235.

(114) D. Seyferth, D. E. Welch, G. Raab, *J. Am. Chem. Soc.* **1962**, *84*, 4266-4269.

(115) P. Tarrant, P. Johncock, J. Savory, *J. Org. Chem.* **1963**, *28*, 839-843.

(116) R. N. Sterlin, L. N. Pinkina, I. L. Knunyants, L. F. Nezgovorov, *Khim. Nauk. Prom.* **1959**, *4*, 809-810.

(117) A. H. Cowley, M. W. Taylor, *J. Am. Chem. Soc.* **1969**, *91*, 1922-1933.

(118) H. G. Horn, R. Koentges, F. Kolkmann, H. C. Marsmann, *Z. Naturforsch., B: Anorg. Chem. Org. Chem.*, **1978**, *33B*, 1422-1426.

(119) J. Burdon, P. L. Coe, I. B. Haslock, R. L. Powell, *Chem. Commun.,* **1996**, 49-50.

(120) P. P. Coe, *J. Fluorine Chem.,* **1999**, *100*, 45.

(121) K. K. Banger, A. K. Brisdon, *J. Organomet. Chem.* **1999**, *582*, 301-309.

(122) K. K. Banger, A. K. Brisdon, A. Gupta, *Chem. Commun.* ,**1997**, 139-140.

(123) A. K. Brisdon, K. K. Banger, *J. Fluorine Chem.*, **1999**, *100*, 35-43.

(124) R. N. Sterlin, R. D. Yatsenko, L. N. Pinkina, I. L. Knunyants, *Khim. Nauk. Prom.*, **1959**, *4*, 810-811.

(125) N. A. Barnes, A. K. Brisdon, F. R. W. Brown, W. I. Cross, I. R. Crossley, C. Fish, J. V. Morey, R. G. Pritchard, L. Sekhri, *New J. Chem.* **2004**, *28*, 828-837.

(126) H. G. Horn, F. Kolkmann, *Z. Naturforsch., B: Anorg. Chem. Org. Chem.* **1978**, *33B*, 1427-1429.

(127) G. Wittig, A. Maercker, *J. Organomet. Chem.* **1967**, *8*, 491-494.

(128) J. W. Middleton, W. H. Sharkey, *J. Am. Chem. Soc.* **1959**, *81*, 803-804.

(129) R. N. Haszeldine, *J. Chem. Soc.* **1951**, 588.

(130) A. L. Henne, M. Nager, *J. Am. Chem. Soc.,* **1951**, *73*, 1042-1043.
(131) W. G. Finnegan, W. P. Norris, *J. Org. Chem.,* **1963**, *28*, 1139-1140.
(132) A. L. Henne, M. Nager, *J. Am. Chem. Soc.,* **1952**, *74*, 650-652.
(133) F. G. Drakesmith, O. J. Stewart, P. Tarrant, *J. Org. Chem.,* **1968**, *33*, 280-285.
(134) R. N. Haszeldine, *Nature,* **1950**, *165*, 152-153.
(135) A. R. Katritzky, M. Qi, A. P. Wells, *J. Fluorine Chem.,* **1996**, *80*, 145-147.
(136) A. K. Brisdon, I. R. Crossley, *Chem. Commun.*, **2002**, 2420-2421.
(137) M. M. Shimizu, *Synlett*, **2007**, 1163.
(138) A. J. Carty, N. K. Hota, T. W. Ng, H. A. Patel, T. J. O'Connor, *Can. J. Chem.*, **1971**, *49*, 2706-2711.
(139) D. H. Lemmon, *Spectrochim. Acta, Part A*, **1973**, *29*, 1899.
(140) D. H. Lemmon, J. A. Jackson, *J. Fluorine Chem.*, **1976**, *8*, 23-42.
(141) K. K. Banger, A. K. Brisdon, C. J. Herbert, H. A. Ghaba, I.S. Tidmarsh, *J. Fluorine Chem.* **2009**, *130*, 1117-1129.
(142) G. F. Jiang, J. Sun, Y. C. Shen, *J. Fluorine Chem.* **2001**, *108*, 207-210.
(143) Y. C. Shen, M. Qi, *J. Chem. Soc., Perkin Trans. 1*, **1993**, 2153-2154.
(144) T. Konno, A. Morigaki, K. Ninomiya, T. Miyabe, T. Ishihara, *Synthesis,* **2008**, 564-572.
(145) I. S. Tidmarsh, MChem Project Report, UMIST, 2003.
(146) A. K. Brisdon, I. R. Crossley, R. G. Pritchard, G. Sadiq, J. E. Warren, *Organometallics,* **2003**, *22*, 5534-5542.
(147) A. B. Burg, W. Mahler, *J. Am. Chem. Soc.*, **1958**, *80*, 2334.
(148) M. Bigorgne, *J. Inorg. Nucl. Chem.* **1964**, *26*, 107-115.
(149) A. B. Burg, G. B. Street, *Inorg. Chem.*, **1966**, *5*, 1532-1537.
(150) A. B. Burg, I. H. Sabherwal, *Inorg. Chem.*, **1970**, *9*, 974-975.
(151) A. B. Burg, G. B. Street, *J. Am. Chem. Soc.*, **1963**, *85*, 3522.
(152) A. B. Burg, R. A. Sinclair, *J. Am. Chem. Soc.*, **1966**, *88*, 5354-5355.
(153) H. Einspahr, J. Donohue, *Inorg. Chem.*, **1974**, *13*, 1839-1843.
(154) R. A. Sinclair, A. B. Burg, *Inorg. Chem.*, **1968**, *7*, 2160-2162.
(155) K. A. Khokhryakov, I. E. Grigorov, N. S. Pamina, V. N. Yakovlev, Y. N. Kukushkin, *Koord. Khim.*, **1987**, *13*, 237-241.
(156) R. C. Dobbie, *J. Chem. Soc. A,* **1971**, 230-233.
(157) A. B. Burg, *Inorg. Chem.,* **1986**, *25*, 4751-4755.
(158) M. Brookhart, W. A. Chandler, A. C. Pfister, C. C. Santini, P. S. White, *Organometallics*, **1992**, *11*, 1263-1274.
(159) J. D. Koola, D. M. Roddick, *J. Am. Chem. Soc* **1991**, *113*, 1450-1451.
(160) B. L. Bennett, S. White, B. Hodges, D. Rodgers, A. Lau, D. M. Roddick, *J. Organomet. Chem.*, **2003**, *679*, 65-71.
(161) M. A. A. Beg, H. C. Clark, *Can. J. Chem.*, **1960**, *38*, 119-124.
(162) K. A. Khokhryakov, I. G. Maslennikov, E. I. Grigorov, Y. N. Kukushkin, *Zh. Obshch. Khim.*, **1985**, *55*, 2622.
(163) A. J. Rest, *J. Chem. Soc. A*, **1968**, 2212-2215.
(164) E. I. Grigorov, K. A. Khokhryakov, *Zh. Obshch. Khim.*, **1984**, *54*, 2389-2390.
(165) M. A. A. Beg, M. A. Qaiser, *Thermochim. Acta*, **1992**, *210*, 123-132.
(166) B. C. Taverner, *J. Comput. Chem.,* **1996**, *17*, 1612-1623.
(167) Butikofer, J. L.; Hoerter, J. M.; Peters, R. G.; Roddick, D. M. *Organometallics*, **2004**, *23*, 400-408.
(168) J. L. Butikofer, T. G. Parson, D. M. Roddick, *Organometallics*, **2006**, *25*, 6108-6114.
(169) M. A. A. Beg, H. C. Clark, *Can. J. Chem.* **1961**, *39*, 595-596.

(170) L. Manojlovic-Muir, D. Millington, K. W. Muir, D. W. A. Sharp, W. E. Hill, J. V. Quagliano, L. M. Vallarino, *J. Chem. Soc. Chem. Commun.*, **1974**, 999-1000.

(171) I. Macleod, L. Manojlovic-Muir, D. Millington, K. W. Muir, D. W. A. Sharp, R. Walker, *J. Organomet. Chem.*, **1975**, *97*, C7-C10.

(172) R. C. Schnabel, D. M. Roddick, *Inorg. Chem.* **1993**, *32*, 1513-1518.

(173) R. G. Peters, J. D. Palcic, R. G. Baughman, *Acta Crystallogr. Sect. E,*, **2003**, *E59*, m1198-m1200.

(174) N. A. Barnes, A. K. Brisdon, F. R. W. Brown, W. I. Cross, C. J. Herbert, R. G. Pritchard, G. Sadiq, *Dalton Trans.* **2008**, 101-114.

(175) N. A. Barnes, A. K. Brisdon, M. Nieuwenhuyzen, R. G. Pritchard, G. C. Saunders, *J. Fluorine Chem.*, **2007**, *128*, 943-951.

(176) N. A. Barnes, A. K. Brisdon, J. G. Fay, R. G. Pritchard, J. E. Warren, *Inorg. Chim. Acta*, **2005**, *358*, 2543-2548.

(177) N. A. Barnes, A. K. Brisdon, M. J. Ellis, R. G. Pritchard, *J. Fluorine Chem.*, **2001**, *112*, 35-45.

(178) L. J. Farrugia, **1997**, *ORTEP 3 for Windows*, University of Glasgow.

(179) J. Fawcett, E. G. Hope, R. D. W. Kemmitt, D. R. Paige, D. R. Russell, A. M. Stuart, *J. Chem. Soc. Dalton Trans.*, **1998**, 3751-3763.

(180) R. G. Peters, J. D. Palcic, R. G. Baughman, *Acta Crystallogr. Sect. E*, **2003**, *59*, m1198-m1200.

(181) *Handbook of Chemistry and Physics*; 58th ed.; CRC Press: Cleveland, OH, 1977-1978.

(182) J. W. Emsley, L. Phillips, V. Wray, *Fluorine Coupling Constants*; 1st Ed., Pergamon Press: Oxford, 1977.

(183) S. Schweizer, J. M. Becht, C. Le Drian, *Adv. Synth. Catal.*, **2007**, *349*, 1150-1158.

(184) S. Ng, C. H. Sederholm, *J. Chem. Phys.*, **1964**, *40*, 2090-2094.

(185) K. Stanek, B. Czarniecki, R. Aardoom, H. Rüegger, A. Togni, *Organometallics*, **2010**, *29*, 2540-2546.

(186) I. R. Crossley, PhD Thesis, UMIST, 2003.

(187) A. K. Brisdon, I. R. Crossley, K. R. Flower, R. G. Pritchard, J. E. Warren, *Angew. Chem. Intl Ed.*, **2003**, *42*, 2399-2401.

(188) S. O. Grim, W. McFarlane, *Nature*, **1965**, *208*, 995-996.

(189) S. O. Grim, W. McFarlane. E. F. Davidoff, *J. Org. Chem.* **1967**, *32*, 781-784.

(190) B. Beutel, Dissertation, University of Marburg, 2009.

(191) H. Ali Gabah, 2nd Year Transfer Report, University of Manchester. 2010.

(192) F. R. W. Brown, MChem Project Report, UMIST, 2002.

(193) C. J. Herbert, MChem Project Report, University of Manchester, 2006.

(194) G. R. Dobson, I. W. Stolz, R. K. Sheline, *Adv. Inorg. Chem. Rad.*, **1966**, *8*, 1.

(195) S. E. Tunney, K. J. Stille, *J. Org. Chem.* **1987**, *52*, 748-753.

(196) J. Balagué, B. Améduri, B. Boutevin, G. Caporiccio, *J. Fluorine Chem.* **1995**, *74*, 49-58.

(197) R. Eujen, R. Mellies, *J. Fluorine Chem.* **1983**, *22*, 263-280.

(198) M. Sako, T. Kihara, K. Okada, Y. Ohtani, H. Kawamoto, H. *J. Org. Chem.*, **2001**, *66*, 3610-3612.

(199) L. C. Lewis-Alleyne, M. B. Murphy-Jolly, X. F. Le Goff, A. J. M. Caffyn, *Dalton Trans.,* **2010**, *39*, 1198-1200.

(200) K. Marat, Spinworks, Version 2.55, University of Manitoba, 2006.

(201) R. Fields, E. F. Mooney, in *Annual Reports on NMR Spectroscopy*; Academic Press Inc: San Diego, 1972; Vol. 5, 99-304.

(202) V. V. Bardin, A. A. Avramenko, G. G. Furin, V. A. Krasilnikov, A. I. Karelin, P. P. Tushin, V. A. Petrov, *J. Fluorine Chem.* **1990**, *49*, 385-400.

(203) P. Bhattacharyya, B. Croxtall, J. Fawcett, D. Gudmunsen, E. G. Hope, R. D. W. Kemmitt, D. R. Paige, D. R. Russell, A. M. Stuart, D. R. W. Wood, *J. Fluorine Chem.*, **2000**, *101*, 247-255.

(204) E. G. Hope, A. M. Stuart, *J. Fluorine Chem.*, **1999**, *100*, 75-83.

(205) G. Vlad, F. U. Richter, I. T. Horvath, *Tetrahedron Lett.* **2005**, *46*, 8605-8608.

(206) I. T. Horvath, G. Kiss, R. A. Cook, J. E. Bond, P. A. Stevens, J. Rabai, E. J. Mozeleski, *J. Am. Chem. Soc.*, **1998**, *120*, 3133-3143.

(207) I. T. Horvath, J. Rabai, *Science,* **1994**, *266*, 72-75.

(208) M. Christl, H. J. Reich, J. D. Roberts, *J. Am. Chem. Soc.*, **1971**, *93*, 3463-&.

(209) R. L. Lipnick, *J. Am. Chem. Soc.* **1974**, *96*, 2941-2948.

(210) K. S. Pitzer, W. E. Donath, *J. Am. Chem. Soc.* **1959**, *81*, 3213-3218.

(211) T. A. Kestner, *J. Fluorine Chem.* **1987**, *36*, 77-82.

(212) V. F. Snegirev, N. I. Delyagina, V. I. Bakhmutov, *Bull. Acad. Sci. USSR Div. Chem. Sci. (Engl. Transl.)*, **1986**, *35*, 1201-1206.

(213) S. I. Pletnev, S. M. Igumnov, E. V. Zakharova, K. N. Makarov, *Russ. Chem. Bull.* **1990**, *39*, 557-560.

(214) V. Matalin, G. Kaurova, V. Berenblit, V. Gribel, *Russ. J. Appl. Chem.* **2007**, *80*, 2090-2092.

(215) S. M. Igumnov, S. I. Pletnev, *Russ. Chem. Bull.*, **1988**, *37*, 2598.

(216) A. N. Wu, D. Cremer, A. A. Auer, J. Gauss, *J. Phys. Chem. A,* **2002**, *106*, 657-667.

(217) M. E. Mkadmi, M. Lazraq, A. Kerbal, J. Escudie, C. Couret, H. Ranaivonjatovo, *Phosphorus, Sulfur,* **1998**, *134*, 151-169.

(218) T. Tanuma, K. Ohnishi, H. Okamoto, T. Miyajima, S. Morikawa, *J. Fluorine Chem.*, *57*, 259-284.

(219) D. D. Elleman, L. C. Brown, D. Williams, *J. Mol. Spectrosc.*, **1961**, *7*, 322-340.

(220) R. A. Bhaskar, B. Sebastian, G. Dietrich, N. Mark, H. Oldamur, N. Laszlo, G. J. Peter, H. Joachim, *Chem.-Eur. J.,* **2009**, *15*, 12263-12272.

(221) S. Aime, R. K. Harris, E. M. McVicker, M. Fild, *J. Chem. Soc. Dalton Trans.*, **1976**, 2144-2153.

(222) E. Vincent, L. Verdonck, G. P. Van Der Kelen, *J. Mol. Struct.* **1980**, *65*, 239-247.

(223) D. D. Denson, G. J. Moore, C. Tamborski, *J. Fluorine Chem.* **1975**, *5*, 475-480.

(224) D. C. England, F. J. Weigert, J. C. Calabrese, *J. Org. Chem.*, **1984**, *49*, 4816-4819.

(225) *CRC Handbook of Chemistry and Physics*; 76th Ed.; Edited by D. R. Lide, CRC Press Inc., 1995-1996.

(226) H. J. Frohn, F. Bailly, D. Welting, V. V. Bardin, *J. Fluorine Chem.*, **2009**, *130*, 301-307.

(227) P. Metrangolo, W. Panzeri, F. Recupero, G. Resnati, *J. Fluorine Chem.*, **2002**, *114*, 27-33.

(228) E. Corradi, S. V. Meille, M. T. Messina, P. Metrangolo, G. Resnati, *Tetrahedron Lett.* **1999**, *40*, 7519-7523.

(229) M. T. Messina, P. Metrangolo, W. Panzeri, E. Ragg, G. Resnati, *Tetrahedron Lett.* **1998**, *39*, 9069-9072.

(230) A. Lunghi, P. Cardillo, T. Messina, P. Metrangolo, W. Panzeri, G. Resnati, *J. Fluorine Chem.*, **1998**, *91*, 191-194.

(231) V. Amico, S. Meille, E. Corradi, M. Mesina, G. Resnati, *J. Am. Chem. Soc.* **1998**, *120*, 8261-8262.

(232) G. W. Parshall, *Org. Synth.*, **1965**, *45*, 102-104.

(233) L. Maier, *J. Inorg. Nucl. Chem.*, **1962**, *24*, 275-283.

(234) H. Liu, J. S. Owen, A. P. Alivisatos, *J. Am. Chem. Soc.*, **2006**, *129*, 305-312.

(235) H. C. E. McFarlane, W. McFarlane, J. A. Nash, *J. Chem. Soc. Dalton Trans.*, **1980**, 240-244.

(236) A. K. Brisdon, Unpublished Results, University of Manchester: 2009.

(237) E. L. Norton, K. L. S. Szekely, J. W. Dube, P. G. Bomben, C. L. B. Macdonald, *Inorg. Chem.*, **2008**, *47*, 1196-1203.

(238) B. D. Ellis, C. L. B. Macdonald, *Inorg. Chem.*, **2006**, *45*, 6864-6874.

(239) K. B. Dillon, P. K. Monks, *Dalton Trans.*, **2007**, 1420-1424.

(240) P. Beck, in *Organic Phosphorus Compounds*; Edited by, G. Kopsaloff, L. Maier, Wiley-Interscience: 1972; Vol. 2.

(241) M. J. Petersson, W. A. Loughlin, I. D. Jenkins, *Chem. Commun.*, **2008**, 4493-4494.

(242) C. Huang, X. Tang, H. Fu, Y. Jiang, Y. Zhao, *J. Org. Chem.*, **2006**, *71*, 5020-5022.

(243) P. G. Jones, Private communication to the CCDC.

(244) P. W. Codding, K. A. Kerr, *Acta Crystallogr. Sect. B*, **1978**, *34*, 3785-3787.

(245) T. S. Cameron, B. Dahlen, *J. Chem. Soc., Perkin Trans. 2*, **1975**, 1737-1751.

(246) J. A. S. Howell, N. Fey, J. D. Lovatt, P. C. Yates, P. McArdle, D. Cunningham, E. Sadeh, H. E. Gottlieb, Z. Goldschmidt, M. B. Hursthouse, M. E. Light, *J. Chem. Soc. Dalton Trans.*, **1999**, 3015-3028.

(247) W. D. Jensen, F. W. Cagle Jr, *Talanta*, **1966**, *13*, 1046-1047.

(248) V. V. Krisyuk, I. A. Baidina, I. K. Igumenov, *Main Group Met. Chem.,* **1998**, *21*, 199.

(249) A. T. Gubaidullin, V. F. Mironov, L. M. Burnaeva, I. A. Litvinov, A. B. Dobrynin, E. I. Goryunov, G. A. Ivkova, I. V. Konovalova, T. A. Mastryukova, *Russ. J. Gen. Chem.*, **2004**, *74*, 842-859.

(250) A. Muller, S. Otto, A. Roodt, *Dalton Trans.,* **2008**, 650-657.

(251) E. Krawczyk, A. Skowronska, J. Michalski, *J. Chem. Soc. Dalton Trans.*, **2002**, 4471-4478.

(252) M. N. Chevykalova, L. F. Manzhukova, N. V. Artemova, Y. N. Luzikov, I. E. Nifant"ev, E. E. Nifant"ev, *Russ. Chem. Bull.*, **2003**, *52*, 78-84.

(253) C. Glidewell, E. J. Leslie, *J. Chem. Soc. Dalton Trans.*, **1977**, 527-531.

(254) R. V. Parish, *NMR, NQR, EPR and Mössbauer Spectroscopy in Inorganic Chemistry*; Ellis Horwood, 1990.

(255) L. Bemi, H. C. Clark, J. A. Davies, C. A. Fyfe, R. E. Wasylishen, *J. Am. Chem. Soc.*, **1982**, *104*, 438-445.

(256) D. L. Thorn, *Organometallics*, **1998**, *17*, 348-352.

(257) D. A. Fletcher, R. F. McMeeking, D. Parkin, *J. Chem. Inf. Comput. Sci.*, **1996**, *36*, 746-749.

(258) O. Kennard, *Chem. Des. Auto. News*, **1993**, *8*, 1.

(259) Y. Lin, P. G. Jones, R. Schmutzler, G. M. Sheldrick, *Eur. J. Solid State Inorg. Chem.*, **1992**, *29*, 887-898.

(260) F. Nief, F. Mathey, *Tetrahedron*, **1991**, *47*, 6673-6680.

(261) M. A. Beswick, N. L. Cromhout, C. N. Harmer, J. S. Palmer, P. R. Raithby, A. Steiner, K. L. Verhorevoort, D. S. Wright, *Chem. Commun.*, **1997**, 583-584.

(262) G. Becker, O. Mundt, M. Rossler, E. Schneider, *Z. Anorg. Allg. Chem.*, **1978**, *443*, 42-52.

(263) G. M. Sheldrick, *Acta Crystallogr. Sect. A*, **2008**, *64*, 112-122.

(264) C. F. Macrae, P. R. Edgington, P. McCabe, E. Pidcock, G. P. Shields, R. Taylor, M. Towler, J. van De Streek, *J. Appl. Crystallogr.* **2006**, *39*, 453-457.